AWARD NUMBER: W81XWH-14-1-0385

TITLE: A New Paradigm for the Treatment of Ovarian Cancer: The Use of Epigenetic Therapy to Sensitize Patients to Immunotherapy and Chemotherapy

PRINCIPAL INVESTIGATOR: Stephen B. Baylin, M.D.

CONTRACTING ORGANIZATION: The Johns Hopkins University
Baltimore, MD 21287

REPORT DATE: October 2017

TYPE OF REPORT: Annual

PREPARED FOR: U.S. Army Medical Research and Materiel Command
Fort Detrick, Maryland 21702-5012

REPORT DOCUMENTATION PAGE

Form Approved
OMB No. 0704-0188

1. REPORT DATE	2. REPORT TYPE	3. DATES COVERED
October 2017	Annual	30 Sept 2016 - 29 Sept 2017

4. TITLE AND SUBTITLE
A New Paradigm for the Treatment of Ovarian Cancer: The Use of Epigenetic Therapy to Sensitize Patients to Immunotherapy and Chemotherapy

5a. CONTRACT NUMBER
W81XWH-15-1-0385

5b. GRANT NUMBER
OC130454

5c. PROGRAM ELEMENT NUMBER

5d. PROJECT NUMBER

5e. TASK NUMBER

5f. WORK UNIT NUMBER

6. AUTHOR(S)

Stephen B. Baylin, M.D.

Email: sbaylin@jhmi.edu

7. PERFORMING ORGANIZATION NAME(S) AND ADDRESS(ES)

Johns Hopkins University
Department of Oncology
1650 Orleans St., Suite 541
Baltimore, MD 21287

8. PERFORMING ORGANIZATION REPORT NUMBER

9. SPONSORING / MONITORING AGENCY NAME(S) AND ADDRESS(ES)

U.S. Army Medical Research and Materiel Command
Fort Detrick, Maryland 21702-5012

10. SPONSOR/MONITOR'S ACRONYM(S)

11. SPONSOR/MONITOR'S REPORT NUMBER(S)

12. DISTRIBUTION / AVAILABILITY STATEMENT

Approved for Public Release; Distribution Unlimited

13. SUPPLEMENTARY NOTES

14. ABSTRACT: Our overall goal remains to bring epigenetic therapy to have major impact for the management of advanced ovarian cancer (OC). This past year, we continue to make exciting advances in our pre-clinical work and are now enrolling a leveraged clinical trial for low dose therapy targeting DNA demethylation paired with immune checkpoint therapy. Moreover, we have now completed two studies of mouse models. First, is an in press (PNAS) study of a serous ovarian cancer in which we have identified that the demethylating agent, 5-aza-cytidine (AZA) potently stimulates tumor immune attraction of T-cells to the tumor microenvironment. The treatment paradigm involves a newly regimen we first derived for addition of a histone deactylase inhibitor (HDACi) in a study of mouse models for lung cancer and this work is also now in press for Cell. In all the above, we document that an AZA induced interferon triggering pathway that we published in Cell in 2015 is a key mechanism triggering the above immune responses. Moreover in the upcoming Cell paper, we also show a key role for down-regulating the CMYC oncogene signaling for the epigenetic therapy to reverse tumor immune evasion and attract activated T-cells.

15. SUBJECT TERMS – key words or phrases identifying major concepts Epigenetic therapy, advanced ovarian cancer, DNA demethylation, histone deactylases, immune checkpoint therapy, viral defense, immune cell attraction

16. SECURITY CLASSIFICATION OF:			17. LIMITATION OF ABSTRACT	18. NUMBER OF PAGES	19a. NAME OF RESPONSIBLE PERSON
a. REPORT	b. ABSTRACT	c. THIS PAGE			USAMRMC
Unclassified	Unclassified	Unclassified	UU	154	19b. TELEPHONE NUMBER *(include area code)*

Standard Form 298 (Rev. 8-98)
Prescribed by ANSI Std. Z39.18

Table of Contents

1. INTRODUCTION

We continue to pursue our goal to develop eventual "epigenetic" therapy strategies, with relatively low toxicities, which can potentially robustly extend the life expectancy of women with advanced ovarian cancer (OC). In this past year we have completed an exciting series of studies which continue to suggest how epigenetic therapy can reverse tumor immune evasion states and thereby potentially enhance the efficacy of immune checkpoint therapy. We continue moving forward in bringing our concepts fully to bear on the treatment of OC. This past year, we have continued to concentrate on **Specific Aim 3:** *to study how epigenetic therapy may sensitize OC cells to subsequent immunotherapies which targets checkpoints which are driving immune tolerance*. As during the previous year, our group of research leaders including Cindy Zahnow, Dennis Slamon, Drew Pardoll, and Peter Jones and the final years of work from our two mentored trainees, Kate Chiappinelli and Meredith Stone, made exciting progress for **Major Task 1**: *to develop the in-vitro pre-clinical systems to outline the sensitivities and derive molecular signatures that track with these,* and **Major Task 2:** *to develop in-vivo pre-clinical systems to outline the potential efficacy of epigenetic therapy sensitization to immunotherapy for targeting checkpoints which drive immune tolerance*. *This progress is all key to our first leveraged clinical trial, headed by Dennis Slamon, which is now enrolling patients with* advanced *serous OC* and which pursues this above potential for epigenetic therapy to improve the efficacy of immune checkpoint therapy. We also continue to use our findings to develop biomarker strategies, with several key new findings to be investigated in the above leveraged trial, which can potentially predict patient responses and monitoring of therapy. Other key progress aspects will also be outlined. We have also focused, and made important progress in **Specific Aim 4:** *Develop new combinations of epigenetic drugs which may provide for the highest level of efficacy for management of OC and :* **Major Task 1:** *Follow biochemical hypotheses for designing combinations of the epigenetic drugs used in all studies above with new agents targeting additional steps in chromatin control of gene expression.*

2. KEYWORDS

1) epigenetic therapy; 2) DNA demethylation; 3) histone deacetylases; 4) immune evasion; 5) immune checkpoint therapy; 6) immune attraction.

3. ACCOMPLISHMENTS

What were the major goals and objectives of the project?

The overall goals remain identical to those outlined in the original proposal. This past year, as introduced earlier, we have concentrated particularly on:

A. Specific Aim 3: *to study how epigenetic therapy may sensitize OC cells to subsequent immunotherapies which targets checkpoints which are driving immune tolerance*. We have, with participants of key leaders, Cindy Zahnow, Dennis Slamon, and Drew Pardoll, with much lead work from the original mentored postdoctoral fellow for our project, Kate Chiappinelli, a second mentored graduate student, Meredith Stone, and a new mentee, Michael Topper made exciting progress for **Major Task 1**: *to develop the in-vitro pre-clinical systems to outline the sensitivities and derive molecular signatures that track with these,* and **Major Task 2:** *to develop in-vivo pre-clinical systems to outline the potential efficacy of epigenetic therapy sensitization to immunotherapy for targeting checkpoints which drive immune tolerance*. The major findings, as detailed directly below, involve discoveries providing key insight into how epigenetic therapy

may help reverse immune evasion to help sensitize to immune checkpoint therapy for OC, and a growing biomarker system for potentially predicting patient responses and monitoring therapy.

***What was accomplished under these goals*?**

A. Specific Aim 3: Major Task 1: *to develop the in-vitro pre-clinical systems to outline the sensitivities and derive molecular signatures that track with these.* Progress is as follows:

1. *In work published in 2015 (Chiappinelli et al, Cell, 2015),* we defined that, in human OC cells, a cytosolic double stranded RNA (dsRNA) viral defense pathway is a core functional circuit for an AZA induced interferon response and we defined the potential for constituent genes and endogenous retroviral transcripts (HERV's) in this drug response for predicting responses to immune checkpoint therapy (**Fig. 1**). Central to this induction is upregulation of a viral defense pathway. We have now markedly extended this work as described in specific aims later below. This has, in large part resulted from using a mouse model of OC (**PNAS, in press, 2017**) with important contributions as well from two mouse models of non-small cell lung cancer (NSCLC) (**Cell, in press, 2017**). The data highly support the functionality of the above pathway for driving tumor induced, immune cell attraction, for deriving key biomarker strategies, and for developing new epigenetic therapy approaches for OC.

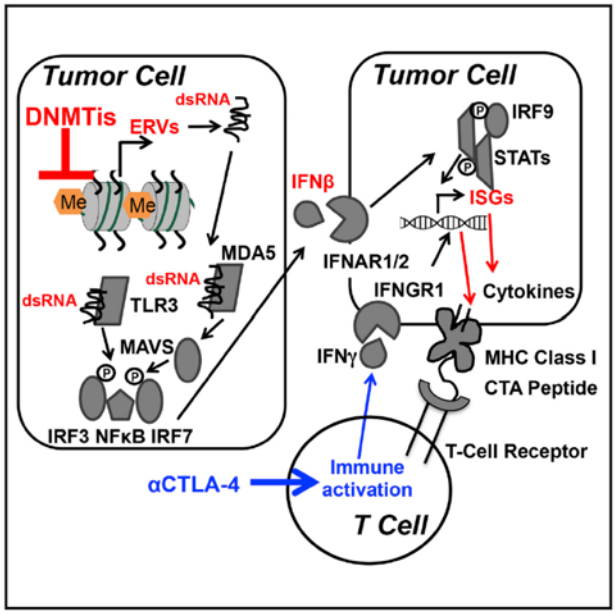

Fig. 1. DNA methyltransferase inhibitors (DNMTis) inhibit DNA methylation of LTR's for endogenous retroviruses (ERVs) to upregulate their transcription in OC tumor cells to induce a growth-inhibiting immune response. High expression of the genes associated with the anti-viral response have the potential to sensitize to immune checkpoint therapy which blocks ligand mediation of immune tolerance including CTLA-4 and PD-L1.

B. Specific Aim 3: Major Task 2: *to develop in-vivo pre-clinical systems to outline the potential efficacy of epigenetic therapy sensitization to immunotherapy for targeting checkpoints which drive immune tolerance*. We are making great progress in this task, as defined in the section below, with Cindy Zahnow continuing to take the lead in a model for OC. She has interacted heavily with Dr. Baylin for his lead in derivation of a new treatment schema in the NSCLC model which has now been fully applied to the OC model. Specific accomplishments are:

1. *Deriving, in mouse models of NSCLC and for simultaneous use in an OC model, a new combinatorial strategy for epigenetic therapy to pair with immune checkpoint therapy*.

A graduate student with Dr. Baylin, Michael Topper, in collaboration with our past TEAL award scholars, post-doctoral fellow Kate Chiappinelli (now a faculty member at George Washington) and graduate student, Meredith Stone (now a Postdoctoral Fellow, at the University of Pennsylvania), has played a seminal role in this study which is the focus of his thesis work. Michael will become a new TEAL mentored scholar as he applies his work now to OC studies.

Michael has taken the work all the way from the bench to the bedside as defined later below. He has addressed the issue, in work now in press (**Topper et al, Cell, 2017**), of how can we improve

a combinatorial, epigenetic therapy paradigm, employing a DNA methyltransferase inhibitor (DNMTi- Azacitidine-AZA), and histone deacetylase inhibitors (HDACi's) for determining whether this can improve the efficacy of immune checkpoint therapy. Although we have already been engaged in trials for this concept for NSCLC and OC, we needed to deeply re-visit what we need to understand about the interaction between the DNMTi, and the HDACi's to optimize our approaches.

We reasoned that a key goal, not yet optimally addressed is how we can, in a patient tolerated manner, develop regimens which placed more chronic pressure on reversing abnormalities of HDAC activity which are central to how abnormal DNA methylation represses gene expression. A very detailed series of initial studies explored which HDAC family members needed to be targeted, and defined the best drugs for this purpose in terms of their known in-vivo half lives in patients and known Ki's for inhibiting the key HDAC's. A chronic administration schema of 5 days of low dose the DNMTi AZA, followed by selected of the above HDACi's was determined to be very well tolerated by mice for up to 3 months or more. A major finding in human NSCLC cells, and in two treatment mouse models of NSCLC, is that there is an Aza induced CMYC driven sensitization to HDACi, which significantly increases the efficacy of these agents when deployed both in vitro and in vivo. This reduced MYC expression and of the entire MYC target signaling pathway potentiates combination epigenetic treatment induced cytostasis, immune gene augmentation and activation of the viral defense pathway in Fig. 1, and robustly reduces both tumor burden and progression in two mouse models of NSCLC. Coupled with this observed therapeutic efficacy, there is increased tumor attraction of activated CD8, T-cells and depletion of immune tolerance inducing, M2 macrophages. Up-regulation of the key, T-cell attracting cytokine, CCL5 is produced in human NSCLC cells, and in the mouse models CCL5 protein is increased in bronchial lavages from the mice. Very importantly, there is a therapy induced skewing of CD8 lymphocytes from an exhausted to a memory, effector phenotype. Thus, these data serve to provide a new treatment schema and suggest that reducing basal levels of MYC and MYC signaling activity by epigenetic treatment may have implications in determining the magnitude and duration of response to immune checkpoint therapy (**results summarized in the graphic for the in press, Cell paper – Fig. 2**).

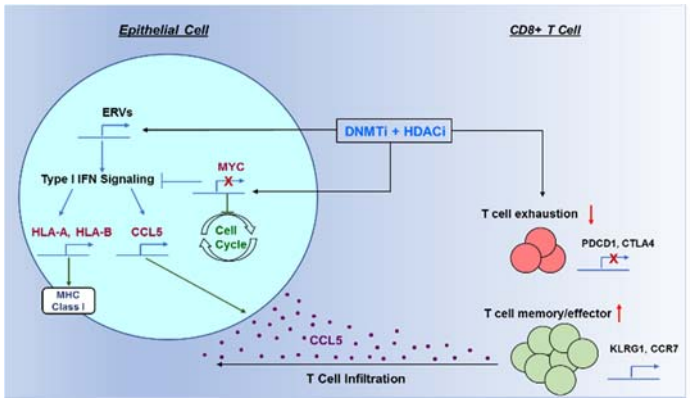

Fig.2. Summary of data in the graphic for our in press paper (Topper et al Cell, 2017). The DNMTi plus HDACi treatment for two mouse models of NSCLC results in up-regulation of ERV's and type 1 interferon signaling to result in increased antigen pentation, upregulation of the cytokine, CCL5 accompanying T-cell attraction to tumors, and reversion of T-cell exhaustion to a cell effector state (up-regulation of genes like KLRG1 and CCR7 as shown). A key step is concomitant down-regulation of CMYC signaling which enhances reversion of tumor immune evasion.

2. *Extrapolating the above, newly derived epigenetic treatment schema to deeply study the syngeneic mouse model for OC described in our last progress report*. Again, the work has involved great participation from our mentored post-doctoral fellow, Dr. Chiappinelli and a graduate student, Meredith Stone. The model is the MOSE mouse model of serous OC and we have now completed a body of work which is now in press (**Stone et al, PNAS, 2017**). In this model, as we have previously outlined, the mice receive tumor cells intraperitoneally and develop ascites in a manner similar to what can occur in patients with advanced OC. This model is known to be poorly immunogenic giving us the opportunity to determine whether our new

epigenetic therapy strategies can alter this scenario and sensitize to immune checkpoint therapy in so doing. The following important data, all in the above in press paper, have emerged:

a) *Treatment model*. The new treatment schema used for all the in vivo studies in the paper is shown in Fig**. 1A**. The selection of the best HDACi employed, Givinostat (ITF) was based on the results from all the studies outlined in Section B1 above.

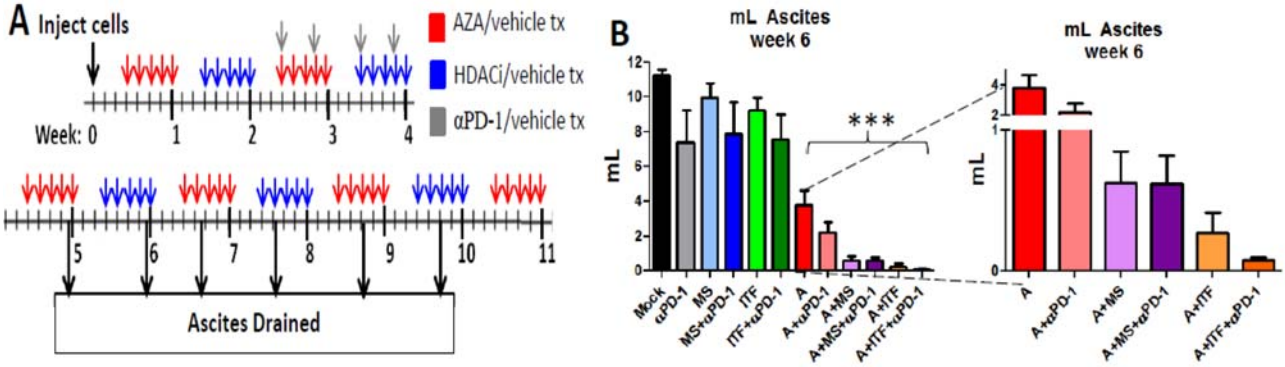

Fig. 2. A. Treatment schema with AZA given each day at 0.5mg/kg and the HDACi's at 0.2 mg/kg with and without anti-PD1. B. Ascites accumulation at 6 weeks. Note the marked blunting with AZA (A) alone and AZA plus especially the HDACi's (ITF and MS) and especially with all 3 drugs.

b) *Summary of results and treatment efficacy*.

All of the work introduced last year, in the now in press paper for OC. It reveals that, in our mouse OC model our newly derived combined epigenetic therapy regimen results in increases in tumor signaling for attraction of activated T-cells and provides for anti-tumor effects as monitored by burden of abdominal ascites **(Fig. 2B)**. This all correlates with prolongation of survival which is further lengthened by addition of the immune checkpoint therapy antibody, anti-PD1 **(Fig. 3)**. These data also provide evidence, as for the NSCLC work in Section B1 above, that our above drug effects substantially rely upon the induced up-regulation of ERV transcripts, viral defense genes, and interferon signaling outlined in Fig. 1 as a major stimulus for the host immune cell attraction to ascites in our model. In this regard, a key new addition to

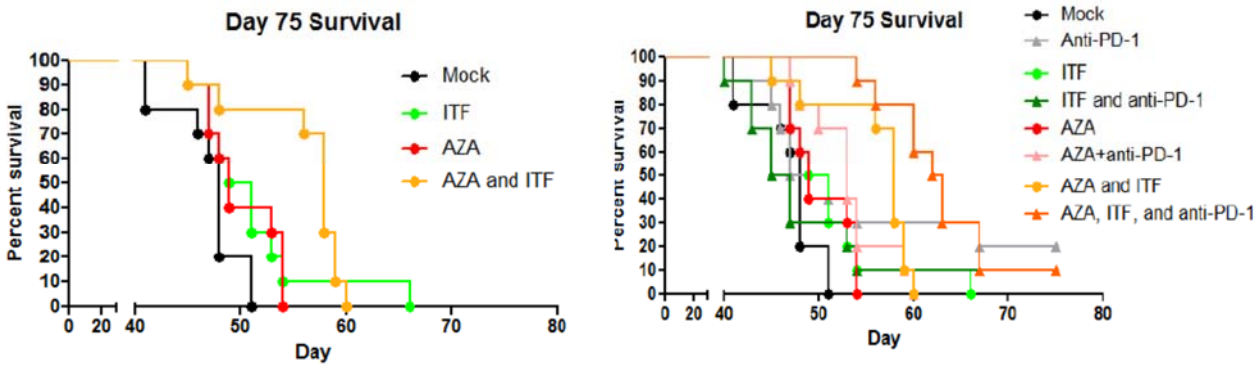

Fig. 3. Effects of in-vivo treatment with the schema in Fig. 4A of AZA and/or entinostat (MS275) and givinostat (ITF) on survival of the mice (left panel) and with the addition of anti-PD-1 treatement (right panel). The color codes for the treatments is shown to the right in the right panel. Sacrifice is always based on mouse discomfort from ascites accumulation. Note that AZA + the HDACi, ITF (orange line), significantly improves survival over the other drugs alone (left panel). Note that the addition of anti-PD-1 to AZA + ITF (dark orange line), provides even further survival advantage (right panel).

this fact, derived during the past year and included in the paper is testing of the hypothesis that a key step in the above drug induced viral defense signaling for T-cell attraction to tumor is obligatory interaction of induced interferon alpha, beta and its interaction with its receptor, α-IFNAR1. While this interaction has been implied to be critical for epigenetic therapy induced tumor signaling for immune cell attraction, it had never been formally proven.

In the in press paper, we now show that the AZA mediated reduction in ascites volume routinely observed in our experiments was inhibited by treatment with in-vivo administration to mice of anti-IFNAR1 (**Figure 4A,B**) and overall survival is decreased (**Figure 4C**). Furthermore, total numbers of CD45+ cells in the ascites were not increased as with the AZA treatment alone, but remained near mock values (**Figure 4D**). Likewise, activation of CD8+ T effector cells and natural killer (NK) cells in response to AZA treatment was also completely blocked and rescued by anti-IFNAR1 (**Figure 4E, F**). Previous in vitro studies have demonstrated that upregulation of a dsRNA sensing pathway by AZA triggers the activation of an intact Type I interferon signaling pathway requiring the interferon alpha and beta receptor subunit 1 (11, 16), and the use of α-IFNAR1 prevented the AZA induced increase in expression normally observed for anti-viral genes, such as ISG15, IFIT1 and ICAM1 in vitro. Our α-IFNAR1 data are the first to indicate that the type I interferon response is, indeed, required for effective in vivo anti-tumorigenic actions of 5-Azacytidine, including reduced tumor burden, extended survival, and increased numbers and activation of immune cells.

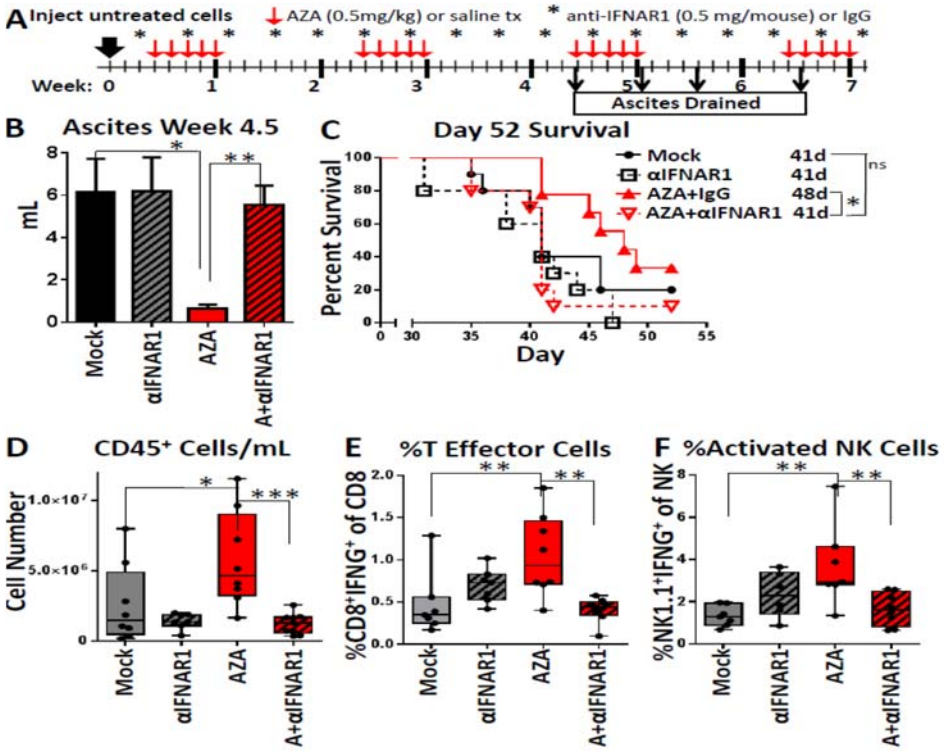

Figure 4: Blockade of IFNAR1 inhibits the actions of AZA. A) Treatment schematic for the 768 mice. Mice were treated with AZA (0.5mg/kg) or saline as described in Figure 3. Anti-IFNAR1 769 was injected i.p. (0.5 mg/mouse) every three days, beginning one day before the AZA regimen. B) Volume of ascites drained from the mice at week 4.5. Mean+SEM is shown and significances are determined by Mann-Whitney T-test. n=8-10 mice per group. C) Survival of the mice in 772 days, with median survival shown. Significances are determined by log rank (Mantel Cox) test. 773 n=10 mice per group. D-F) Median, 25th and 75th percentiles, and range are plotted, and significances are determined by Mann-Whitney T-test. n=6-9 mice per group. D) CD45+ cells/mL of ascites. E) %T effector cells (CD8+IFNγ+) of CD3+ T cells. F) % activated NK cells 776 (NK1.1+, IFNγ+) of NK1.1+ cells.

C. Summary of progress for Specific Aim 3 and majors tasks 1 and 2: As outlined in the sections above, our progress has been extensive in the past year in further understanding how use of epigenetic drugs which inhibit DNA methylation (AZA) and inhibit histone deactylases (HDACi) may be used to increase the efficacy of immune checkpoint therapy in patients with OC. Our new strategy to augment the effects of AZA alone by combining this drug with a deeply researched plan for chronic administration of low dose HDACi's has now been extensively explored over the past years as outlined in Figs. 2-6. Importantly, this includes fully taking this therapy strategy to in vivo treatment to our mouse MOSE OC model and in combination with

immune checkpoint therapy. All of this now shows that the combined epigenetic therapies increase tumor signaling for attraction of activated T-cells and provide for anti-tumor effects with prolongation of survival. These data provide substrate for our honing this treatment regimen further during the next year, and our continuing to explore the implications of all of these studies towards the present leveraged clinical trial for patients with advanced OC and for designing future trials.

D. Specific Aim 4: *Develop new combinations of epigenetic drugs which may provide for the highest level of efficacy for management of OC*: **Major Task 1:** *Follow biochemical hypotheses for designing combinations of the epigenetic drugs used in all studies above with new agents targeting additional steps in chromatin control of gene expression – the goal is to improve reversal of abnormal gene silencing in OC*: These studies, under the direction of Dr. Peter Jones at the Van andel Research Institute (VARI), with close collaboration from Dr. Baylin has made continued progress during the past year. We are moving towards a first paper on this work which will describe the effects of adding a specific inhibitor of the histone methyltransferase, G9A, UNC0638, to the DNMTi, AZA. G9a adds the transcriptionally repressive mark, histone 3, lysine 9, di methyl (H3K9me2) to chromatin and the enzyme interacts with the major enzyme which maintains abnormal DNA methylation in cancer, DNMT1. The Baylin lab has shown in the past that G9a, and the H3K9me2 mark is tightly tied to the start sites of genes affected by abnormal DNA methylation in cancer. This mark, and G9A, leave these genes when the abnormal methylation is reversed by AZA, the key drug being used in our studies of OC in the previous sections and in the now ongoing clinical trial.

Overall, in assessing gene expression levels in TCGA primary cancer samples, G9a is overexpressed compared to multiple normal samples and levels are highest in OC. By RNA-seq analyses, with pathway determinations, the G9a inhibitor (G9ai), UNC0638 added to AZA, synergistically enhances the viral defense signaling (Fig.1) effects induced by AZA in three cancer cell lines (**Fig. 5**).

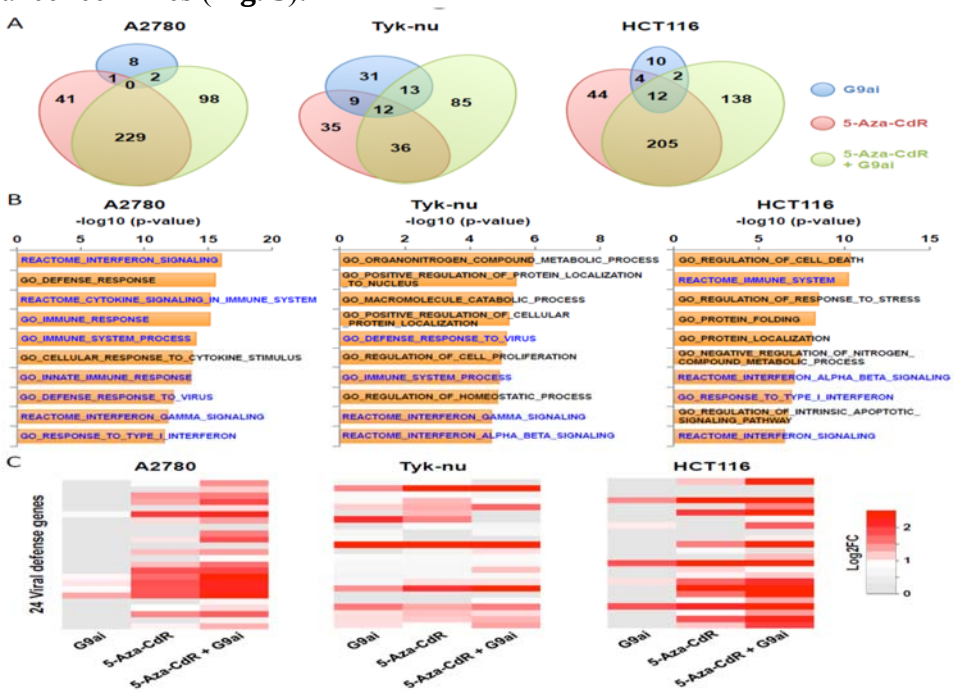

Fig. 5 In RNA-seq data, protein coding genes are upregulated by combined AZA +G9ai treatment with the genes largely overlapping with those overlapped with those up regulated by AZA treatment alone (panel A). Immune pathways are prominent among those upregulated most by the combination (panel B) and compared to AZA treatment alone, the combination treatment further up regulated viral defense genes in all three cell lines (panel C).

With this above increased viral defense signaling, in the two OC lines and the HCT116 colon cancer cells, the combination of drugs upregulates expression of ERV's over effects of AZA

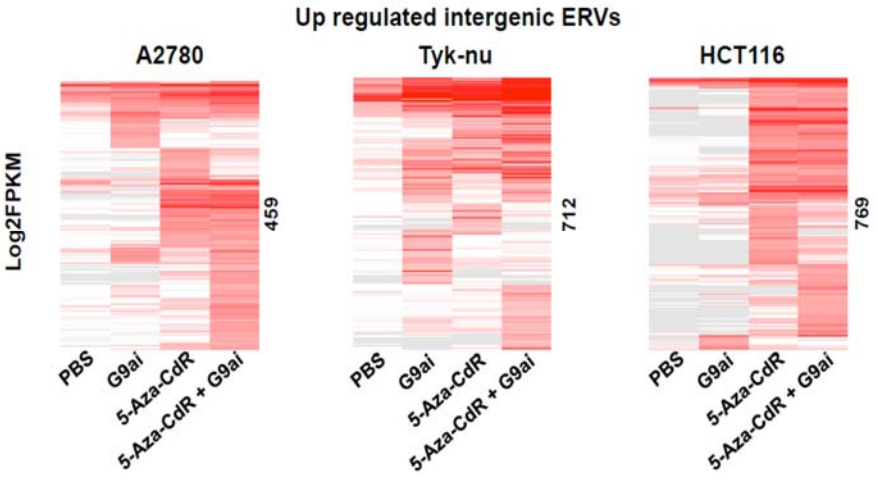

Fig. 6 Combination treatment of G9ai with 5-Aza upregulates ERV expression in A2780 and Tyknu OC cells, but not in HCT116 cells. Effects are greater than for aZA treatment alone and the G9i has little effects on its own.

alone and the G9ai drug has little effects on its own (**Fig. 6**). With the above effects on immune signaling, the G9ai also synergistically induced apoptosis and inhibited cell growth in A2780 and Tyknu OC cells, but not significantly in HCT116 colon cancer cells.

The mechanism for the gene expression effects of the combination treatment involves globally decreases the transcriptional repressive marks, H3K9 mono, di and tri methylation levels, and decreases the key mark, H3K9me2 levels directly at the long terminal repeat (LTR) regions of ERVs. This is also accompanied by increases in transcriptional active marks, H3K4me3 and H3K27ac at these loci after the combination treatment.

In summary, addition of an inhibitor of G9a to AZA suggest a potentially new epigenetic therapy combination which may serve as a novel therapeutic strategy for OC patients. We are continuing to define the mechanisms underlying the combined effects of the drugs. Importantly while the G9ai, UNC0638 works only at high, uM levels to specifically inhibit G9a, and is not soluble for in-vivo administration, we are now in a position to receive new drug from the company GBT. This G9ai works at nM doses to block G9a and can be given orally to mice with no toxic effects. We plan to pursue our combination strategies with this drug over the next year and, most critically to test its combination with AZA in pre-clinical therapy regimens with tumor bearing mice.

What opportunities for training and professional development did the project provide?

The first three years year of this grant have been exceptionally important as discussed in preceding sections in this regard. *Dr. Chiappinelli*, our mentored fellow trainee, has benefitted enormously from participation in all of the work outlined in the above sections and the work and become a real leader in these multiple projects. She is now a faculty member in the Cancer Center at George Washington University and pursuing her studies in OC. A graduate student, *Meredith Stone*, whose work is also outlined earlier has also benefitted tremendously from principally working with TEAL faculty investigator, Dr. Cindy Zahnow, on the MOSE mouse model and is the first author on the paper outlined above that is now in press for PNAS. She has just received a Ph.D. for her studies and is now a Postdoctoral Fellow at the University of Pennsylvania continuing to pursue work in OC. Finally, the work of graduate student, Michael Topper, a new mentee, has also been outlined in preceding sections. He has also just received his Ph.D. for his studies with Dr. Baylin based on the paper now in press for Cell.

How were the results disseminated to communities of interest?

As outlined last year, over the three years of studies, and outlined in multiple sections below, key studies during the first year were published in Cell (Chiappinelli et al, 2015) and have been

presented in several research forums for OC research including an AACR sub-meeting on OC and the general AACR meeting. In addition, during the second year Dr. Chiappinelli's work has been the subject of a requested review article (Chiappinelli et al, Cancer research, 2016) and also received an editorial in the New England Journal of Medicine (Dear AE. Epigenetic Modulators and the New Immunotherapies. NEJM 374(7):684-6, 2016). Finally, in the past year as outlined in this report in sections above, we have the paper by Topper et al now in press in Cell, as well as the paper by Stone et al now in press for PNAS (both included in Appendix).

What do you plan to do during the next reporting period to accomplish the goals and objectives?

During the next year we are hopeful to continue the same pace and volume of work as during this past one.

4. IMPACT

***What was the impact on the development of the principal discipline(s) of the project*?**

The work in the past year, as is hopefully apparent from the progress report, continues to bring the PI into work on the biology of serous OC and for developing new means to treat this disease. He is widely asked to lecture at national and international meetings specifically regarding the potential for epigenetic therapy to increase the efficacy of immune checkpoint therapy and for providing insight into the mechanisms that may be involved. As per sections above, the trainees and faculty involved with the TEAL have also been called upon for many lectures at OC specialty meetings and general cancer research meetings. Our great hope is that the new therapy regimens described earlier in this year's report can be brought into a clinical trial for OC including pairing with immune checkpoint therapy. We are now in discussions with Dr. Slamon to try and move this possibility forward.

***What was the impact on other disciplines*?**

Our studies of OC outlined in this third year Progress Report continue to have widespread impact as defined just above. The new combination regimen of AZA plus HDACi's, given with immune checkpoint therapy, as defined in the in press Cell and PNAS papers has just entered, as discussed earlier, a major trial for NSCLC. This will include an intense pre- and post-treatment battery of correlative science studies including much emphasis on testing potential predictive value for the viral defense related markers in tumor biopsies and also looking at effects on immune cells for the findings outlined in the above outlined pre-clinical work now in the in press Cell and PNAS papers. We are extremely hopeful that any positive results emerging in this trial over the next 6 to 12 months will help extrapolate this combined treatment paradigm to a trial for patients with serous OC.

***What was the impact on technology transfer*?**

As outlined in last year's report, and now augmented by the work over the past year, viral defense signature, inclusive of the ERV transcripts has a patent applied for status as a biomarker system to predict and monitor the efficacy of applying epigenetic therapy to sensitize patients with advanced OC and all cancer types, to immune checkpoint therapy. The work in the ongoing, leveraged OC trial with AZA plus immune checkpoint therapy, and the new trial for NSCLC will hopefully help Hopkins push forward the potential to license this biomarker signature.

***What was the impact on society beyond science and technology*?**

Hopefully, as outlined in our previous reports, the biggest impact of our studies will be for patients. As mentioned in the progress report, two trials are now testing our therapy paradigms for sensitizing to immune checkpoint therapy in patients with advanced OC and NSCLC. Hopefully, efficacies observed in these trials may provide the greatest impact we could seek for our work.

5. CHANGES/PROBLEMS

Changes in approach and reasons for change

At present, we do not anticipate any major changes to our work scope and directions. We will continue to focus on Specific Aims 3 and 4 and trying to maximize our epigenetic therapies for OC. We will also pursue the new work with the G9ai to develop in-vivo pre-clinical studies during the coming year as defined in Specific Aim 4.

Actual or anticipated problems or delays and actions or plans to resolve them

None anticipated at this time. We have been moving at a rapid pace during the past year and hope to continue this.

Changes that had a significant impact on expenditures

None anticipated at this time.

Significant changes in use or care of human subjects, vertebrate animals, biohazards, and/or select agents

None anticipated at this time.

6. PRODUCTS

Publications, conference papers and presentations

Publications

Stone ML, Chiappinelli KB, Li H, Murphy LM, Travers ME, Topper M, Mathios D, Lim M, Shih I-M, Wang T-L, Hung C-F, Bhargava V, Wiehagen KR, Cowley GS, Bachman KE, Strick R, Strisse PL, Baylin SB, Zahnow CA. Epigenetic therapy activates type I interferon signaling in murine ovarian cancer to reduce immunosuppression and tumor burden. In Press PNAS, 2017.

Topper MJ, Vaz M, Chiappinelli KB, DeStefano Shields C, Wenzel A, Hicks J, Ballew M, Stone M, Tran PT, Zahnow CA, Hellmann MD, Strissel PL, Strick R, Baylin SB. A combination epigenetic therapy ties blocking MYC to reversing immune evasion and treating lung cancer. In Press Cell, 2017.

Presentations

Stephen B. Baylin, M.D.
2017 SU2C Summit – Santa Monica CA
2017 AACR Annual Meeting – Washington DC

University of California San Diego – San Diego CA
Baylor College of Medicine – Waco TX
Gordon Research Conference – Tuscany Italy
George Washington University – Washington DC
Institute of Molecular Biology - Mainz Germany
2nd European Cancer Epigenetics Conference 2017 – Heidelberg Germany
VARI Summer Retreat – Grand Rapids, MI
8th Mildred Scheel Cancer Conference - Bonn Germany
2017 TRIST Symposium - Northwestern University – Chicago IL
Ludwig Oxford 10th Anniversary Symposium – Oxford London
6th Annual Mayo Clinic Individualizing Medicine Conference – Rochester MN
Translational Genomics and Epigenomics Symposium - Roswell Park Cancer Institute- Buffalo NY
AbbVie Celebration of Science – Chicago IL

Cynthia A. Zahnow, Ph.D.
Baylor College of Medicine - Houston TX
Fels Institute for Cancer Research and Molecular Biology - Temple University - Philadelphia PA
Biology Research Seminar Series, Baylor University - Waco TX
In Vivo Cellular & Molecular Imaging Center, Division of Radiology, Johns Hopkins School of Medicine - Baltimore MD

Website(s) or other Internet site(s)

Nothing to report

Technologies or techniques

Nothing to report

Inventions, patent applications, and/or licenses

Nothing to report

Other Products

Nothing to report

7. PARTICIPANTS & OTHER COLLABORATING ORGANIZATIONS

Individuals who have worked on the project

Johns Hopkins University

Name:	Stephen B. Baylin, M.D.
Project Role:	PI (Senior/Key Personnel)
Research Identifier:	N/A
Nearest person month worked:	4
Contribution to Project:	Dr. Baylin oversees all studies and activities conducted under this proposal.
Funding Support:	See Other Support

Name:	Cynthia Zahnow, Ph.D.
Project Role:	Co-Investigator (Senior/Key Personnel)
Research Identifier:	N/A
Nearest person month worked:	2
Contribution to Project:	Dr. Zahnow collaborates with Dr. Baylin on all of the studies in the lab.
Funding Support:	See Other Support

Name:	Drew Pardoll, M.D., Ph.D.
Project Role:	Co-Investigator (Senior/Key Personnel)
Research Identifier:	N/A
Nearest person month worked:	1
Contribution to Project:	Dr. Pardoll works with the Baylin group for all of the studies on how epigenetic therapy can sensitize ovarian cancers to immune checkpoint therapy.
Funding Support:	See Other Support

Name:	Ray-Whay Yen
Project Role:	Research Associate
Research Identifier:	N/A
Nearest person month worked:	8
Contribution to Project:	Ms. Yen is responsible for working with the entire Hopkins group for all of the pre-clinical work on ovarian cancer.
Funding Support:	No change

Name:	Katherine Chiappinelli, Ph.D.
Project Role:	Postdoctoral Fellow / Teal Junior Scientist
Research Identifier:	N/A
Nearest person month worked:	0 (salary is covered by F32 CA183214)
Contribution to Project:	Dr. Chiappinelli has become a real leader in multiple projects as per her accomplishments discussed extensively in the sections above. Her academic growth is discussed in detail in Section 8, Special Reporting.
Funding Support:	Dr. Chiappinelli termed from JHU on 12/31/16. She is now an Assistant Professor at George Washington University Cancer Center

Name:	Meredith Stone
Project Role:	Graduate Student
Research Identifier:	N/A
Nearest person month worked:	6
Contribution to Project:	Ms. Stone works along with Dr. Zahnow.
Funding Support:	Meredith received her Ph.D. in March '17. She termed from JHU on 6/30/17 to pursue a Postdoc position at the University of Pennsylvania.

Has there been a change in the active other support of the PD/PI(s) or senior/key personnel since the last reporting period?

Yes. See next pages for Drs. Baylin, Zahnow and Pardoll's Other Support.

OTHER SUPPORT

BAYLIN, STEPHEN B.

CURRENT

P30 CA006973 (PI: Nelson)
Title: Regional Oncology Research Center – Senior Leader
Time Commitment: 0.6 calendar
Supporting Agency: NIH/NCI
Procuring Contracting/Grants Officer: Devi Vembu
Address of Grants Officer: National Cancer Institute, Building 6116-700, 6116 Executive Blvd, Rockville, MD 20852
Performance Period: 5/7/1997-4/30/2022
Level of Funding: $12,529 (salary support only)
Project's Goal(s): CORE grant for the Johns Hopkins Oncology Center. Stephen Baylin receives salary support only for leadership and microarray core responsibilities.
Specific Aims: N/A
Project Overlap or Parallel: No scientific or budgetary overlap.

R01 ES011858 (PI: Baylin)
Title: DNA Methyltransferase Gene Expression in Colon Cancer
Time Commitment: 1.44 calendar
Supporting Agency: NIH/NIEHS
Procuring Contracting/Grants Officer: Frederick Tyson
Address of Grants Officer: National Institute of Health, Keystone Park 3064, 615 Davis Dr, Durham, NC 27709
Performance Period: 4/1/1991-5/31/2019
Level of Funding: $270,498
Project's Goal(s): Understand, further, the role of altered regulation and patterns of DNA methylation in the progression of colon cancer.
Specific Aims: 1. To determine mechanisms by which SOX17 blocks Wnt activation in CRC evolution. 2. To develop mouse models for CRC evolution based on epigenetic loss of Hic1. 3. To explore specific stages of CRC tumorigenesis mediated by epigenetic silencing of stem/progenitor cell related genes. 4. To define molecular determinants which initiate and/or maintain gene promoter DNA hypermethylation and gene silencing in CRC evolution.
Project Overlap or Parallel: No scientific or budgetary overlap.

90046519 (PI: Baylin/Casero/Zahnow)
Title: Novel Therapies Targeting Epigenetic Silencing of Tumor Suppressors
Time Commitment: 0.12 calendar
Supporting Agency: Samuel Waxman Cancer Research Foundation
Procuring Contracting/Grants Officer: Carole Asher
Address of Grants Officer: 420 Lexington Ave., Suite 825, New York, NY 10170
Performance Period: 7/1/2011-6/30/2019
Level of Funding: $45,000
Project's Goal(s): The goals of this project are: Project 1: To examine newly identified lysine specific demethylase 1 (LSD1) inhibitors in order to advance the understanding of the functioning and targeting of LSD1 for clinical utility. Project 2: To show that epigenetic therapy at very low, non-toxic doses, can dramatically blunt the tumorigenic properties of subpopulations of leukemic and solid tumor populations of "stem-like" cells. Project 3: To demonstrate that low dose epigenetic therapy re-

sensitizes drug tolerant breast cancer cells to conventional, single agent chemotherapeutics or targeted therapy.
Specific Aims: 1. To perform, in Kasumi AML cells, and other lines, genome-wide studies of DNA methylation, chromatin and, gene expression patterns, including pathway analyses, for activating and repressive marks in separated populations of tumorigenic CD34+/CD38- versus non-tumorigenic CD34- cells. 2. To examine changes in the above genome-wide patterns induced by low doses of DNA demethylating and histone deacetylation inhibiting drugs, already shown to inhibit the leukemic engraftment of the whole cell population, alone and together, on the above separated populations. 3. To derive markers for prediction and monitoring of epigenetic therapy from the above studies and which can be studied in primary tumor samples, and patient samples.
Project Overlap or Parallel: No scientific or budgetary overlap.

90075114 (PI: Baylin)
Title: Bringing Epigenetic Therapy to the Management of Ovarian and Other Cancers
Time Commitment: 1.8 calendar
Supporting Agency: Miriam & Sheldon Adelson Medical Research Foundation
Procuring Contracting/Grants Officer: Joseph Bigley
Address of Grants Officer: OncoMethylome Sciences, 2505 Meridian Parkway, Suite 310, Durham, NC 27713
Performance Period: 10/1/2014-9/30/2019
Level of Funding: $467,420
Project's Goal(s): We are embarked on in-depth pre-clinical studies designed to directly bring "epigenetic" therapy, using existing DNA de-methylating agents and histone deactylase inhibitors (HDACi's), to the therapeutic management of advanced ovarian and other cancers.
Specific Aims: N/A
Project Overlap or Parallel: While both of these projects are aimed at taking novel approaches to radically improving the management of women with ovarian cancer, and can inform one another, they fund separate activities vital to this quest. First, while both grants seek to use information to leverage key clinical trials for ovarian cancer, only the Adelson supports activities for implementation of these trials, the bulk of biopsy acquisitions, and any other partial trial costs not otherwise covered. Second, many aspects for studies of host immune cell responses to epigenetic drugs are covered only in the Adelson funding, including work and support of collaborators, and genomics studies, in this effort, while the TEAL funds primarily work for response of ovarian cancer cells. Third, Only the TEAL award supports the efforts of the junior investigator mentored by Dr. Baylin to dissect how increased expression of endogenous viruses induced by epigenetic agents elicit up-regulation of ovarian cancer cell viral defense pathways. Lastly, only the Adelson supports work to use epigenetic agents to sensitize ovarian cancer to PARP inhibitors and work, with other collaborators for bring novel epigenetic therapy agents to treatment of ovarian cancer. However, this information can all be brought to bear on work in the TEAL in later years of the grant if indicated.

W81XWH-13-1-0199 (PI: Chan/Baylin)
Title: Targeting Master Regulators of the Breast Cancer Metastasis Transcriptome
Time Commitment: 0.24 calendar
Supporting Agency: Memorial Sloan-Kettering Cancer Center
Procuring Contracting/Grants Officer: Unknown
Address of Grants Officer: Unknown
Performance Period: 7/1/2013-6/30/2018
Level of Funding: $61,555
Project's Goal(s): The Baylin lab will help perform CHIP seq and help analyze the chromatin state data for both the isogenic cell line systems that model differential metastatic ability.
Specific Aims: Aim 1: N/A
Justification: This grant has no overlap with the current proposal.

Project Overlap or Parallel: No scientific or budgetary overlap.

W81XWH-14-1-0385 (Baylin)
Title: A New Paradigm for the Treatment of Ovarian Cancer: The Use of Epigenetic Therapy to Sensitize Patients to Immunotherapy and Chemotherapy
Effort: 4.2 calendar
Supporting Agency: CDMRP
Name of Procuring Contracting/Grants Officer: Susan Dellinger, Grants Officer
Address of Funding Agency: 1077 Patchel St., Bldg 1077, Fort Detrick, MD 21702
Period of Performance: 09/30/2014-09/29/2019
Level of Funding: $501,318 annual direct costs
Project's Goal: The major goal of this project is to robustly prolong the survival of patients with serous ovarian cancer (OC) through introducing epigenetic therapy paradigms
Specific Aims: 1) To uncover the mechanisms through which epigenetic therapy may, alone, achieve robust, durable responses in patients with advanced ovarian cancer (OC) 2) Study how epigenetic therapy may sensitize OC cells to subsequent chemotherapies 3) Study how epigenetic therapy may sensitize OC cells to subsequent immunotherapies which targets checkpoints which are driving immune tolerance 4) Develop new combinations of epigenetic drugs which may provide for the highest level of efficacy for management of OC 5) Bring all of the above studies to bear on leveraging clinical trials of epigenetic therapy on OC
Role: PI
Overlap: None

R01 CA185357 (PI: Ahuja)
Title: (PQD3) Molecular Profiles associated with Long-Term Survival in pancreas Cancer
Time Commitment: 0.24 calendar
Supporting Agency: NCI
Procuring Contracting/Grants Officer: Unknown
Address of Grants Officer: Unknown
Performance Period: 6/1/2014-5/30/2018
Level of Funding: $303,066
Project's Goal(s): Identify genomic and epigenomic signatures of pancreas cancer patients who have long-term survival using a large dataset.
Specific Aims: N/A
Project Overlap or Parallel: No scientific or budgetary overlap.

(PI: Baylin)
Title: Clinical trials of epigenetic therapy sensitized patients with advanced non-small cell lung cancer to chemotherapy and immunotherapy
Time Commitment: 0.12 calendar
Supporting Agency: AACR – Jim Toth Sr. Breakthrough Prize in Lung Cancer
Procuring Contracting/Grants Officer: Unknown
Address of Grants Officer: Unknown
Performance Period: 7/1/2014-6/30/2018
Level of Funding: $340,380
Project's Goal(s): N/A
Specific Aims: N/A
Project Overlap or Parallel: No scientific or budgetary overlap.

(PI: Baylin)
Title: Clinical trials of epigenetic therapy in non-small cell lung cancer
Time Commitment: 0.3 calendar

Supporting Agency: Rising Tide Foundation
Procuring Contracting/Grants Officer: Unknown
Address of Grants Officer: Unknown
Performance Period: 1/1/2015-12/31/2018
Level of Funding: $331,360
Project's Goal(s): We are addressing the hypothesis that reversal of cancer-specific DNA methylation and chromatin abnormalities can potently change the management of NSCLC.
Specific Aims: N/A
Project Overlap or Parallel: No scientific or budgetary overlap.

R01 HD082098 (PI: Zambidis)
Title: Functional vascular progenitors from naïve human iPSC
Time Commitment: 0.24 calendar
Supporting Agency: Natl Ins of Child Health & Human
Procuring Contracting/Grants Officer: Unknown
Address of Grants Officer: Unknown
Performance Period: 5/1/2015-2/29/2020
Level of Funding: $186,750
Project's Goal(s): To develop novel gene targeting and regeneration approaches for treating pediatric and adult vascular disorders using a newly discovered class of human iPSC converted to a ground state of naïve pluripotency.
Specific Aims: N/A
Project Overlap or Parallel: No scientific or budgetary overlap.

(PI: Baylin)
Title: VARI-SU2C Epigenetics Dream Team
Time Commitment: 0.12 calendar
Supporting Agency: Van Andel Research Institute
Procuring Contracting/Grants Officer: Unknown
Address of Grants Officer: Unknown
Performance Period: 10/1/2014-9/30/2018
Level of Funding: $50,000
Project's Goal(s): Our Dream Team unites scientists at major cancer research institutions who are poised to propel the early promise of epigenetic therapy in blood malignancies to the forefront of management for patients with breast, colon and lung cancer.
Specific Aims: N/A
Project Overlap or Parallel: No scientific or budgetary overlap.

AWARDED SINCE LAST SUBMISSION

90061810 (PI: Yegnasubramanian)
Title: Enhancing Prostate Cancer Immunotherapy Through Epigenetic Reprogramming
Time Commitment: 0.6 calendar
Supporting Agency: Prostate Cancer Foundation
Procuring Contracting/Grants Officer: Unknown
Address of Grants Officer: Unknown
Performance Period: 12/24/14-12/24/17
Level of Funding: $210,000
Project's Goal(s): The main goal of this project is to test the hypothesis that epigenetic therapy plus immunotherapy can be effective in the control of advanced prostate cancer.
Specific Aims: N/A
Project Overlap or Parallel: No scientific or budgetary overlap.

90067293 (PI: Baylin)
Title: Understanding the mechanisms underlying how epigenetic therapy may sensitize patients with multiple human cancer types to immune checkpoint therapy
Time Commitment: 0.36 calendar
Supporting Agency: Janssen Research & Development LLC
Procuring Contracting/Grants Officer: Unknown
Address of Grants Officer: Unknown
Performance Period: 2/26/2016-2/25/2018
Level of Funding: $145,110
Project's Goal(s): A collaboration between Janssen Res & Dev and The Cancer Center at Johns Hopkins to study mechanisms underlying how epigenetic therapy may sensitize patients with multiple human cancer types to immune checkpoint therapy.
Specific Aims: N/A
Project Overlap or Parallel: No scientific or budgetary overlap.

(PI: Baylin)
Title: Developing a lab model for lung cancer initiation, risk and prevention
Time Commitment: 0.36 calendar
Supporting Agency: Am Lung Association
Procuring Contracting/Grants Officer: Unknown
Address of Grants Officer: Unknown
Performance Period: 7/1/2017-6/30/2018
Level of Funding: $100,000
Project's Goal(s): Our preliminary data and proposed studies for this proposal aim to use a new approach to study, in human lung epithelial cells *in-vitro*, the consequences of chronic exposure to low doses of cigarette smoke extract (CSC).
Specific Aims: N/A
Project Overlap or Parallel: No scientific or budgetary overlap.

R21 CA212495 (PI: Easwaran)
Title: High-efficiency microfluidic-assisted single-cell DNA methylome sequencing
Time Commitment: 0.24 calendar
Supporting Agency: NCI
Procuring Contracting/Grants Officer: Unknown
Address of Grants Officer: Unknown
Performance Period: 8/3/2017-7/30/2020
Level of Funding: $100,000
Project's Goal(s): The goal of this project is to devise a novel methodology for high-efficiency multiplexed profiling of DNA methylation in single cells by bisulfite sequencing.
Specific Aims: N/A
Project Overlap or Parallel: No scientific or budgetary overlap.

90075113 (PI: Velculescu)
Title: Ovarian Cancer Genome Analysis Platform
Time Commitment: 0.36 calendar
Supporting Agency: Miriam & Sheldon Adelson Medical Research Foundation
Procuring Contracting/Grants Officer: Joseph Bigley
Address of Grants Officer: OncoMethylome Sciences, 2505 Meridian Parkway, Suite 310, Durham, NC 27713
Performance Period: 10/1/2017-9/30/2019
Level of Funding: $1,630,366

Project's Goal(s):
Specific Aims: N/A
Project Overlap or Parallel: No scientific or budgetary overlap.

COMPLETED SINCE LAST SUBMISSION

U01 HL099775 (PI: Friedman)
Title: Basic and Translational Research of iPSC-Based Hematologic & Vascular Therapies – Project 2
Time Commitment: 0.46 calendar
Supporting Agency: NIH/NHLBI
Procuring Contracting/Grants Officer: Denis Buxton
Address of Grants Officer: NHLBI, Two Rockledge Center, Suite 8216, 6701 Rockledge Dr., Bethesda, MD 20817
Performance Period: 9/30/2009-4/30/2017
Level of Funding: $245,000
Project's Goal(s): This work will provide basic insight into how stem cells can be generated from adult cells and how these cells can be directed to develop into blood cells or blood vessel cells to benefit patients with hematologic or vascular disorders.
Specific Aims: 1. Precisely characterize the degree of cellular transformation observed at early stages of iPSC generation that are caused by reprogramming factor-mediated epigenetic changes, and the role that various factors, and protocols for introducing these factors, play in eliciting these alterations. 2. Determine the molecular mechanisms that induce abnormal epigenetic events during iPSC generation. 3. Determine whether refining use of DAC and TSA during iPSC generation, together with manipulation of DNMTs or other members of the repressive complex, can increase the efficiency of obtaining iPSC, while maximally reducing their tumorigenic potential and enhancing their regeneration potential.
Project Overlap or Parallel: No scientific or budgetary overlap.

R01 CA170550 (PI: Laird/Jones)
Title: Epigenetic Drivers of Cancer
Time Commitment: 0.6 calendar
Supporting Agency: University of Southern California
Procuring Grants Officer: Emily Greenspan
Address of Grants Officer: 31 Center Drive, Room 10A-33, Bethesda, MD 20892
Performance Period: 9/1/2012-6/30/2016
Level of Funding: $130,119
Project Goals: We propose to address PQ10: As we improve methods to identify epigenetic changes that occur during tumor development, can we develop approaches to discriminate between "driver" and "passenger" epigenetic events?
Specific Aims: 1. To develop a probabilistic framework for predicting and prioritizing candidate epigenetic driver loci. 2. To select candidate epigenetic drivers of colon, breast, and lung cancer. 3. To functionally test candidate epigenetic drivers of colon, breast, and lung cancer.
Project Overlap or Parallel: No scientific or budgetary overlap.

(PI: Baylin)
Title: The intersection of epigenetic and immune checkpoint therapy
Time Commitment: 0.12 calendar
Supporting Agency: AACR – Phillip A. Sharp Innovation in Collaboration Award
Procuring Contracting/Grants Officer: Unknown
Address of Grants Officer: Unknown
Performance Period: 7/1/2014-12/31/2015 (NCE)
Level of Funding: $227,275

Project's Goal(s): Utilize results from all studies to help craft leveraged clinical trials for lung, melanoma and other cancers which are based on hypotheses derived from the data.
Specific Aims: N/A
Project Overlap or Parallel: No scientific or budgetary overlap.

P50 CA058184 (PI: Baylin)
Title: SPORE in Lung Cancer (Project 1)
Time Commitment: 0.36 calendar
Supporting Agency: NIH/NCI
Procuring Contracting/Grants Officer: Peter Ujhazy
Address of Grants Officer: National Cancer Institute, Building 6116, 6116 Executive Blvd, Rockville, MD 20852
Performance Period: 9/5/1997-11/30/2015
Level of Funding: $242,211 (NCE)
Project's Goal(s): This project involves DNA methylation changes in cancer concerned with their translational implications for lung neoplasms.
Specific Aims: 1. To determine if novel biomarkers added to the current gene panel can enhance the predictive index, for tumor recurrence and death, of a DNA hypermethylation marker system for re-staging of stage I NSCLC. 2. To validate prospectively our findings that changes in promoter DNA methylation can molecularly restage stage I to stage III lung NSCLC and predict early disease recurrence and death. 3. To determine in a prospective controlled clinical trial of stage I NSCLC cancer patients, whether adjuvant epigenetic therapy improves overall and disease-free survival.
Project Overlap or Parallel: No scientific or budgetary overlap.

P50 CA058184 (PI: Baylin)
Title: SPORE in Lung Cancer (Administrative Core)
Time Commitment: 0.36 calendar
Supporting Agency: NIH/NCI
Procuring Contracting/Grants Officer: Peter Ujhazy
Address of Grants Officer: National Cancer Institute, Bldg. 6116-7109, 6116 Executive Blvd, Rockville, MD 20852
Performance Period: 9/5/1997-11/30/2015
Level of Funding: $80,250 (NCE)
Project's Goal(s): This project involves DNA methylation changes in cancer concerned with their translational implications for lung neoplasms.
Specific Aims: N/A
Project Overlap or Parallel: No scientific or budgetary overlap.

OTHER SUPPORT

ZAHNOW, CYNTHIA A.

ACTIVE

90046519 (PI: Casero/Baylin/Zahnow)
Title: Novel therapies targeting epigenetic silencing of tumor suppressors
Time Commitment: .12 calendar
Supporting Agency: Samuel Waxman Cancer Research Foundation
Procuring Contracting/Grants Officer: Carole Asher
Address of Grants Officer: 420 Lexington Ave., Suite 825, New York, NY 10170
Performance Period: 7/1/2011-6/30/2019
Level of Funding: $45,000
Project's Goal(s): The goals of Dr. Zahnow's project within this Collaborative Grant is to demonstrate that low dose epigenetic therapy re-sensitizes drug tolerant breast cancer cells to conventional, single agent chemotherapeutics or targeted therapy.
Specific Aims: 1. To test whether Azacytidine can sensitize endocrine-resistant breast cancers to anti-estrogen therapy. 2. To continue our investigation of the role of the immune system in the anti-tumorigenic response of breast cancer cells to epigenetic therapy with a special focus on interferon signaling and activation. **Justification:** This grant has no overlap with the current proposal.
Project Overlap or Parallel: No scientific or budgetary overlap.

P30 CA006973 (PI: Nelson)
Title: Regional Oncology Research Center – Resource Director
Time Commitment: 3.6 calendar
Supporting Agency: NIH/NCI
Procuring Contracting/Grants Officer: Devi Vembu
Address of Grants Officer: National Cancer Institute, Building 6116-700, 6116 Executive Blvd, Rockville, MD 20852
Performance Period: 5/7/1997-4/30/2022
Level of Funding: $154,400 (salary support only)
Project's Goal(s): CORE grant for the Johns Hopkins Oncology Center. Dr. Zahnow receives salary support only for serving as the Director of the Animal Facility and administrative duties to the Oncology Center.
Specific Aims: N/A
Justification: This grant has no overlap with the current proposal.
Project Overlap or Parallel: No scientific or budgetary overlap.

Award ID: W81XWH-14-1-0385(Baylin)
Title: A New Paradigm for the Treatment of Ovarian Cancer: The Use of Epigenetic Therapy to Sensitize Patients to Immunotherapy and Chemotherapy
Effort: 1.8 calendar
Supporting Agency: CDMRP
Name of Procuring Contracting/Grants Officer: Susan Dellinger, Grants Officer
Address of Funding Agency: 1077 Patchel St., Bldg 1077, Fort Detrick, MD 21702
Period of Performance: 09/30/2014-09/29/2019
Level of Funding: $501,318 annual direct costs
Project's Goal: The major goal of this project is to robustly prolong the survival of patients with serous ovarian cancer (OC) through introducing epigenetic therapy paradigms
Specific Aims: 1) To uncover the mechanisms through which epigenetic therapy may, alone, achieve robust, durable responses in patients with advanced ovarian cancer (OC), 2) Study

how epigenetic therapy may sensitize OC cells to subsequent chemotherapies, 3) Study how epigenetic therapy may sensitize OC cells to subsequent immunotherapies which targets checkpoints which are driving immune tolerance, 4) Develop new combinations of epigenetic drugs which may provide for the highest level of efficacy for management of OC, 5) Bring all of the above studies to bear on leveraging clinical trials of epigenetic therapy on OC.
Role: PI
Overlap: None

90075114 (PI: Baylin)
Title: Bringing Epigenetic Therapy to the Management of Ovarian and Other Cancers
Time Commitment: 3 calendar
Supporting Agency: Miriam & Sheldon Adelson Medical Research Foundation
Procuring Contracting/Grants Officer: Marissa White
Address of Grants Officer: 300 First Avenue, Suite 330, Needham, MA 02494
Performance Period: 10/01/2014-9/30/2019
Level of Funding: $467,420
Project Goals: We are embarked on in-depth pre-clinical studies designed to directly bring "epigenetic" therapy, using existing DNA de-methylating agents and histone deactylase inhibitors (HDACi's), to the therapeutic management of advanced ovarian and other cancers.
Specific Aims: N/A
Justification: This grant has no overlap with the current proposal.
Project Overlap or Parallel: While both of these projects are aimed at taking novel approaches to radically improving the management of women with ovarian cancer, and can inform one another, they fund separate activities vital to this quest. First, while both grants seek to use information to leverage key clinical trials for ovarian cancer, only the Adelson supports activities for implementation of these trials, the bulk of biopsy acquisitions, and any other partial trial costs not otherwise covered. Second, many aspects for studies of host immune cell responses to epigenetic drugs are covered only in the Adelson funding, including work and support of collaborators, and genomics studies, in this effort, while the TEAL funds primarily work for response of ovarian cancer cells. Third, Only the TEAL award supports the efforts of the junior investigator mentored by Dr. Baylin to dissect how increased expression of endogenous viruses induced by epigenetic agents elicit up-regulation of ovarian cancer cell viral defense pathways. Lastly, only the Adelson supports work to use epigenetic agents to sensitize ovarian cancer to PARP inhibitors and work, with other collaborators for bring novel epigenetic therapy agents to treatment of ovarian cancer. However, this information can all be brought to bear on work in the TEAL in later years of the grant if indicated.

(PI: Baylin)
Title: Clinical trials of epigenetic therapy in non-small cell lung cancer
Time Commitment: 0.3 calendar
Supporting Agency: Rising Tide Foundation
Procuring Contracting/Grants Officer: Unknown
Address of Grants Officer: Unknown
Performance Period: 1/1/2015-12/31/2018
Level of Funding: $331,360
Project's Goal(s): We are addressing the hypothesis that reversal of cancer-specific DNA methylation and chromatin abnormalities can potently change the management of NSCLC.
Specific Aims: N/A
Project Overlap or Parallel: No scientific or budgetary overlap.

AWARDED SINCE LAST SUBMISSION

R01 CA184165 (PI: Pandey)

Title: Personalized Therapy of Hormone Refractory Breast Cancer
Time Commitment: 0.6 calendar
Supporting Agency: NIH/NCI
Procuring Contracting/Grants Officer: Unknown
Address of Grants Officer: Unknown
Performance Period: 4/1/2015-3/31/2020
Level of Funding: $228,750
Project's Goal(s): Unknown
Specific Aims: N/A
Project Overlap or Parallel: No scientific or budgetary overlap.

90067293 (PI: Baylin)
Title: Understanding the mechanisms underlying how epigenetic therapy may sensitize patients with multiple human cancer types to immune checkpoint therapy
Time Commitment: 1.2 calendar
Supporting Agency: Janssen Research & Development LLC
Procuring Contracting/Grants Officer: Unknown
Address of Grants Officer: Unknown
Performance Period: 2/26/2016-2/25/2018
Level of Funding: $145,110
Project's Goal(s): A collaboration between Janssen Res & Dev and The Cancer Center at Johns Hopkins to study mechanisms underlying how epigenetic therapy may sensitize patients with multiple human cancer types to immune checkpoint therapy.
Specific Aims: N/A
Project Overlap or Parallel: No scientific or budgetary overlap.

R01 CA204555 (PI: Sharma)
Title: Evaluation of molecular determinants of racial disparity in triple-negative breast cancer
Time Commitment: 0.48 calendar
Supporting Agency: NIH/NCI
Procuring Contracting/Grants Officer: Unknown
Address of Grants Officer: Unknown
Performance Period: 4/1/2017-3/31/2022
Level of Funding: $250,000
Project's Goal(s): Our studies focus on examining the key molecules involved in racial disparity in triple negative breast cancer focusing on the role and importance of loss of tumor suppressor genes and resulting 'oncogene addiction' in triple negative breast cancer growth and progression.
Specific Aims: N/A
Project Overlap or Parallel: No scientific or budgetary overlap.

(PI: Shih)
Title: Development of Targeted Therapies for Recurrent Ovarian Cancer
Time Commitment: 0.6 calendar
Supporting Agency: Ovarian Cancer Research Fund
Procuring Contracting/Grants Officer: Unknown
Address of Grants Officer: Unknown
Performance Period: 1/1/2017-12/31/2019
Level of Funding: $272,727
Project's Goal(s): Unknown
Specific Aims: N/A
Project Overlap or Parallel: No scientific or budgetary overlap.

COMPLETED SINCE LAST SUBMISSION

R01 CA170550 (PI: Laird/Jones)
Title: Epigenetic Drivers of Cancer
Time Commitment: 1.2 calendar

Supporting Agency: University of Southern California
Procuring Contracting/Grants Officer: Emily Greenspan
Address of Grants Officer: 31 Center Dr., Rm. 10A-33, Bethesda, MD 20892
Performance Period: 9/01/2012-6/30/2016
Level of Funding: $130,119
Project Goals: We propose to address PQ10: As we improve methods to identify epigenetic changes that occur during tumor development, can we develop approaches to discriminate between "driver" and "passenger" epigenetic events?
Specific Aims: 1) To develop a probabilistic framework for predicting and prioritizing candidate epigenetic driver loci 2) To select candidate epigenetic drivers of colon, breast, and lung cancer. 3) To functionally test candidate epigenetic drivers of colon, breast, and lung cancer.
Justification: This grant has no overlap with the current proposal.
Project Overlap or Parallel: No scientific or budgetary overlap.

(PI: Baylin)
Title: The intersection of epigenetic and immune checkpoint therapy
Time Commitment: 0.6 calendar
Supporting Agency: AACR – Phillip A. Sharp Innovation in Collaboration Award
Procuring Contracting/Grants Officer: Unknown
Address of Grants Officer: Unknown
Performance Period: 7/1/2014-12/31/2015
Level of Funding: $227,275
Project's Goal(s): Utilize results from all studies to help craft leveraged clinical trials for lung, melanoma and other cancers which are based on hypotheses derived from the data.
Specific Aims: N/A
Project Overlap or Parallel: No scientific or budgetary overlap.

(PI: Brahmer/Baylin)
Title: Viral Defense Gene Expression Patterns and Response to Immune Checkpoint Blockade in NSCLC
Time Commitment: 1.2 calendar
Supporting Agency: Bristol-Myers Squibb
Procuring Contracting/Grants Officer: Unknown
Address of Grants Officer: Unknown
Performance Period: 7/1/2015-8/13/2017
Level of Funding: $62,447
Project's Goal(s): This project seeks to develop a biomarker to predict benefit from immunotherapy and to define if epigenetic modulation synergizes with immune checkpoint blockade.
Specific Aims: N/A
Project Overlap or Parallel: No scientific or budgetary overlap.

OTHER SUPPORT

PARDOLL, DREW M.

ACTIVE

Award ID: P50CA098252 (Wu)
Title: SPORE in Cervical Cancer
Effort: 0.24 calendar months
Supporting Agency: NIH/NCI
Name of Procuring Contracting/Grants Officer: Jason Gill
Address of Funding Agency: 9609 Medical Center Drive, Rockville, MD 20850
Performance Period: 09/01/04 – 08/31/19
Level of Funding: $1,702,596 annual direct costs
Project's Goal: The development research program role is to identify and select pilot projects with potential for development into full- fledged translational research avenues, collaborations, and new methodologies for integration into other research projects based on the described review criteria.
Specific Aims: 1) Provide initiating funds for novel explorations related to cervical cancer. 2) Integrate the awardee into the SPORE community by participation in monthly meetings, group communications, and opportunities for expanded funding and for collaborations. 3) Review progress and recommend avenues for continuation of successful projects
Role: Co- Director, Developmental Research Program
Overlap: None

Award ID: P30CA06973 (Nelson)
Title: Regional Oncology Research
Center
Effort: 0.6 calendar months
Supporting Agency: NIH/NCI
Name of Procuring Contracting/Grants Officer: Jason Gill
Address of funding agency: 9609 Medical Center Drive, Rockville, MD 20850
Performance Period: 08/09/2012-04/30/2022
Level of Funding: $12,529 annual direct costs (*salary support only)
Project's Goal: The major goal of this project is to support research programs and shared resources at the National Cancer Institute Designated Cancer Center. The central goal of the Cancer Immunology program is the development of new effective cancer immunotherapies that are based on understanding the molecular recognition and regulation.
Specific Aims: N/A
Role: Co-Program Leader for Cancer Immunology
Overlap: None

Award ID: 308121 (Vogelstein)
Title: Mutational Density and Response to Immunotherapy with Checkpoint Blockade
Effort: 1.2 Calendar months
Supporting Agency: Melanoma Research Alliance
Name of Procuring Contracting/Grants Officer: Laura Brockway-Lunardi, Ph.D.
Address of Funding Agency: 1101 New York Avenue, Suite 620, Washington, DC 20005
Period of Performance: 05/15/2014-05/14/2017
Level of Funding: $300,000 annual direct costs
Projects Goal: The goal of this project is to lay the groundwork for a biomarker to predict response to anti-PD-1 antibodies and also for the generation of personalized melanoma vaccines that could be used in combination with anti-PD-1 therapy.

Specific Aims: 1.) Determine whether overall mutational load in melanoma correlates with PD-1 ligand (PD-L1 and PD-L2) expression and clinical response to anti-PD-1 treatment. 2.) Using algorithms for HLA binding, proteasome processing and TAP transport, determine whether predicted mutation-derived neoepitopes correlate with PD-1 ligand expression and clinical response to anti-PD-1 treatment and 3.) In selected cases, analyze T cell responses to predicted *neoepitopes* from peripheral blood lymphocytes and compare them with responses to epitopes from index *shared* melanosomal and cancer-testes antigens.
Role: Co-investigator
Overlap: None

Award ID: N/A (Pardoll)
Title: Analysis of novel immunomodulatory ligands and receptors
Effort: .6 calendar months
Supporting Agency: Compugen Ltd.
Name of Procuring Contracting/Grants Officer: Anat Cohen-Dayag, Ph.D
Address of Funding Agency: 72 Pichas Rosen St., Tel Aviv 69512, Israel
Period of Performance: 01/01/2015-06/30/2019
Level of Funding: $203,488 annual direct costs
Project's Goal: The major goal of this project is to study the immunobiology and cancer immunotherapy relevance of multiple novel gene products identified as potentially immunomodulatory
Specific Aims: 1) Determine in-house phage display vs conventional hybridoma depending on level of conservation of molecule across species. 2) Expression studies in mice and humans-define target's expression tumor components of the TME, sorted cell populations, purified tumor infiltrates, myeloid and lymphocyte human-on selected targets. 3) In vitro testing of murine and human antibodies and Fc fusion molecules 4)Antibody/Recombinant Fc fusion experiments with emphasis on antibodies 5) Therapeutic synergy experiments
Role: PI
Overlap: None

Award ID: W81XWH-14-1-0385(Baylin)
Title: A New Paradigm for the Treatment of Ovarian Cancer: The Use of Epigenetic Therapy to Sensitize Patients to Immunotherapy and Chemotherapy
Effort: .36 cal months
Supporting Agency: CDMRP
Name of Procuring Contracting/Grants Officer: Susan Dellinger, Grants Officer
Address of Funding Agency: 1077 Patchel St., Bldg 1077, Fort Detrick, MD 21702
Period of Performance: 09/30/2014-09/29/2019
Level of Funding: $435,304 annual direct costs
Project's Goal: The major goal of this project is to robustly prolong the survival of patients with serous ovarian cancer (OC) through introducing epigenetic therapy paradigms
Specific Aims: 1) To uncover the mechanisms through which epigenetic therapy may, alone, achieve robust, durable responses in patients with advanced ovarian cancer (OC) 2) Study how epigenetic therapy may sensitize OC cells to subsequent chemotherapies 3) Study how epigenetic therapy may sensitize OC cells to subsequent immunotherapies which targets checkpoints which are driving immune tolerance 4) Develop new combinations of epigenetic drugs which may provide for the highest level of efficacy for management of OC
5) Bring all of the above studies to bear on leveraging clinical trials of epigenetic therapy on OC
Role: Co-Investigator
Overlap: None

Award ID: 90062513 (Pardoll)
Title: The role of neuritin/sema4 interactions to promote expansion and persistence of Tregs
Effort: 1.2 calendar Months
Supporting Agency: Potenza Therapeutics, Inc
Name of Procuring Contracting/Grants Officer: Daniel J. Hicklin, PhD
Address of Funding Agency: 1030 Massachusetts Avenue, Suite 210, Cambridge, MA 02138
Performance Period: 04/01/2015-03/31/2017
Level of Funding: $348,837 annual direct costs
Project goal: The major goal of this project is to further delineate the role of the neuritin/sema4 interaction in promoting the expansion and persistence of Tregs
Specific Aims: 1) Generate panel of monoclonal antibodies with high affinity for neuritin. 2) Define in vitro and in vivo activity of these antibodies, particularly regarding Treg maintenance and function. Benchmark against Neutitin KO. 3) Define in vitro and in vivo activity of peptides that block Neuritin- Seama4A/D interaction and recombinant Neuritin protein. 4) Confirming and mapping the interaction between neuritin and semaphoring 4D. 5) Generate and screen for blocking antibodies which disrupt the neuritin/sema4D interaction. 6) Examine the expression of neuritin on Tregs in human peripheral blood and tumor infiltrating leukocytes. 7) Pharmacology studies to examine the activity of mAbs targeting the neuritin/sema4 interaction in several murine models of cancer (alone or in combination with other immunotherapies)
Role: PI
Overlap: None

Award ID: 305021 (Topalian)
Title: Crossroads of Genetic and Immunologic Heterogeneity of Melanoma Metastasis
Effort: .24 calendar months* effort, no salary
Supporting Agency: Melanoma Research Alliance
Name of Procuring Contracting/Grants Officer: Laura Brockway-Lunardi, Ph.D.
Address of Funding Agency: 1101 New York Avenue, Suite 620, Washington, DC 20005
Period of Performance: 05/15/2014-05/14/2017
Level of Funding: $75,000 annual direct costs
Project's Goal: The major goal of this project is to characterize interactions between heterogeneous genetic and immunological factors in melanoma, by studying primary and metastatic tumors obtained through a rapid autopsy program
Specific Aims: 1) Establish a rapid autopsy biospecimen bank of primary and metastatic melanoma lesions from 8-10 patients. 2) Characterize genetic features of tumor clonal evolution through space (anatomic location) and time (primary lesion to metastasis). 3) Explore the immunological heterogeneity of metastasis. 4) Correlate genetic and immunological signatures in order to understand factors driving tumor-induced immunosuppression and progression
Role: Co-Investigator
Overlap: None

Award ID: N/A (Pardoll)
Title: The role of neuritin/sema4 interactions to promote expansion and persistence of Tregs
Effort: 1.2 cal months
Supporting Agency: Potenza Therapeutics
Name of Procuring Contracting/Grants Officer: Daniel J. Hicklin, PhD
Address of Funding Agency: 1030 Massachusetts Avenue, Suite 210, Cambridge, MA 02138
Period of Performance: 04/01/2015-03/31/2017
Level of Funding: $348,837 annual direct costs
Project's Goal: The major goal of this project is to further delineate the role of the neuritin/sema4 interaction in promoting the expansion and persistence of Tregs

Specific Aims: 1) Generate panel of monoclonal antibodies with high affinity for neuritin 2) Define in vitro and in vivo activity of these antibodies, particularly regarding Treg maintenance and function. Benchmark against Neutitin KO. 3) Define in vitro and in vivo activity of peptides that block Neuritin- Seama4A/D interaction and recombinant Neuritin protein. 4) Confirming and mapping the interaction between neuritin and semaphoring 4D. 5) Generate and screen for blocking antibodies which disrupt the neuritin/sema4D interaction. 6) Examine the expression of neuritin on Tregs in human peripheral blood and tumor infiltrating leukocytes. 7) Pharmacology studies to examine the activity of mAbs targeting the neuritin/sema4 interaction in several murine models of cancer (alone or in combination with other immunotherapies)
Role: PI
Overlap: None

AWARDED SINCE LAST SUBMISSION

Award ID: CA-209-358 (Topalian)
Title: Analysis of PD-1 Blockade in Virus-Associated Cancers on CA-209-358
Effort: .12 Calendar months
Supporting Agency: Bristol Myers Squibb Co
Name of Procuring Contracting/Grants Officer: Les Enterline
Address of Funding Agency: Route 206 and Providence Line Road, Princeton, NJ 08543
Period of Performance: 07/01/2016-12/31/2018
Level of Funding: $203,524 annual direct costs
Projects Goal: The goal of this project is to characterize changes in the tumor immune microenvironment in pre/post therapy biopsies from patients with advanced virus-associated cancers receiving anti-PD-1 therapy on clinical trial CA209-358, in order to understand response and resistance to therapy.
Specific Aims: N/A
Role: PI
Overlap: None

Award ID: R01CA142779-06A1 (Pardoll/Topalian/Taube)
Title: B7-H1/PD1 modulation in cancer therapy
Effort: .96 Calendar months
Supporting Agency: NIH/NCI
Name of Procuring Contracting/Grants Officer: Jacquelyn Saval
Address of Grants Officer: 9609 Medical Center Drive, Rockville, MD 20850
Period of Performance: 12/01/2015-11/30/2020
Level of Funding: $271,296 annual direct costs
Project's Goal: The major goals of this multi-PI project are to define mechanisms regulating the expression of B7-H1 (PD-L1) by tumor cells and PD-1 by tumor-specific T cells, and to explore the molecular and immunological mechanisms contributing to the clinical effects of B7-H1/PD-1 blockade in therapeutic trials for patients with advanced metastatic cancers
Specific Aims: 1) Define mechanisms regulating PD-L1 expression by tumor cells and other cell types in the tumor microenvironment 2) Characterize factors influencing PD-1 expression by T cells. 3) Characterize immunological mechanisms underlying the clinical effects of PD-L1/PD-1 blockade in cancer therapy, including the co-expression of multiple checkpoint pathways that might provide resistance pathways to therapy
Overlap: None
Role: MPI (Contact PI)

Award ID: N/A (Pardoll)
Title: The Johns Hopkins University Bloomberg-Kimmel Institute for Cancer Immunology

Effort: 2.88 calendar months
Supporting agency: Bloomberg Philanthropies
Procuring Contracting/Grants Officer: Patricia Harris
Address of Grants Officer: 25 E. 78th St, New York, NY 10075
Performance period: 01/01/2016-12/31/2020
Level of funding: $10,000,000 annual direct costs
Project's Goal(s): The goal of the Institute is to develop, within 10 years, immunotherapies that can place 50% of people with inoperable cancer into lifelong remission.
Specific Aims: N/A
Role: Institute Director
Overlap: None

Award ID: N/A (Brahmer)
Title: Stand Up To Cancer-American Cancer Society Lung Cancer Translational Research Dream Team Grant: Targeting KRAS Mutant Lung Cancers
Effort: .6 calendar months
Supporting Agency: Mass General Hospital (AACR Prime)
Name of Procuring Contracting/Grants Officer: Ashley Gleason, Manager, Partners Research Management
Address of Grants Officer: 101 Huntington Ave, Suite 200 Boston, MA 02199
Period of Performance: 08/01/2015-07/31/2018
Level of Funding: $391,875 annual direct costs
Project's Goal: As part of the Stand up to Cancer-American Society lung Cancer Translational Research Dream Team, efforts will focus on implementing advances in lung cancer research as rapidly as possibly through the creation of a collaborative, translational, cancer research "Dream Team**".**
Specific Aims: N/A
Role: Co-Investigator
Overlap: None

Award ID: N/A (Bollinger)
Title: miLab
Effort: .6 calendar months
Supporting agency: MiDiagnostics
Procuring Contracting/Grants Officer: 3001 Leuven, Kapeldreef 75, Belgium
Address of Grants Officer: Luc Van den Hove
Performance period: 06/01/2015-09/30/018
Level of funding: 6,205,635 annual direct costs
Project's Goal(s): miLab is an *in-vitro* diagnostic system that integrates a complete clinical laboratory process including sample prep and bio-sensing capability on a single disposable chip-set. The platform will bring diagnostic tests to the point of need and to the point of care fundamentally changing the way we manage our health in the future.
Specific Aims: N/A
Role: Management Board Participant
Overlap: None

Award ID: BMSC1259 (Pardoll)
Title: Strategic Research Collaboration Agreement
Effort: 2.88 calendar months
Supporting agency: Bristol Myers Squibb
Procuring Contracting/Grants Officer: Fouad Namoun
Address of Grants Officer: 345 Park Avenue, New York, New York 10154

Performance period: 01/01/2017-12/31/2022
Level of funding: $3,141,044 annual direct costs
Project's Goal(s): This overarching contract funds multiple immunotherapy research projects and clinical trials in an effort to determine the IO agents or combination treatments incorporating IO agents that provide the optimal benefit risk ratio for cancer populations and subpopulations.(when applicable)
Specific Aims: N/A
Role: PI
Overlap: None

Award ID: CA209-596(Lim)
Title: ABTC: A Phase I Trial of Anti-LAG-3 or Anti-CD137 Alone and in Combination with Anti-PD-1 in Patients with Recurrent GBM (ABTC 1501)
Effort: .02 calendar months
Supporting agency: Bristol Myers Squibb
Procuring Contracting/Grants Officer: Fouad Namoun
Address of Grants Officer: 345 Park Avenue, New York, New York 10154
Performance period: 04/29/2016-05/01/2020
Level of funding: $488,373 annual direct costs
Project's Goal(s): The major goal of this project is assaying and analyzing the correlatives of CA209-596/ABTC1501 study.
Specific Aims: N/A
Role: Co-Investigator
Overlap: None

Award ID: N/A (Lim)
Title: Pre-Immunization During Delta24-RGD Therapy in Intracranial Gliomas
Effort: .24 calendar months
Supporting agency: DNATrix
Procuring Contracting/Grants Officer:
Address of Grants Officer: 2450 Holcombe Blvd Suite X+200 Houston, Texas 77021
Performance period: 08/02/2017-07/31/2018
Level of funding: $85,684 annual direct costs
Project's Goal(s): See aims below
Specific Aims: 1.) To assess the optimal dosing strategy of Delta24-RGD therapy in GL261 gliomas (*pilot experiment*). 2.) To assess the anti-tumor effect of pre-immunization during Delta24-RGD therapy in GL261 gliomas 3.) To characterize immune cells involved in pre-immunized mice with GL261 gliomas during Delta24-RGD therapy
Role: Co-Investigator
Overlap: None

Award ID: W81XWH-17-1-0627 (Elisseeff)
Title: Removal of trauma induced senescent cells as a new treatment for osteoarthritis
Effort: .24 calendar months
Supporting agency: US Department of Defense
Procuring Contracting/Grants Officer: TBD
Address of Grants Officer: Unknown
Performance period: 09/30/2017-09/29/2020
Level of funding: $392,845 annual direct costs
Project's Goal(s): The goal of this project is to answer the fundamental questions on how senescent cells induce OA after trauma (with implications also for age-related OA).

Specific Aims: 1.) Define the senescence and immunological profile of the articular joint after ACLT injury
2.) Determine the impact of senolytics and clearance of senescent cells on the immune profile and PTOA disease 3.) Develop and test controlled release senolytics in the PTOA murine model
Role: Co-Investigator
Overlap: None

COMPLETED SINCE LAST SUBMISSION

Award ID: 90054364 (Pardoll)
Title: International Immuno-Oncology Network (IION) Resource Model
Effort: 1.2 calendar months
Supporting Agency: Bristol- Myers Squibb Co
Name of Procuring Contracting/Grants Officer: Les Enterline
Address of Funding Agency: Route 206 and Providence Line Road, Princeton, NJ 08543
Period of Performance: 05/07/2013-05/06/2017
Level of Funding: $486,987 annual direct cost
Project's Goal: The major goals of this project are to dissect the tumor immune microenvironment in the context of therapy with immune checkpoint blockade and to monitor tumor burden using circulating tumor DNA (ctDNA)
Specific Aims: 1.) Analyze immune-inhibitory networks in resected tumors employing 3 techniques for geographic localization: (i) IHC, (ii) amplified ISH, and (iii) qRT-PCR analysis of laser capture micro-dissected (LCM) regions of leukocytic infiltration. 2.) Complementary to the studies in 1, we will sort myeloid, lymphoid and cancer cells from freshly dissociated tumors in cases where enough tumor is available, allowing analysis by flow cytometry and mRNA profiling of cellular subsets for co-expression of inhibitory ligands, receptors and druggable metabolic enzymes. 3.) Using qRT-PCR, amplified ISH and multiplex ELISA, we will analyze the spectrum of cytokines within the tumor microenvironment.
Role: PI
Overlap: None

Award ID: 273686 (Pardoll)
Title: CTLA-4 and anti-PD1 blockade: Correlative assessments for discovery
Effort: .36 calendar months
Supporting Agency: Bristol-Myers Squibb Co
Name of Procuring Contracting/Grants Officer: Les Enterline
Address of Funding Agency: Route 206 and Providence Line Road, Princeton, NJ 08543
Period of Performance: 07/10/2013-07/09/2016
Level of Funding: $125,000 annual direct costs
Projects Goal: The major goal of this project is to help guide optimal therapeutic combinations of co-inhibitory agents, to identify novel therapeutic Immune modulatory targets, and to predict, understand and overcome disease resistance.
Specific Aims: 1. Characterize changes in tumor infiltrating lymphocytes (TILs) and circulating peripheral blood cells from serially acquired tumor and blood samples from patients with therapeutic response to ipi, nivo and combination therapy with comparison to non-responders. 2. Characterize changes in metastatic melanoma cells, myeloid cells and tumor aSSOCiated fibroblasts from tumor samples from patients with therapeutic response 10 ipi, nivo and combination therapy with comparison to non-responders. 3. Compare finding from pre- and post-therapy specimens from patients treated with ipi and nivo as single agents vs combination therapy to identify unique potential biomarkers predictive of therapeutic response to combinatorial blockade.
Role: PI

Overlap: Overlaps with grant below. This is an Academic-Industry sponsored award with MRA being the prime sponsor and BMS being the industry sponsor. Each sponsor provides 50% support for the project.

Award ID: 273686
Title: CTLA-4 and anti-PD1 blockade: Correlative assessments for discovery
Effort: .36 calendar months
Supporting Agency: Memorial Sloan Kettering Cancer Center (Prime sponsor, Melanoma Research Alliance)
Name of Procuring Contracting/Grants Officer: Richard K. Naum
Address of Funding Agency: 1275 York Ave, New York, New York 10065
Performance Period: 07/10/2013-07/09/2016
Level of Funding: $125,000 annual direct costs
Project's Goal: The major goal of this project is to help guide optimal therapeutic combinations of co-inhibitory agents, to identify novel therapeutic Immune modulatory targets, and to predict, understand and overcome disease resistance
Specific Aims: 1. Characterize changes in tumor infiltrating lymphocytes (TILs) and circulating peripheral blood cells from serially acquired tumor and blood samples from patients with therapeutic response to ipi, nivo and combination therapy with comparison to non-responders. 2. Characterize changes in metastatic melanoma cells, myeloid cells and tumor aSSOCiated fibroblasts from tumor samples from patients with therapeutic response 10 ipi, nivo and combination therapy with comparison to non-responders. 3. Compare finding from pre- and post-therapy specimens from patients treated with ipi and nivo as single agents vs combination therapy to identify unique potential biomarkers predictive of therapeutic response to combinatorial blockade.
Role: PI
Overlap: Overlaps with grant above. This is an Academic-Industry sponsored award with MRA being the prime sponsor and BMS being the industry sponsor. Each sponsor provides 50% support for the project.

Award ID: SU2C-AACR-DT10
Title: Immunologic Checkpoint Blockade and Adoptive Cell Transfer in Cancer Therapy
Effort: 2.4 calendar months (20% effort, 10% salary support)
Supporting Agency: MD Anderson Cancer Center -Prime Sponsor-AACR (SU2C)
Name of Procuring Contracting/Grants Officer: Melinda Cotten
Address of Funding Agency: 1515 Holcombe Blvd, Houston, TX 77030-4000
Performance Period:3/1/2013-02/28/2016
Level of Funding: $468,182 annual direct cost
Project's Goal: The major goal of this project is to 1.) develop an increased understanding of immune cells and pathways within the tumor microenvironment that contribute to tumor resistance vs. rejection, 2.) identify the antigenic targets of both T and B cells response to checkpoint blockade, including unique neoantigens that arise as a result of missense mutations in the tumors and 3.) develop rationale combinatorial treatment regiments.
Specific Aims: Aim 1: Interrogation of the immune responses within the tumor microenvironment before and after treatment with immune checkpoint blockade. Aim 2: Interrogation of the targets of T and B cell responses after checkpoint blockade. Aim 3: Development of combinatorial cancer therapies based on checkpoint blockade.
Role: PI
Overlap: None

Award ID: N/A (Pardoll)
Title: CTLA-4 and anti-PD1 blockade: Correlative assessments for discovery

Effort: .12 calendar months
Supporting Agency: Bristol-Myers Squibb Co
Name of Procuring Contracting/Grants Officer: Les Enterline
Address of Funding Agency: Route 206 and Providence Line Road, Princeton, NJ 08543
Period of Performance: 07/10/2013-07/09/2016
Level of Funding: $125,000 annual direct costs
Projects Goal: The major goal of this project is to help guide optimal therapeutic combinations of co-inhibitory agents, to identify novel therapeutic Immune modulatory targets, and to predict, understand and overcome disease resistance.
Specific Aims: 1. Characterize changes in tumor infiltrating lymphocytes (TILs) and circulating peripheral blood cells from serially acquired tumor and blood samples from patients with therapeutic response to ipi, nivo and combination therapy with comparison to non-responders. 2. Characterize changes in metastatic melanoma cells, myeloid cells and tumor aSSOCiated fibroblasts from tumor samples from patients with therapeutic response 10 ipi, nivo and combination therapy with comparison to non-responders. 3. Compare finding from pre- and post-therapy specimens from patients treated with ipi and nivo as single agents vs combination therapy to identify unique potential biomarkers predictive of therapeutic response to combinatorial blockade.
Role: PI
Overlap: Overlaps with grant below. This is an Academic-Industry sponsored award with MRA being the prime sponsor and BMS being the industry sponsor. Each sponsor provides 50% support for the project.

Award ID: BMSC192 (Topalian/Pardoll)
Title: Analysis of PD-1 Blockade in Virus-Associated Cancers
Effort: .24 Calendar months
Supporting Agency: Bristol Myers Squibb Co
Name of Procuring Contracting/Grants Officer: Les Enterline
Address of Funding Agency: Route 206 and Providence Line Road, Princeton, NJ 08543
Period of Performance: 11/01/2014-10/31/2015
Level of Funding: $168,042 annual direct costs
Projects Goal: The major goal of this project is to characterize immune cell types and the expression of immune-modulating molecules (PD-1, PD-L1 and others) in the microenvironment of select cancers associated with EBV or HPV
Specific Aims: N/A
Role: PI
Overlap: None

Individuals who have worked on the project

The Regents of the University of California

Name:	Dennis Slamon, M.D., Ph.D.
Project Role:	PI (Senior/Key Personnel)
Research Identifier:	N/A
Nearest person month worked:	1
Contribution to Project:	Dr. Slamon contributes clinical, translational, and genomic expertise to the project and is involved in the overall direction.
Funding Support:	See Other Support

Name:	Judy Dering, Ph.D.
Project Role:	Sr Public Analyst
Research Identifier:	N/A
Nearest person month worked:	1
Contribution to Project:	Dr. Dering is responsible for analyzing data from the microarray experiments.
Funding Support:	No change

Has there been a change in the active other support of the PD/PI(s) or senior/key personnel since the last reporting period?

Yes. See next pages for Dr. Slamon's Other Support.

OTHER SUPPORT

SLAMON, DENNIS

CURRENT

P30 CA016042 (PI: Dorskind)
Title: "Cancer Support Grant"
Time Commitment: 1.80 calendar
Supporting Agency: NIH/NCI
Procuring Contracting/Grants Officer: Amy Connolly, Grant Management Specialist
Address of Grants Officer: National Cancer Institute, Room 700, Mail Stop 8335
6116 Executive Blvd, Bethesda, MD 20852-8335
Performance Period: 4/23/2003-11/30/2017
Level of Funding: $57,825
Project's Goal(s): This Funding supports activities to increase scientific interaction among members of the Signal Transduction Program Area at Jonsson Cancer Center.
Specific Aims: N/A
Project Overlap or Parallel: No scientific or budgetary overlap.

A5481023 (PI: Slamon)
Tittle: Multicenter, Randomized, Double-Blind, Placebo-Controlled, Phase 3 Trial of Fulvestrant (Faslodex®) With or Without PD-0332991 (Palbociclib) ± Goserelin in Women with Hormone Receptor-Positive, HER2-Negative Metastatic Breast Cancer Whose Disease Progressed After Prior Endocrine Therapy.
Time Commitment: 0.12
Supporting Agency: Pfizer
Procuring Contracting/Grants Officer: Soo Y. Bang
Address of Grants Officer: Address of Contract officer: 235 E. 42nd Street, MS 685/13/1,
New York, New York 10017
Performance Period: 11/26/13-11/26/17
Level of Funding: 345,811
Project's Goal(s): is to demonstrate the superiority of palbociclib in combination with fulvestrant (with or without goserelin) over fulvestrant alone (with or without goserelin) in prolonging investigator-assessed PFS in women with HR+/HER2-negative metastatic breast cancer whose disease has progressed on prior endocrine therapy.
Specific Aims: N/A
Project Overlap or Parallel: No scientific or budgetary overlap.

CIRM DR3-07067 (PI: Slamon)
Title: "A Phase I dose escalation and expansion clinical trial of the novel first-in-class Polo-like Kinase 4 (PLK4) inhibitor, CFI-400945 in patients with advanced solid tumors"
Time Commitment: 3.60 calendar
Supporting Agency: California Institute for Regenerative Medicine
Procuring Contracting/Grants Officer: Doug Kearney, Grants Management Office
Address of Grants Officer: California Institute for Regenerative Medicine, 210 King Street
San Francisco, CA 94107
Performance Period: 05/01/2014-04/30/2018
Level of Funding: $8,469,697
Project's Goal(s): This proposal is aimed at a phase I clinical trial of CFI-400945, a first-in-class inhibitor of Polo-like Kinase 4 (PLK4). PLK4, a serine/threonine kinase functions at the intersection

Procuring Contracting/Grants Officer: Soo Y. Bang
Address of Grants Officer: Address of Contract officer: 235 E. 42nd Street, MS 685/13/1, New York, New York 10017
Performance Period: 11/26/13-11/26/17
Level of Funding: 345,811
Project's Goal(s): is to demonstrate the superiority of palbociclib in combination with fulvestrant (with or without goserelin) over fulvestrant alone (with or without goserelin) in prolonging investigator-assessed PFS in women with HR+/HER2-negative metastatic breast cancer whose disease has progressed on prior endocrine therapy.
Specific Aims: N/A
Project Overlap or Parallel: No scientific or budgetary overlap.

CIRM DR3-07067 (PI: Slamon)
Title: "A Phase I dose escalation and expansion clinical trial of the novel first-in-class Polo-like Kinase 4 (PLK4) inhibitor, CFI-400945 in patients with advanced solid tumors"
Time Commitment: 3.60 calendar
Supporting Agency: California Institute for Regenerative Medicine
Procuring Contracting/Grants Officer: Doug Kearney, Grants Management Office
Address of Grants Officer: California Institute for Regenerative Medicine, 210 King Street San Francisco, CA 94107
Performance Period: 03/01/2014-2/28/2017
Level of Funding: $8,469,697
Project's Goal(s): This proposal is aimed at a phase I clinical trial of CFI-400945, a first-in-class inhibitor of Polo-like Kinase 4 (PLK4). PLK4, a serine/threonine kinase functions at the intersection of mitosis, DNA repair, hypoxia and metabolism, and is expressed in a variety of solid tumors. Overexpression of PLK4 results in the excessive formation of centrioles and multinucleation in cells suggesting that the elevated expression of PLK4 in tumors could contribute to chromosomal instability (CIN) and aneuploidy. Of interest, PLK4 overexpression in neural stem cells drives centrosome amplification and is associated with tumor formation. Conversely, depletion of PLK4 in cancer cells by RNA interference prevents centriole duplication, causing mitotic defects and cell death. Notably, these effects are amplified in hypoxic conditions. Thus, PLK4 is an attractive target for the development of small-molecule therapeutics in cancer. The candidate molecule, CFI-400945 was developed as part of a collaborative effort funded by CIRM/CSCC (PIs: Dennis Slamon and Tak Mak) that supported a drug discovery effort, preclinical assessment, and IND enabling studies.
Specific Aims: This clinical trial described herein will be carried out in two parts. Part A will consist of the dose escalation phase of the first-in-human trial, where the primary objective will be to determine the maximum tolerated dose (MTD) of CFI-400945. In Part A, patients with any solid tumor refractory to conventional treatment will be enrolled in order to reach the MTD expeditiously. Part B will consist of the expansion phase, where the primary objectives are to further refine the MTD to assist in determination of the recommended phase II dose (RP2D), to further assess plasma pharmacokinetics and to evaluate preliminary evidence of antitumor activity patient populations dosed at the MTD. Up to 4 expansion cohorts of 6-12 patients each would be enrolled which may include: 1) cohorts restricted to a specific tumor histology and/or specific biomarker (predicated upon preclinical data) and a 2) a biomarker cohort to obtain tumor biopsy samples at pre-treatment, on-treatment, with the exploratory objective of evaluating pharmacodynamic effects and potential resistance mechanisms. We expect that the dose escalation will complete enrollment in approximately 1 year and an additional 12-18 months for completion of the expansion cohorts. We then expect an additional one year period will be required to collect data and complete a clinical study report (CSR). We believe that this Phase 1/1B trial will provide critical clinical and biomarker data that will demonstrate clinical proof of concept which will

inform the Phase 2 development plan. Over the next 4 years, our Phase I trial will also advance a successfully completed CIRM funded-project for which an IND has already been filed
Project Overlap or Parallel: No scientific or budgetary overlap.
W81XWH-14-1-0385 (PI: Baylin)
Title: A New Paradigm for the treatment of Ovarian Cancer: The use of Epigenetic Therapy to Sensitize Patients to Immunotherapy and Chemotherapy.
Time Commitment: 0.60 Calendar Months
Supporting Agency: US Army Subaward with John Hopkins University
Procuring Contracting/Grants Officer: Melody Snow, M.H.S, Assistant Director, Outgoing Awards
Address of Grants Officer: John Hopkins University, School of Medicine, 1629 Thames Street, Suite 200
Baltimore, Maryland 21231
Performance Period: 9/30/2014-9/29/19
Level of Funding: $314,280
Project's Goal(s): To robustly prolong the survival of patients with serous ovarian cancer (OC) through introducing epigenetic therapy paradigms.
Specific Aims: 1) To uncover the mechanisms through which epigenetic therapy may, alone, achieve robust, durable responses in patients with advanced ovarian cancer (OC) 2) Study how epigenetic therapy may sensitize OC cells to subsequent chemotherapies 3) Study how epigenetic therapy may sensitize OC cells to subsequent immunotherapies which targets checkpoints which are driving immune tolerance 4) Develop new combinations of epigenetic drugs which may provide for the highest level of efficacy for management of OC
5) Bring all of the above studies to bear on leveraging clinical trials of epigenetic therapy on OC
Project Overlap or Parallel: No scientific or budgetary overlap.

AWARDED SINCE LAST SUBMISSION

R01CA182514-01A1 (PI: Curtis)
Title: Intergrated genomic analysis and multi-scale modeling of therapeutic resistance
Time Commitment: 0.24
Supporting Agency: NIH Subaward with Stanford University
Procuring Contracting/Grants Officer: Aida Vasquez, Vasquez@mail.nih.gov
240-276-6319
Performance Period: 09/12/14-8/31/19
Level of Funding: $74,773
Project's Goal(s): The major goals of this project are to i) perform an integrated genomic analysis of serial tissue specimens from HER2-positive patients enrolled in clinical trials to evaluate the efficacy of single or dual agent neoadjuvant lapatinib and or trastuzumab targeted therapy (NCT00769470/TRIO B07) in order to characterize mechanisms of resistance ii) delineate temporal patterns of clonal expansions under treatment selective pressure by analyzing longitudinal samples collected prior to, at run-in, and after therapy iii) to functionally characterize mechanisms of resistance to single and dual agent therapy in HER2-positive tumors and to phenotype resistant cell populations by analyzing patient-derived xenograft models and short-term primary cultures.
Specific Aims: N/A
Project Overlap or Parallel: No scientific or budgetary overlap.

COMPLETED SINCE LAST SUBMISSION

Stand Up to Cancer Dream Team (PI: Slamon)
Title: "An integrated Approach to Targeting Molecular Breast Cancer Subtypes and Their Resistance Phenotypes"
Time Commitment: 1.20 calendar
Supporting Agency: American Association for Cancer Research
Procuring Contracting/Grants Officer: Michael Stewart, CFO
Address of Grants Officer: American Association for Cancer Research, 615 Chestnut Street, 17th FL
Philadelphia, PA 19106-4404
Performance Period: 10/01/2009-09/30/2014
Level of Funding: $15,000,000
Project's Goal(s): The goals and objectives of this "Stand Up to Cancer" (SU2C)/AACR Breast Cancer Dream Team is to undertake a fully-integrated, molecular, genomic, biologic and "informatics" translational research approach directed at development of new and more effective therapies for the spectrum of diseases that comprise human breast cancer.
Specific Aims: ***Specific Aim I*** – Expand our understanding of the known "driving" initial molecular mechanisms responsible for the pathogenesis and clinical behavior of the three known therapeutic breast cancer subtypes, i.e. estrogen (E2)/estrogen receptor (ER-positive), HER2-positive and triple-negative (TN) subtypes of breast cancers. This will be accomplished using existing and/or creating new, relevant preclinical models as well as querying annotated clinical materials with the latest technologies and informatics platforms. The ultimate objective of this effort will be the design, development and clinical testing of new and innovative therapies for the known molecular subtypes of breast cancer;
Specific Aim II - Study the "driving" mechanisms responsible for *de novo* as well as acquired resistance to appropriately targeted treatments of the three known therapeutic breast cancer subtypes, i.e. estrogen (E2)/estrogen receptor (ER-positive), HER2-positive and triple-negative (TN) breast cancers. As in Specific Aim I, this will be accomplished utilizing existing and/or creating new, relevant preclinical models of resistance to current therapeutics as well as querying annotated clinical materials exhibiting the "resistance" phenotype using the latest technologies and informatics platforms. Again, the ultimate objective will be the design, development and clinical testing of new and innovative therapies for the "resistance" phenotype in the known breast cancer subtypes;
Specific Aim III - Investigate the potential initial "driving" pathogenetic as well as *de novo* or acquired "resistance" mechanisms mediated by "stem/progenitor" breast cancer cells within each or across all of the three known breast cancer therapeutic subtypes with the ultimate objective being the design, development and clinical testing of new and innovative therapies for the "tumorigenic" and "resistance" phenotypes potentially mediated by these stem/progenitor cells;
Specific Aim IV - Develop new and/or characterize existing relevant and representative cell line and xenograft models as well as utilize annotated clinical material to query the contributions of "normal" and "malignancy-derived" matrix/stromal components of each breast cancer subtype including those that might contribute to or mediate the "resistance" phenotype to targeted therapeutics. The ultimate objective will again be the design, development and clinical testing of new and innovative therapies for the "tumorigenic" and "resistance" phenotypes potentially mediated by these matrix/stromal components;
Specific Aim V - Develop an integrated discovery and informatics research unit that cuts across the above Specific Aims that is designed to deploy, inform and facilitate implementation of relevant discovery and informatics platforms needed for these aims. This will include utilization of robust informatics and systems biology efforts to not only manage, integrate and disseminate relevant data between Dream-Team members and the greater scientific community, but also to execute genome-wide analyses of relevant genes/pathways and "nodes" critical to breast cancer subtype

pathogenesis and directed at identification of "resistance" mechanisms. This effort will also lead to further refinement of the current molecular classification of known breast cancer therapeutic subtypes. As with all other Specific Aims, this Aim will have as its ultimate objective, the design, development and clinical testing of novel and hopefully more effective, less toxic therapies for women challenged with breast cancer both in the adjuvant and metastatic settings.
Project Overlap or Parallel: No scientific or budgetary overlap.

DR1-01477 (PI: Slamon)
Title: "Therapeutic Opportunities to Target Tumor Initiating Cells in Solid Tumors"
Time Commitment: 3.60 calendar
Supporting Agency: CIRM (Disease Team Awards)
Procuring Contracting/Grants Officer: Doug Kearney, Grants Management Office
Address of Grants Officer: California Institute for Regenerative Medicine, 210 King Street San Francisco, CA 94107
Performance Period: 05/01/2010-04/30/2014
Level of Funding: $19,979,660
Project's Goal(s): The purpose of the California Institute for Regenerative Medicine (CIRM) Disease Team Research Awards is to accelerate potential therapies based on stem cell research toward clinical testing. To facilitate this goal, CIRM intends to support actively managed multidisciplinary teams engaged in milestone-driven translational research. We propose to develop novel therapeutic drugs that target solid tumors affecting the brain, colon and ovaries.
Specific Aims: (1) increase the number of characterized xenografts and CIC-enriched cell lines, (2) carry out genomic characterization of these xenografts and cell lines, (3) carry out genomic characterization of available tumor bank samples, (4) test candidate PLK4 and TTK inhibitors supplied by the drug discovery group, (5) carry out combination drug testing, and (6) analyze the data en masse to determine how various CIC subtypes and tumor samples respond to the drugs so that optimal compounds can be selected and a targeted clinical plan developed.
Project Overlap or Parallel: No scientific or budgetary overlap.

OAM4861g (PI: Slamon)
Title: "A Randomized, Phase II, MultiCenter, Double-Blind, Placebo-Controlled study evaluating the safety and efficacy of Metmab and/or Bevacizumab in combination with Paclitaxel in patients with metastatic triple negative breast cancer"
Time Commitment: 0.12 calendar
Supporting Agency: Genentech, Inc
Procuring Contracting/Grants Officer: See-Chun Phan, M.D.
Address of Grants Officer: 1 DNA way, South San Francisco, CA 94080-4990
Performance Period: 12/01/11-02/28/15
Level of Funding: $192,211
Project's Goal(s): The goals of the OAM4861g study are to estimate the clinical benefit of MetMAb + bevacizumab + paclitaxel and MetMab + Placebo + Paclitaxel Relative to Placebo + bevacizumab + paclitaxel.
Specific Aims: To characterize the safety and tolerability of MetMAb + bevacizumab + paclitaxel and MetMAb + placebo + paclitaxel relative to placebo + bevacizumab + paclitaxel, To evaluate drug exposure of MetMAb, paclitaxel, and bevacizumab, To evaluate the serum levels and incidence of anti-therapeutic antibodies (ATAs) against MetMAb,To evaluate the effect of MetMAb on the following electrocardiogram (ECG) parameters: corrected QT (QTc) interval, heart rate, uncorrected QT interval, PR interval, QRS duration, and T-wave and U-wave morphology.
Project Overlap or Parallel: No scientific or budgetary overlap.

BCIRG#006 (PI: Slamon)
Title: "MC, PH III R, Trial Comp (AC-T), (AC-TH), oor (TCH) in the TX of NODE = & high risk node – adjuvant w Operable breast cancer containing ain HER2NEU alter"
Time Commitment: 0.12 calendar
Supporting Agency: Breast Cancer International Research Group
Procuring Contracting/Grants Officer: Ira Steinberg, M.D.
Address of Grants Officer: 55 Cambridge Parkway, Cambridge, Massachusetts 02142
Performance Period: 06/01/01-12/31/14
Level of Funding: $2,177,946
Project's Goal(s): The goals of the BCIRG #006 study is to compare disease free survival after treatment with doxorubicin and cyclophasphamide followed by docetaxel with doxorubicin and cyclophosphamide followed by docetaxel and trastuzumab and with docetaxel in combination with platinum salt and herceptin in the treatment of node positive and high risk node negative adjuvant patients.
Specific Aims: Compare overall survival between above mentioned arms. Compare toxicity and quality of life between mentioned arms, evaluate pathologic and molecular markers for predicting efficacy**.**
Project Overlap or Parallel: No scientific or budgetary overlap.

BCIRG#005 (PI: Slamon)
Title: "MC/P3/R Trial comparing Docetaxel in COMB w/ Doxorubicon & Cyclophosphamide followed by Docetaxel"
Time Commitment: 0.10 calendar
Supporting Agency: Breast Cancer International Research Group
Procuring Contracting/Grants Officer: Dominique Mery-Mignard, Medical Director
Address of Grants Officer: 42-50 Qua de la rapee, 75012 Paris, France
Performance Period: 06/01/2001-12//31/2013
Level of Funding: $1,066,299
Project's Goal(s): The Goals of the BCIRG#005 study is to compare disease free survival after treatment with Docetaxel in combination with doxorubicin and cyclophosphamide (TAC) in operable breast cancer HER2neu negative patients with positive axillary lymph nodes.
Specific Aims: Compare overall survival between above mentioned arms. Compare toxicity and quality of life between mentioned arms, evaluate pathologic and molecular markers for predicting efficacy**.**
Project Overlap or Parallel: No scientific or budgetary overlap.

Individuals who have worked on the project

Van Andel Research Institute

Name:	Peter Jones, Ph.D.
Project Role:	PI (Senior/Key Personnel)
Research Identifier:	N/A
Nearest person month worked:	1
Contribution to Project:	Dr. Jones serves as PI on this project.
Funding Support:	See Other Support

Has there been a change in the active other support of the PD/PI(s) or senior/key personnel since the last reporting period?

Yes. See next pages for Dr. Jones' Other Support.

OTHER SUPPORT

JONES, PETER A.

CURRENT

W81XWH14-1-0385 (PI: Baylin)

Title:	A New Paradigm for the Treatment of Ovarian Cancer: The Use of Epigenetic Therapy to Sensitize Patients to Immunotherapy and Chemotherapy
Time Commitment:	0.3 calendar
Supporting Agency:	DoD/Department of the Army via Johns Hopkins University
Procuring/Contracting/Grants Officer:	Barbara Schneider, Johns Hopkins University,
Address of Grants Officer:	The Sidney Kimmel Comp Cancer Ctr, 1650 Orleans St., CRBI Rm352, Baltimore, MD, 21287-0013, schneba@jhmi.edu
Performance Period:	9/30/14 – 9/30/19
Level of Funding:	$38,591 Annual Direct
Project Goals:	The goal of this project is to determine how DNMTs activate drug response pathways in ovarian cancer.
Specific Aims:	1) To uncover the mechanisms through which epigenetic therapy may, alone, achieve robust, durable responses in patients with advanced ovarian cancer (OC); 2) Study how epigenetic therapy may sensitize OC cells to subsequent chemotherapies; 3) Study how epigenetic therapy may sensitize OC cells to subsequent immunotherapies which targets checkpoints which are driving immune tolerance; 4) Develop new combinations of epigenetic drugs which may provide for the highest level of efficacy for management of OC; 5) Bring all of the above studies to bear on leveraging clinical trials of epigenetic therapy on OC
Project Overlap or Parallel:	No scientific or budgetary overlap.

AWARDED SINCE LAST SUBMISSION

R35 CA209859 (PI: Jones)

Title:	Targeting DNA Methylation and the Cancer Epigenome
Time Commitment:	6.0 calendar
Supporting Agency:	NIH/NCI
Procuring Contracting/Grants Officer:	Long Nguyen
Address of Grants Officer:	National Cancer Institute, Executive Plaza North, Suite 5024, 6130 Executive Blvd., Rockville, MD 20852
Performance Period:	01/01/17-12/31/23
Level of Funding:	$521,523 Annual Direct
Project's Goals:	This major goal of this project is to provide new approaches to treating cancers through the many epigenetic changes seen in the genomes of cancer cells.
Specific Aims:	Future Question 1: Why are there so many mutations in chromatin modifiers and what are the effects of these mutations on the structure of the epigenome? Future Question 2: What are the functional consequences of activating the expression of cancer/testis genes by 5-Aza-CdR? Future Question 3: What double-stranded RNAs are activated by 5-Aza-CdR and how do

these relate to cellular responses? Future Question 4: Can we design combinations of epigenetic drugs which might increase the effectiveness of 5-azanucleoside treatment? Future Question 5: Can cryo-EM help to visualize complexes relevant to chromatin structure and functions?

Project Overlap or Parallel: No scientific or budgetary overlap.

COMPLETED SINCE LAST SUBMISSION

R01 CA 082422 (PI: Jones) Previously R37

Title: Mechanisms of *De Novo* Methylation in Cancer
Time Commitment: 3.0 calendar
Supporting Agency: NIH/NCI
Procuring Contracting/Grants Officer: Sy Shakleford
Address of Grants Officer: National Cancer Institute, Executive Plaza North, Suite 5024, 6130 Executive Blvd., Rockville, MD 20852
Performance Period: 09/17/99-7/31/17
Level of Funding: $290,706 Annual Direct
Project's Goals: The major goals of this project are to study mechanisms of *de novo* methylation in culture systems and to probe the potential roles of chromatin structure in defining DNA methylation patterns.
Specific Aims: 1) To determine the role of DNA methylation on the structure of the cancer epigenome and to elucidate the potential mechanisms by which histone methyltransferases and chromatin alter the stability and output of the human epigenome; 2) determine the immediate epigenome-wide outcomes of treating cells with the global DNA methylation inhibitor 5-aza-2'-deoxycytidine and then probe the kinetics of remethylation and its link to chromatin remodeling with a particular focus on gene body methylation; 3) to complete the first pilot epigenome maps of a small number of uncultured human colon tumors and compare them to adjacent tissue collected from same patients.
Project Overlap or Parallel: No scientific or budgetary overlap.

5 R01 CA 083867 (PI: Jones/Liang)

Title: *De Novo* DNA Methylation in Bladder Cancer
Time Commitment: 1.80 calendar
Supporting Agency: NIH/NCI
Procuring Contracting/Grants Officer: Paul Okano
Address of Grants Officer: National Cancer Institute, Executive Plaza North, Suite 5024, 6130 Executive Blvd., Rockville, MD 20852
Performance Period: 03/01/2000-04/30/2016
Level of Funding: No Cost Extension
Project's Goals: The goal of this project, which has been funded for almost 30 years, is to understand the genetic and epigenetic basis of human bladder cancer.
Specific Aims: 1) Use a series of eight hypermethylation markers to complete the examination of DNA in urine sediments obtained from individuals with low grade tumors to determine whether we can

detect the frequent recurrences of these tumors; 2) complete the analysis of DNA from healthy individuals of different ages to determine whether age-related changes in DNA methylation can be detected in urine sediments; 3) determine the functional significance of an observed hypomethylation phenotype by analyzing directly whether methylation of non- CpG island regions which constitute the bulk of the phenotype might be involved in gene activation and have chromatin properties associated with active genes; 5) take advantage of ongoing clinical trials in which patients with myelodysplastic syndrome are being treated with the hypomethylating drug 5-azacytidine (5-aza-CR). This grant does not overlap with the proposed research as it does not investigate the role of ascorbic acid in cancer treatment.

Project Overlap or Parallel: No scientific or budgetary overlap.

1 R01 CA170550 (PI: Laird)
Title: Epigenetic Drivers of Cancer (PQ 10)
Time Commitment: 1.20 calendar
Supporting Agency: NIH/NCI
Procuring Contracting/Grants Officer: Roy W. Tarnuzzer
Address of Grants Officer: National Cancer Institute, 31 Center Drive, BG 31 Room 3A20, Bethesda MD 20814

Performance Period: 09/01/2012-06/30/2016
Level of Funding: $589,952
Project's Goals: The major goals of this project are addresses an unmet need to develop methods of finding out which epigenetic changes contribute directly to cancer formation.

Specific Aims: 1. We will develop a probabilistic framework for predicting and prioritizing candidate epigenetic driver loci. This approach is unique in that it fully integrates the wealth of available data, using complementary data types derived from primary genomic data, experimental data, and supporting curated information, resulting in a composite Epigenetic Driver Score (EDS), reflecting the posterior probability that each gene is an epigenetic driver. 2. Will provide experimental data on epigenetic addiction, using cell lines depleted of DNA methyltransferases, and thus selected to retain only the most essential silencing events, in addition to data obtained with embryonic and adult stem-cell and progenitors. These experimental data sets will be used to complement primary epigenomic data we have generated in the context of TCGA, to provide Epigenetic Driver Scores for each locus in each tumor type, using the methodology developed in Aim 1. 3a. We will functionally test the top-ranked candidate epigenetic drivers of colon, breast, and lung cancer in vitro, by reintroducing expression of candidate genes into appropriate human cancer cells lines containing the relevant silencing events. These experiments will be complemented by shRNA approaches in cell lines to modulate the functional expression of the candidate epigenetic drivers. *In vitro* proliferation and apoptosis assays will be used to assess phenotypic effects. 3b. We will assess the

	functional contributions of the candidate epigenetic drivers *in vivo*, using the stable cell lines created in Aim 3a in xenograft mouse models.
Project Overlap or Parallel:	No scientific or budgetary overlap.

8. SPECIAL REPORTING REQUIREMENTS

Progress of the Teal Junior Scientists, Drs. Kate Chiappinelli, Meredith Stone, Ph.D, and Michael Topper, Ph.D

Scientific training – Dr. Chiappinelli: As mentioned in the progress report, Dr. Chiappinelli benefitted enormously from her time with us. For her studies in the Cell, 2015 paper, she worked with collaborators in Germany, Drs. Reiner Strick and Pamela Strissel for learning how to profile, knockdown, and overexpress several of the endogenous retroviruses (ERVs). She was also mentored extensively with Dr. Cindy Zahnow's group for the mouse model work she participated in and for which she is a co-author on Meredith's Stone's PNAS paper, in press as outlined in the progress report. As mentioned last year, she benefitted enormously from Drew Pardoll's mentorship as part of her training learning how to isolate and profile mouse immune cells, both from the spleen and from tumor. Kate left a little less than a year ago to take a faculty position at George Washington University in the Cancer Center where she has gotten off to a great start. She still has some collaborative work with us and continues to focus on ovarian cancer research.

Scientific training – Dr. Meredith Stone: For her year as a mentee Meredith Stone worked with Cindy Zahnow for her dissertation studies and was co-mentored by Dr. Baylin. She benefitted from all of the activities listed above for Dr. Chiappinelli and, as fully outlined in the progress report, her work resulted in her paper now in press in PNAS on the mouse OC model. All of the educational activities and mentoring activities outlined for Dr. Chiappinelli were engaged in by Dr. Stone. All of this resulted in her successful application for a Postdoctoral fellowship at University of Pennsylvania in the Cancer Center where she will continue to work on aspects of immunology related to OC.

Scientific training – Dr. Michael Topper: Our new mentee, to begin in year 4, is Dr. Topper whose work for his dissertation, done with Dr. Baylin with co-mentoring from Dr. Zahnow, has been fully defined in the progress report and resulted in his first author Cell paper, now in press. This work, developing a new epigenetic therapy schema to pair with immune checkpoint therapy through initial studies of NSCLC was then extrapolated to the mouse OC model studied by Dr. Stone and Michael is also a co-author on her in press, PNAS paper. He will be mentored for postdoctoral studies over this next year by Dr. Baylin and will focus his work on further extending the above therapy to OC and aimed towards leveraging a clinical trial for patients with this cancer. He will also focus on dissecting further the upstream mechanisms by which the epigenetic therapy down regulates MYC signaling to help reverse tumor evasion.

Presentations for the above trainees:

Posters (National)

Topper, M., Hannigan, C.L., Vaz, M., et al, The American Association for Cancer Research Annual Meeting, New Orleans, LA. April 2016.

Participation in Hopkins groups: All three mentees participated in the following:

1) Methylation Data Group: attended these weekly meetings, and presented several times per year.
2) Methylation Journal Club: attended these weekly meetings, and presented many times.
3) Tumor Biology Lab Meeting: attended these weekly meetings, and presented at least twice per year.
4) All three met with co-investigator Peter Jones and his group at the Van Andel Research Institute in Grand Rapids, Michigan in 2016 and again with this group when they came to Baltimore this year.

Professional development:

As above all three mentees had great development of their professional careers directly dependent on their training time.

1) Dr. Chiappinelli was recruited as a faculty member to George Washington University as previously outlined.
2) Dr. Stone received her Ph.D. based on the dissertation work supported by this grant and, and as previously outlined, successfully applied for a postdoctoral position at the University of Pennsylvania.
3) Dr. Topper, in the lead up to his mentoring involvement with this grant, received his Ph. D. based on the dissertation work partially supported by this grant.

Additional training: As above, Drs. Stone and Topper are now engaged in postdoctoral fellowship work based on their studies outlined for this grant.

Individual Development Plan (IDP) for Postdoctoral Fellows:
Johns Hopkins University School of Medicine requires postdoctoral fellows and their mentors to fill out an annual IDP. This allows the fellow and mentor to identify long-term and short-term goals for the postdoc's research progress as well as career development. All three mentees have completed IDP's and this has been reviewed annually with Drs. Baylin and Zahnow.

Teal Innovator's Ovarian Cancer ambassadorship activities

More this past year than ever, Dr. Baylin has been requested to discuss the exciting results which are outlined in the progress report and which constitute the Cell and PNAS papers in press. Which have evolved to date and which are outlined in the Progress Report. He has given plenary section lectures at the national AACR meeting in 2017, at multiple national conferences including among others at Northwestern University, the Mayo Clinic, Abbvie Pharmaceuticals, Roswell Park, and at international events including, among others, the Epigenetics Gordon Conference in Lucca, Italy (April 2017), and symposia in Heidleberg, Mainz, and Bonn Germany, and Ludwig Symposium, Oxford England.

9. APPENDICES

Stone ML, Chiappinelli KB, Li H, Murphy LM, Travers ME, Topper M, Mathios D, Lim M, Shih I-M, Wang T-L, Hung C-F, Bhargava V, Wiehagen KR, Cowley GS, Bachman KE, Strick R, Strisse PL, Baylin SB, Zahnow CA. Epigenetic therapy activates type I interferon signaling in murine ovarian cancer to reduce immunosuppression and tumor burden. In Press PNAS, 2017.

Topper MJ, Vaz M, Chiappinelli KB, DeStefano Shields C, Wenzel A, Hicks J, Ballew M, Stone M, Tran PT, Zahnow CA, Hellmann MD, Strissel PL, Strick R, Baylin SB. A combination epigenetic therapy ties blocking MYC to reversing immune evasion and treating lung cancer. In Press Cell, 2017.

Epigenetic therapy activates type I interferon signaling in murine ovarian cancer to reduce immunosuppression and tumor burden

Short title: Epigenetic drugs reduce ovarian cancer immunosuppression

Classification: BIOLOGICAL SCIENCES; Medical Sciences

Meredith L. Stone[1*7], Katherine B. Chiappinelli[1, 8*], Huili Li[1], Lauren M. Murphy[1], Meghan E. Travers[1], Michael Topper[1], Dimitrios Mathios[2], Michael Lim[2], Ie-Ming Shih[3], Tian-Li Wang[4], Chien-Fu Hung[4], Vipul Bhargava[5], Karla R. Wiehagen[5], Glenn S. Cowley[5], Kurtis E. Bachman[5], Reiner Strick[6], Pamela L. Strissel[6], Stephen B. Baylin[1§], and Cynthia A. Zahnow[1§].

[1]Department of Oncology, The Sidney Kimmel Comprehensive Cancer Center at Johns Hopkins, 1650 Orleans Street, Baltimore, MD 21287.

[2]Department of Neurosurgery, The Sidney Kimmel Comprehensive Cancer Center at Johns Hopkins, 1650 Orleans Street, Baltimore, MD 21287.

[3]Department of Gynecology and Obstetrics, The Sidney Kimmel Comprehensive Cancer Center at Johns Hopkins, 1650 Orleans Street, Baltimore, MD 21287.

[4]Department of Pathology, The Sidney Kimmel Comprehensive Cancer Center at Johns Hopkins, Baltimore, 1650 Orleans Street, Baltimore, MD 21287.

[5]Janssen Research & Development, 1400 McKean Road, Spring House, PA 19477, USA.

[6]Department of Gynaecology and Obstetrics, Laboratory for Molecular Medicine, University-Clinic Erlangen, 91054 Erlangen, Germany.

[7]Current address: Division of Hematology-Oncology, Department of Medicine, Perelman School of Medicine, University of Pennsylvania, 3400 Civic Center Boulevard, Bldg 421, Philadelphia, PA.

[8]Current address: Department of Microbiology, Immunology &Tropical Medicine and the GW Cancer Center, George Washington University, 800 22nd Street N.W. Washington, DC 20052

*These authors contributed equally to this work.

[§]Corresponding authors:

Cynthia A. Zahnow: 1650 Orleans Street, Baltimore, MD 21287. (410)-955-8506.

Stephen B. Baylin: 1650 Orleans Street, Baltimore, MD 21287. (410)-955-8506.

Conflicts of interest: CAZ and SBB have a collaborative research agreement with Janssen. VB, KRW, GSC, and KEB are employed by Janssen.

Key words: 5-azacytidine, DNA methyltransferase inhibitors, histone deacetylase inhibitors, immune cell activation, tumor microenvironment, ovarian cancer, type I interferon.

Abstract

Ovarian cancer (OC) is the most lethal of all gynecological cancers and there is an urgent unmet need to develop new therapies. Epithelial ovarian cancer (EOC) is characterized by an immune suppressive microenvironment and response of ovarian cancers to immune therapies has thus far been disappointing. We now find, in a mouse model of EOC, that clinically relevant doses of DNA methyltransferase (DNMTi) and histone deacetylase (HDACi) inhibitors reduce the immune suppressive microenvironment through Type I interferon signaling and improve response to immune checkpoint therapy. These data are the first to indicate that the Type I interferon response is required for effective *in vivo* anti-tumorigenic actions of the DNMTi, 5-Azacytidine (AZA). Through type I interferon signaling, AZA increases numbers of $CD45^+$ immune cells and the percentage of active $CD8^+$ T and NK cells in the tumor microenvironment, while reducing tumor burden and extending survival. AZA also increases viral defense gene

expression in both tumor and immune cells, and reduces the percentage of macrophages and myeloid derived suppressor cells in the tumor microenvironment. The addition of an HDACi to AZA enhances the modulation of the immune microenvironment, specifically increasing T and natural killer cell activation and reducing macrophages over AZA treatment alone, while further increasing the survival of the mice. Finally, a triple combination of the DNMTi/HDACi plus the immune checkpoint inhibitor α-PD-1 provides the best anti-tumor effect and longest overall survival, and may be an attractive candidate for future clinical trials in ovarian cancer.

Statement of Significance

Therapies that activate the host immune system have shown tremendous promise for a variety of solid tumors. However, in most cancer types, fewer than half of patients respond to these immunotherapies. We propose epigenetic therapy as a mechanism to sensitize tumors to immune checkpoint therapy. We have shown that inhibiting DNA methylation triggers a viral defense pathway in tumors. Here we show that epigenetic therapy in a mouse model of ovarian cancer increases the numbers of activated immune cells, and this is dependent on the interferon anti-viral response. The combination of epigenetic therapy and immune checkpoint blockade leads to the greatest reduction in tumor burden and increases in survival and may hold the greatest promise for patients.

\body

Introduction

Ovarian carcinoma is the leading cause of death from gynecological malignancies in the United States (1). Epithelial ovarian cancer (EOC) is characterized by an immunosuppressive microenvironment (2) and patient responses to immunotherapy have been disappointing (3). In

particular, the response of ovarian cancer to the immune checkpoint inhibitors α-PD-1 or α-PD-L1 has thus far been modest in comparison to the robust responses observed for melanoma, non-small cell lung cancer, and renal cell cancers (4). New treatment strategies are needed to reverse the immunosuppressive microenvironment of ovarian cancer and sensitize these tumors to immune checkpoint blockade.

One promising approach for reversing the tumor immune evasion phenotype and improving the efficacy of immune checkpoint therapy of cancers in general and ovarian cancers in particular is epigenetic therapy. The first suggestion for this approach came from a clinical observation in trials involving patients with advanced, pre-treated non-small cell lung cancer (NSCLC) (5). These individuals initially received the DNA methyltransferase inhibitor (DNMTi), Vidaza (5-azacytidine, AZA) and the histone deactylase inhibitor (HDACi) Entinostat (MS275). This coupling was based on pre-clinical data that DNMTIs and HDACIs in combination enhance reactivation of aberrantly silenced genes in tumor cells and cause reductions in tumor burden that are more effective with the combined agents (6-9). After disease progression, these patients entered the first trials of immune checkpoint therapy for NSCLC and several of these patients had durable responses compared to those who received the immunotherapy alone (10). Clinical trials are being conducted to validate this preliminary observation (10), but preclinical work to optimize this combinatorial approach of HDACIs and DNMTIs has not been explored.

Compelling data is emerging to show that this combinatorial approach in pre-clinical studies induces immune signaling in both tumor and immune cells. Studies by our group and others have shown that DNMTIs can upregulate a wide range of genes involved in immune signaling in breast, lung, colon, and ovarian cancer cells (11-15). A particularly important

component of this in ovarian and colon cancer cells is that DNMTIs can induce an upregulation of a cytosolic sensing double stranded RNA (dsRNA) anti-viral pathway which results in Type I interferon production and downstream signaling for upregulation of interferon stimulated genes including immune cell attracting chemokines and cytokines (11, 14). Furthermore, epigenetic changes, specifically *de novo* methylation, have been shown to play an important role in the promotion of $CD8^+$ T cell exhaustion, which is a barrier to immune cell activation during checkpoint inhibition therapy (16). While this study showed that demethylation is important for T cell reactivation, our data in the present study show that treatment of isolated tumor cells with DNMT inhibitors is sufficient to increase immune cell numbers in the tumor microenvironment. Taken together, both the tumor and the immune microenvironment are responsive to epigenetic therapy.

Others have utilized mouse models of ovarian cancer to explore how epigenetic therapy affects the response to immune checkpoint blockade, finding that the DNMTi, decitabine, can increase activated immune cells in ovarian ascites and sensitize tumors to α-CTLA4 (cytotoxic T lymphocyte associated protein 4) (14). Similarly, another study showed that epigenetic therapy induced tumor expression of CXCL10 which led to an increase in T effector cells in the tumor microenvironment and to an improved response to α-PD-L1 therapy (15). However, the precise mechanisms underlying their findings and the link to a DNMTi/HDACi induced anti-viral, cellular response remain to be clarified.

Recently, using human NSCLC cells, and a mouse model of these diseases, our group has approached this question by trying to elucidate the best HDACIs to use based on their pharmacologic half-lives and K_i effects on key members of the HDAC family. Moreover, we have optimized the ability to combine DNMTIs and HDACIs to develop a chronic, tolerable, low

dose schema to keep constant pressure on reversing not only DNA methylation abnormalities but the repressive chromatin events which accompany these. A potent regimen has been developed for inducing pre-clinical anti-tumor responses and reversing tumor evasion (Topper *et al*, *Cell* in press). We now employ this new regimen in a mouse model of ovarian cancer, outlining not only a potent potential paradigm for an ovarian cancer clinical trial combining epigenetic with immune checkpoint therapy, but, importantly, mechanistically tying induction of viral defense to the above anti-tumor responses by finding, in a mouse model of ovarian cancer, that DNMTIs and HDACIs increase both the number and activation of immune cells in the tumor microenvironment, reduce tumor burden, and extend overall survival of the mice. This modulation of the tumor microenvironment stems in part from an AZA induced, interferon mediated, upregulation of an immune gene signature including genes involved in viral defense, chemokines, cytokines, interferon signaling, and cancer testis antigens (11, 13). We also now verify that that type I interferon signaling caused by AZA induced immune signaling is required for this drug to increase the number of $CD45^+$ immune cells in the tumor microenvironment and activation of $CD8^+$ T cells and natural killer (NK) cells. Moreover, we demonstrate that when HDACIs are combined with AZA *in vivo*, these drugs act on the immune compartment to further improve the activation of $CD8^+$ T cells, natural killer (NK) cells, and to decrease myeloid cells to create a less immunosuppressed tumor microenvironment. Together, the actions of these drugs on tumor cells and the tumor microenvironment indicate that combination epigenetic therapy may offer an approach to optimize immune checkpoint therapy for patients with ovarian cancer, and that AZA, the HDACi Givinostat (ITF2357, ITF), and α-PD-1 may hold the most promise.

Results

Pre-treatment of tumor epithelial cells *ex vivo*

To study how DNMTIs and HDACIs directly affect tumor epithelial cells to regulate response and immune cell interactions, we pre-treated cultured, syngeneic mouse ovarian surface epithelial cancer cells, ID8-VEGF-Defensin (17-20), with epigenetic agents, injected the cells into untreated mice, and analyzed ascites volume as a measure of tumor burden (21). The ID8 parental cells were derived from ovarian surface epithelium, instead of from the fallopian tube which is hypothesized to be the origin of most ovarian tumors (22, 23). While genetic models of the development of ovarian cancer in the fallopian tube exist (24, 25), the ID8 model is one of very few transplantable syngeneic murine models of ovarian cancer routinely available (26), that is able to be transplanted into immunocompetent mice, and creates an immunosuppressed tumor microenvironment (21), making it well suited to our studies. Parental ID8 cells (20) were modified to overexpress VEGF and Defensin (17, 19) to make them more aggressive and more like some human ovarian cancers (27, 28). The ID8-VEGF-Defensin cells also consistently generate hemorrhagic ascites approximately 4 weeks after transplantation of only 250,000 cells. The ascites generated by the ID8-VEGF-Defensin cells is easily drained for analysis of tumor and immune cells, and is representative of tumor burden (17, 21, 29-33). The number of tumor cells in the ascites fluid correlates positively with the volume drained, while the number of immune cells is inversely correlated, showing that the increase in tumor cells is not a general increase in cellularity of the fluid (Figure S1A, B).

Ten or 17 (A10, A17), but not 3 (A3-10), days of AZA pre-treatment of tumor cells (Figure 1A) led to significantly less ascites (Figure 1B), reflected as a reduction in weight gain (Figure S1C), and increased mouse survival compared to vehicle (Mock) or HDACi pre-treated

tumor cells (Figures 1A-D, Figure S1C, D). Combination pre-treatment of AZA and Entinostat (A+MS17) or AZA and Givinostat (A+ITF17) decreased ascites compared to mock, but did not decrease ascites (Figure 1C) or improve survival (Figure 1D) compared to AZA treatment alone. The slight antagonistic effect of AZA+MS17 compared to AZA alone is not observed when the whole mouse is treated (Figure 3B, C), and may be due to effects on the tumor cells that are not observed in an *in vivo*, immunocompetent setting. Overall, the decrease in ascites volume and increase in survival with AZA or AZA+HDACi pre-treatment appears to be driven by an AZA mediated effect on tumor cells.

AZA pre-treatment of tumor epithelial cells in these *ex vivo*, pre-treatment studies led to changes in the immune microenvironment with increased numbers of immune cells ($CD45^+$) in the ascites of A10 pre-treated tumor cells (Figure 2A, B). Entinostat or Givinostat treatment of cultured tumor cells did not alter the number of $CD45^+$ cells/ml (Figure 2C), but did lead to decreases in the percent of T effector and T helper cells (Figure 2I, J) in the ascites. Neither the addition of Givinostat (A+ITF17), nor Entinostat (A+MS17), to AZA increased the number of $CD45^+$ cells above AZA treatment alone (Figure 2C); however, there were some significant changes in the percentage of activated NK cells (Fig 2F). These changes are particularly interesting in light of the fact that the immune cells, associated with the tumor microenvironment, were not treated in the *ex vivo*, pretreatment model.

AZA induced immune signaling in tumor cells

Treatment with AZA at doses that degrade its molecular target, DNA methyltransferase 1, in ID8-VEGF-Defension cells (Figure S1E-G) caused an upregulation of an immune related viral defense signature in these murine cells, as was previously described for human ovarian

cancer cells (11), (Figure S2A). This expression, also seen in cancer testis antigens (CTAs), was especially robust with prolonged treatment (Figure S2A, B). HDACIs have been shown to synergize with DNMT inhibitors to re-express silenced genes in cancer (7, 9), but Entinostat (MS275) or Givinostat (ITF) treatment (HDACi17) alone or in combination with AZA caused only small or moderate changes in the expression of the antiviral and CTA genes in these mouse ovarian cancer cells (Figure S2C, D).

We previously demonstrated that AZA treatment of human ovarian carcinoma cell lines induced the expression of RNA from endogenous retroviruses (ERVs), which led to increased interferon signaling and viral defense gene expression (11, 14). We now demonstrate in mouse ovarian ID8-VEGF-defensin cells that AZA significantly increased several mERVs in both cultured tumor cells (Figure S2E) and tumor cells sorted from ascites from treated C57Bl/6 mice (Figure S2F, Figure S4A, Supplemental Table 1). While the ERVs are increased early in this treatment (Day 3), they sharply decrease at later time points (Days 4, 7 and 10). This is reminiscent of the increase and subsequent decrease in ERV transcripts observed in (11). We hypothesize that antiviral proteins upregulated by the interferon response may destroy the ERV RNA. Interestingly, *in vivo* (Figure S2F) we observe a long-term increase in ERV transcripts. We have previously shown that these ERVs, silenced by DNA methylation, lose methylation and increase transcription upon DNMTi treatment (11).

Lastly, AZA treatment *in vitro* (A10) and *in vivo* (See schematic, Figure S4A) altered the secreted protein levels of chemokines and cytokines. In an array of 40 chemokines and cytokines, CD54, IL-1RA, CXCL10, CCL2, CCL5 were significantly upregulated *in vitro*, while CXCL12 was downregulated. In the ascites fluid of AZA treated mice, IL-1RA was significantly downregulated, while CXCL10 and CXCL1 were significantly upregulated. Only

CXCL10 was significantly increased by AZA in both the media and the ascites fluid (Figure S2G, H).

Treatment of mice with AZA, HDACi, and α-PD-1

Having shown that pre-treatment of ovarian tumor cells led to increased immune cells in the tumor microenvironment and improved survival of the mice, we next asked whether the addition of α-PD-1 would provide added benefit. Mice bearing ovarian tumors treated intraperitoneally with AZA, an HDACi, and α-PD-1 had improved overall survival, decreased tumor burden, and alterations of immune cell populations that would promote immune cell killing of tumor cells (Figure 3, 4). AZA as a single agent or in combination with either HDACi or α-PD-1 significantly reduced ascites volume (Figure 3B, expansion), while HDACIs or HDACIs+α-PD-1 were ineffective (Figure 3B). Mirroring these ascites data, α-PD-1, HDACIs alone, or HDACIs plus α-PD-1 did not affect survival (Figure S3B), while the combination of AZA with either HDACi significantly improved this key parameter over AZA treatment alone (Figure 3C). This is in contrast to the *ex vivo* treatment model, where the addition of HDACi to AZA did not affect the tumor burden or overall survival (Figure 1C, D). The improved survival with *in vivo* treatment may reflect the effects of the epigenetic drugs on the host immune cells. Adding α-PD-1 to AZA+ITF further significantly increased survival over AZA+ITF or AZA+MS+α-PD-1 (Figure 3D-F. In summary, the triple combination of AZA+ITF+α-PD-1 was the most effective at decreasing ascites volume and increasing overall survival (Figure 3F).

Immune cell subpopulations in the ascites fluid of tumor bearing mice were changed by epigenetic therapy and α-PD-1, but immune cells in non-malignant tissues, such as the spleen, were not affected (Figure S4B). In the tumor microenvironment, AZA treatment moderately but significantly increased the percentage of activated $CD4^+$ and $CD8^+$ T cells and NK cells, and

when combined with ITF or either HDACi+α-PD-1, this activation was markedly enhanced (Figure 4A, B, C). All treatments containing AZA led to an increase in the percentage of T cells (Figure 4F), though this effect was less consistently observed in replicate experiments than the increases in activation of $CD8^+$ T and NK cells. None of the treatment groups altered the percentages of T regulatory, $CD4^+$, $CD8^+$, $CD4^+PD\text{-}1^+$, or $CD8^+PD\text{-}1^+$cells, or the CD4/CD8 ratio (Figure S5). The addition of Givinostat or either HDACi+α-PD-1 to AZA therapy increased the activation of key tumor-killing subsets of immune cells.

Myeloid derived suppressor cells, which aid in tumor immune evasion (34), were significantly decreased by almost all therapies, with the exception of ITF and ITF+α-PD-1; however, this exception may be due to limitations in sample number and high variability (Figure 4D). All treatments containing AZA decreased the percentage of macrophages, which can influence tumor growth (35) (Figure 4E). Compared to AZA alone, the addition of an HDACi significantly decreased the percentage of macrophages further. Overall, increased numbers of $CD45^+$ immune cells, increased activation of $CD8^+$ T cells and NK cells and decreases in macrophages and MDSCs were the most consistent, significant changes resulting from epigenetic therapy. Differences were observed between the changes of the immune cell subpopulations in the *ex vivo* (Figure 2D-J) and in *vivo* (Figure 4) models. This was not unexpected as the immune cells were exposed to drug in the *in vivo* model, but not in the *ex vivo*, pretreatment model. Further investigation is needed regarding the response of immune cell populations to epigenetic treatment.

In support of the fact that *in vivo* epigenetic treatment alters host immune cell populations in the tumor microenvironment, we find that AZA treatment increases expression of viral defense genes in $CD8^+$ and $CD4^+$ T cells and in $CD11b^+$ myeloid cells in the ascites fluid of

253 treated, tumor bearing mice (Figure S6A, B). Ingenuity analysis also identified interferon
254 associated genes as top upstream regulators of the transcriptional program in these *in vivo* AZA
255 treated cells (Supplemental Table 2). These results suggest that the AZA induced increase in
256 gene expression of interferon associated genes in both tumor and host immune cells may be an
257 integral component of the improved outcome of mice treated with epigenetic therapy and
258 immune checkpoint inhibitors.
259 In summary, the combinations of epigenetic agents, as well as the addition of α-PD-1 to
260 AZA+HDACi, increase the numbers and activation of key tumor killing immune cells to the
261 tumor microenvironment and decrease numbers of MDSCs and macrophages (Figure 4). We
262 hypothesize that these effects contribute to the reduction in tumor burden and survival when
263 treating with AZA, its combination with HDACIs, and importantly these agents combined with
264 α-PD-1.
265
266 **Blockade of IFNAR1 inhibits the actions of AZA**
267 Our expression data show that AZA treatment leads to increased interferon signaling and
268 viral defense gene expression in ID8-VEGF-Defensin cells (Figure S2A). We therefore
269 questioned the role and importance that interferon signaling plays in the AZA induced decrease
270 in tumor burden and alterations in immune cells observed in Figures 3 and 4. To test this
271 hypothesis, we used an antibody targeting the interferon alpha, beta receptor 1 (α-IFNAR1).
272 Mice harboring ID8-VEGF-Defensin tumor cells were injected with α-IFNAR1 (i.p.,
273 0.5mg/mouse) every 3 days and simultaneously treated with AZA or vehicle control (Mock)
274 (Figure 5A). The AZA mediated reduction in ascites volume routinely observed in our
275 experiments was inhibited by treatment with α-IFNAR1 (Figure 5B) and total numbers of $CD45^+$

cells in the ascites were not increased as with the AZA and IgG control treatment, but remained near Mock values (Figure 5D). Likewise, activation of $CD8^+$ T effector cells and natural killer (NK) cells in response to AZA treatment was also completely blocked by α-IFNAR1 (Figure 5E, F) and there was no survival benefit for mice treated with AZA and α-IFNAR1 (Figure 5C). Previous *in vitro* studies have demonstrated that upregulation of a dsRNA sensing pathway by AZA triggers the activation of an intact Type I interferon signaling pathway requiring the interferon alpha and beta receptor subunit 1 (11, 14), and here the use of α-IFNAR1 prevented the AZA induced increase in expression normally observed for anti-viral genes, such as ISG15, IFIT1 and ICAM1 *in vitro* (Figure S7A-C) Our α-IFNAR1 data are the first to indicate that the type I interferon response is, indeed, required for effective *in vivo* anti-tumorigenic actions of 5-azacytidine, including reduced tumor burden, extended survival, and increased numbers and activation of immune cells.

AZA+HDACi efficacy requires a treated immune system

To further assess the role of the immune cells in the anti-tumorigenic response, we compared the response to epigenetic agents in treated immune-deficient NSG mice that lack functional B, T and NK cells (36) (Figure 6A) to the response in the treated immunocompetent mice (Figure 3). In the NSG immunodeficient mice, AZA treatment reduced ascites volume and increased survival as in the C57Bl/6 mice, and HDACi treatment alone did not significantly affect ascites volume or survival in either mouse model. Combination treatment was more effective than AZA as a single agent in the treated immune competent C57Bl/6 mice (Figure 6B, C), and not in the immunodeficient mice or in the pretreatment model (Figure 1C, D), suggesting that when combined with AZA, HDACIs may act on the immune microenvironment to reduce

tumor burden. Taken together, these data imply that AZA can act on both tumor and immune cells, while the added benefit of the combination with the HDACi may rely on the treatment and presence of an intact host immune microenvironment. Specifically, the activation of T and NK cells and decreases in macrophages were all significantly enhanced by the HDACi addition to AZA and may be responsible for the reduction in tumor burden in the treated mice in an immune intact setting (Figure 4A, B, C, E). Interestingly, α-IFNAR1 treatment (Figure 5A) did not inhibit the reduction in ascites burden in AZA treated NSG mice (Figure 6D), as it did in the C57Bl/6 mice, shown again here for comparison, suggesting that the role interferon signaling is playing in the response to AZA is dependent on functional immune cells in the tumor microenvironment These data also suggest that there are additional mechanisms responsible for the anti-tumorigenic effect of AZA that are not dependent on interferon signaling.

AZA has direct anti-tumorigenic effects

Even in the absence of tumor killing immune cells in the NSG model, we noted increased numbers of dead cells in the $CD45^-$ (non-immune cell) population with AZA and AZA+ITF treatment, the two groups with the longest median survival (Figure 6E). This could be explained by the fact that the anti-tumor effects of AZA can be mediated through mechanisms that are not immune or interferon dependent, such as apoptosis and disruption of the cell cycle (11, 37-39). Indeed, three or 10 days of *in vitro* treatment of the tumor cells (A3-3, A10) with 500nM AZA caused a significant decrease in cultured cell numbers (Figure 7A, B) associated with signs of apoptosis reflected by increased cleaved-PARP protein levels and percentage of cells positive for Annexin V and 7-AAD (Figure 7C- F). These data confirm that nanomolar doses of AZA induce a low level of apoptosis in cancer cells, as we have previously described (11, 37), which appears

to be too small to account for the large decrease in tumor cells observed in culture (Figure 7B). A more important factor in the decrease in tumor cell number could be that A3 and A10 treatment *in vitro* decreased the percentage of tumor cells in S phase and increased those in G2-M arrest (Figure 7G, H), as has been observed in other models (38, 39). In summary, AZA directly affects intrinsic, anti-tumorigenic mechanisms in the tumor cells, leading to increased apoptosis and cell cycle arrest. However, the changes in the cell cycle and small increases in apoptosis were not inhibited *in vitro* by treatment with the α-IFNAR1 blocking antibody described previously (Figure S7D, E), suggesting that while interferon signaling is important for the recruitment and activation of immune cells, AZA also has non-immune related and interferon independent effects.

Overall, our data demonstrate that AZA reduces tumor burden and increases the number of immune cells in the tumor microenvironment, in part through effects on the tumor cells themselves. AZA treatment upregulates immune gene expression in tumor cells and in immune cells, and type I interferon signaling is required for some anti-tumorigenic effects of *in vivo* AZA, such as decreased ascites burden, extended survival, and activation of immune cells. When tumor bearing mice are treated *in vivo*, the addition of an HDACi to AZA further reduces tumor burden and increases survival, perhaps due to an increase in activated T and NK cells and a decrease in macrophages. Finally, the combination of AZA, Givinostat, and α-PD-1 was the most effective in improving overall survival.

Discussion

The use of different treatment models in this study has enabled us to understand how 5-azacytidine (AZA) and HDACIs act individually and in combination on ovarian tumor epithelial

cells and immune cells in the microenvironment to establish anti-tumor responses and to enhance immune checkpoint therapy. Low doses of AZA, but not HDACIs, directly induce multiple anti-tumorigenic mechanisms in tumor cells, most notably increased immune signaling, increased apoptosis, and disruptions of the cell cycle, as well as increasing immune cell activation in the tumor microenvironment via type I interferon signaling. When an HDACi, especially Givinostat, is combined with AZA *in vivo*, these agents can enhance the activation of specific immune subsets such as T and NK cells. Our data now show that that the addition of an HDACi to a DNMTi may be optimal to achieve a maximal sensitization to checkpoint inhibitors. We hypothesize that other DNMTIs such as decitabine may behave similarly to AZA used in this study, as decitabine has also been shown to trigger an antiviral response in tumor cells (11, 40). The triple combination of AZA, Givinostat, and anti-PD-1 extended median survival by 14.5 days compared to Mock treated mice. This change is significantly greater than the benefit derived from paclitaxel, a common chemotherapy for OC, treatment in this fast-growing model (41). The addition of Givinostat, but not Entinostat, to AZA was able to sensitize the tumors to α-PD-1 therapy. The reasons why Givinostat outperforms Entinostat in overall survival when combined with AZA and α-PD-1 are currently under investigation. Other studies have shown that HDAC inhibition can affect tumor associated immune cells, with one finding that B cells as well as interferon-γ receptor signaling in the tumor cells were important for the anti-tumorigenic effect of the HDACIs vorinostat and panobinostat in syngeneic models of colon cancer and lymphoma (42).

In our study, blockade of type 1 interferon signaling with an antibody against IFNAR1 impairs the anti-tumorigenic effects of AZA. Although it had been observed that AZA treatment could stimulate interferon pathway induction by the viral defense pathway signaling, it was not

known which *in vivo* consequences would be linked to this pathway upregulation. Importantly, our data now demonstrate that many of the anti-tumorigenic actions of AZA in ovarian cancer are mediated via the interferon α, β receptor subunit 1, including decreased tumor burden, increased $CD45^+$ immune cells in the tumor microenvironment, and increased activation of $CD8^+$ T and NK cells. We show that Type I interferon signaling is responsible for the anti-tumor effects of AZA in immune competent mice (Figure 6D). However, AZA has an effect that leads to decreased tumor burden in NSG mice that is not mediated by the interferon response (Figure 6D). Thus we conclude that the antiviral response caused by AZA primarily reduces tumor burden by recruitment and activation of immune cells to kill tumor cells in this model. Separately, (Figure S7) we show that AZA also has interferon independent effects such as cycle disruptions in ID8-VEGF-Defensin cells (Figure S7F, G) which may account for the anti-tumorigenic effect of AZA in the NSG mice. AZA induced low levels of apoptosis that were not significantly affected by blocking IFNAR1 (Figure S7D, E), in contrast to previous work from our group and others that indicated an intrinsic apoptotic effect of AZA in human ovarian tumor cells (11, 14). Thus, in this mouse model, the primary effect of the AZA-induced interferon response is through recruitment and activation of host immune cells, while AZA also causes interferon-independent signaling to inhibit tumor cell growth.

Interestingly, P53 was identified as an upstream regulator of signaling induced by AZA in immune cells. P53 and DNMTs may cooperate to regulate repetitive elements that when transcribed trigger the interferon response (43). P53 is known to transcriptionally regulate specific interferon stimulated genes, including IRF9 and TLR3. In addition, STAT1 and PKR upregulate P53, leading to transcription of pro-apoptotic genes (44). Previous work has shown upregulation of P53 through the DNA damage repair pathway by the DNMTi decitabine (45).

Thus P53 signaling may be activated by either the interferon response or DNA damage in the immune cells in question.

Others have tested whether the interferon response can play a role in sensitization to immune checkpoint blockade, as stabilization of IFNAR1 improves efficacy of anti-PD-1 therapy (46), and the loss of interferon-γ pathway genes is a mechanism of resistance to anti-CTLA-4 (47). Interferon-γ has also been shown to suppress genes related to M2-like function in macrophages (48). On the other hand, prolonged tumor interferon signaling has been shown to induce resistance to immune checkpoint blockade over time (49), implying that perhaps the timing and duration of the response is important. Our study provides a greater understanding of how interferon signaling may sensitize tumors to immune checkpoint blockade.

The AZA induced increases in immune signaling observed in ID8-VEGF-defensin mouse ovarian cancer cells are consistent with our results for AZA treated human ovarian cancer cells (11, 13). Thus, in both the human and murine tumor cells, AZA treatment leads to an increase in the expression of endogenous retroviral transcripts (ERVs), viral defense genes, cancer testis antigens and chemokines/cytokines (11, 13, 14). Chemokine CXCL10 was significantly increased in both the cell culture media of AZA treated murine cells and the ascites fluid of AZA treated mice. CXCL10 has been identified in humanized models of ovarian cancer (15), validating the relevance of the ID8-VEGF-defensin mouse model of ovarian cancer to human disease, and suggesting that these chemokines/cytokines may play a role in the AZA induced recruitment of immune cells to the tumor associated ascites (50-52). In fact, CXCL10 is linked to decreased tumor burden in the ID8 model (53).

Our work now provides mechanistic insight for previous studies showing that epigenetic agents may alter the tumor associated microenvironment to potentially sensitize tumors to

immunotherapy. Our study defines the cellular targets of AZA and HDACIs using a more comprehensive panel of immune cells and proves a requirement for Type I interferon signaling in the AZA-induced immune response. We have also shown that the addition of an HDACi to AZA can increase the activation of immune subsets, using doses of epigenetic therapy that are clinically relevant and can be immediately applied in clinical trials. The preclinical data in this manuscript helped to initiate a Celgene sponsored, phase II randomized study of pembrolizumab with or without epigenetic modulation with CC-486 (oral AZA) in patients with platinum-resistant or -refractory epithelial ovarian, fallopian tube or primary peritoneal cancer (54). This trial started enrollment December 2016 and will hopefully reveal that addition of a DNMTi to checkpoint inhibitor therapy provides benefit beyond that of immunotherapy alone. The addition of an HDACi to the DNMTi in future trials may provide more benefit, and our data suggest that this combination can most effectively decrease the immunosuppression in the ovarian tumor microenvironment to sensitize to immune checkpoint blockade therapy.

Materials and Methods

Cell culture treatments

MOSE ID8-Defb29/Vegf-a (ID8-VEGF-Defensin) cells, kindly provided by Dr. Chien-Fu Hung, Johns Hopkins Pathology, which tested negative for mycoplasm in December 2016, were grown in RPMI medium, and treated with AZA (500nM), at the same “low dose” established by Tsai et al (37). The A3 treatment paradigm had AZA in the media on days 0, 1 and 2, while the A10 paradigm was also treated with AZA on days 3, 6, 7, 8 and 9. Cells were split on days 3 and 6, and harvested on Day 10 (A3 and A10).

Entinostat (MS275) treatment followed the AZA paradigms above, but with 100nM MS275 for 3 days, or 30nM MS275 for 3 or 10 days (HDACi3 or 10).

For the sequential combination of AZA and HDACi treatment, cells were treated with the A10 paradigm described above, followed by 3 doses of 100nM MS275 or ITF. The cells were collected on day 17 (AZA17, HDACi17, and AZA+HDACi17, Figure 1A). AZA (Sigma) was suspended in 0.9% saline. Entinostat (Syndax Pharmaceuticals) and Givinostat (SelleckChem) were both suspended in DMSO and diluted 1:1000 in media, so that the percentage of DMSO did not exceed 0.1%

Gene Expression Analysis

RNA extraction, RNA quality analysis, hybridization to Agilent 4x44k Human Gene Expression v2 arrays (Agilent Technologies) and analysis of the arrays were done as previously described (13). In some cases, tumor cells were isolated from ascites fluid by FACS and RNA was isolated using the Qiagen RNeasy Micro Kit (cat. no. 74004). After total cellular RNA was extracted using the Trizol method (Life Technologies, Carlsbad, California), RNA concentration was determined using the Nanodrop machine and software (Thermo Fisher Scientific, Rockville, Maryland). 1 μg total RNA was used to generate cDNA with the QuantiTect Reverse Transcription Kit (Qiagen, Venlo, The Netherlands). Quantitative reverse transcription PCR (q-RT-PCR) of ISG15, IFIT1, and ICAM1 mRNA was performed using TaqMan assays or Custom Taqman Gene Expression Array Cards (Life Technologies, Carlsbad, California) and the Applied Biosystems 7500 Fast real-time PCR system and software. TBP and was used as a reference gene. The ΔΔCT method was used to calculate relative expression levels. Reverse transcriptase negative cDNA synthesis reactions were performed for at least one sample per plate.

Mouse endogenous retrovirus and SINE qPCR

Cells with A10 treatment were collected on days 3, 4, 7, and 10. RNAs were DNAseI treated and cDNA synthesis was performed (High-Capacity cDNA Reverse Transcription Kit, ThermoFisher). Expression of 9 mERVs genes (two IAP gag genes, an IAP-LTR, Mtv 7/8/9 sequences specific for C57Bl/6 mouse strains, and placental mERVs including syncytin-A, mErv-3, Peg11 and Mart8) and the B1 SINE gene was quantified by qPCR (ABI 7300) (see Supplemental Table 1 for primer sequences and q-PCR methodology). Mouse housekeeping genes:18S rRNA, β-actin and GAPDH were used for normalization (Supplemental Table 1). Ascites tumor cells were sorted using FACS at week 4.5 following *in vivo* AZA treatment (Figure S6A). We examined gene expression for all 9 mERVs and B1 SINE gene expression in sorted ascites tumor cells. The full qPCR protocol was previously described(55),(56).

All mouse experiments

Tumor burden was assessed via measurement of body weight and amount of ascites drained from the mice at the point where they had gained 20-30% of their body weight. Statistical outliers were removed using Pierce's criterion. Mice were cared for in accordance with the policies of the JHU ACUC. n=10 mice for all treatment groups. While each experimental group started with 10 mice, at the time ascites was drained some mice had died, and other treated mice did not have ascites yet. Furthermore, some mice only yielded enough cells to run one panel for flow cytometry, which led to decreases in mouse numbers and differences between groups in some figures.

Mouse experiments with *ex vivo* epigenetic treatment of cancer cells.

Single agent therapy: $2.5x10^5$ cells (A10) or $5x10^5$ cells (HDACi3, HDACi10, and A3) were injected i.p. into 8-10 (A10) or 6-8 (HDACi3, HDACi10, and A3) week old female C57Bl/6 mice. Immune cells were isolated from the ascites fluid via a Percoll gradient, and stained for FACS.

Combination therapy: $2.5x10^5$ cells treated with A17, HDACi17, or A+HDACi17 schedules were injected i.p. into 8-10 week old female C57Bl/6 mice. All cells from the ascites fluid were filtered and stained for FACS.

Mouse experiments with *in vivo* treatment

$2.5x10^5$ ID8-VEGF-Defensin cells were injected i.p. into 8-10 week old female C57BL/6NHsd (C57Bl/6) mice or NOD.Cg-*Prkdc*^{scid} *Il2rg*^{tm1Wjl}/SzJ (NSG) mice 3 days after injection. 0.5mg/kg AZA or saline was given i.p., for 5 days a week. The following week, 2mg/kg Givinostat or Entinostat or 1% DMSO in saline was injected i.p. for 5 days. For the rest of the experiment, the treatment alternated AZA/HDACi every other week. α-PD-1 (200ug/mouse) was given on days 17, 20, 24, and 27 after injection in the C57Bl/6 mouse experiment. α-PD-1 (1mg/mL in saline) was kindly provided by Dr. Michael Lim of the SKCCC, Johns Hopkins University, and has been described previously (57, 58). Blocking of IFNAR1 was achieved with the anti-mouse IFNAR1 antibody (clone MAR1-5A3), injected every 3 days (0.5mg/mouse)(59). Anti-IFNAR1 and the mouse IgG isotype control were purchased from Leinco Technologies and diluted in PBS.

Flow cytometry

Ascites were drained or spleens were collected from 5-10 mice per group and incubated in ACK buffer (Thermo Fisher) to lyse red blood cells for 10 minutes, then washed. Ascites from each mouse was individually lysed and prepared for flow cytometry. Mononuclear cells collected were cultured for 4 hours in RPMI with 5% Fetal Bovine Serum and in the presence of Cell Stimulation Cocktail (plus protein transport inhibitors; eBioscience). Cells were then washed and stained for cell surface markers including Live/Dead (eBioscience), CD45 (BD Biosciences), CD3 (BD Biosciences), CD4 (BD Biosciences), CD8 (BD Biosciences), PD-1 (eBioscience), NK1.1 (BD Biosciences), F4/80 (Biolegend), MHC II (Biolegend, Isotype Control #400627), GR1 (Biolegend, Isotype Control #400635), and CD11b (Biolegend). After incubation, the cells were permeabilized (FoxP3 staining buffers, eBioscience). Intracellular staining was performed for FoxP3 (eBioscience, Isotype Control #12-4321) and IFNγ (BD Biosciences, Isotype Control #554686). Flow cytometry acquisition was performed on an LSRII cytometer (BD Biosciences) and data were analyzed using FlowJo software version 10.2.

Chemokine and Cytokine Array

Cultured cells were treated with an A10 treatment schedule and media was collected at day 10. Ascites from mice treated with AZA as described above was collected at week 4 after injection of cells. Cells were removed from ascites and supernatant collected. Media and ascites samples were analyzed with the Proteome Profile Array, Mouse Cytokine Panel A (R&D Systems) according to manufacturer instructions.

Cell Cycle and Apoptotic Analysis

Cells were treated with an A10 treatment schedule and collected on Days 3 and 10. For cell cycle analysis, BrdU (10uM, Sigma) was incubated with cells for 2 hours. Cells were fixed, treated with DNase (300ug/mL), and stained with anti-BrdU (Biolegend) and 7-AAD (Life Technologies). For apoptosis analysis, cells were stained for FACS and were measured as apoptotic based on positive Annexin V (eBioscience) and 7-AAD (Life Technologies) staining. Flow cytometry was performed on a FACS Calibur cytometer (BD Biosciences) and data were analyzed with FlowJo V10 software.

Western Blots

Protein extracts were quantified and immunoblotted using the 4%–20% Mini-PROTEAN TGX gel system (Bio-Rad) and PVDF membranes (Millipore). β-actin or GAPDH was used as a loading control. Antibodies used were as follows: polyclonal rabbit anti-mouse cleaved PARP (Cell Signaling, 1:1000), polyclonal rabbit anti-DNMT1 (Sigma, 1:1000), mouse anti-β-Actin (Sigma, 1:10,000), and polyclonal rabbit anti-GAPDH (Trevigen, 1:10,000). Band intensities were quantified using the program Adobe Photoshop Elements 6.0.

RNA extraction and sequencing library generation for immune cells

$CD8^+$ and $CD4^+$ T cells and $CD11b^+$ myeloid cells were sorted using a FACS Aria II from ascites derived from mock and AZA treated mice. Approximately 10,000 cells were collected for each sorted population, based on viability, size- and lineage-exclusion. Cells were pelleted at 300 x g for 10 mins. The supernatant was carefully removed and 100 µL of Arcturus PicoPure extraction buffer (ThermoFisher Scientific) was added. Total RNA was extracted using Arcturus PicoPure RNA isolation kit according to the manufacturer's protocol. Low-input RNA

sequencing libraries were generated from 200 pg of total RNA using SMART-seq v4 Ultra Low Input RNA kit (Clontech). All samples were subjected to 13 PCR amplification cycles to minimize PCR biases. Amplified cDNA libraries were later fragmented through sonication to obtain 200 – 500 bp fragments. Standard Illumina sequencing libraries were prepared using Rubicon ThruPLEX DNA-seq kit (Rubicon Genomics) according to manufacturer's protocol. Sample barcoded libraries were sequenced on Illumina's NextSeq 500 instrumentation using NextSeq 300 Cycle Kit, High Output, V1 reagents (Illumina) and data analysis workflow, bcl2fastq -v2.17.1.14, to obtain 150 bp paired-end reads.

Paired-end RNA sequencing reads were trimmed to remove Illumina's adapter sequences. Sequencing reads were further processed to remove poor quality reads and/or reads mapping to mouse rRNA and tRNA sequences using ArrayStudio package (www.omicsoft.com/array-studio). Following criteria was used to remove poor quality reads: Trim reads with base quality score (Sanger Quality Score) <10; Filter out reads if trim length is < 25 bp; Filter out reads if maximal base quality score is < 15, Filter out reads if average quality score is < 10; Filter out reads if poly AGCT rate is >= 80%; Filter out the pair if either read fails the filtering criteria. Sequencing reads were aligned to the mouse reference genome (Build38) using OSA version 4 (PMID: 22592379). To obtain transcript counts data, RSEM package (PMID: 21816040) and NCBI mouse RefSeq gene model (release July 2015) annotations were used. Transcripts with zero counts in more than two third of the samples were discarded from downstream analysis to reduce noise in the expression data. Filtered counts data was later normalized using quantile normalization and differentially expressed transcripts were identified using Limma Voom (PMID: 24485249). A p-value cutoff of 0.05 was used to classify transcripts as differentially expressed in treatment condition. Upstream regulator and pathway analyses on

differentially expressed transcripts were performed using QIAGEN's Ingenuity Pathway Analysis (www.qiagen.com/ingenuity).

Statistical Analysis

Data was graphed in GraphPad PRISM 5.0, and significance was determined by a Mann-Whitney t-test or by multiple pairwise comparisons using the one-way ANOVA test with Bonferroni Correction. Significances in survival data were determined by Mantel-cox (log rank) test. Differences were deemed significant with a p-value of less than 0.05. Outliers were removed from ascites volume data sets and ascites immune cell data sets using the Peirce's Criterion (60) Significances are shown with $p<0.05$ (*); $p<0.01$ (**) or $p<0.001$ (***).

Footnotes: To whom correspondence should be addressed: zahnoci@jhmi.edu

Acknowledgements: The authors would like to acknowledge Ada Tam for her help with flow cytometry, Peter Ordentlich from Syndax Pharmaceuticals for generously providing Entinostat, and Robert Schreiber of the Washington University in St. Louis School of Medicine for assistance in obtaining the IFNAR1 blocking antibody. We also greatly acknowledge Mrs. Elizabeth Stiegler for her expert technical assistance. This work was supported by the Defense Health Program, through the Department of Defense Ovarian Cancer Research Program, Teal Innovator Award under Award No. OC130454 / W81XWH-14-1-0385. Opinions, interpretations, conclusions and recommendations are those of the author and no necessarily endorsed by the Department of Defense. Research reported in this publication was supported by the National Cancer Institute under award number P30CA006973. The content is solely the

responsibility of the authors and does not necessarily represent the official views of the National Institutes of Health. This work was also supported in part by Janssen, the SWCRF Collaboration for a Cure Grant, the Irving Hansen Fund, and the Dr. Miriam and Sheldon G. Adelson Medical Research Foundation.

References

1. Siegel RL, Miller KD, & Jemal A (2016) Cancer statistics, 2016. *CA Cancer J Clin* 66(1):7-30.
2. Preston CC, Goode EL, Hartmann LC, Kalli KR, & Knutson KL (2011) Immunity and immune suppression in human ovarian cancer. *Immunotherapy* 3(4):539-556.
3. Chester C, Dorigo O, Berek JS, & Kohrt H (2015) Immunotherapeutic approaches to ovarian cancer treatment. *J Immunother Cancer* 3:7.
4. Brahmer JR*, et al.* (2012) Safety and activity of anti-PD-L1 antibody in patients with advanced cancer. *N Engl J Med* 366(26):2455-2465.
5. Juergens RA*, et al.* (2011) Combination epigenetic therapy has efficacy in patients with refractory advanced non-small cell lung cancer. *Cancer Discov* 1(7):598-607.
6. Arrowsmith CH, Bountra C, Fish PV, Lee K, & Schapira M (2012) Epigenetic protein families: a new frontier for drug discovery. *Nature reviews. Drug discovery* 11(5):384-400.
7. Zahnow CA*, et al.* (2016) Inhibitors of DNA Methylation, Histone Deacetylation, and Histone Demethylation: A Perfect Combination for Cancer Therapy. *Adv Cancer Res* 130:55-111.
8. Allis CD, Caparros M-L, Jenuwein T, Reinberg D, & Lachlan M (2015) *Epigenetics* (Cold Spring Harbor Laboratory Press) Second Edition Ed.
9. Cameron EE, Bachman KE, Myohanen S, Herman JG, & Baylin SB (1999) Synergy of demethylation and histone deacetylase inhibition in the re-expression of genes silenced in cancer. *Nat Genet* 21(1):103-107.
10. Wrangle J*, et al.* (2013) Alterations of immune response of Non-Small Cell Lung Cancer with Azacytidine. *Oncotarget* 4(11):2067-2079.
11. Chiappinelli KB*, et al.* (2015) Inhibiting DNA Methylation Causes an Interferon Response in Cancer via dsRNA Including Endogenous Retroviruses. *Cell* 162(5):974-986.
12. Matei D*, et al.* (2012) Epigenetic resensitization to platinum in ovarian cancer. *Cancer Res* 72(9):2197-2205.
13. Li H*, et al.* (2014) Immune regulation by low doses of the DNA methyltransferase inhibitor 5-azacitidine in common human epithelial cancers. *Oncotarget* 5(3):587-598.
14. Roulois D*, et al.* (2015) DNA-Demethylating Agents Target Colorectal Cancer Cells by Inducing Viral Mimicry by Endogenous Transcripts. *Cell* 162(5):961-973.
15. Peng D*, et al.* (2015) Epigenetic silencing of TH1-type chemokines shapes tumour immunity and immunotherapy. *Nature* 527(7577):249-253.
16. Ghoneim HE*, et al.* (2017) De Novo Epigenetic Programs Inhibit PD-1 Blockade-Mediated T Cell Rejuvenation. *Cell*.
17. Conejo-Garcia JR*, et al.* (2004) Tumor-infiltrating dendritic cell precursors recruited by a beta-defensin contribute to vasculogenesis under the influence of Vegf-A. *Nat Med* 10(9):950-958.

18. Hung CF, *et al.* (2007) Vaccinia virus preferentially infects and controls human and murine ovarian tumors in mice. *Gene Ther* 14(1):20-29.
19. Zhang L, *et al.* (2002) Generation of a syngeneic mouse model to study the effects of vascular endothelial growth factor in ovarian carcinoma. *Am J Pathol* 161(6):2295-2309.
20. Roby KF, *et al.* (2000) Development of a syngeneic mouse model for events related to ovarian cancer. *Carcinogenesis* 21(4):585-591.
21. Duraiswamy J, Freeman GJ, & Coukos G (2013) Therapeutic PD-1 pathway blockade augments with other modalities of immunotherapy T-cell function to prevent immune decline in ovarian cancer. *Cancer Res* 73(23):6900-6912.
22. Lee Y, *et al.* (2007) A candidate precursor to serous carcinoma that originates in the distal fallopian tube. *J Pathol* 211(1):26-35.
23. Singh N, *et al.* (2016) Primary site assignment in tubo-ovarian high-grade serous carcinoma: Consensus statement on unifying practice worldwide. *Gynecol Oncol* 141(2):195-198.
24. Perets R, *et al.* (2013) Transformation of the fallopian tube secretory epithelium leads to high-grade serous ovarian cancer in Brca;Tp53;Pten models. *Cancer Cell* 24(6):751-765.
25. Sherman-Baust CA, *et al.* (2014) A genetically engineered ovarian cancer mouse model based on fallopian tube transformation mimics human high-grade serous carcinoma development. *J Pathol* 233(3):228-237.
26. Walton J, *et al.* (2016) CRISPR/Cas9-Mediated Trp53 and Brca2 Knockout to Generate Improved Murine Models of Ovarian High-Grade Serous Carcinoma. *Cancer Res* 76(20):6118-6129.
27. Hata K, Watanabe Y, Nakai H, Hata T, & Hoshiai H (2011) Expression of the vascular endothelial growth factor (VEGF) gene in epithelial ovarian cancer: an approach to anti-VEGF therapy. *Anticancer Res* 31(2):731-737.
28. Li Z, *et al.* (2016) The inflammatory microenvironment in epithelial ovarian cancer: a role for TLR4 and MyD88 and related proteins. *Tumour Biol* 37(10):13279-13286.
29. Janat-Amsbury MM, Yockman JW, Anderson ML, Kieback DG, & Kim SW (2006) Comparison of ID8 MOSE and VEGF-modified ID8 cell lines in an immunocompetent animal model for human ovarian cancer. *Anticancer Res* 26(4B):2785-2789.
30. Baert T, *et al.* (2015) The dark side of ID8-Luc2: pitfalls for luciferase tagged murine models for ovarian cancer. *J Immunother Cancer* 3:57.
31. Peter S, Bak G, Hart K, & Berwin B (2009) Ovarian tumor-induced T cell suppression is alleviated by vascular leukocyte depletion. *Transl Oncol* 2(4):291-299.
32. Abiko K, *et al.* (2013) PD-L1 on tumor cells is induced in ascites and promotes peritoneal dissemination of ovarian cancer through CTL dysfunction. *Clin Cancer Res* 19(6):1363-1374.
33. Wei H, *et al.* (2013) Combinatorial PD-1 blockade and CD137 activation has therapeutic efficacy in murine cancer models and synergizes with cisplatin. *PLoS One* 8(12):e84927.
34. Ostrand-Rosenberg S & Sinha P (2009) Myeloid-derived suppressor cells: linking inflammation and cancer. *J Immunol* 182(8):4499-4506.
35. Bingle L, Brown NJ, & Lewis CE (2002) The role of tumour-associated macrophages in tumour progression: implications for new anticancer therapies. *J Pathol* 196(3):254-265.
36. Shultz LD, Ishikawa F, & Greiner DL (2007) Humanized mice in translational biomedical research. *Nat Rev Immunol* 7(2):118-130.
37. Tsai HC, *et al.* (2012) Transient low doses of DNA-demethylating agents exert durable antitumor effects on hematological and epithelial tumor cells. *Cancer Cell* 21(3):430-446.
38. Weller EM, Poot M, & Hoehn H (1993) Induction of replicative senescence by 5-azacytidine: fundamental cell kinetic differences between human diploid fibroblasts and NIH-3T3 cells. *Cell Prolif* 26(1):45-54.

39. Alexander VM, Roy M, Steffens KA, Kunnimalaiyaan M, & Chen H (2010) Azacytidine induces cell cycle arrest and suppression of neuroendocrine markers in carcinoids. *Int J Clin Exp Med* 3(2):95-102.
40. Liu M*, et al.* (2016) Vitamin C increases viral mimicry induced by 5-aza-2'-deoxycytidine. *Proc Natl Acad Sci U S A* 113(37):10238-10244.
41. Janat-Amsbury MM, Yockman JW, Anderson ML, Kieback DG, & Kim SW (2006) Combination of local, non-viral IL12 gene therapy and systemic paclitaxel chemotherapy in a syngeneic ID8 mouse model for human ovarian cancer. *Anticancer Res* 26(5A):3223-3228.
42. West AC*, et al.* (2013) An intact immune system is required for the anticancer activities of histone deacetylase inhibitors. *Cancer Res* 73(24):7265-7276.
43. Leonova KI*, et al.* (2013) p53 cooperates with DNA methylation and a suicidal interferon response to maintain epigenetic silencing of repeats and noncoding RNAs. *Proc Natl Acad Sci U S A* 110(1):E89-98.
44. Muller PA & Vousden KH (2013) p53 mutations in cancer. *Nat Cell Biol* 15(1):2-8.
45. Karpf AR, Moore BC, Ririe TO, & Jones DA (2001) Activation of the p53 DNA damage response pathway after inhibition of DNA methyltransferase by 5-aza-2'-deoxycytidine. *Mol Pharmacol* 59(4):751-757.
46. Katlinski KV*, et al.* (2017) Inactivation of Interferon Receptor Promotes the Establishment of Immune Privileged Tumor Microenvironment. *Cancer Cell* 31(2):194-207.
47. Gao J*, et al.* (2016) Loss of IFN-gamma Pathway Genes in Tumor Cells as a Mechanism of Resistance to Anti-CTLA-4 Therapy. *Cell* 167(2):397-404 e399.
48. Kang K*, et al.* (2017) Interferon-gamma Represses M2 Gene Expression in Human Macrophages by Disassembling Enhancers Bound by the Transcription Factor MAF. *Immunity* 47(2):235-250 e234.
49. Benci JL*, et al.* (2016) Tumor Interferon Signaling Regulates a Multigenic Resistance Program to Immune Checkpoint Blockade. *Cell* 167(6):1540-1554 e1512.
50. Carr MW, Roth SJ, Luther E, Rose SS, & Springer TA (1994) Monocyte chemoattractant protein 1 acts as a T-lymphocyte chemoattractant. *Proc Natl Acad Sci U S A* 91(9):3652-3656.
51. Xu LL, Warren MK, Rose WL, Gong W, & Wang JM (1996) Human recombinant monocyte chemotactic protein and other C-C chemokines bind and induce directional migration of dendritic cells in vitro. *J Leukoc Biol* 60(3):365-371.
52. Dufour JH*, et al.* (2002) IFN-gamma-inducible protein 10 (IP-10; CXCL10)-deficient mice reveal a role for IP-10 in effector T cell generation and trafficking. *J Immunol* 168(7):3195-3204.
53. K KA*, et al.* (2017) CXCL10 alters the tumour immune microenvironment and disease progression in a syngeneic murine model of high-grade serous ovarian cancer. *Gynecol Oncol*.
54. Fresco R, Glaspy J, & Palodichuk C (2016) Phase II Randomized Study of Pembrolizumab With or Without Epigenetic Modulation With CC-486 in Patients With Platinum-resistant Epithelial Ovarian, Fallopian Tube or Primary Peritoneal Cancer, NCT02900560. (Bethesda (MD): National Library of Medicine (US). ClinicalTrials.gov).
55. Henke C*, et al.* (2013) Regulation of murine placentogenesis by the retroviral genes Syncytin-A, Syncytin-B and Peg10. *Differentiation* 85(4-5):150-160.
56. Henke C*, et al.* (2015) Selective expression of sense and antisense transcripts of the sushi-ichi-related retrotransposon--derived family during mouse placentogenesis. *Retrovirology* 12:9.
57. Mathios D*, et al.* (2016) Anti-PD-1 antitumor immunity is enhanced by local and abrogated by systemic chemotherapy in GBM. *Sci Transl Med* 8(370):370ra180.
58. Hirano F*, et al.* (2005) Blockade of B7-H1 and PD-1 by monoclonal antibodies potentiates cancer therapeutic immunity. *Cancer Res* 65(3):1089-1096.

59. Swann JB*, et al.* (2007) Type I IFN contributes to NK cell homeostasis, activation, and antitumor function. *J Immunol* 178(12):7540-7549.
60. Ross SM (2003) Peirce's criterion for the elimination of suspect experimental data. *Journal of Engineering Technology* 20(2):38-41.
61. Munclinger P, Boursot P, & Dod B (2003) B1 insertions as easy markers for mouse population studies. *Mamm Genome* 14(6): 359-366.

Figure Legends

Figure 1: Pretreatment of tumor epithelial cells with AZA and transplantation into untreated C57Bl/6 mice leads to decreased tumor associated ascites and increased overall survival. A) Treatment schematic for *in vitro* treatment of cultured ID8-VEGF-Defensin cells (AZA 500nM, MS275 30nM or 100nM, ITF 100nM).(A= AZA, MS=Entinostat, ITF= Givinostat) **B-C)** Ascites volume drained from mice 4-5 weeks after pre-treated tumor injection. Mean+SEM is shown. A10, MS3, MS10: n=7-30 mice, 3 biological replicates; A3-10: n=9 mice, 2 biological replicates; MS17, ITF17, A17, A+MS17, and A+ITF17 n=9-10 mice, 1 biological replicate. Statistical outliers were removed using Pierce's criterion, and significance was determined by a Mann-Whitney t-test. **D)** Survival of mice in days, with median survival shown. Significance was determined using a log rank (Mantel-Cox) test.

Figure 2: Pretreatment of tumor epithelial cells with AZA and an HDACi lead to alterations in the numbers and activation of immune cell populations in tumor associated ascites. ID8-Vegf-Defensin cells were pretreated, AZA (A) 500nM, Entinostat (MS, MS275) 30nM or 100nM, Givinostat (ITF) 100nM, and injected into mice. Cells were analyzed from the drained ascites fluid (Figure 1A-C). **A)** Immune cells/mL separated via Percoll gradient (n=6-12 mice, 2-3 biological replicates). **B)** $CD45^+$cells/mL identified via Percoll gradient and FACS (n=6-11 mice, 2 biological replicates). Mean+SEM is shown in A-B, and significances are determined by Mann-Whitney t-test. **C-J)** All cells from ascites were analyzed via FACS (n=5-9

mice, 1 biological replicate). Mean+SEM is shown and significances are determined by one-way ANOVA. **C)** CD45+ cells/mL of ascites. **D-J)** Response of immune cell subpopulations to tumor cells pretreated *ex vivo* with AZA (A10).

Figure 3: The addition of immune checkpoint inhibition to epigenetic therapy in an intact mouse model decreases tumor burden and increases survival. A) *In vivo* treatment schematic of AZA (A, 05.mg/kg), Entinostat (MS, 2mg/kg), Givinostat (ITF, 2mg/kg) and α-PD-1 (200ug/mouse). **B)** Volume of ascites fluid drained at week 6. Mean+SEM is shown and significances are determined by one-way ANOVA. All significances are compared to Mock, *=p<0.05, **=p<0.01, ***=p<0.00.1 n=8-10 mice per group. **C-F)** Survival of the mice in days, with median survival shown**.** Significances are determined by log rank (Mantel Cox) test n=10 mice per group.

Figure 4: Epigenetic therapy and α-PD-1 increases the number and activation of immune cells in the tumor microenvironment. Mice were treated as described in Figure 3A. Cells from ascites fluid drained at week 6.5 were analyzed via FACS. Median, 25^{th} and 75^{th} percentiles, and range are plotted for each experimental arm and significances are determined by Mann Whitney T test. Significances compared to Mock are marked with *, and significances compared to AZA are marked with #. */#-p<0.05, **/##-p<0.01, ***/###-p<0.001. **A)** %T effector cells ($CD8^+IFN\gamma^+$) of T cells. **B)** %T helper cells ($CD4^+IFN\gamma^+$) of T cells. **C)** % activated NK cells ($NK1.1^+$, $IFN\gamma^+$) of $NK1.1^+$ cells; **D)** %Myeloid derived suppressor cells ($GR\text{-}1^+$, $CD11b^+$, $F4/80^-$, $MHCII^-$) of $CD45^+$ cells; **E)** %Macrophages ($CD11b^+$, $F4/80^+$) of $CD45^+$ cells. **F)** %$CD3^+$ T cells of $CD45^+$ cells. **A, B, C, F)** n=4-9 mice per group. **D, E)** n=2-9 mice per group.

Figure 5: Blockade of IFNAR1 inhibits the actions of AZA. A) Treatment schematic for the mice. Mice were treated with AZA (0.5mg/kg) or saline as described in Figure 3. Anti-IFNAR1 was injected i.p. (0.5 mg/mouse) every three days, beginning one day before the AZA regimen. **B)** Volume of ascites drained from the mice at week 4.5. Mean+SEM is shown and significances are determined by Mann-Whitney T-test. n=8-10 mice per group. **C)** Survival of the mice in days, with median survival shown**.** Significances are determined by log rank (Mantel Cox) test. n=10 mice per group. **D-F)** Median, 25^{th} and 75^{th} percentiles, and range are plotted, and significances are determined by Mann-Whitney T-test. n=6-9 mice per group. **D)** $CD45^+$ cells/mL of ascites. **E)** %T effector cells ($CD8^+IFN\gamma^+$) of $CD3^+$ T cells. **F)** % activated NK cells ($NK1.1^+$, $IFN\gamma^+$) of $NK1.1^+$ cells.

Figure 6: AZA+HDACi combination therapy is less effective at reducing tumor burden and increasing survival in an immunodeficient mouse model. A) Treatment schematic for *in vivo* treatment of NSG mice with AZA (A) and HDACIs Entinostat (MS) or Givinostat (ITF). **B)** Fold change in ascites volume drained at week 5.5 (NSG) or 6 (C57Bl/6). The C57Bl/6 data from Figure 3A is shown here for direct comparison. n=3-10 mice per group. **C)** NSG mice survival in days, with median survival shown. Significances are determined by a log rank (Mantel Cox) test. n=10 mice per group. **D)** Ascites volume drained at week 4.5 or 4 from C57Bl/6 or NSG mice, respectively, treated with AZA and anti-IFNAR1 as shown in Fig. 5A and B. n=8-10 mice per group. **E)** % dead, $CD45^-$, non-immune ascites cells (Live/dead $stain^+$, $CD45^-$) from the NSG ascites fluid. n=5-10 mice per group. **B, D, E)** Mean+SEM is shown and significances are determined by a Mann-Whitney t-test.

804

805 **Figure 7: Ex vivo treatment of ID8-VEGF-Defensin cells with low dose AZA decreases**
806 **viable cell number, increases apoptosis, and disrupts the cell cycle. A)** 3 or 10 day *in vitro*
807 treatment with 500nM AZA. **B)** Total number of cells relative to mock. n=3. **C)** Quantification
808 of c-PARP levels in AZA treated cells relative to Mock. n=3. **D)** A representative western blot
809 of c-PARP levels. **E-F)** Percentage of annexin V^+ and 7-AAD^+ apoptotic cells. Representative
810 flow cytometry data is shown (E) along with quantification (F). n=3. **G-H)** Cell cycle analysis,
811 determined by BrdU incorporation and 7-AAD staining of DNA content. n=3. Mean+SEM is
812 shown, and significances are determined by Mann-Whitney t-tests.

Figure 1: *Ex vivo* treatment of tumor cells

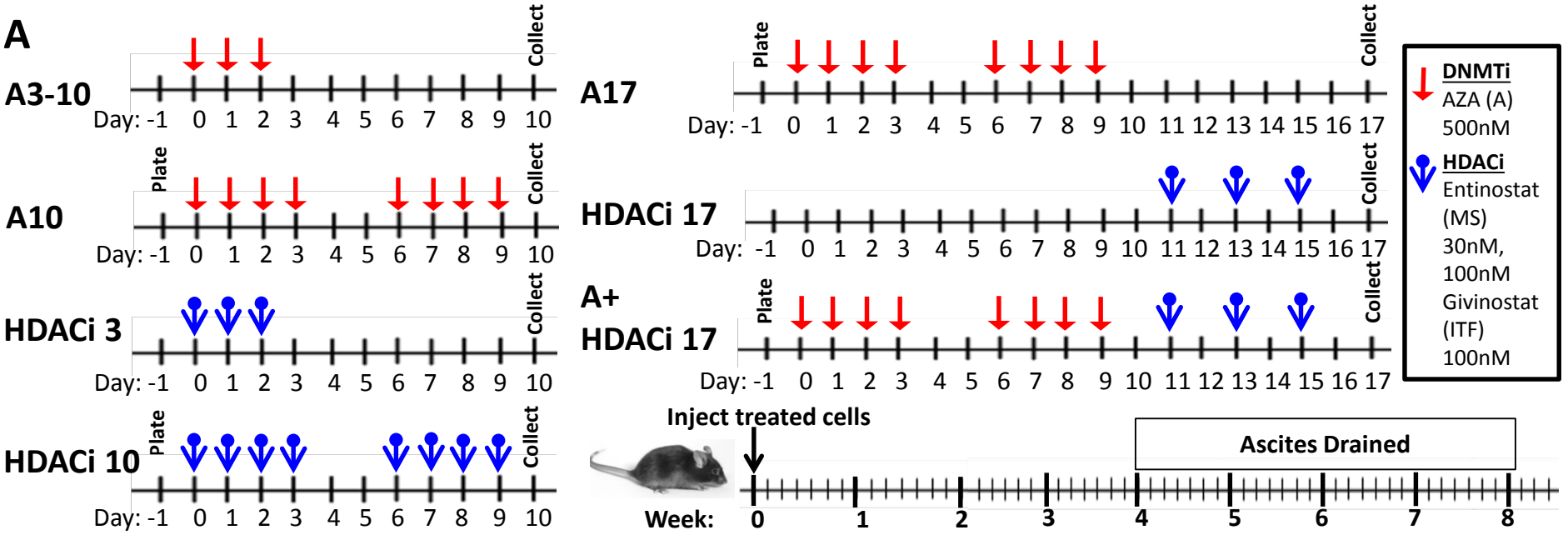

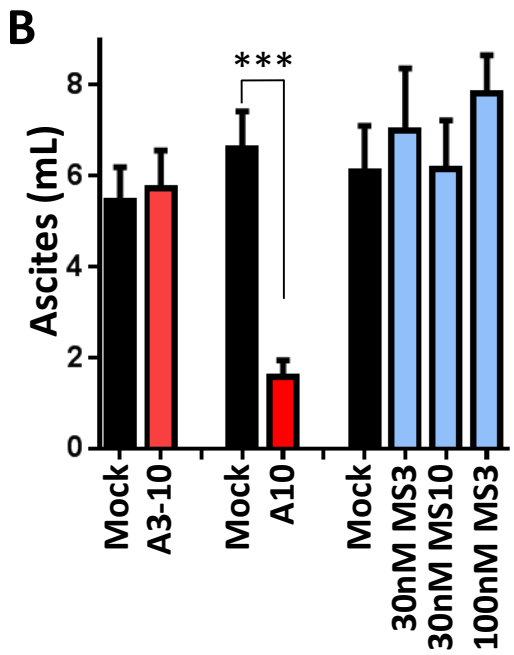

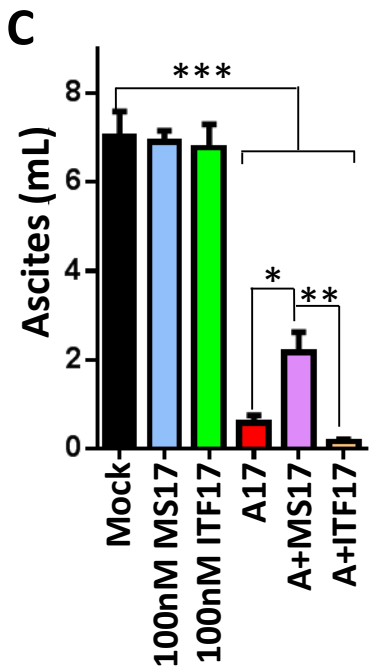

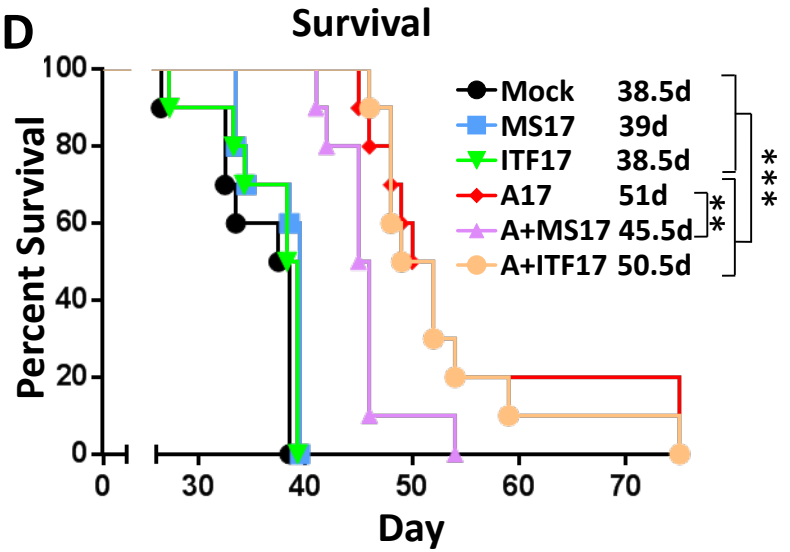

Figure 2: *Ex vivo* treatment of tumor cells

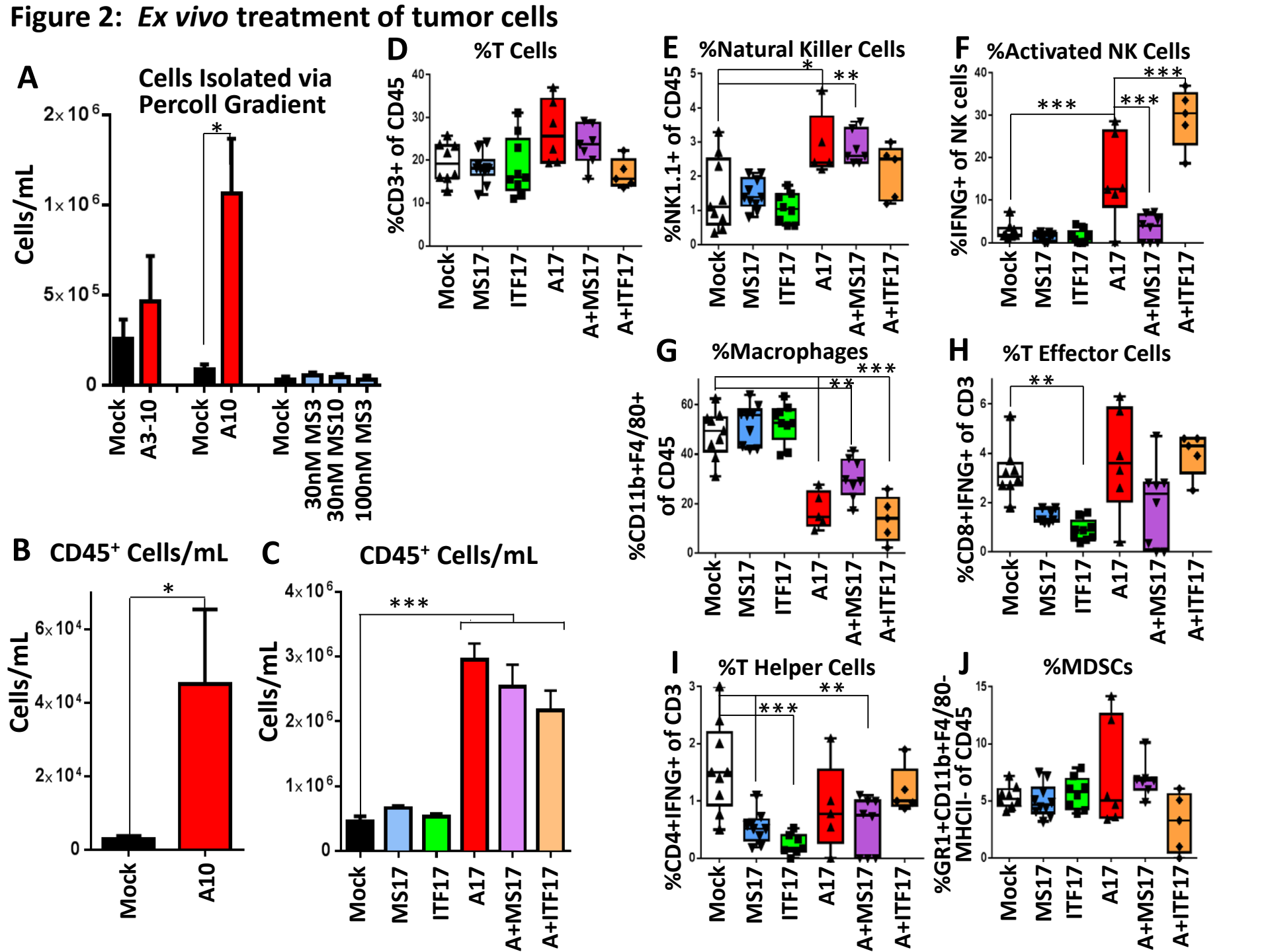

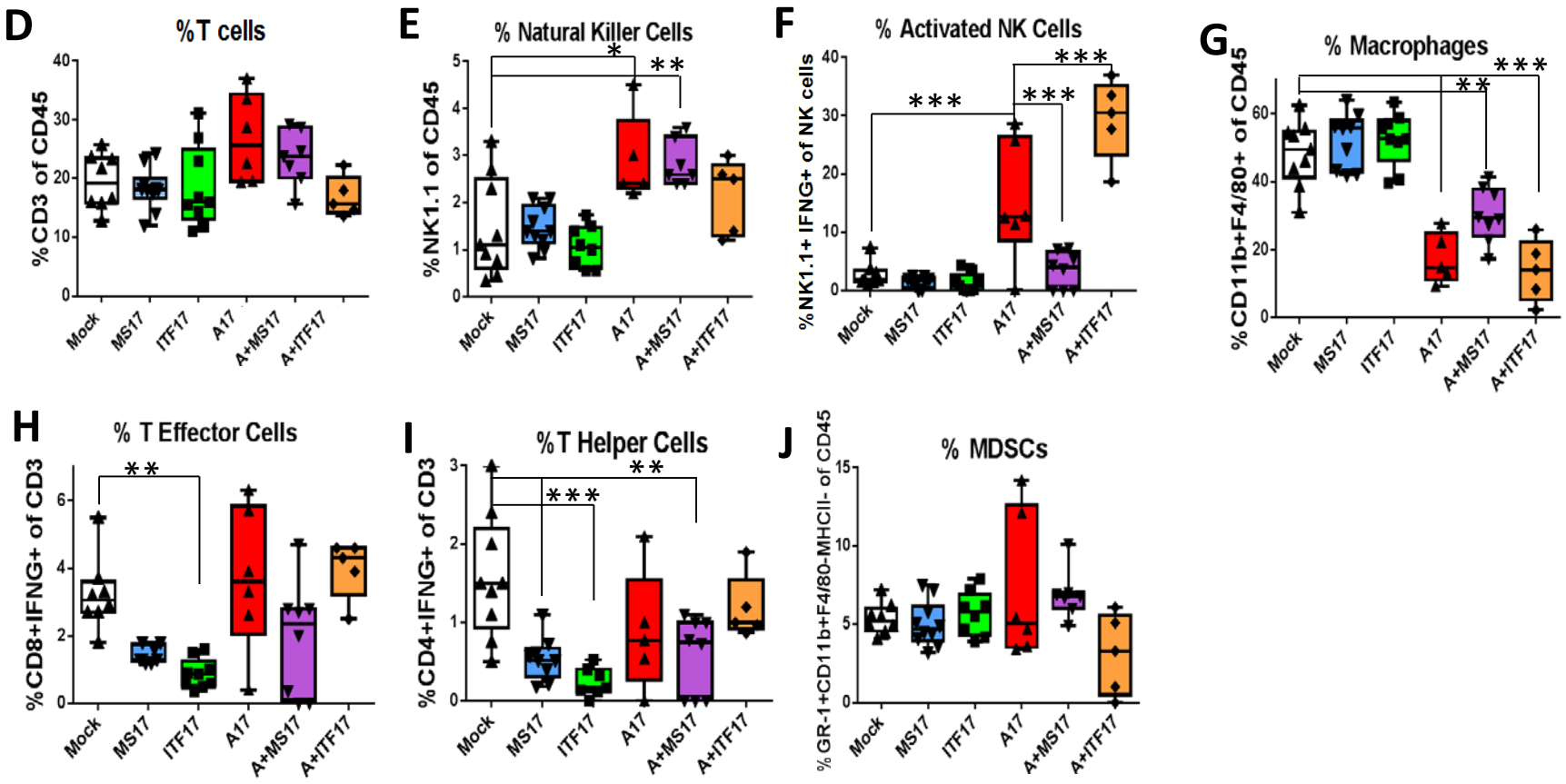
D
%T cells
% CD3 of CD45
Mock
MS17
ITF17
A17
A+MS17
A+ITF17
E
% Natural Killer Cells
% NK1.1 of CD45
*
**
F
% Activated NK Cells
% NK1.1+ IFNG+ of NK cells
***
***
***
G
% Macrophages
% CD11b+F4/80+ of CD45
**
***
H
% T Effector Cells
%CD8+IFNG+ of CD3
**
I
%T Helper Cells
%CD4+IFNG+ of CD3
**
***
J
% MDSCs
% GR-1+CD11b+F4/80-MHCII- of CD45

Figure 3

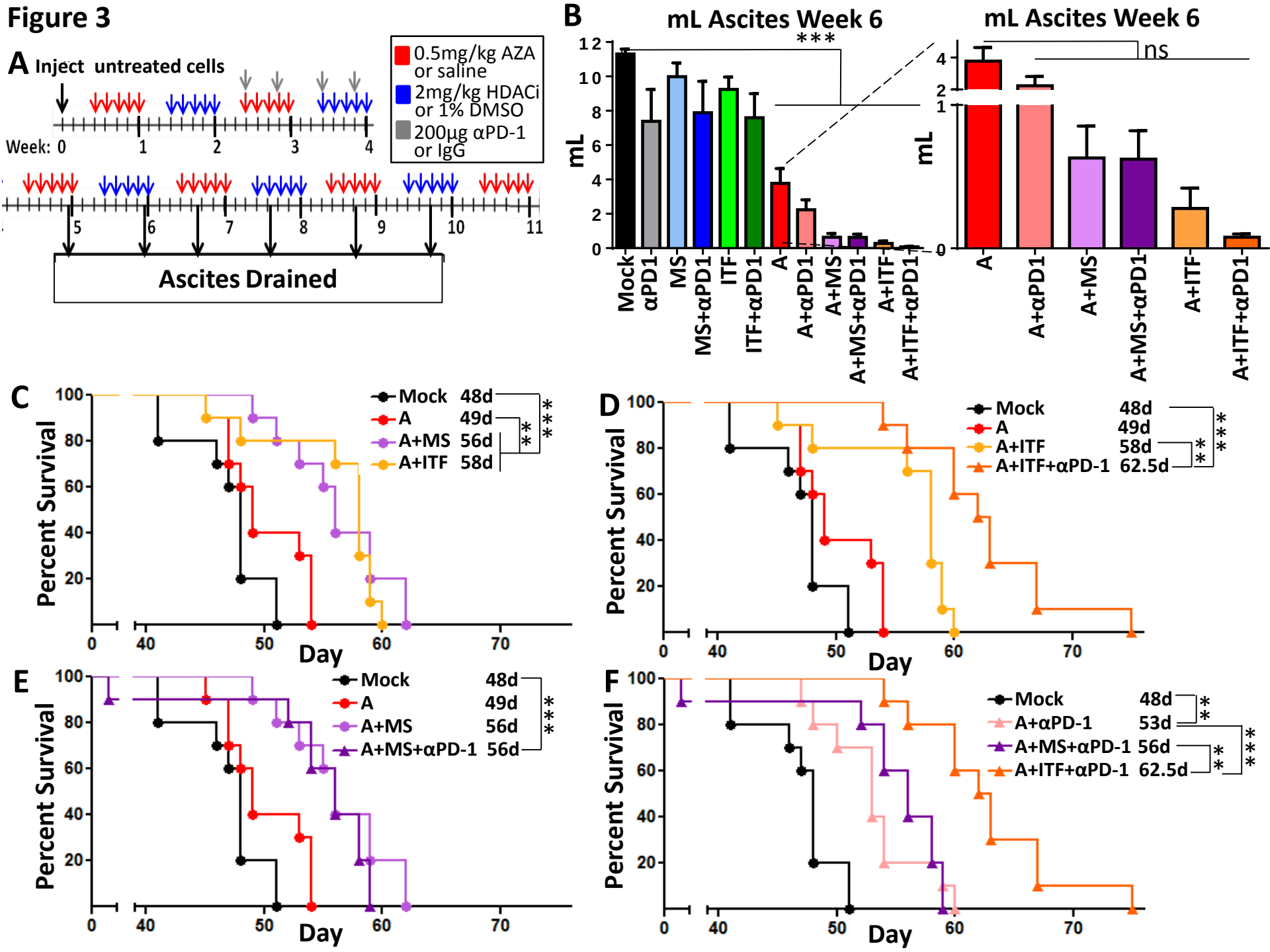
A
Inject untreated cells
0.5mg/kg AZA or saline
2mg/kg HDACi or 1% DMSO
200µg αPD-1 or IgG
Week: 0 1 2 3 4
5 6 7 8 9 10 11
Ascites Drained
B
mL Ascites Week 6
***
ns
mL
Mock
αPD1
MS
MS+αPD1
ITF
ITF+αPD1
A
A+αPD1
A+MS
A+MS+αPD1
A+ITF
A+ITF+αPD1
C
Percent Survival
Day
Mock 48d
A 49d
A+MS 56d
A+ITF 58d
D
Mock 48d
A 49d
A+ITF 58d
A+ITF+αPD-1 62.5d
E
Mock 48d
A 49d
A+MS 56d
A+MS+αPD-1 56d
F
Mock 48d
A+αPD-1 53d
A+MS+αPD-1 56d
A+ITF+αPD-1 62.5d

Figure 4

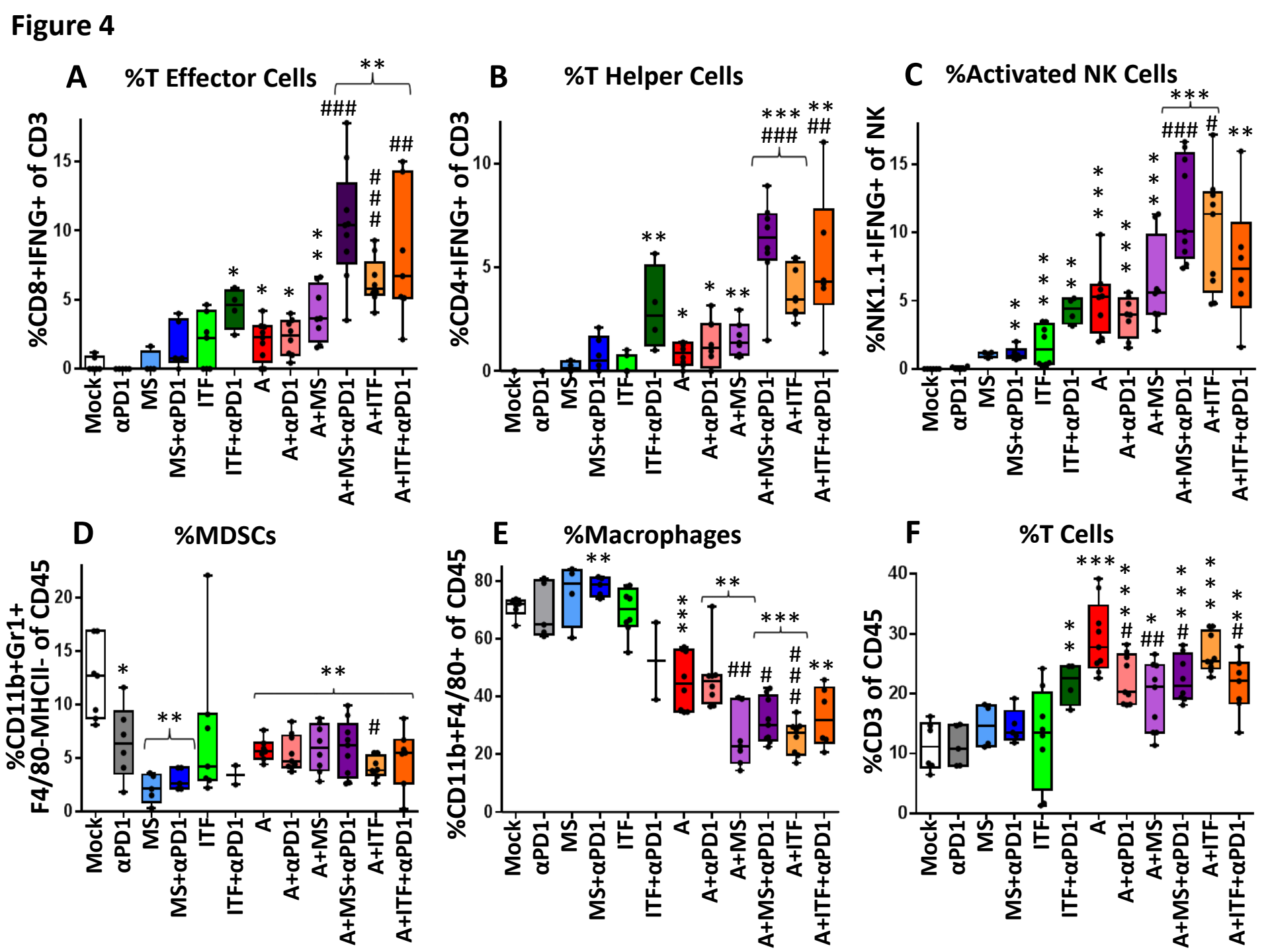
A
%T Effector Cells
%CD8+IFNG+ of CD3
B
%T Helper Cells
%CD4+IFNG+ of CD3
C
%Activated NK Cells
%NK1.1+IFNG+ of NK
D
%MDSCs
%CD11b+Gr1+ F4/80-MHCII- of CD45
E
%Macrophages
%CD11b+F4/80+ of CD45
F
%T Cells
%CD3 of CD45
Mock
αPD1
MS
MS+αPD1
ITF
ITF+αPD1
A
A+αPD1
A+MS
A+MS+αPD1
A+ITF
A+ITF+αPD1

Figure 5

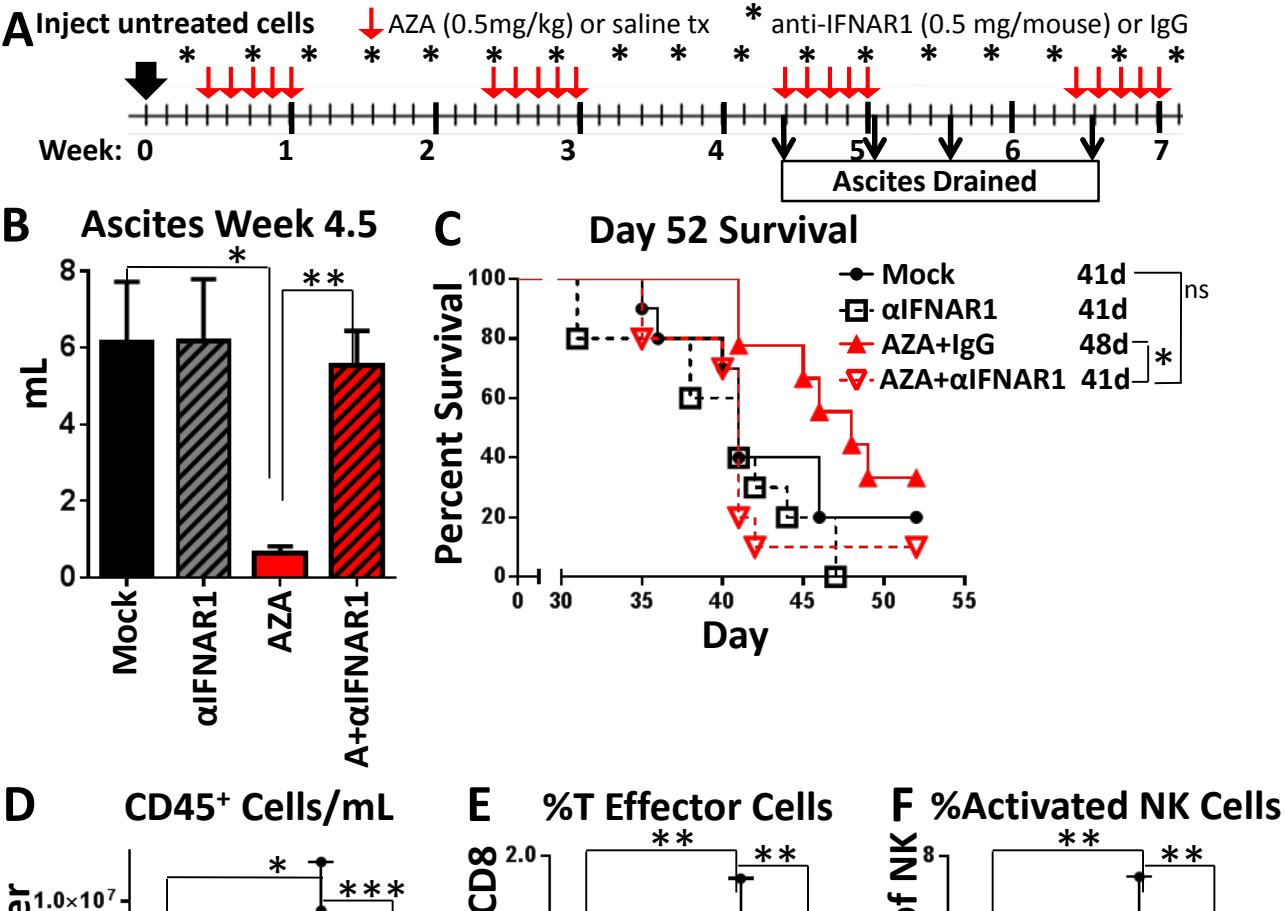
A
Inject untreated cells
AZA (0.5mg/kg) or saline tx
anti-IFNAR1 (0.5 mg/mouse) or IgG
Week: 0 1 2 3 4 5 6 7
Ascites Drained
B
Ascites Week 4.5
mL
Mock
αIFNAR1
AZA
A+αIFNAR1
C
Day 52 Survival
Percent Survival
Day
Mock 41d
αIFNAR1 41d
AZA+IgG 48d
AZA+αIFNAR1 41d
ns
D
CD45+ Cells/mL
Cell Number
E
%T Effector Cells
%CD8+IFNG+ of CD8
F
%Activated NK Cells
%NK1.1+IFNG+ of NK

Figure 6

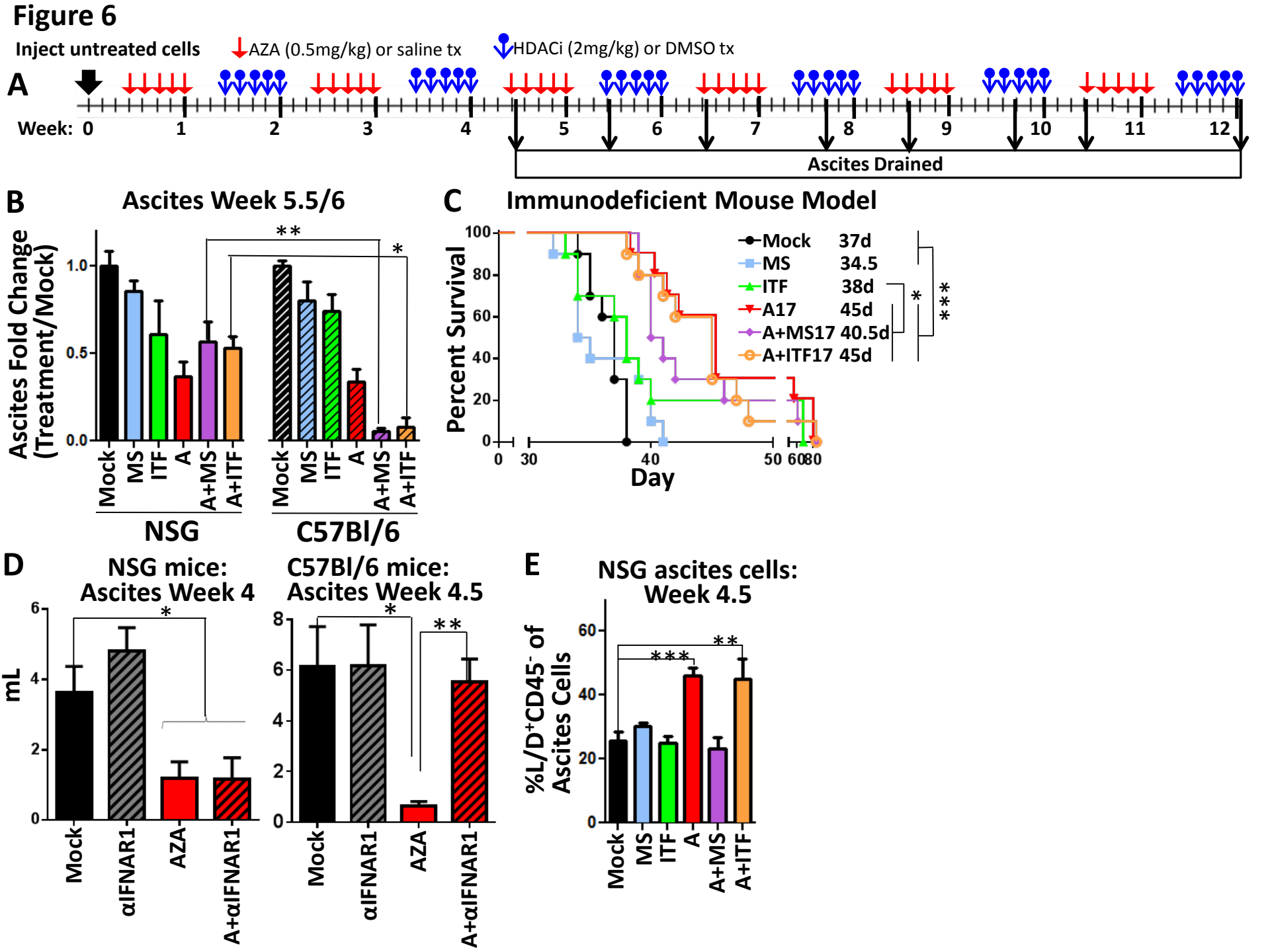
Inject untreated cells
AZA (0.5mg/kg) or saline tx
HDACi (2mg/kg) or DMSO tx
A
Week: 0 1 2 3 4 5 6 7 8 9 10 11 12
Ascites Drained
B
Ascites Week 5.5/6
Ascites Fold Change (Treatment/Mock)
1.0
0.5
0.0
**
*
Mock MS ITF A A+MS A+ITF
Mock MS ITF A A+MS A+ITF
NSG
C57Bl/6
C
Immunodeficient Mouse Model
Percent Survival
100
80
60
40
20
0
0 30 40 50 60 80
Day
Mock 37d
MS 34.5
ITF 38d
A17 45d
A+MS17 40.5d
A+ITF17 45d
*
***
D
NSG mice: Ascites Week 4
C57Bl/6 mice: Ascites Week 4.5
mL
6
4
2
0
8
6
4
2
0
*
*
**
Mock αIFNAR1 AZA A+αIFNAR1
Mock αIFNAR1 AZA A+αIFNAR1
E
NSG ascites cells: Week 4.5
%L/D+CD45- of Ascites Cells
60
40
20
0
***
**
Mock MS ITF A A+MS A+ITF

Figure 7

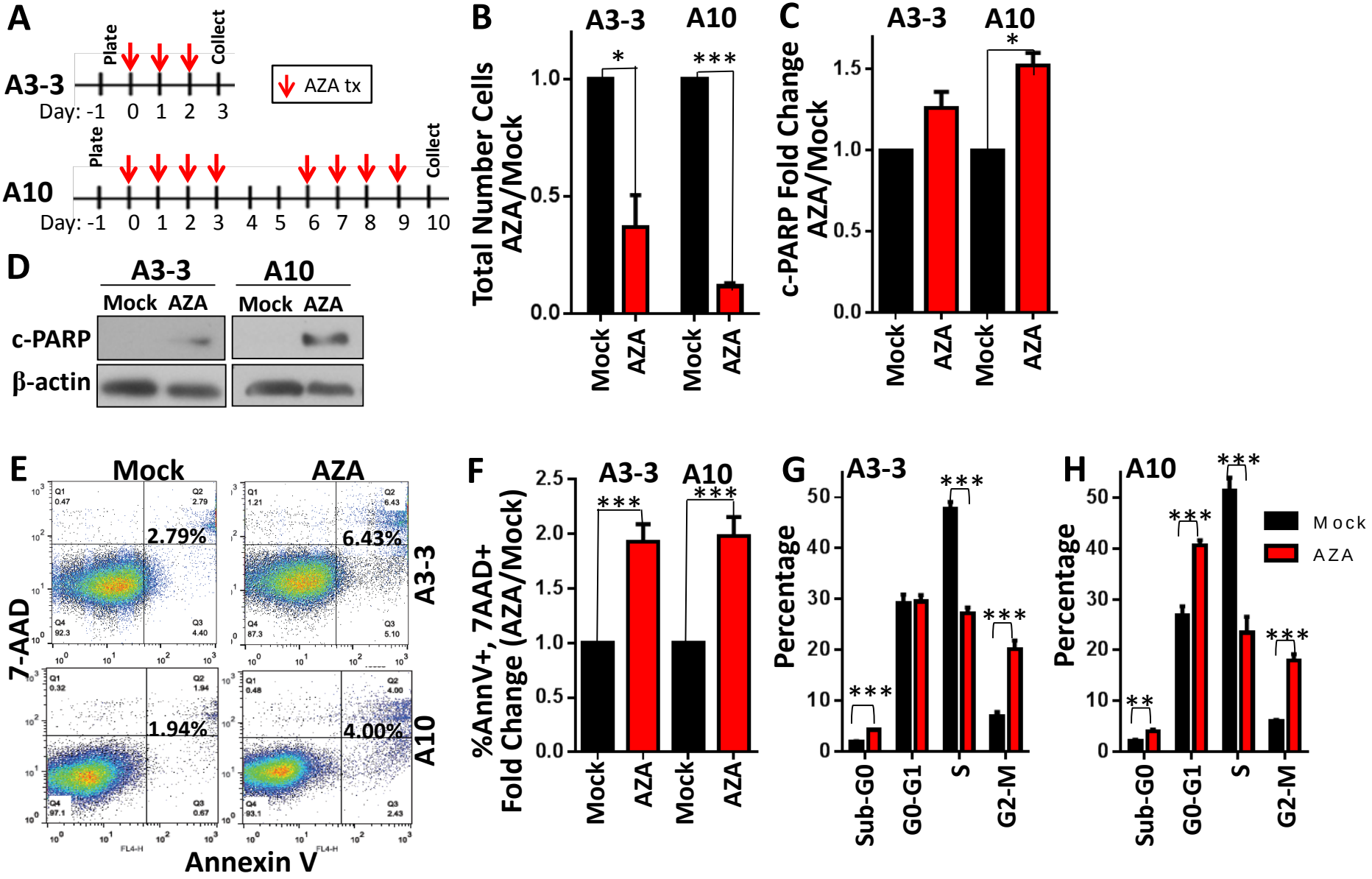
A
A3-3
Plate
Collect
Day: -1 0 1 2 3
AZA tx
A10
Plate
Collect
Day: -1 0 1 2 3 4 5 6 7 8 9 10
B
A3-3
A10
Total Number Cells AZA/Mock
Mock
AZA
C
A3-3
A10
c-PARP Fold Change AZA/Mock
D
A3-3
A10
Mock AZA
Mock AZA
c-PARP
β-actin
E
Mock
AZA
2.79%
6.43%
1.94%
4.00%
A3-3
A10
7-AAD
Annexin V
F
A3-3
A10
%AnnV+, 7AAD+ Fold Change (AZA/Mock)
G
A3-3
Percentage
Sub-G0
G0-G1
S
G2-M
H
A10
Percentage
Mock
AZA

Cell

A combination epigenetic therapy ties MYC depletion to reversing immune evasion and treating lung cancer

--Manuscript Draft--

Manuscript Number:	
Full Title:	A combination epigenetic therapy ties MYC depletion to reversing immune evasion and treating lung cancer
Article Type:	Research Article
Keywords:	DNMTi, HDACi, lung cancer, Immune, Myc, tumor associated macrophages
Corresponding Author:	Stephen B Baylin The Sidney Kimmel Comprehensive Cancer Center at Johns Hopkins Baltimore, MD UNITED STATES
First Author:	Michael J Topper
Order of Authors:	Michael J Topper
	Michelle Vaz
	Katherine B Chiappinelli
	Christina DeStefano Shields
	Alyssa Wenzel
	Jessica Hicks
	Matthew Ballew
	Meredith Stone
	Phuoc T Tran
	Cynthia A Zahnow
	Matthew D Hellmann
	Pamela L Stissel
	Reiner Strick
	Stephen B Baylin
Abstract:	While combination epigenetic treatment involving DNA demethylating agents (DNMTi's) with histone deacetylase inhibitors (HDACi's) holds promise as a cancer therapy further optimization is required. We present a new, low dose regimen for sequentially pairing these agents based on the isoform specificity of HDAC's and pharmacologic properties of HDACi's. This pairing reverses tumor immune evasion through augmentation of Interferon signaling and potent DNMTi-induced sensitization for HDACi through c-MYC depletion. The former results from predominant inhibition of HDAC's 1, 2 and 6 isoforms and the latter, which triggers reduced cell proliferation, is driven by targeting HDAC's 1, 2, and 3. Our regimen exacts a potent anti-tumor response in a mouse model of lung cancer correlating with attraction of CD8 T cells and reduction of tumor associated macrophages. This schema of combination epigenetic therapy with immune checkpoint blockade is now entering a Stand up to Cancer trial for patients with NSCLC.
Opposed Reviewers:	Timothy Bestor, PhD Professor, Columbia University thb12@columbia.edu Conflict of interest
	Rudolf Jaenisch, MD Professor, Whitehead Institute kemske@wi.mit.edu Conflict of interest

	Weiping Zou Professor, University of Michigan, Ann Arbor wzou@umich.edu
Suggested Reviewers:	Jonathan Licht, MD Associate Profssor, Norhtwestern University j-licht@northwestern.edu
	Anthony G Letai, MD, PhD Associate Professor of Medicine, Harvard Medical School anthony_letai@dfci.harvard.edu
	George Coukos, M.D., Ph.D Ovarian Cancer Research Center, University of Pennsylvania george.coukos@chuv.ch

Dear Dr. Mao,

Please find our manuscript, " **A combination epigenetic therapy ties MYC depletion to reversing immune evasion and treating lung cancer**" by Topper et al, which we submit for consideration for publication in *Cell*. In this work, we have devised a new regimen for combination epigenetic therapy which deeply considers how to best pair histone deactylase inhibitors (HDACi's) with DNA methyltransfrase inhibitors (DNMTi's) for targeting reversal of cancer immune tolerance. In previous studies published in *Cell*, predominantly using human ovarian cancer cells, we revealed how DNMTi's trigger a viral defense pathway to drive key aspects of interferon signaling. This scenario is predicted to trigger tumors to reverse an immune evasion to an immune active scenario key and we now reveal this. We now show how our combined strategy, indeed, reverts an immune desert situation by attracting and diminishing key subsets of immune cell to the tumor microenvironment and alters key cytokines levels fundamental to this. We now report how careful addition of HDACi's to DNMTi's can derive a new therapeutic approach for driving each of the above immune attraction parameters. To accomplish this , we deeply considered which HDAC family members must be targeted by HDACi's to complement DNMTi's, which of these agents are optimal in terms of the differential Ki's for the multiple HDAC family members, what $T_{1/2}$ best synergizes with DMNTi's and, ultimately, how to incorporate all of these parameters to acheive a low-dose combinatorial strategy that may be tolerable and effective clinically. Our approach not only augments the above interferon signaling by the DNMTi, but also reveals new molecular parameters for sensitizing tumor cells to this immune activation. In the emergent scenario, our approach reveals how DNMTi's can sensitize the capacity of HDACi's to robustly down-regulate signaling from the potent oncogene, CMYC. Blockade of MYC signaling is inversely related to the achieved levels of tumor interferon signaling activation.

Having worked out the above therapy paradigm using human non-small lung cancer (NSCLC) cells, the greatest cause of cancer related death worldwide, we take it to treatment of a KRAS mutant transgenic NSCLC mouse model. This allows examination of the therapeutic potential in mice with a competent immune system. The well tolerated, combination epigenetic therapy has a potent anti-tumor effect tightly tied to reversal of basally reduced tumor immune attraction signaling. The precise signaling pathways identified above for the human NSCLC cells are seen in post-treatment analyses of tumors with the inverse scenario for the role of downregulating MYC signaling and activating viral defense and interferon signaling. The result is induction of CD8 T-cells to the tumors and decrease of a population of immune tolerance inducing macrophages. Key cytokines for mediating these effects are identified.

We recognize that a paper by Evan and colleagues with highly related findings has recently been submitted to Cell, and we have had a transparent exchange of manuscripts between our groups. We both agree that the papers might have great impact when considered together. In short, Evan's group has seen virtually the same MYC related dynamics for immune attraction consequences, using precisely the same mouse NSCLC model. They have utilized genetic manipulation for MYC to achieve what we have seen with our pharmacologic approach. We, thus hope the papers might be considered for joint review and that you might share our enthusiasm for possible publication of both. Importantly, the new strategy we have derived for combining DNMTi's and HDACi's is about enter a Stand-up to Cancer (SU2C) clinical trial for patients with NSCLC. On the basis of the work described in this paper, this

combination regimen will be paired with immune checkpoint therapy (pembrolizuamb) and the trial will be fully supported by a SU2C/Merck Catalyst Research Grant award received by our team.

Sincerely,

Michael Topper, graduate student,

Michelle Vaz, Ph.D.

Stephen B. Baylin, M.D.

A combination epigenetic therapy ties MYC depletion to reversing immune evasion and treating lung cancer

Michael J. Topper [1,2,9], Michelle Vaz [1,9], Katherine B. Chiappinelli [4], Christina DeStefano Shields [1], Alyssa Wenzel [8], Jessica Hicks [7], Matthew Ballew [3], Meredith Stone [1, 2], Phuoc T. Tran [3], Cynthia A. Zahnow [1], Matthew D. Hellmann [5], Pamela L. Strissel [6], Reiner Strick [6], Stephen B. Baylin [1*]

1. Department of Oncology, The Johns Hopkins School of Medicine, The Sidney Kimmel Comprehensive Cancer Center, Baltimore, MD, 21287, USA

2. The Graduate Program in Cellular and Molecular Medicine, Johns Hopkins University School of Medicine, Baltimore, MD 21287, USA

3. Dept. of Radiation Oncology & Molecular Radiation Sciences, The Johns Hopkins School of Medicine, The Sidney Kimmel Comprehensive Cancer Center, Baltimore, MD 21287, USA

4. Department of Microbiology, Immunology, and Tropical Medicine, The George Washington University Cancer Center, 800 22nd Street, NW, Suite 8860, Washington, DC 20052, USA

5. Dept. of Medicine; Memorial Sloan-Kettering Cancer Center; New York, NY 10065, USA

6. Department of Gynaecology and Obstetrics, Laboratory for Molecular Medicine, University-Clinic Erlangen, 91054 Erlangen, Germany

7. Department of Urologic Pathology, The Johns Hopkins School of Medicine, The Sidney Kimmel Comprehensive Cancer Center, Baltimore, MD, 21287, USA

8. The Johns Hopkins University, Baltimore, MD 21218, USA

9. Co-first Authors

* Contact: Email: sbaylin@jhmi.edu ; phone: (410) 955-8506; fax: (410) 614-9884

Summary

While combination epigenetic treatment involving DNA demethylating agents (DNMTi's) with histone deacetylase inhibitors (HDACi's) holds promise as a cancer therapy further optimization is required. We present a new, low dose regimen for sequentially pairing these agents based on the isoform specificity of HDAC's and pharmacologic properties of HDACi's. This pairing reverses tumor immune evasion through augmentation of Interferon signaling and potent DNMTi-induced sensitization for HDACi through c-MYC depletion. The former results from predominant inhibition of HDAC's 1, 2 and 6 isoforms and the latter, which triggers reduced cell proliferation, is driven by targeting HDAC's 1, 2, and 3. Our regimen exacts a potent anti-tumor response in a mouse model of lung cancer correlating with attraction of CD8 T cells and reduction of tumor associated macrophages. This schema of combination epigenetic therapy with immune checkpoint blockade is now entering a Stand up to Cancer trial for patients with NSCLC**.**

Keywords: DNMTi, HDACi, lung cancer, Immune, Myc, tumor associated macrophages

Highlights

Azacitidine depletes c-MYC and induces dsRNA to sensitize NSCLC to HDACi.

This sensitization invokes HDAC isoform specific effects.

Combination epigenetic treatment induces potent anti-tumor response in vivo.

This anti-tumor response is correlated with tumor associated macrophage depletion.

Introduction

The development of effective therapeutic schemas for the treatment of patients with lung cancer, especially non-small cell lung carcinoma (NSCLC), the world's leading cause of cancer related death, is of paramount concern. While much progress has been made, the 5-year survival rate for NSCLC remains dismal (Molina et al., 2008). The advent of immune checkpoint therapy has been a tremendous step forward (Borghaei et al., 2015), but only a minority of unselected patients benefit. Thus increasing the overall 21 percent response rate represents a major challenge for the field (Reck and Brahmer, 2017; Reck et al., 2016).

One promise for improving the proportion of patients who benefit from immune therapy is the development of rational combination therapy that augments anti-tumor immunity. Combination epigenetic therapy is one such approach. Previously we identified durable responses in a small percentage of NSCLC patients who were initially treated with low dose of DNA methyltransferase inhibitor (DNMTi) combined with intermittent high dose histone deacetylase inhibitor (HDACi), followed by treatment with immune checkpoint therapy (Juergens et al., 2011). Clinical trials are ongoing in our Stand Up to Cancer (SU2C) group and by others seeking to validate this above efficacy for combined epigenetic and immune checkpoint therapy.

Clinically relevant combination epigenetic treatment regimens, as for our work cited above, most commonly utilize cytidine analogs, Azacitidine (5-AC) or Decitabine (DAC) in combination with HDACi's on the premise that the latter can enhance re-expression of abnormally DNA methylated genes, produced by low doses of the former (Cameron et al., 1999; Jones et al., 2016). However, for this above combination, most pre-clinical work has concentrated on the DNMTi's. Low doses of these impart durable changes in both genome –wide DNA methylation and transcriptome, while avoiding acute cytotoxicity (Tsai et al., 2012).

Most important for our present study, is the well-known ability of DNMTi's to upregulate key facets of immune signaling, including antigen expression (Moreno-Bost et al., 2011; Oi et al., 2009; Weiser et al., 2001). In our recent studies, aiming to understand the possibilities of enhancing immunotherapy, we have discovered that DNMTi's induce an epithelial, cancer immune attraction signature for NSCLC and other cancer types with a characteristic augmentation of interferon and antigen presentation related transcription (Li et al., 2014; Wrangle et al., 2013). Most excitingly, a key component of this signaling is an interferon response observed in ovarian and colon cancer cells induced through the activation of endogenous retroviruses transcription and a cytoplasmic, double stranded RNA (dsRNA) response. This has been termed DNMTi induced viral mimicry (Chiappinelli et al., 2015; Roulois et al., 2015).

While all the above actions of DNMTi's are emerging, the contribution of HDACi's in this paradigm of viral mimicry and immune responses has not been investigated. This is a key focus of our present study. In this regard, the zinc chelating HDACi's are comprised of 3 major classes: benzamide, hydroxamic acid, and cyclic tetrapeptides (Bradner et al., 2010; Falkenberg and Johnstone, 2014; Rasheed et al., 2007; Zahnow et al., 2016). Benzamide class HDACi's target class I HDAC isoforms, while hydroxamic acid class HDACi's target both Class I and Class II HDAC's, although differences in isoform targeting can be noted (Bradner et al., 2010). How this above information for HDACi's contributes to potentiating clinical efficacy for cancer management and enhancing immune therapy specifically remains to be elucidated.

Herein, we investigate how targeting with specific HDACi's enables the full exploitation of the DNMTi mediated responses, through the consideration of both isoform specific Ki's and pharmacokinetic parameters. These findings bring together anti-tumor responses based on reducing c-MYC related cell proliferation and importantly, link this parameter to enhanced immune signaling. From these data, a treatment paradigm emerges, which maximizes the

potential of combined epigenetic therapy to achieve alteration of tumor immune environment, thus providing the underpinning for an upcoming SU2C Merck Catalyst Trial for patients with NSCLC.

RESULTS

Selection of optimal HDACi's, and their timing and doses for exerting chronic effects on chromatin when paired with Aza

Selection of HDACi's was instituted by pairing these agents with low dose (500 nM) Azacitidine (Aza), which we have studied across many common epithelial and hematological cancer cell lines (Li et al., 2014; Tsai et al., 2012; Vendetti et al., 2015; Wrangle et al., 2013). A transient three-day exposure for this dose of Aza has a lasting reprogramming effect, while avoiding inducing initial, potentially off target cytotoxicity. This noted reprogramming effect has a phenotypic correlate consisting of decreases in colony formation and growth of tumor cells in untreated, immune-deficient mice. This is accompanied by decreasing gene promoter DNA methylation, upregulation of gene transcription and alterations for multiple important signaling pathways (Li et al., 2014; Tsai et al., 2012; Vendetti et al., 2015; Wrangle et al., 2013).

Clinically relevant HDACi's were selected for their known pharmacokinetic parameters (cmax and half-life) and their enzymatic Ki's against key HDAC family members (Figure S1D). The half-life issue is of paramount importance, as our goal is to achieve constant drug pressure, thereby enabling the reversion of basal acetylation and thus maintaining upregulation of gene expression. The consideration of Ki to cmax ratio is also key for elucidating HDACi's, which have the greatest potential to impart significant inhibition of relevant HDAC isoforms. For these attributes, ITF-2357 is the more potent, with Ki's of 2 to 3nM against the above HDAC's, as

compared with 22nM for MS-275 against HDAC1 and 360 nM against HDAC3 (Bradner et al., 2010).

Additionally, ITF-2357 strongly inhibits cytoplasmic HDAC6 isoform (Bradner et al., 2010), which we demonstrate in the current study to be of importance when combined with Aza. ITF-2357 also has a much shorter half-life, enabling frequent administration, and a higher cmax relative to MS-275 (**Figure S1D**). The influence of these drug characteristics on multiple aspects of this study will be apparent in the following sections.

Combination Aza + ITF-2357 induces profound drug synergy when applied to human NSCLC

To gain an initial perspective on the use of the agents outlined above, we first examined the implications of therapeutic scheduling on the alteration of proliferation in human NSCLC cell lines. We deployed Aza and ITF-2357, both sequentially and concurrently (**Figure S1A**). These studies reveal only the former schedule to be the inducer of both formal synergy and robust potentiation of HDACi by Aza (**Figures 1A, 1B, S1B and S1C**).The benzamide class inhibitor MS-275, the HDACi previously deployed in combination with Aza for the treatment of NSCLC patients (Juergens et al., 2011), while demonstrating significant reduction of IC50, when utilized in our current schema, is still inferior to that of Aza+ITF-2357 (**Figure 1C**). This advantage of adding ITF-2357 to Aza, over MS-275, has a pharmacologic basis with respect to both, HDAC's targeted and their associated Ki's. This emerges through the finding that sequential application of Aza with HDAC3 or HDAC6 isoform specific inhibitors (RGFP996 and Tubastatin A) robustly reduces the IC50 of these agents (**Figure 1D**) and increases the potency of inhibition when combined with MS-275 (**Figure 1E**).

As an extension to the above assays, we probed the effect of ITF-2357 and MS-275 on DNA synthesis. We find the application of Aza with ITF-2357 at 100nM, a concentration roughly one

third cmax (Furlan et al., 2011), has a demonstrable antiproliferative advantage over 100nM MS-275, a supra-physiological concentration of this agent (Gore et al., 2008; Ryan et al., 2005) (**Figure 1F**).

To further delineate the Aza + ITF-2357 DNA synthesis inhibition mechanism, we deployed HDAC isoform specific inhibitors. We normalized these isoform HDACi's to the potency of 100nM ITF-2357 through the assessment of histone acetylation and tubulin acetylation, targets of HDAC1, 2 and HDAC6 isoforms, respectively (Asthana et al., 2013; Fournel et al., 2008; Khan et al., 2008). The resulting equivalent doses were estimated to be 200nM for Mocetinostat (HDAC1 ,2i) and 1000nM for Tubastatin A (HDAC6i) (**Figure S1E**). Selection of 2000nM RGFP996 (HDAC3i) dose was based on extrapolation of Ki's for each inhibitor, due to lack of pharmacodynamic targets (Malvaez et al., 2013). Using the aforementioned doses, we determine that inhibition of HDACs 1, 2, and 3 in combination with Aza induce profound proliferative arrest (**Figure S1F**).

We verified the specificity of Aza induced depletion of DNMT's as a driver of the combination induced proliferation inhibition. Aza, while a potent initiator of DNA hypomethylation, is a pleotropic agent, especially at higher doses. shRNA mediated depletion of DNMT1, the major pharmacodynamic target of this drug (Cai et al., 2014), achieves potent augmentation of the combination drug treatment synergy seen in the above studies combining Aza with HDACi's **(Figures S6A and B**).

All the above findings come into therapeutic relevance when in-vivo treatment of immune-incompetent mice, bearing explants of NSCLC, are examined. In this setting, Aza+ITF-2357 provided a 60% reduction in tumor volume while all other therapeutic conditions tested failed to significantly reduce tumor volume (**Figure 1F**). These data, in total, provide strong evidence of the superiority of ITF-2357 over MS-275, elicited through the robust inhibition of HDACs 1, 2, 3 and 6.

Effects of the drug combination paradigm on the transcriptome in NSCLC lines

Assessment of drug combination induced effect on gene expression yields important insight for signaling pathway alterations that may relate to eventual clinical efficacy. When examined on day 8 of sequential drug treatment (**Figure S1A**), transcriptional analyses reveal that both ITF-2357 and MS-275 alone produced modest changes when compared to the effects of Aza or combination epigenetic treatment (**Figure 2A**). The application of combination epigenetic treatment induces an increase in differential gene expression relative to monotreatment conditions, with a clear advantage noted from the application of Aza + ITF-2357 over all other conditions tested (**Figure 2B**). Matrix correlation analysis of relative expression distribution depict an Aza driven probe spreading, which is further augmented by combination epigenetic treatment (**Figure S2A**). Clustering of top 500 genes, as delineated by median absolute deviation (MAD) analysis, shows a divergence between HDACi monotreatment and Aza containing regimens (**Figure 2C**). DAVID pathway analysis of these top 500 MAD derived genes revealed epigenetic treatment alteration of pathways related to immune signaling, c-MYC regulation and metabolism (**Figure 2D)**.

A key parameter when considering the application of Aza and HDACi, is the further potentiation of demethylating agent inducible genes. To assay this parameter, we chose to focus on top tier genes, a category of transcriptionally induced genes which are DNA hypermethylated in cancer cells, which are responsive to Aza, but not inducible by HDACi alone (Schuebel et al., 2007) (**Figure S2B)**. The application of the schedule derived here, coupled with HDACi ITF-2357, more effectively induces robust upregulation of this gene subset (**Figure S2C)**.

In the drug treatment schema devised above, the most potent combination of Aza + ITF-2357 affects the transcriptome in a very focused way for altering pathway signaling (**Figure 2**). The resultant changes have key implications for use of the drugs to potentially increase tumor immune signaling, as assessed later in our studies and as now related to the blunting of cell

proliferation identified in the sections immediately above. Using GSEA analyses, with both KEGG and REACTOME gene ontologies, a total of 690 pathways per drug condition were queried. This analysis led to the identification of 3 significantly induced pathways conserved across NSCLC cell lines that are inducible by combination epigenetic treatment, 2 of which are immune signaling specific (**Figures 3A and B**). Immune related gene signatures induced by transient Aza treatment, and especially their convergence on interferon signaling, have been described (Chiappinelli et al., 2015; Li et al., 2014; Wrangle et al., 2013). Indeed, when we focused further scrutiny exclusively on combination driven pathway augmentation, the interferon alpha/ beta signaling demonstrates the most prominent pathway induction with combination epigenetic treatment (**Figure 3C**).The immune pathway induction noted here includes a significant augmentation of interferon responsive genes with the inclusion of HDACi in our combination paradigm and this is dissected further below.

While pathway upregulation was intrinsically driven by Aza and thus consistent between the Aza + HDACi conditions tested, pathway downregulation was more variable with 11 unique gene sets present in the Aza + ITF-2357 treatment group (**Figure 3D**). Comparative analysis of the conserved Aza + HDACi pathways revealed 7 of 12 shared pathways to be cell cycle related (**Figure 3E**). The corresponding enrichment plots for the top downregulated pathway confirms a conserved signature for KEGG DNA replication in both combinatorial treatments tested (**Figure 3F**). The above transcriptional downregulation of cell cycle related pathways elicited by combinatorial epigenetic treatment matches the observed proliferative arrest induced by combination epigenetic treatment (**Figures 1F**).

The potential of combinatorial epigenetic treatment to stimulate signals for immune related genes

One of the primary goals for combined epigenetic therapy, as introduced above, is to increase the efficacy of immune checkpoint and other immunotherapies. Further scrutiny of the pathway induction for immune related cell signaling derived from GSEA in the data above, delineates the implications of combinatorial epigenetic treatment on the alteration of AIM (Aza induced immune) genes and viral mimicry (Chiappinelli et al., 2015; Li et al., 2014). In human NSCLC cells, there is superiority of ITF-2357 over MS-275 when paired with Aza, in terms of both the magnitude and number of interferon alpha-beta pathway related genes induced, most notably observed for H23 and A549 cells (**Figures 4A and B**). As defined earlier, this superiority could be based on greater potency or broader targeting of HDAC's, and deploying HDACi's at concentrations mimicking 100nM ITF-2357 helps delineate these possibilities. We find the advantage of ITF-2357 over benzamide class inhibitors in the induction of interferon stimulated genes is the result of HDAC6 coupled with HDAC's 1, 2 based inhibition, but not HDAC3. This is based on our observation of the ability of specific inhibitors of HDAC1/2 (MCGD0103) and HDAC6 (Tubastatin A) to cause significant induction of these genes over Aza treated cells. This induction was not seen when an HDAC3 inhibitor RGFP996 was uses along with Aza (**Figures 4C, 4D, S3B and S3D**). We further tested the efficacy of ITF-2357 against SAHA, another hydroxamic acid derivative HDACi and observed a superior augmentation of interferon genes by ITF-2357 when deployed in combination with Aza. This result is suggestive of enhanced ITF-2357 stability over SAHA, as other parameters between the two agents are roughly equivalent (**Figures S3A and S3C**). These studies define a combination epigenetic induction of interferon stimulated genes which is potentiated by Aza, but further augmented by the application of HDACi's targeting isoforms 1, 2 and 6.

The induction of antigen presentation machinery is critical to facilitate the presentation of mutated peptides and neoantigens to immune cells, thereby enabling recognition and ablation of cancerous lesions (DuPage et al., 2011). The augmentation of this parameter, in contrast to other effects probed thus far, is potentiated through the application of HDACi's, with further increases noted for Aza and most notably, Aza + ITF-2357 (**Figures 4A, E and F**). Cancer/testis antigens are epigenetic-treatment responsive and have an established role in facilitating the recognition of tumors through immune surveillance (Moreno-Bost et al., 2011; Oi et al., 2009; Weiser et al., 2001). We find in agreement with previous studies, the induction of cancer/testis antigens is induced by the application of Aza, but a significant additional benefit is noted with the combination of Aza + ITF-2357 (**Figures S4D-4G**). All other HDACi's deployed failed to facilitate meaningful increases in the expression of these antigens over Aza alone. These studies on cancer/testis antigens and class I antigen presentation suggest a system where the application of demethylating agents in combination with broader targeting HDACi's impart the most potential to simultaneously induce transcription and presentation of immune-reactive antigens.

Our combinatorial drug treatments augment, in our lines of human NSCLC, the interferon alpha beta pathway induction by Aza, which partially relies on increasing dsRNA species including endogenous retroviruses (ERV) transcripts (Chiappinelli et al., 2016; Roulois et al., 2015; Stengel et al., 2010; Strissel et al., 2012). Indeed, combination HDACi with Aza augmented multiple ERV's across all cell lines tested, suggestive of a common response to epigenetic treatment (**Figures 4G, 4H, S4A and S4B**) The most differentially expressed ERV induced by Aza + ITF-2357 was found to be ERV9-1. To delineate the specific HDAC isoform mediating this response, we tested isoform specific inhibitors in combination with Aza in our two most immune-responsive cell lines. We observed a subtle increase in ERV9-1 transcription by class I HDACi, but a larger increase is noted through the application of HDAC6 targeting agents (**Figures 4I**

and J). This explains the large induction of this ERV driven by ITF-2357. This ERV alteration specifically results from DNMT depletion in combination with HDACi as assessed by its transcriptional induction in the presence of DNMT1 knockdown (**Figure S6C**). The inducibility of interferon signaling from ERV transcription is linked in our NSCLC cells as evidenced by the demonstrated sufficiency of single ERV overexpression to induce transcription of OASL1, an interferon responsive gene (**Figure S4C**).

In summary, HDACi's enhance Aza induced interferon responsive gene transcription, particularly with inhibition of HDAC's 1, 2, and 6. Class I antigen presentation is augmented through the inhibition of HDAC's 1, 2, 3, and 6 in combination with Aza. The induction of cancer/testis antigen transcription requires potent HDACi's, such as ITF-2357, to mediate significant upregulation over Aza alone.

Perturbation of c-MYC by Aza drives sensitization to HDACi

Using our agnostic transcriptome approach, at least one key mechanism identified through which our drug schema acts, is the down regulation of the cell cycle. When we sort, and identify the top 500 genes displaying the greatest median absolute deviation of expression, and conduct DAVID analysis, 3 of the top 8 pathways were c-MYC related (**Figure 2D**), suggesting the perturbation of c-MYC as an epigenetic therapy actionable parameter.

Critically, in the tested NSCLC cell lines, Aza produces a significant and conserved transcriptional downregulation of c-MYC, with an at least 1.4-fold reduction observed across all cell lines assayed (**Figure 5A**). These transcription data are matched with downregulation of c-MYC protein in A549 and H460 cells (**Figure 5B**). Combinatorial Aza + HDACi acts to further deplete c-MYC over Aza treatment alone **(Figure S5A).** The application of Aza and Aza + HDACi treatment induces potent repression of the top 200 c-MYC targets, which is especially

biased to the Aza + ITF-2357 treatment group (**Figure 5C**). Importantly, knockdown of c-MYC protein phenocopies the Aza repression of c-MYC, sensitizing NSCLC to HDACi induced cytostasis (**Figure 5D and S5C**). Additionally, the stable overexpression of c-MYC partially rescues the Aza induced sensitization to HDACi induced cell depletion (**Figure 5E and S5B**). These data are suggestive of an Aza induced c-MYC depletion as a potent sensitizer to HDACi induced proliferative arrest and accordingly implicate c-MYC signaling as a phenotypic driver.

High c-MYC tumors have been reported to display resistance to interferon gamma signaling and the action of cytotoxic T lymphocytes (Casey et al., 2016; Schlee et al., 2007a; Schlee et al., 2007b). In this regard, exogenous c-MYC overexpression results in antagonism of interferon stimulated gene induction and antigen presentation induced by epigenetic treatment (**Figure 5F and G).** Thus, the c-MYC depletion signature imparted by Aza sensitizes to the actions of HDACi induced cytostasis and augments NSCLC interferon signaling.

The anti-tumor effects and accompanying immune activation parameters for combination epigenetic treatment of a Kras G12D mouse model for NSCLC

We next examined the translational significance of all the above studies by utilizing our chronic schema of 1 week Aza, followed by 1 week ITF-2357 as an alternating schedule, for the treatment of a genetically engineered, mutant *Kras* induced, mouse model of NSCLC **(Figure 6A)**. Mice were treated 16 weeks following the lung specific activation of the *Kras* G12D mutation (Jackson et al., 2001) with AdenoCre. The appearance of adenomas as determined by both CT scan and H&E histology was confirmed prior to the start of treatment. Treatment was continued for 3 months. This treatment paradigm, as defined earlier was highly anti-tumorigenic, and well tolerated in the human H460 xenograft model (**Figure 1F**). To evaluate the implications of this treatment schema in combination with immune checkpoint blockade, we added treatment with anti-PD1 antibody to the described regimen (**Figure S7C**).

The combination epigenetic therapy alone, proved to be exceptionally efficacious and much more so than the anti-PD-1 therapy alone. Combination epigenetic treatment, in fact, virtually prevents the occurrence of macroscopically discernable adenocarcinomas and caused a discernible decrease in tumor area in the treated mice as compared to the vehicle treated controls **(Figure 6B, S7A and S7B).** Consistent with all the studies in the human NSCLC cells, there is a corresponding reduction in any remaining histologic, adenomatous lesions of tumor cell proliferation as assessed by ki67 positivity (**Figure 6C**). When anti-PD1 administration is combined with epigenetic therapy, the latter fully dominated the therapeutic effect (**Figure S7D**).

Importantly, as outlined below, a profound immune effect correlates with the above efficacy of the epigenetic therapy alone. Analysis of RNA extracted from tumors from mock and treated mice show that the combination epigenetic treatment profoundly altered the transcriptome with 5167 significantly upregulated and 4540 downregulated genes (**Figure 6D**). GSEA of relative expression identified 18 gene sets upregulated and 52 gene sets downregulated by the combination treatment and these were predominantly associated with immune and cell cycle pathways, respectively (**Figure 6E**). Similar to the results for human NSCLC lines, 12 of 18 gene sets upregulated were immune related, with a strong induction of cytokine and interferon related gene sets (**Figure 6F**). Evaluation of the hallmark inflammatory response pathway revealed 24 genes displaying significant induction by combination epigenetic treatment (**Figure 6G**). As again observed in human NSCLC lines, most of the down-regulated pathways were cell cycle related, including the *c-myc* target hallmark set (**Figure 6H**) and 30 *c-myc* pathway related genes (**Figure 6I**). These data demonstrate a potent reduction in tumor proliferation, progression and burden induced by combination epigenetic treatment, which is correlated with the repression of *c-myc* related signaling.

Combination epigenetic treatment alters the tumor microenvironment, facilitating tumor associated macrophage depletion and CD8 T cell infiltration

The endogenous immune environment of the *Kras* G12D mouse model presents with an immune desert phenotype, with a characteristic high tumor associated macrophages, and low CD8 T-cell infiltrate (DuPage et al., 2011; Okayama et al., 2013). The application of epigenetic therapy induces a reversion of this tumor immune microenvironment characterized first by inducing intra-tumor infiltration of CD8 T cells (**Figure 7A**). This is accompanied by interferon gamma pathway activation with a corresponding augmentation of pathway responsive genes (**Figure 7B**). Moreover, we find transcriptional augmentation of CCL5, a secreted chemokine involved in lymphocyte attraction (**Figure 7C**). An important protein corollary to this transcriptional augmentation was the finding of increased levels of bronchoalveolar accumulation of CCL5 in mice treated with combination epigenetic therapy as compared to controls (**Figure 7D**). This protein and its ligand have been identified as the primary factors influencing T cell infiltration of melanoma post-chemotherapy (Hong et al., 2011). The induction of CCL5 is a conserved response to epigenetic treatment in human NSCLC cell lines with upregulation again triggered as a drug-specific effect on the epithelial compartment (**Figure 7E**). Additionally, over-expression of exogenous c-MYC to A549 cells acts as a potent repressor of CCL5 transcriptional induction in response to epigenetic treatment, further linking c-MYC perturbation to the alteration of immune correlates **(Figure 7F).** Finally, the potential repressive role of c-MYC on CCL5 is apparent in TCGA primary, patient lung adenocarcinoma (LUAD) samples, where there is an inverse relationship between CCL5 and c-MYC RNA transcripts, most profoundly apparent when considering the c-MYC low patient samples **(Figure 7G).**

In addition to the noted increase of intra-tumor CD8 lymphocyte infiltration, combination epigenetic treatment induces a marked reduction in both density and area of F4/80 positive tumor associated macrophages (**Figure 7H**). These tumor associated cells have a clear role in

the progression of the *Kras* G12D model (Okayama et al., 2013) and have been associated with mediating the establishment of a tumor immunosuppressive environment (Koyama et al., 2016; Motz and Coukos, 2013). As the reduction of intratumor macrophages could be multi-factorial, we focused on 2 important parameters: direct drug toxicity and indirect effect of the drug on epithelial cell secretion. In an in vitro bone marrow derived macrophage (BMDM) culture system, from wild type C57BL6 mice, we find combination epigenetic treatment induces a direct drug elicited reduction in macrophage proliferation (**Figure 7I**). Culturing of BMDM's in media derived from Lewis Lung Carcinoma (LLC) cells treated with epigenetic agents, revealed a potent decrease in macrophage proliferation (**Figure 7J**). In summary, these immune related data reveal a reversion of the immunosuppressive environment of our mouse model and suggest epigenetic treatment can both induce direct toxicity on macrophages, as well as reduce epithelial support of macrophages.

Discussion

We have derived a paradigm for epigenetic therapy that demonstrates its role in decreasing c-MYC signaling which drives a substantial anti-tumor response and a reversion of the tumor immunophenotype. Previously, we and others have shown how DNMTi's can induce a cytoplasmic, dsRNA sensing pathway for interferon signaling, or a viral mimicry effect (Chiappinelli et al., 2015; Roulois et al., 2015). Now, using careful selection of specific HDACi's, based upon their pharmacological targeting and potency characteristics, we find these agents can complement the therapeutic effects of DNMTi's by augmenting the above inverse relationship between tumor immune attraction and c-MYC signaling.

The effects of our therapeutic paradigm on decreasing c-MYC signaling appears to be the result of true cellular re-programming. We have previously shown that low doses of DNMTi's do not

immediately trigger DNA damage and cell cycle checkpoints, which might otherwise acutely stop cell proliferation and secondarily downregulate c-MYC expression (Tsai et al., 2012). Rather, in the present study the c-MYC downregulation and decreased cell proliferation are later events occurring on day 8 and day 9 after start of drug administration, respectively **(Figures 5A, 1F and S1F).** Furthermore, DAVID pathway analysis implicates upstream perturbation of TGFβ, Hippo, and stem cell regulatory pathways as potential mediators of the observed c-MYC downregulation by Aza **(Figure 2D)**. Our present data emphasize the importance of considering the pharmacological parameters of HDACis for pairing these agents with DNMTi's to devise epigenetic therapy strategies. By considering these for isoform targeting and duration of drug action, we have derived a simultaneous effect for tying c-MYC mediated proliferative and tumor immune attraction to achieve a robust anti-tumor effect. We find the inhibition of HDAC1, 2, and 3 isoforms are key for inducing a profound proliferative arrest, imparting most of this effect at clinically relevant concentrations of ITF-2357. The inhibition of HDAC6 appears to play an important role, possibly involving its known function for regulating Stat-1 dependent NF-kB signaling (Kramer et al., 2006). Our data then, in the aggregate, appear to explain our noted benefit of this HDACi relative to the benzamide class agents studied. The potent inhibitory properties, however, of the benzamide class HDACi, Mocetinostat for HDAC's 1 and 2, coupled with its short half-life, enable this compound to be very effective in our chronic administration schema. This drug will be utilized with a DNMTi and an anti-PD1 reagent in in our upcoming SU2C trial for patients with NSCLC.

The culmination of our studies is the application of our developed regimen for chronic administration of combined Aza plus ITF-2357 in a genetically engineered mouse model harboring a *Kras* mutation. These studies demonstrate the ability of this treatment paradigm to be administered chronically, thereby enabling continuous pressure for reversing abnormal DNA methylation and preventing deacetylation. This model allows the assessment of immune effects

of the regimen with respect to tumors and their microenvironment. In this scenario, we demonstrate the ability of epigenetic treatment to reduce burden, proliferation and progression of disease in a manner where the transcriptome effects mimic those seen for our regimens in the first studies of human NSCLC cells. Notable among these effects is the downregulation of c-MYC and MYC targets (Figure 6I). Interesting, inhibition of MYC and its targets has been shown to eradicate lung tumor lesions in a Kras driven mouse lung cancer model (Soucek et al., 2013). In addition to these effects on tumor epithelial cells, we observe a reversion of an immune desert phenotype, noted to be a basal characteristic for the NSCLC lesions in this mouse model (DuPage et al., 2011). Specifically, there is depletion of tumor associated macrophages, cells known for promoting tumorigenesis and inducing immune tolerance (Laoui et al., 2014; Levinson et al., 1989; Pyonteck et al., 2013) and an increase in tumor infiltrating CD8+ T cells. The attraction of the latter to the tumor microenvironment are essential for anti-PD1 therapy to then block their tolerance features and exert an anti-tumor effect (Liu and Giaccone, 2016; Topalian et al., 2016).

An important parameter altered, which may have implications for the induced infiltration of CD8+ T cells into the tumor microenvironment, is the simultaneous upregulation of CCL5 protein secretion into the bronchioloalveolar compartment. The forced overexpression of this secreted protein has been found to induce tumor recruitment of T cells (Lavergne et al., 2004). Importantly, higher levels of CCL5 have also been found to serve as an independent prognostic indicator for longer overall survival with a noted induction of an active tumor associated lymphocyte compartment, in NSCLC patients (Moran et al., 2002).

In patient tumors, CCL5 augmentation by epigenetic therapy may prove crucial both functionally and as a biomarker in pre- and post-epigenetic treatment. As a biomarker, these data indicate that such findings for basal levels of CCL5 may be especially valuable when combined with the other immune related markers studied, particularly in patients with c-MYC high, NSCLC tumors.

Considering these relationships may enable the prediction of those most likely to respond to combination epigenetic therapy. This c-MYC high, CCL5 low population seems both primed to respond to epigenetic, as well as immune therapy. This hypothesis is being pursued in the above mentioned pending trial of the DNA demethylating agent SGI-110 + Mocetinostat + anti-PD-1 for patients with advanced NSCLC.

In summary, we believe that epigenetic therapy induced depletion of c-MYC can remove a barrier to interferon responsiveness in NSCLC tumors, as well as cause sensitization to the direct anti-proliferative actions of HDACi's when these agents are combined with DNMTi's. This, coupled with the reversion of immune evasion, as constituted by depletion of macrophages and increased secretion of CCL5, may act to increase the infiltration of T cells to the tumor micro-environment. This appears to help mediate tumor responses to epigenetic therapy alone and/or enhancing the efficacy of immune checkpoint therapy.

Author Contributions:

MJT, MV, and SBB designed experiments, performed data analyses, and wrote the manuscript. MJT, MV, KBC, AW, JH performed experiments. PLS and RS analyzed ERV data. CDS assisted with data analyses and manuscript review. MB and PTT performed and analyzed CT scans. CAZ assisted with xenograft studies. MDH, PTT, KBC participated in writing of the manuscript and aspects of experimental studies.

Acknowledgements:

This work was supported by grants from The Hodson Trust, The Dr. Miriam and Sheldon G. Adelson Medical Research Foundation and the SWCRF Collaboration for a Cure. This work is also supported by The Defense Health Program, through the Department of Defense Ovarian

Cancer Research Program, Teal Innovator Award under Award No. OC130454 / W81XWH-14-1-0385 (opinions, interpretations, conclusions and recommendations are those of the author and no necessarily endorsed by the Department of Defense). Research funding also provided by Van Andel Research Institute through the Van Andel Research Institute – Stand Up To Cancer Epigenetics Dream Team. Stand Up To Cancer is a program of the Entertainment Industry Foundation, administered by AACR. We acknowledge Mrs. Elizabeth Stiegler and Lauren Murphy for expert technical help. We thank Kathy Bender for help with manuscript preparation. We acknowledge the support of the Johns Hopkins SKCC Microarray Core for expression arrays.

References

Asthana, J., Kapoor, S., Mohan, R., and Panda, D. (2013). Inhibition of HDAC6 deacetylase activity increases its binding with microtubules and suppresses microtubule dynamic instability in MCF-7 cells. The Journal of biological chemistry *288*, 22516-22526.

Borghaei, H., Paz-Ares, L., Horn, L., Spigel, D.R., Steins, M., Ready, N.E., Chow, L.Q., Vokes, E.E., Felip, E., Holgado, E.*, et al.* (2015). Nivolumab versus Docetaxel in Advanced Nonsquamous Non-Small-Cell Lung Cancer. The New England journal of medicine *373*, 1627-1639.

Bradner, J.E., West, N., Grachan, M.L., Greenberg, E.F., Haggarty, S.J., Warnow, T., and Mazitschek, R. (2010). Chemical phylogenetics of histone deacetylases. Nature chemical biology *6*, 238-243.

Cai, Y., Geutjes, E.J., de Lint, K., Roepman, P., Bruurs, L., Yu, L.R., Wang, W., van Blijswijk, J., Mohammad, H., de Rink, I.*, et al.* (2014). The NuRD complex cooperates with DNMTs to maintain silencing of key colorectal tumor suppressor genes. Oncogene *33*, 2157-2168.

Cai, Y., Tsai, H.C., Yen, R.C., Zhang, Y.W., Kong, X., Wang, W., Xia, L., and Baylin, S.B. (2017). Critical threshold levels of DNA methyltransferase 1 are required to maintain DNA methylation across the genome in human cancer cells. Genome research.

Cameron, E.E., Bachman, K.E., Myohanen, S., Herman, J.G., and Baylin, S.B. (1999). Synergy of demethylation and histone deacetylase inhibition in the re-expression of genes silenced in cancer. Nature genetics *21*, 103-107.

Casey, S.C., Tong, L., Li, Y., Do, R., Walz, S., Fitzgerald, K.N., Gouw, A.M., Baylot, V., Gutgemann, I., Eilers, M.*, et al.* (2016). MYC regulates the antitumor immune response through CD47 and PD-L1. Science *352*, 227-231.

Chiappinelli, K.B., Strissel, P.L., Desrichard, A., Li, H., Henke, C., Akman, B., Hein, A., Rote, N.S., Cope, L.M., Snyder, A.*, et al.* (2015). Inhibiting DNA Methylation Causes an Interferon Response in Cancer via dsRNA Including Endogenous Retroviruses. Cell *162*, 974-986.

Chiappinelli, K.B., Strissel, P.L., Desrichard, A., Li, H., Henke, C., Akman, B., Hein, A., Rote, N.S., Cope, L.M., Snyder, A.*, et al.* (2016). Inhibiting DNA Methylation Causes an Interferon Response in Cancer via dsRNA Including Endogenous Retroviruses. Cell *164*, 1073.

DuPage, M., Cheung, A.F., Mazumdar, C., Winslow, M.M., Bronson, R., Schmidt, L.M., Crowley, D., Chen, J., and Jacks, T. (2011). Endogenous T cell responses to antigens expressed in lung adenocarcinomas delay malignant tumor progression. Cancer cell *19*, 72-85.

Falkenberg, K.J., and Johnstone, R.W. (2014). Histone deacetylases and their inhibitors in cancer, neurological diseases and immune disorders. Nature reviews Drug discovery *13*, 673-691.

Fournel, M., Bonfils, C., Hou, Y., Yan, P.T., Trachy-Bourget, M.C., Kalita, A., Liu, J., Lu, A.H., Zhou, N.Z., Robert, M.F.*, et al.* (2008). MGCD0103, a novel isotype-selective histone deacetylase inhibitor, has broad spectrum antitumor activity in vitro and in vivo. Molecular cancer therapeutics *7*, 759-768.

Furlan, A., Monzani, V., Reznikov, L.L., Leoni, F., Fossati, G., Modena, D., Mascagni, P., and Dinarello, C.A. (2011). Pharmacokinetics, safety and inducible cytokine responses during a phase 1 trial of the oral histone deacetylase inhibitor ITF2357 (givinostat). Molecular medicine *17*, 353-362.

Gore, L., Rothenberg, M.L., O'Bryant, C.L., Schultz, M.K., Sandler, A.B., Coffin, D., McCoy, C., Schott, A., Scholz, C., and Eckhardt, S.G. (2008). A phase I and pharmacokinetic study of the oral histone deacetylase inhibitor, MS-275, in patients with refractory solid tumors and lymphomas. Clinical cancer research : an official journal of the American Association for Cancer Research *14*, 4517-4525.

Hong, M., Puaux, A.L., Huang, C., Loumagne, L., Tow, C., Mackay, C., Kato, M., Prevost-Blondel, A., Avril, M.F., Nardin, A.*, et al.* (2011). Chemotherapy induces intratumoral expression of chemokines in cutaneous melanoma, favoring T-cell infiltration and tumor control. Cancer research *71*, 6997-7009.

Huang da, W., Sherman, B.T., and Lempicki, R.A. (2009a). Bioinformatics enrichment tools: paths toward the comprehensive functional analysis of large gene lists. Nucleic acids research *37*, 1-13.
Huang da, W., Sherman, B.T., and Lempicki, R.A. (2009b). Systematic and integrative analysis of large gene lists using DAVID bioinformatics resources. Nature protocols *4*, 44-57.
Jackson, E.L., Willis, N., Mercer, K., Bronson, R.T., Crowley, D., Montoya, R., Jacks, T., and Tuveson, D.A. (2001). Analysis of lung tumor initiation and progression using conditional expression of oncogenic K-ras. Genes & development *15*, 3243-3248.
Johnson, C.R., Kitz, D., and Little, J.R. (1983). A method for the derivation and continuous propagation of cloned murine bone marrow macrophages. J Immunol Methods *65*, 319-332.
Jones, P.A., Issa, J.P., and Baylin, S. (2016). Targeting the cancer epigenome for therapy. Nature reviews Genetics *17*, 630-641.
Juergens, R.A., Wrangle, J., Vendetti, F.P., Murphy, S.C., Zhao, M., Coleman, B., Sebree, R., Rodgers, K., Hooker, C.M., Franco, N.*, et al.* (2011). Combination epigenetic therapy has efficacy in patients with refractory advanced non-small cell lung cancer. Cancer discovery *1*, 598-607.
Khan, N., Jeffers, M., Kumar, S., Hackett, C., Boldog, F., Khramtsov, N., Qian, X., Mills, E., Berghs, S.C., Carey, N.*, et al.* (2008). Determination of the class and isoform selectivity of small-molecule histone deacetylase inhibitors. The Biochemical journal *409*, 581-589.
Koyama, S., Akbay, E.A., Li, Y.Y., Aref, A.R., Skoulidis, F., Herter-Sprie, G.S., Buczkowski, K.A., Liu, Y., Awad, M.M., Denning, W.L.*, et al.* (2016). STK11/LKB1 Deficiency Promotes Neutrophil Recruitment and Proinflammatory Cytokine Production to Suppress T-cell Activity in the Lung Tumor Microenvironment. Cancer research *76*, 999-1008.
Kramer, O.H., Baus, D., Knauer, S.K., Stein, S., Jager, E., Stauber, R.H., Grez, M., Pfitzner, E., and Heinzel, T. (2006). Acetylation of Stat1 modulates NF-kappaB activity. Genes & development *20*, 473-485.
Laoui, D., Van Overmeire, E., De Baetselier, P., Van Ginderachter, J.A., and Raes, G. (2014). Functional Relationship between Tumor-Associated Macrophages and Macrophage Colony-Stimulating Factor as Contributors to Cancer Progression. Frontiers in immunology *5*, 489.
Lavergne, E., Combadiere, C., Iga, M., Boissonnas, A., Bonduelle, O., Maho, M., Debre, P., and Combadiere, B. (2004). Intratumoral CC chemokine ligand 5 overexpression delays tumor growth and increases tumor cell infiltration. Journal of immunology *173*, 3755-3762.
Levinson, W., Ward, G., and Valleroy, M. (1989). Care of spinal-cord-injured patients after the acute period. Journal of general internal medicine *4*, 336-348.
Li, H., Chiappinelli, K.B., Guzzetta, A.A., Easwaran, H., Yen, R.W., Vatapalli, R., Topper, M.J., Luo, J., Connolly, R.M., Azad, N.S.*, et al.* (2014). Immune regulation by low doses of the DNA methyltransferase inhibitor 5-azacitidine in common human epithelial cancers. Oncotarget *5*, 587-598.
Liu, S.V., and Giaccone, G. (2016). Lung cancer: First-line immunotherapy in lung cancer - taking the first step. Nature reviews Clinical oncology *13*, 595-596.
Malvaez, M., McQuown, S.C., Rogge, G.A., Astarabadi, M., Jacques, V., Carreiro, S., Rusche, J.R., and Wood, M.A. (2013). HDAC3-selective inhibitor enhances extinction of cocaine-seeking behavior in a persistent manner. Proceedings of the National Academy of Sciences of the United States of America *110*, 2647-2652.
Molina, J.R., Yang, P., Cassivi, S.D., Schild, S.E., and Adjei, A.A. (2008). Non-small cell lung cancer: epidemiology, risk factors, treatment, and survivorship. Mayo Clinic proceedings *83*, 584-594.
Moran, C.J., Arenberg, D.A., Huang, C.C., Giordano, T.J., Thomas, D.G., Misek, D.E., Chen, G., Iannettoni, M.D., Orringer, M.B., Hanash, S.*, et al.* (2002). RANTES expression is a predictor of survival in stage I lung adenocarcinoma. Clinical cancer research : an official journal of the American Association for Cancer Research *8*, 3803-3812.
Moreno-Bost, A., Szmania, S., Stone, K., Garg, T., Hoerring, A., Szymonifka, J., Shaughnessy, J., Jr., Barlogie, B., Prentice, H.G., and van Rhee, F. (2011). Epigenetic modulation of MAGE-A3 antigen

expression in multiple myeloma following treatment with the demethylation agent 5-azacitidine and the histone deacetlyase inhibitor MGCD0103. Cytotherapy *13*, 618-628.
Motz, G.T., and Coukos, G. (2013). Deciphering and reversing tumor immune suppression. Immunity *39*, 61-73.
Oi, S., Natsume, A., Ito, M., Kondo, Y., Shimato, S., Maeda, Y., Saito, K., and Wakabayashi, T. (2009). Synergistic induction of NY-ESO-1 antigen expression by a novel histone deacetylase inhibitor, valproic acid, with 5-aza-2'-deoxycytidine in glioma cells. Journal of neuro-oncology *92*, 15-22.
Okayama, H., Saito, M., Oue, N., Weiss, J.M., Stauffer, J., Takenoshita, S., Wiltrout, R.H., Hussain, S.P., and Harris, C.C. (2013). NOS2 enhances KRAS-induced lung carcinogenesis, inflammation and microRNA-21 expression. International journal of cancer *132*, 9-18.
Pyonteck, S.M., Akkari, L., Schuhmacher, A.J., Bowman, R.L., Sevenich, L., Quail, D.F., Olson, O.C., Quick, M.L., Huse, J.T., Teijeiro, V.*, et al.* (2013). CSF-1R inhibition alters macrophage polarization and blocks glioma progression. Nature medicine *19*, 1264-1272.
Rasheed, W.K., Johnstone, R.W., and Prince, H.M. (2007). Histone deacetylase inhibitors in cancer therapy. Expert opinion on investigational drugs *16*, 659-678.
Reck, M., and Brahmer, J.R. (2017). Pembrolizumab in Non-Small-Cell Lung Cancer. The New England journal of medicine *376*, 997.
Reck, M., Rodriguez-Abreu, D., Robinson, A.G., Hui, R., Csoszi, T., Fulop, A., Gottfried, M., Peled, N., Tafreshi, A., Cuffe, S.*, et al.* (2016). Pembrolizumab versus Chemotherapy for PD-L1-Positive Non-Small-Cell Lung Cancer. The New England journal of medicine.
Roulois, D., Loo Yau, H., Singhania, R., Wang, Y., Danesh, A., Shen, S.Y., Han, H., Liang, G., Jones, P.A., Pugh, T.J.*, et al.* (2015). DNA-Demethylating Agents Target Colorectal Cancer Cells by Inducing Viral Mimicry by Endogenous Transcripts. Cell *162*, 961-973.
Ryan, Q.C., Headlee, D., Acharya, M., Sparreboom, A., Trepel, J.B., Ye, J., Figg, W.D., Hwang, K., Chung, E.J., Murgo, A.*, et al.* (2005). Phase I and pharmacokinetic study of MS-275, a histone deacetylase inhibitor, in patients with advanced and refractory solid tumors or lymphoma. Journal of clinical oncology : official journal of the American Society of Clinical Oncology *23*, 3912-3922.
Schlee, M., Holzel, M., Bernard, S., Mailhammer, R., Schuhmacher, M., Reschke, J., Eick, D., Marinkovic, D., Wirth, T., Rosenwald, A.*, et al.* (2007a). C-myc activation impairs the NF-kappaB and the interferon response: implications for the pathogenesis of Burkitt's lymphoma. International journal of cancer *120*, 1387-1395.
Schlee, M., Schuhmacher, M., Holzel, M., Laux, G., and Bornkamm, G.W. (2007b). c-MYC impairs immunogenicity of human B cells. Advances in cancer research *97*, 167-188.
Schuebel, K.E., Chen, W., Cope, L., Glockner, S.C., Suzuki, H., Yi, J.M., Chan, T.A., Van Neste, L., Van Criekinge, W., van den Bosch, S.*, et al.* (2007). Comparing the DNA hypermethylome with gene mutations in human colorectal cancer. PLoS genetics *3*, 1709-1723.
Soucek, L., Whitfield, J.R., Sodir, N.M., Masso-Valles, D., Serrano, E., Karnezis, A.N., Swigart, L.B., and Evan, G.I. (2013). Inhibition of Myc family proteins eradicates KRas-driven lung cancer in mice. Genes & development *27*, 504-513.
Stengel, S., Fiebig, U., Kurth, R., and Denner, J. (2010). Regulation of human endogenous retrovirus-K expression in melanomas by CpG methylation. Genes, chromosomes & cancer *49*, 401-411.
Stewart, S.A., Dykxhoorn, D.M., Palliser, D., Mizuno, H., Yu, E.Y., An, D.S., Sabatini, D.M., Chen, I.S., Hahn, W.C., Sharp, P.A.*, et al.* (2003). Lentivirus-delivered stable gene silencing by RNAi in primary cells. Rna *9*, 493-501.
Strissel, P.L., Ruebner, M., Thiel, F., Wachter, D., Ekici, A.B., Wolf, F., Thieme, F., Ruprecht, K., Beckmann, M.W., and Strick, R. (2012). Reactivation of codogenic endogenous retroviral (ERV) envelope genes in human endometrial carcinoma and prestages: Emergence of new molecular targets. Oncotarget *3*, 1204-1219.

Subramanian, A., Tamayo, P., Mootha, V.K., Mukherjee, S., Ebert, B.L., Gillette, M.A., Paulovich, A., Pomeroy, S.L., Golub, T.R., Lander, E.S*., et al.* (2005). Gene set enrichment analysis: a knowledge-based approach for interpreting genome-wide expression profiles. Proc Natl Acad Sci U S A *102*, 15545-15550.
Topalian, S.L., Taube, J.M., Anders, R.A., and Pardoll, D.M. (2016). Mechanism-driven biomarkers to guide immune checkpoint blockade in cancer therapy. Nature reviews Cancer *16*, 275-287.
Tsai, H.C., Li, H., Van Neste, L., Cai, Y., Robert, C., Rassool, F.V., Shin, J.J., Harbom, K.M., Beaty, R., Pappou, E*., et al.* (2012). Transient low doses of DNA-demethylating agents exert durable antitumor effects on hematological and epithelial tumor cells. Cancer cell *21*, 430-446.
Vendetti, F.P., Topper, M., Huang, P., Dobromilskaya, I., Easwaran, H., Wrangle, J., Baylin, S.B., Poirier, J.T., and Rudin, C.M. (2015). Evaluation of azacitidine and entinostat as sensitization agents to cytotoxic chemotherapy in preclinical models of non-small cell lung cancer. Oncotarget *6*, 56-70.
Weischenfeldt, J., and Porse, B. (2008). Bone Marrow-Derived Macrophages (BMM): Isolation and Applications. CSH Protoc *2008*, pdb prot5080.
Weiser, T.S., Guo, Z.S., Ohnmacht, G.A., Parkhurst, M.L., Tong-On, P., Marincola, F.M., Fischette, M.R., Yu, X., Chen, G.A., Hong, J.A*., et al.* (2001). Sequential 5-Aza-2 deoxycytidine-depsipeptide FR901228 treatment induces apoptosis preferentially in cancer cells and facilitates their recognition by cytolytic T lymphocytes specific for NY-ESO-1. Journal of immunotherapy *24*, 151-161.
Wrangle, J., Wang, W., Koch, A., Easwaran, H., Mohammad, H.P., Vendetti, F., Vancriekinge, W., Demeyer, T., Du, Z., Parsana, P*., et al.* (2013). Alterations of immune response of Non-Small Cell Lung Cancer with Azacytidine. Oncotarget *4*, 2067-2079.
Zahnow, C.A., Topper, M., Stone, M., Murray-Stewart, T., Li, H., Baylin, S.B., and Casero, R.A., Jr. (2016). Inhibitors of DNA Methylation, Histone Deacetylation, and Histone Demethylation: A Perfect Combination for Cancer Therapy. Advances in cancer research *130*, 55-111.

Figure Legends

Figure 1: Azacitidine synergizes with sequential HDACi.

A. Log dose response curves showing effect of sequential treatment with 500nM Aza or vehicle (mock) and various concentrations of ITF-2357 on growth of A549 and H460 cells (day 11, n=5). **B.** Combination index (CI) plots for sequential application of Aza + ITF-2357 in A549 and H460 cells (n=5). **C.** Log dose response curves showing effect of sequential treatment with 500nM Aza or vehicle (mock) and various concentrations of MS-275 on growth of A549 and H460 cells (day 11, n=3). **D**. Drug dose response matrix for A549 and H460 cells treated sequentially with vehicle (mock) or Aza (500nM) and HDACi's at concentrations defined in the figure. Color gradation based on mean viability (day 11, n=3). **E.** Normalized BrdU percent positivity for Aza +/- 100nM MS-275 or 100nM ITF-2357 (day 9, n=4 (MS-275), n=6 (ITF-2357)). All error bars indicative of SEM between biological replicates. **F**. Average volumes of tumor xenografts obtained from NOD-SCID mice subcutaneous injected with H460 cells following treatment with vehicle, 0.5mg/kg Aza, 2.0mg/kg MS-275, 2.0mg/kg ITF-2357 or a combination of these agents as outlined in the figure, (n=5), significance calculated using ANOVA.. Data are presented as mean ± SEM, * p value< .05 relative to mock, # p value< .05 relative to Aza + MS-275. See also Figures S1 and S6.

Figure 2: Epigenetic treatment of NSCLC cell lines induces robust alteration of cell transcriptome.

Analysis of RNA expression obtained from microarrays with NSCLC cells treated sequentially with vehicle (mock) or Aza and HDACi's at Day 8. **A.** Dot plot quantile distribution of relative RNA expression following treatment with the indicated drugs. **B.** Quantitation of the differentially expressed genes for each treatment condition (differential gene expression cutoff Log2 fold change over mock >0.5). **C.** Unsupervised hierarchical clustering of relative RNA expression by

median absolute deviation (MAD). RNA expression is Log2 fold change over mock, blue to red color gradation is based on the ranking of each cell line, inhibitor condition from minimum (blue) to maximum (red). The top 500 genes are depicted. **D.** DAVID analysis of the top 500 MAD genes using KEGG gene ontology. (Aza=500nM, ITF-2357=100nM, MS-275=100nM). See also Figure S2.

Figure 3: GSEA of transcriptional data reveal interferon alpha/ beta induction and cell cycle repression induced by combination epigenetic treatment.

GSEA (KEGG, REACTOME, and C5BP gene ontologies) of relative RNA expression from microarrays with NSCLC cells treated sequentially with vehicle or Aza and HDACi (8 days) (Aza=500nM, ITF-2357=100nM, MS-275=100nM) **A.** Venn diagrams showing numbers of overlapping and unique pathways upregulated by combination treatment among the indicated cell lines with the respective HDACi. (NES >2.0, FDR <0.25) Depicted pathways demonstrate significant upregulation in at least 3 cell lines. **B.** Venn diagram of pathways commonly upregulated following sequential combination treatment with Aza and the respective HDACi. **C.** GSEA enrichment plots for the top upregulated pathway (Interferon alpha beta signaling) following combination epigenetic treatment with the indicated HDACi. **D.** Venn diagrams showing overlapping and unique pathways down regulated by combination treatment among the indicated cell lines with the respective HDACi. (NES <2.0, FDR <0.25). Depicted pathways demonstrate significant repression in at least 3 cell lines. **E.** Venn diagram of pathways commonly down regulated following sequential combination treatment with Aza and the respective HDACi. **F.** GSEA enrichment plots for the top downregulated pathway(DNA replication).

Figure 4: Combination epigenetic treatment augments interferon alpha beta pathway associated immune genes and endogenous retrovirus transcription.

A. Heatmap of relative RNA expression for core enriched genes from the interferon alpha beta signaling pathway across NSCLC cell lines (microarray, day 8, Aza=500nM, MS275= 100nM, ITF-2357=100nM). **B.** Quantification of interferon alpha beta pathway core enriched genes differentially expressed by the indicated treatment conditions across NSCLC cell lines (microarray, day 8, Aza=500nM, MS275= 100nM, ITF-2357=100nM; differential gene expression cutoff Log2 fold change over mock >0.5). **C and D.** Expression of the viral defense gene subset of interferon alpha beta pathway genes induced by sequential treatment with Aza + HDACi (analyzed on genecard, day 8, 500nM Aza, 100nM ITF-2357, 200nM MCGD0103, 1000nM Tubastatin A). **E and F.** Quantitation of selected MHC class I gene subset of interferon alpha beta pathway in response to Aza and/or HDACi (qRT-PCR, day 8, 500nM Aza, 100nM ITF-2357, 200nM MCGD0103, 2000nM RGFP996, 1000nM Tubastatin A, n=3). **G and H.** Quantitation of endogenous retrovirus transcripts in response to Aza and/or HDACi (qRT-PCR, day 8, 500nM Aza, 100nM ITF-2357, 100nM MS-275; n=4) **I, J.** Quantitation of ERV9_1 in response to Aza and/or HDACi (500nM Aza, 100nM ITF-2357, 200nM MCGD0103, 2000nM RGFP996, 1000nM Tubastatin A, n=3). Data are presented as mean ± SEM. * p value< .05 relative to mock, # p value< .05 relative to Aza. See also Figures S3, S4 and S6.

Figure 5: MYC perturbation drives sensitization to HDACi and interferon alpha beta pathway gene augmentation

A. Quantitation of relative MYC RNA expression (microarray, day 8, Aza=500nM). **B.** Immunoblot showing expression of MYC on day 9 of treatment. Beta actin used as loading control (Aza=500nM, n=3). **C.** Unsupervised hierarchical clustering of relative RNA expression for HALLMARK MYC TARGETS gene set. Color gradation based on Z score ranking of log2 fold change over mock (microarray, day 8, Aza=500nM, MS-275=100nM, ITF-2357=100nMD.

Quantitation of cell proliferation, normalized to untreated control, for GFP and shMYC infected A549 and H460 cells treated with the indicated HDACi's for 5 days (n=3). The presented data are the ratio of normalized colorimetric absorbance between the GFP treated and shMYC treated cells, displayed as a percentage of GFP cells. **E.** Quantitation of cell proliferation, normalized to untreated controls, for A549 and H460 cells infected with Empty vector or MYC overexpression constructs followed by treatment with increasing concentration of the indicated HDACi's for 5 days (n=3 overexpression clones) The presented data are the ratio of normalized colorimetric absorbance between the empty vector treated and MYC overexpression construct containing cells, displayed as a percentage of Empty vector cells. **F.** Relative RNA expression of interferon alpha beta pathway responsive genes in A549 cells infected with empty vector or MYC overexpression construct and treated with vehicle or 500nM Aza + 100nM ITF-2357 (genecard, day 8). **I.** Relative RNA expression of interferon alpha beta pathway responsive MHC class I genes in A549 cells infected with empty vector or MYC overexpression construct and treated with vehicle or 500nM Aza + 100nM ITF-2357 (qRT-PCR, day 8, n=3). Data are presented as mean ± SEM. * p value< .05 relative to mock, * p value< .05 relative to EV + Epigenetic treatment. See also Figure S5.

Figure 6: Combination epigenetic treatment reduces lung tumor burden, progression and proliferation in a *Kras* G12D mouse model with corresponding alterations of the tumor transcriptome

A. In vivo treatment schema for sequential combination epigenetic treatment with 0.5mg/kg Aza + 2.0mg/kg ITF-2357 applied to a *Kras* G12D murine model of NSCLC. **B**. Representative macroscopic images of lungs from mice treated for 12 weeks post disease initiation with vehicle or epigenetic drugs as indicated in the schema (n=7 per group). **C**. Representative H & E and Ki67 stained IHC images of murine lung sections treated with vehicle and combination epigenetic treatment (n=7 per group). Images scanned using the Aperio Scanscope sytem. **D.**

Volcano plot of relative RNA expression from lung tumors obtained from mice treated with combination epigenetic treatment as compared to control mice. Genes in upper left and right quadrants are significantly, differentially expressed (microarray, n=2 mice per group). **E.** GSEA (KEGG, REACTOME, HALLMARK gene ontologies) derived NES and FDR plot of relative RNA expression from mice treated with combination epigenetic treatment. Horizontal line denotes FDR significance cutoff of 0.25. Immune and cell cycle related gene sets are demarcated by green and red dot coloration (microarray, n=2 per group). **F**. Gene sets upregulated (<FDR 0.25 and >NES 1.5) by combination epigenetic treatment; color gradation based on GSEA NES. **G.** Representative upregulated gene set enrichment plots with corresponding core enriched genes; color gradation representative of Log2 fold change over vehicle treated RNA expression. **H**. Gene sets downregulated (<FDR 0.25 and <NES 1.5) following combination epigenetic treatment; color gradation based on GSEA NES. **I**. Representative downregulated gene set enrichment plot with core enriched genes; color gradation representative of Log2 fold change over vehicle treated RNA expression.

Figure 7: Combination epigenetic treatment induces CCL5 secretion, T cell infiltration and macrophage depletion in tumor microenvironment.

A. IHC staining of CD8 positive cells in lung tumors of vehicle and combination epigenetic drug treated mice following 12 weeks of treatment post disease initiation (n=7 per group). Images scanned using the Aperio Scanscope sytem **B**. Relative RNA expression based enrichment plot for HALLMARK INTERFERON GAMMA RESPONSE gene set in lung tumors from mice treated with combination epigenetic treatment as compared to vehicle treated mice. Color gradation is representative of Log2 fold change over vehicle RNA expression (microarray, n=2 per group). **C.** Expression of CCL5 RNA in mouse lung tumors in response to treatment with vehicle or combination epigenetic drugs (microarray, n=2, p value <.05). **D**. Quantitation of CCL5 chemokine levels in bronchoalveolar lavage from mice treated with either vehicle or

combination epigenetic drugs (n=3, error bars=SD, p value <.05) **E.** Relative CCL5 RNA expression in human NSCLC cell lines treated in vitro with Aza and/or HDACi (day 8, microarray, Aza=500nM, MS-275=100nM, ITF-2357=100nM). **F.** Relative CCL5 RNA expression in GFP or MYC overexpressing A549 cells treated with 500nM Aza and/or 100nM ITF-2357 (qRT-PCR, Day 8, n=3, error bars=SEM). **G.** Profile interaction plots of TCGA RNA seq data for CCL5 and MYC expression across LUAD samples. 576 LUAD samples were ranked by expression of CCL5 and MYC into: low, intermediate and high expression groups. These 3 expression categories for MYC and CCL5 were then compared as follows, where gene(y) is sorted based on low, intermediate or high expression of other gene: MYC high:CCL5(y), MYCintermediate:CCL5(y), MYClow:CCL5(y), MYC(y):CCL5high, MYC(y):CCL5intermediate, MYC(y):CCL5low. **H.** Representative images of IHC staining of macrophages with F4/80 in lung tumor sections from mice treated with vehicle or combination epigenetic drugs for 12 weeks. Upper panel: Images scanned using the Aperio Scanscope sytem; Lower panel: Positive pixel transformation of images displayed in upper panel to depict saturation of F4/80 staining, degrees of saturation arbitrary units: blue=0, yellow=1, orang=2, red=3. (n=7 per group). **I.** Quantitation of in vitro cultured bone marrow derived macrophages isolated from C57Bl/6 mice following sequential treatment with 500nM Aza and/or 100nM ITF-2357(3 day Aza, 3-day ITF-2357, error bars=SD, n=4). **J.** Quantitation of in vitro cultured bone marrow derived macrophages isolated from C57Bl/6 mice and treated with the supernatants obtained from Lewis Lung Carcinoma cells treated with 500nM Aza and/or 100nM ITF-2357 (3 day Aza, 3-day ITF-2357, error bars=SD, n=4). * p value< .05 relative to mock, # p value< .05 relative to Aza, * p value< .05 relative to EV + Epigenetic treatment. See also Figure S7.

METHODS

Cell culture and Treatments

A549, H460, H23 and H1299 human non small cell lung cancer (NSCLC) cells lines were obtained from ATCC. Cells were maintained in (RPMI-1640) and cultured at 37ºC in the presence of 5% CO_2. Details of drug used and treatment conditions are described in detailed methods.

Cell viability assay

Cell titer 96 aqueous one (MTS) (Promega) was deployed according to standard protocol. Absorbance and dose response data were analyzed as described in detailed methods.

BrdU Proliferation Assay

Assay performed according to standard protocol using Calbiochem BrdU Cell Proliferation ELISA (Millipore). Detailed methods and analysis parameters described in detailed methods.

shRNA/Overexpression vectors

shRNA vectors: shGFP (Chiappinelli et al., 2015), shMYC (TRCN0000010391), and shDNMT1 (Cai et al., 2017); Overexpression vectors: MYC vector (Addgene plasmid # 46970) and Empty vector (Addgene plasmid # 72299) were deployed using established methods (Stewart et al., 2003). Analysis of cell viability in the presence of c-MYC knockdown and overexpression vectors are detailed in the Supplemental Experimental Procedures. ERV overexpression vectors: The description and transfection methodology (JetPei transfection reagent) of the expression vectors *Syncytin-1* (5' LTR-Syn-1-pGL3)*, ERV-3* (p3Xflag-CMV-14) and pE-GFP-N1 (Clontech Laboratories, Inc.) was previously described by us (Chiappinelli et al., 2016).

RNA extraction and analysis of gene expression

Total RNA was isolated from cultured cells or mouse lung tumors using the RNeasy Mini kit (Qiagen), RNA was analyzed by quantiatative RT-PCR, processed for hybridization on an Agilent Human Gene Expression v2 4x44K Microarray chip two color, Agilent Mouse Gene Expression 4x44k Microarray chip single color, or using taqman microfluidic genecards. The R/Bioconductor package limma was used to process expression data, which were analyzed as describe in detailed methods.

Protein Extraction and Immunoblotting

Cells were collected at the indicated time points. Cells were lysed with 4% SDS and passed through QIAshredder (Qiagen) to obtain whole cells extracts. A comparable amount of total protein from each sample was separated on a 4-12% % BOLT Bis-Tris gels (Thermo Fischer Scientific). Membranes were probed with the indicated antibodies specific: Total Histone 3, c-MYC, acetylated tubulin, (Cell signaling Technology); β-actin, DNMT1 (Sigma, St. Louis, MO and Acetylated histone 3 (Upstate). The blots were developed using an ECL kit (Pierce, Rockford, IL). Band densitometry for western blots were quantitated using Image lab software (Bio-Rad).

Xenograft Studies

H460 xenografts were initiated by subcutaneously injecting 5x 10^4 viable cells in the flank of male *NOD-SCID mice (*5-6 weeks). Mice were monitored every 3 days for duration of xenograft study, tumor volume was quantified by 0.5(LxWxH) formula and measured by a blinded investigator. All animal care was in accord with institutional guidelines and approved Institutional Animal Care and Use Committee (IACUC) protocols. Drugs used to treat mice as well as the duration of treatment are described in detailed methods.

KrasG12D Mouse Model Studies

LSL-Kras^{G12D} (Jackson et al., 2001) mice were obtained from Jackson laboratories and bred to generate heterozygous *Kras*^{G12D} mice. *Kras*^{G12D} mice (8-10 weeks, both genders) were infected intratracheally with Adenoviral vectors encoding *Cre* (obtained from University of Iowa*)* to activate *Kras*. IHC was conducted on fixed, paraffin imbedded sections with the following primary antibodies: CD8(eBiosciences), F4/80 (Serotec), Ki67(Cell Signaling), All experimental animal protocols were performed in accordance with guidelines approved by the animal care and use committee at the Johns Hopkins University (Baltimore, MD). Drugs used to treat mice, duration of treatment, IHC methods and histological analysese are described in detailed methods.

Mouse Cytokine Analysis

Cytokine levels in cell-free BAL fluid samples obtained from the mice were quantitated using Mouse Cytokine Array Q1 (Raybiotech). The BAL fluid samples were thawed, and run per the manufacturer's protocol, and measured as pg/mL of BAL fluid (n = 3).

Isolation of bone marrow derived macrophages (BMDMs): BMDMs were isolated from femurs and tibias of 8 week old mice as described previously (Johnson et al., 1983; Weischenfeldt and Porse, 2008). Cells were grown in DMEM medium supplemented with 10ng/mL macrophage-colony stimulating factor. After 7 days in culture adherent cells were approximately 95 % pure macrophages and were used for experiments.

TCGA Analysis

Broad Morpheus tool was used to analyze TCGA lung adenocarcinoma data for the relationship between CCL5 and MYC expression as described in detailed methods.

Statistical Analysis

qRT-PCR and BrdU proliferation data are presented as the mean ± standard error of mean (SEM), data analyzed by two-way ANOVA between drug conditions. c-MYC shRNA and overexpression vector experiments data are mean ± SEM, with two-tail student t-test used to test for significance. Mouse cytokine data are presented as mean ± standard deviation (SD), with two-tail student t-test used to test for significance. p values of <0.05 were considered statistically significant for all tests and are demarcated by * or #.

DETAILED METHODS

Cell Culture

The cells were cultured as described below in RPMI1640 media (Corning) containing FBS (Gemini) at 10% v/v. Cells were passaged every 3 days.

Drug Reagents

Azacidine (Sigma) was dissolved in PBS to concentration of 500uM (in vitro) and 7.1 mg/mL (in vivo), aliquoted, and stored at -80C for single use. ITF-2357 (Apexbio) was dissloved in DMSO to concentrations of: 1mM, 500uM, 250uM, 100uM, 50uM and 25uM (in vitro) and 50mg/mL (in vivo), aliquoted and stored at -20C. MS-275 (Syndax) was dissloved in DMSO to concentrations of: 2.5mM, 1mM, 500uM, 250uM, 125uM (in vitro) and 50mg/mL (in vivo), aliquoted and stored at -20C. MCGD0103 (Apexbio) was dissloved in DMSO to concentrations of: 1mM, 500uM, 250uM, 100uM, 50uM and 25uM (in vitro), aliquoted and stored at -20C. RGFP996 (Apexbio) was dissloved in DMSO to concentrations of: 10mM, 5mM, 2.5uM, 1uM, 500uM and 100uM (in vitro), aliquoted and stored at -20C. Tubastatin (Apexbio) was dissloved in DMSO to concentrations of: 10mM, 5mM, 2.5mM, 1mM, 500uM and 250uM (in vitro), aliquoted and stored at -20C. Vorinostat (Cell signaling) was dissloved in DMSO to concentrations of 300uM (in

vitro), aliquoted, and stored at -20C. Puromycin (Sigma), dissolved to 1mg/mL, aliquoted and stored -20C.

Azacitidine Treatments

Cell lines were plated at the following densities: 1.0*10^5 cells per T75 flask (H460, A549, H1299), 2.0*10^5 cells per T75 flask. Allowed to adhere for 24 hours before the onset of treatment. Cells were treated with 500uM Azacitidine diluted 1:1000 or PBS vehicle in complete RPMI1640 media every 24 hours for the indicated treatement duration.

Cell Viability Assays (MTS colorimetric)

Cells treated as described in Azacitidine treatment section, were trypsinized, enumerated, and assesed for viability by trypan blue exclsuion assay. Equal numbers of viable cells were plated in 96 well plates at the following densities, in technical triplicate: 1000 cells per well: H460, A549, H1299 and 2000 cells per well: H23. Cells were allowed to adhere for 24 hours in the presence of complete media prior to the onset of treatment. Adhered cells were incubated with 100uL drug supplemented media every 3 days, treated with DMSO(vehicle) at .1% or the following drugs/concentrations standarized to .1% DMSO final concentration. ITF-2357: 25nM, 50nM, 100nM, 250nM, 500nM, 1uM; MCGD0103: 25nM, 50nM, 100nM, 250nM, 500nM, 1uM; RGFP996: 250nM, 500nM, 1uM, 2.5uM, 5.0uM and 10uM; Tubastatin A: 250nM, 500nM, 1uM, 2.5uM, 5.0uM and 10uM;; MS-275: 125nM, 250nM, 500nM, 1uM, 2.5uM. Treatments were applied for a period of 5 days, afterwhich, MTS colorimetric assay (promega) waas conducted. MTS reagent was diluted 20uL per mL in complete and vortexed to ensure the resultant solution was homogenous. Drug treated was gently removed from treated cells by multichannel pipette and replaced MTS supplemented media. Cells were incubated in 37C incubator to allow the colorietric reaction to occur. 490nm absorbance was read using the BioRad iMark microplate reader for media+MTS, vehicle treated+MTS and drug treated+MTS cells. Absorbance values

were imported to Graphpad prism. Data were normalized the vehcicle treated cells for both mock and Aza treated condtion. Drug doses were log transformed. These normalized, lofg transformed data were analyzed by 4 parameter nonliner regreesion to generte log dose response curves for each cell line and drug condition and determination of drug effect at dose. The resultant dose repsonse curves are a representation of these data, with the indicated biolofical replicates being a represention of the mean for each condtion. These dose response data were utlitized for drug synergy analysis using chou talay method intrinsci to the Compusyn software. The fractional affect data for each drug condtion were imported for drugs both alone and in combination with Aza. These data were anayzed and used to generate combination index output as an indicator of drug synergy.

Brdu Cell Prolifertion Assay, colorimetric ELISA

Cells were plated in technical triplate in 96 well fomat at the densities described in the Cell viabilty section. Vehicle or Aza treated cells were allowed to adhere for 24 hrs prior to the onset of treatment. Cell were subsequently treated with the following inhibtiors for 3 days. MCGD0103: 200nM, ITF-2357: 100nM, Tubastatin A: 1uM, RGFP996: 2uM. On day 3 of treatment, Stock Brdu (Calbiochem BrdU Cell Proliferation Assay) was diluted 1:1000 in complete media and added to 100uL of drug treated media. Cells were incubated with BrdU at 37C for 5 hours to allow for DNA synthese based incorporation. The reaminder of protocol was carried out as decribed in Calbiochem protocol, with the lot specifc 1:2400 dilution of secondary antibody. 450nm absorbance values derived from ELISA were measured using the Biorad iMark plate reader. The triplacate measurements per conditon were imported to graphpad prism and the data background subtracted, normalized to vehicle treated control to gnerate the normalized proliferation. Error bars depicted as SEM between the means of experimental replicates, after computing the mean of technical triplicates. Statistical signifcance is the result of two way anova conducted between the experimental conditions depicted.

Gene expression analysis

Gene expression was studied across NSCLC cell lines: H460, A549, H1299, H23. With the following drug conditions assayed on day 8 of treatment: Mock, 100nM MS275. 100nM ITF-2357, 500nM Azacitidine, 500nM Azacitidine + 100nM ITF-2357, and 500nM Azacitidine + 100nM MS-275. The R/Bioconductor package limma was used to process expression data. Within- and between-array normalizations were performed using the loess and aquantile methods, respectively. The normexp option was used for background correction. Raw files read in using the read.maimages function. Log2 fold change in transcription for drug treated conditions over mock treated was obtained for each sample at each time point studied. Ranked lists of log2 fold change were analyzed using Gene Set Enrichment Analysis (GSEA) by the Broad Institute and data packages (KEGG, C5BP and Reactome) (Subramanian et al., 2005). Pathways enriched with a false discovery rate less than 0.25 were selected with cutoff of 2.0 normalized enrichment score in human and 1.5 normalized enrichment score cutoff in mouse studies. Median absolute deviation analysis of Log2 fold change transcription data were obtained using Morpheus program (Broad). Top 500 genes were selected and depicted as heatmap representative of minimum to maximum value ranking for each gene across cell lines and conditions.

DAVID analysis of median absolute deviation derived genes (KEGG Pathways)

Top 500 genes derived by median absolute deviation were obtained as described above were analyzed for Gene Ontology (GO) enrichment for KEGG pathways using the DAVID Bioinformatics resources database (Huang da et al., 2009a, b). Only categories that were below the DAVID p value of .05, and containing at least 5 genes per pathway are reported.

MYC targets heatmap:

MYC targets heat maps are based on hierarchical clustering of Log2 fold change over mock using Euclidean distance and complete linkage of MYC hallmarks gene set v2.

qPCR Primers

Gene	Fwd	Rev
OASL1	TCGTGAAACATCGGCCAACT	ACCTGGCTTTCACATACTGCT
HLA-A	TCAGATAGAAAAGGAGGGAGTTACA	ACAAGCTGTGAGGGACACAT
HLA-B	CCTGAGATGGGAGCCGTCTT	CTCCGATGACCACAACTGCT
CCL5	TGCTGCTTTGCCTACATTGC	CTTGACCTGTGGACGACTGC
CT45A1	GCACCTGTGGGAGGAAACG	CCTGACTGCAGTAGGTCCTTG
SPANXB1	TGTGAATCCAACGAGGCCAACG	CCACTAGTATGGTCGAGGACTC
Beta Actin	CAACCGCGAGAAGATGACC	TAGCACAGCCTGGATAGCAA

ERV absolute quantitative real time PCR (qPCR)

Eleven codogenic and partially codogenic ERV envelope (env) gene families (see Figure 4 and Figure S4 for ERV env genes used in this investigation), one ERV gag (ERV-W5) and two ERV pols (ERVFXA34, erv9-1) were quantified using qPCR and have been previously described by us (Chiappinelli et al, 2015). Additionally, some of these ERV primers could potentially hybridize with other ERV transcripts among the ERV family members, e.g. the ERV-K env primers could hybridize with 8 transcripts derived from ERV-K102 (1q22), -107 (5q33.3), -108 (7p22.1), -109 (6q14.1), -113 (19p13.11), -115 (8p23.1), -17833 (19q12), -74261 (12q14.1) according to sequence alignments (Chiappinelli et al, 2015).

The qPCR methodology detecting the ERV genes has been previously described by us (Chiappinelli et al, 2015). Briefly, ERV genes were amplified by qPCR from 40 ng of cell line cDNA with SYBR-green technology and then analyzed with an ABI7300 (ABI, Darmstadt, Germany). Expression values were calculated as molecules per ng total RNA using a standard curve of each cloned gene determined by real time PCR and calculated as mean +/- standard deviation of the mean (s.e.m.). TBP and beta-actin were used as housekeeping genes where a mean from both genes was used for normalization of NSCLC cell lines.

DNMT1 Knockdown Cell Viability Assay

DNMT1 knockdown was initated, see refernce for sequence (PMID: 2823247) and control vector shGFP 5′- GCAAGCTGACCCTGAAGTTCAT3-3′. Clonal selection was initated with puromycin selection. Selected clones were plated at cell densities, treated and analyzed as described in Cell viabilty Assay section of methods. Error bars are representative of SEM between experimental replicates.

MYC Knockdown Cell Viability Assay

MYC knockdown was initated using Broad TRCN0000010391 clone and control vector shGFP 5′- GCAAGCTGACCCTGAAGTTCAT3-3′. Clonal selection was initated with puromycin selection. Selected clones were plated at cell densities and treated as described in Cell viabilty Assay section of methods. MTS was used to quantify numbers of proliferating cells. Bar graphs depicted are representative of the percent of MYC knockdown cells present as a percentage of the Empty vector treated controls for same dose of drug. Error bars are representative of SEM between experimental replicates. Statistical significance was determined by two tailed t test between empty vector and MYC shRNA treated cells at each dose.

MYC Overexpression Cell Viability Assay

MYC vector (Addgene plasmid # 46970) and Empty vector (Addgene plasmid # 72299). Clonal selection was initated with puromycin selection. Selected clones were plated at cell densities and treated as described in Cell viabilty Assay section of methods. MTS was used to quantify numbers of proliferating cells. Bar graphs depicted are representative of the percent of MYC overexpression cells present as a percentage of the Empty vector treated controls for same dose of drug. Error bars are representative of SEM between experimental replicates. Statistical significance was determined by two tailed t test between empty vector and MYC overexpression vector treated cells at each dose.

In-vivo Drug Studies

Mice were treated as follows: Azacitdine 0.5 mg/kg (PBS vehicle) IP injected daily for 5 days sequentially, every 14 days. ITF-2357 2.0 mg/kg (1% DMSO in PBS vehicle) IP injected daily for 5 days sequentially, every 14 days. MS-275 2.0 mg/kg (1% DMSO in PBS vehicle) IP injected daily for 5 days sequentially, every 14 days. InVivoMAb mouse Anti-PD1 (BioXcell RMPI 14 clone) injected 10ug/kg on the 12^{th} day of a 14 day cycle. InVivoMAb Rat IgG2a Isotype control (BioXcell 2A3 clone) injected 10ug/kg on the 12^{th} day of a 14 day cycle. For xenograft studies, drug application iniated 10 days post injection when palpable tumors sould be discerned and continued for 37 days. For KrasG12D mouse model studies, drug application initated 16 weeks post Ad-Cre instillation, and applied for 12 weeks as described in the Kras G12D animal model section.

Kras G12D Mice

LSL-KrasG12D (Jackson et al., 2001) mice were obtained from Jackson laboratories and bred to generate heterozygous KrasG12D mice. KrasG12D mice (8-10 weeks, both genders) were infected intratracheally with Adenoviral vectors encoding Cre (obtained from University of Iowa)

to activate Kras. LSL-KrasG12D mice harbor a latent point-mutant allele of Kras (KrasG12D) and infection with an adenoviral vector encoding Cre leads to Cre-mediated deletion of a transcriptional termination sequence (Lox-Stop-Lox, LSL) and the oncogenic Kras production, thereby resulting in very high frequency of lung tumors (Jackson et al., 2001). All experimental animal protocols were performed in accordance with guidelines approved by the animal care and use committee at the Johns Hopkins University (Baltimore, MD). Mice were examined for presence of disease at 16 weeks post infection with AdenoCre. Mice were sacrificed and lungs were examined histologically. At this stage most of the mice showed presence of significant regions of hyperplasia as well as adenomas. Drug treatments were started as per the schedule shown in Figure 6 A. Mice were divided in two groups. Once group was injected with vehicle control while the other was injected with combination epigenetic drugs. Mice were uniformly distributed into the two treatment groups so that each group had comparable numbers of age and weight matched male and female mice. Drug treatments were continued for 12 weeks following which mice were sacrificed and the lungs were processed for histological studies, RNA extraction on analysis of cytokine levels in lung bronchoalveolar lavage (BAL) fluid as described as described in main methods.

Assessment of lung tumor formation

Mice were sacrificed by and the left lung was fixed in formalin for histologic examination. The right lung in some mice was lavaged by instilling with 1.0ml of sterile PBS to collect Bronchoalveolar lavage (BAL) fluid. In some mice right lung was used to macro dissect tumors for RNA extraction.

Histological analysis

Lungs tissues were fixed in 10% formalin overnight, and subsequently transferred into 70% ethanol, embedded in paraffin and sectioned (5 μM) at 3 levels at regular intervals. Sections

were stained with Hematoxylin and eosin (H&E) and scanned using the Aperio whole slide scanning system (Scanscope CS) The entire left lung lobe was scanned for presence of adenomas/adenocarcinomas using the Aperio ImageScope analysis software. For each sample, sections from 3 levels were analyzed. Unstained sections of the left lung were also used for Immunohistochemistry (IHC) staining. All Images were scanned using the Aperio Scanscope system.

Immunohistochemistry (IHC):

Immunostaining of lung sections was performed with the PowerVision kit according to the manufacturer's protocol (Leica Biosystems). Briefly, slides were heated at 60°C for 10 min,deparaffinized and hydrated through xylene, graded ethyl alcohols, dH2O, dH2O with 20% Tween 20 (P-7949, Sigma-Aldrich). After antigen retrieval (45 minutes of steaming in Target Retrieval Solution (Dako S170084-2) using Black and Decker Handy Steamer Plus), sections were treated 5 minutes with Dual Endogenous Enzyme Block (S2003, Dako). Sections with primary antibodies Ki67 (Cell signalling, 9101, 1:500) were incubated at room temperature for 45 minutes. Additional blocking steps were used for CD8 and F4/80 slides using DakoCytomation Biotin Blocking System (X0590). Antibody incubations for CD8 (eBiosciences, 14-0808, 1:800) and F4/80 (Serotec, MCAP497, 1:1000) were carried out at room temperature for 45 minutes, soaked an additional 45 min in PBS-Tween, and followed by mouse adsorbed biotinylated anti Rat IgG (Vector, BA-4001, 1:500) for 15 minutes. For all, the secondary used was anti-rabbit IgG-reagent provided in the Powervision kit (PV6119, Leica Biosystems) for 30 minutes. Immunostaining was visualized with DAB chromogen (D4293, Sigma-Aldrich) and sections were counterstained with Mayer's hematoxylin. Control slides: No primary for each, CD8 (spleen), F480 (tumor)

F4/80 Intratumor Macrophage Analysis

F4/80 IHC stained sections were scanned used the Aperio system as described earlier, these images were analyzed use imagescope software. To generate the false color images depicted, used to demarcate pixel saturation by macrophage infiltration, the images were analyzed by the positive pixel v4 algorythm.

TCGA Analysis

Broad Morpheus tool was used to analyze TCGA LUAD data for the relationship between CCL5 and MYC. First the 2 genes were selected from available RNA seq data of 576 patients available. These data were used to generate a new heat map. This new heat map was sorted based on CCL5 and MYC expression and the samples were separated into low, intermediate and high expression groups. These subsets were than compared using the profile interaction tool, to generate the depicted plots.

Supplementary Legends

Figure S1: Sequential but not concurrent Aza + HDACi potently enhances HDACi effect on cell proliferation. Related to Figure 1

A. In vitro treatment schema for sequential and concurrent application of Aza and/or HDACi to NSCLC cell lines. **B.** Log dose response curve for H460 cells treated concurrently with 500nM Aza and variable concentrations of ITF-2357 (day 5, n=3). **C.** Log dose response curves showing effect of sequential treatment with 500nM Aza or vehicle (mock) and various concentrations of ITF-2357 on growth of H23 and H1299 cells (day 11, n=3). **D.** Table of pharmacokinetic and pharmacodynamic parameters for clinically relevant HDAC inhibitors used in study. **E.** Evaluation of pharmacodynamic targets for HDAC1/2: histone acetylation and HDAC6: tubulin acetylation by immunoblotting. Total histone 3 and beta Actin used as loading controls (24-hour treatment, n=2). **F.** Normalized BrdU percent positivity for mock or Aza treated cells in combination with the indicated HDACi's (day 9, MCGD0103=200nM, RGFP996=2000nM, Tubastatin A=1000nM; n=6). All error bars indicative of SEM between biological replicates. * p value< .05 relative to mock.

Figure S2: Combination epigenetic treatment induces significant differential gene expression. Related to Figure 2

A. Relative RNA expression correlation matrix for inhibitor conditions and cell lines indicated in figure (microarray, day 8, Aza=500nM, MS-275=100nM, ITF-2357=100nM), Axis are Log2 Fold change over mock relative RNA expression. **B.** Total number of identified Top Tier genes by cell line **D.** Relative RNA expression distribution of Aza + HDACi normalized for the induction by Azacitidine alone, plotted as log2 fold axis are Log2 Fold change over Aza for each combination drug treatment. (microarray, day8, Aza=500nM, MS-275=100nM, ITF-2357=100nM)

Figure S3: HDACi isoform specific induction of interferon signaling. Related to Figure 4

A and C. Expression of Interferon stimulated genes induced by Aza and/or HDACi depicted in the figure in A549 cells and H23 cells (Genecard, day 8, Aza=500nM, ITF-2357=100nM, A, 200nM MCGD0103, SAHA=300nM). **B and D**. Expression of Interferon stimulated genes induced by Aza and/or HDACi depicted in figure in A549 and H23 cells (Genecard, day 8, Aza=500nM, , 1000nM Tubastatin A, 2000nM RGFP996).

Figure S4: Sequential Aza + HDACi imparts significant amplification of Aza response. Related to Figure 4

A and B. ERV expression in H1299 and H460 cells treated sequentially with Aza and/ or HDACi (day 8, qRT-PCR, Aza=500nM, MS-275=100nM, ITF-2357=100nM, n=4). **C.** Effect of ERV overexpression on transcription of the interferon stimulated gene, OASL, in A549 and H23 cells (48-hour post transfection, qRT-PCR, ERV3 overexpressed in A549, SYN1 overexpressed in H23, n=4). **D.** Heatmap of relative RNA expression for cancer/testis antigen genes across NSCLC cell lines (microarray, day 8, Aza=500nM, MS275= 100nM, ITF-2357=100nM). **E.** Quantification of cancer/testis antigen transcriptional induction by combination Aza + HDACi treatment over Aza alone across NSCLC cell lines (microarray, day 8, Aza=500nM, MS275= 100nM, ITF-2357=100nM; differential gene expression cutoff Log2 fold change over Aza >0.5). **F and G**. Quantitation of selected cancer/testis antigen transcriptional response to Aza and/or HDACi (qRT-PCR, day 8, 500nM Aza, 100nM ITF-2357, 200nM MCGD0103, 2000nM RGFP996, 1000nM Tubastatin A, n=3). All error bars indicative of SEM between biological replicates**.** * p value< .05 relative to mock or Empty vector.

Figure S5: Validation of MYC perturbations. Related to Figure 5

A. Immunoblotting for c-MYC in H460 cells treated with Aza with or without HDACi. Beta Actin used as loading control (Day 9, 500nM Aza, 100nM ITF-2357, 200nM MCGD0103, 2000nM

RGFP996, 1000nM Tubastatin A, n=2) **B.** Immunoblotting for c-MYC in H460 and A549 cells infected with empty or c-MYC overexpression vector. Beta Actin used as loading control. (day 5, n=2). **C.** Immunoblotting for c-MYC in H460 and A549 cells infected with GFP or c-MYC shRNA vector. Beta Actin used as loading control (day 4, n=2).

Figure S6: Direct targeting of DNMT1 mimics Aza sensitization to HDACi. Related to Figure 1 and 4

A. Immunoblotting for DNMT1 in A549 and H460 cells infected with GFP or shDNMT1 vector. Beta Actin used as loading control (day 5, n=2). **B.** Log dose response for A549 and H460 cells infected with GFP or shDNMT1 vector and treated with HDACi as indicated in figure (5 day HDACi exposure, n=2) **C.** Relative ERV9-1 expression in A549 cells treated with HDACi in the presence of GFP orshDNMT1 constructs (2 day HDACi exposure, ITF-2357=100nM, 1000nM Tubastatin A, 2000nM RGFP996, 200nM MCGD0103, n=2) All error bars indicative of SEM between biological replicates.

Figure S7: Combination epigenetic treatment reduces disease burden *in vivo*. Related to Figure 7

A. Additional macroscopic images of murine lungs treated with vehicle or 0.5mg/kg Aza and 2.0mg/kg ITF-2357, for 12 weeks' post onset of disease initiation (n=7 mice treated). **B.** Quantitation of total tumor area occupied by lesions in lungs of *Kras* G12D mice treated with vehicle or Aza + ITF-2357 as estimated with use of the Aperio software, 3 sections were used per mouse, with the resultant values averaged (n=4) **C.** In vivo treatment schema for addition of anti-PD1 to Kras G12D mice **D.** Representative H&E sections of lungs from anti-PD1 and Aza + ITF-2357 + anti-PD1 treated mice (n=2 anti-PD1, n=5 anti-PD1 + Aza + ITF-2357). * p value< .05 relative to mock.

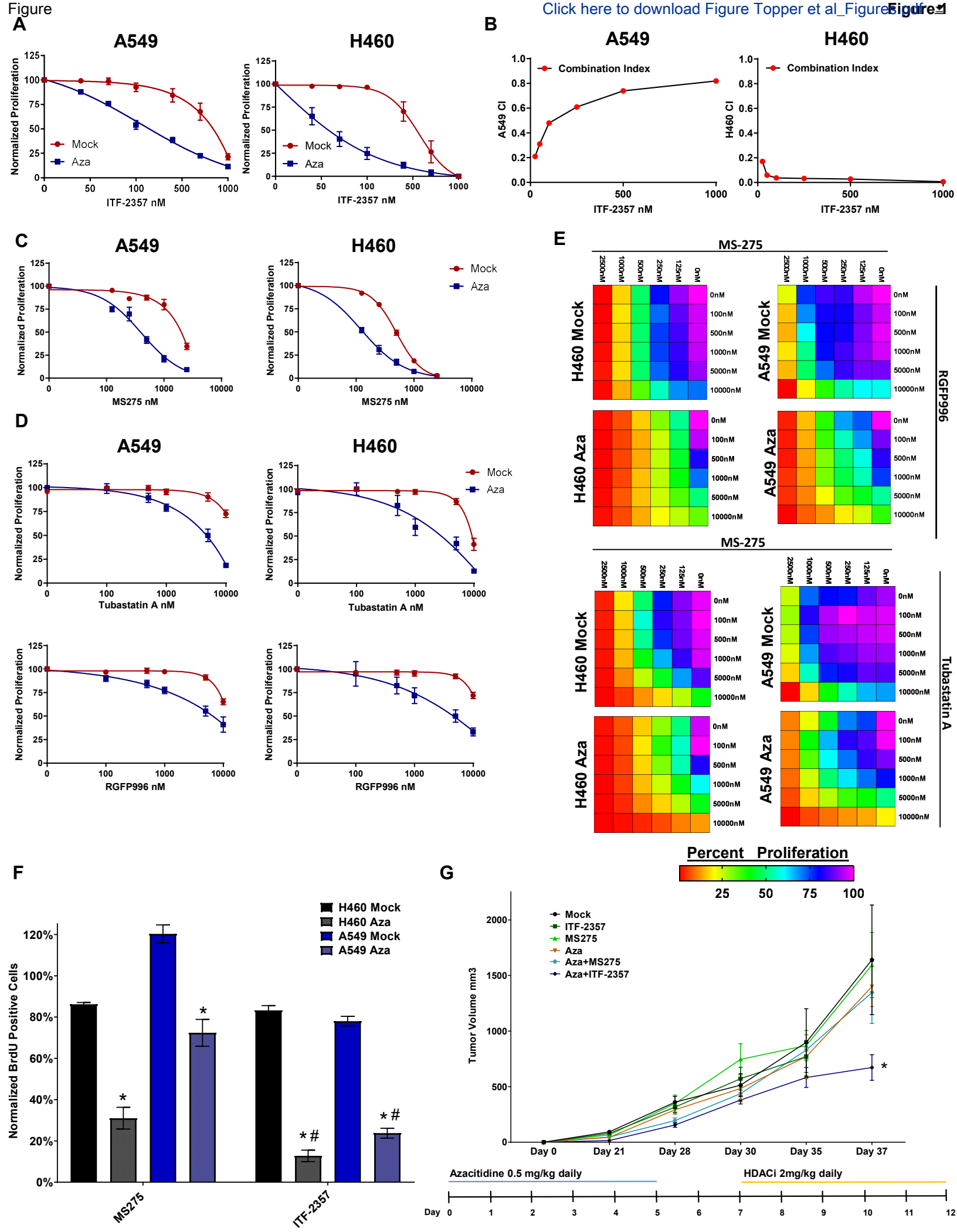
A
A549
H460
Normalized Proliferation
Mock
Aza
ITF-2357 nM
B
A549
H460
Combination Index
A549 CI
H460 CI
ITF-2357 nM
C
A549
H460
Mock
Aza
Normalized Proliferation
MS275 nM
D
A549
H460
Mock
Aza
Normalized Proliferation
Tubastatin A nM
RGFP996 nM
E
MS-275
H460 Mock
A549 Mock
H460 Aza
A549 Aza
RGFP996
Tubastatin A
Percent Proliferation
F
H460 Mock
H460 Aza
A549 Mock
A549 Aza
Normalized BrdU Positive Cells
MS275
ITF-2357
G
Mock
ITF-2357
MS275
Aza
Aza+MS275
Aza+ITF-2357
Tumor Volume mm3
Day 0
Day 21
Day 28
Day 30
Day 35
Day 37
Azacitidine 0.5 mg/kg daily
HDACi 2mg/kg daily
Day

Figure 2

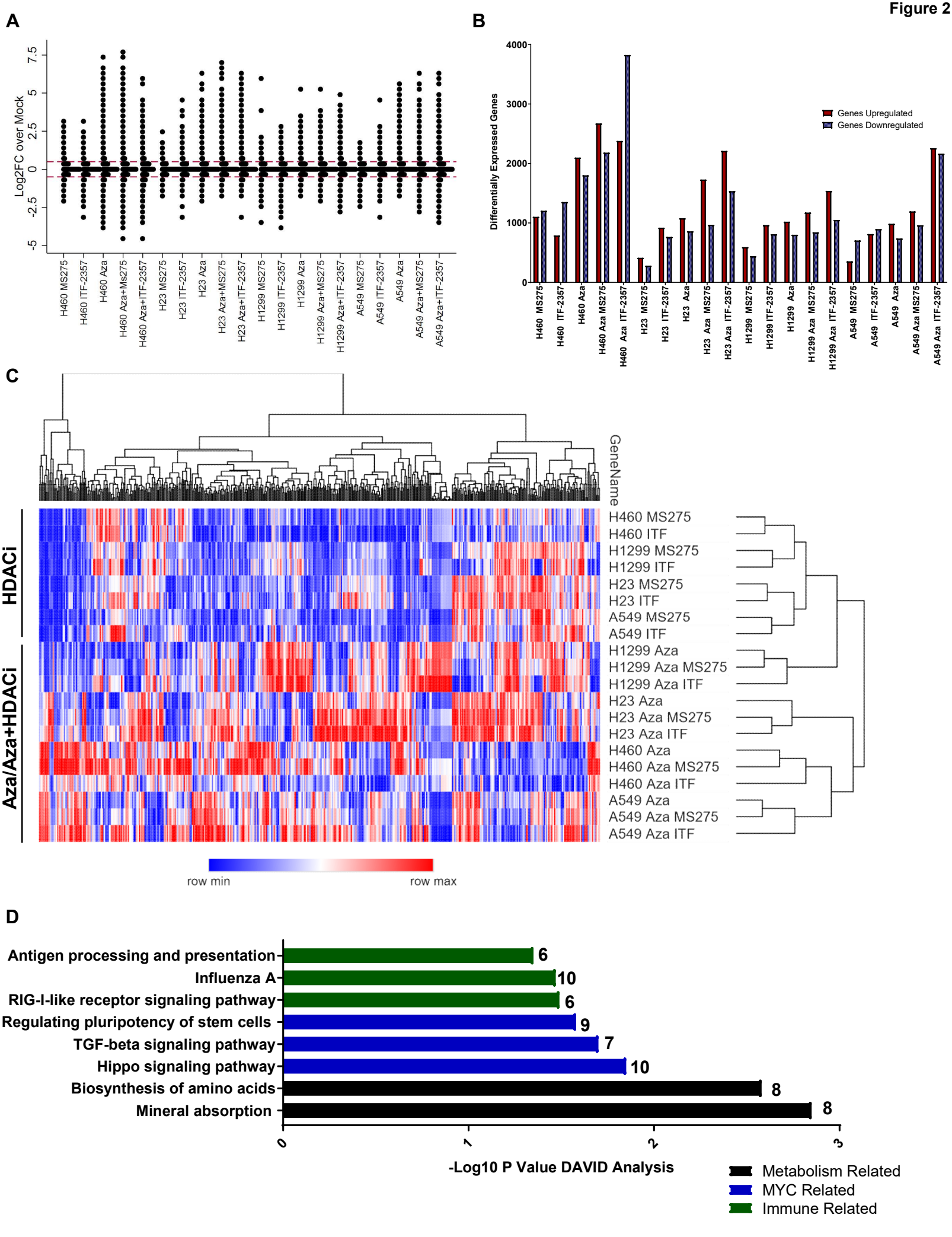
A
Log2FC over Mock
H460 MS275
H460 ITF-2357
H460 Aza
H460 Aza+Ms275
H460 Aza+ITF-2357
H23 MS275
H23 ITF-2357
H23 Aza
H23 Aza+MS275
H23 Aza+ITF-2357
H1299 MS275
H1299 ITF-2357
H1299 Aza
H1299 Aza+MS275
H1299 Aza+ITF-2357
A549 MS275
A549 ITF-2357
A549 Aza
A549 Aza+MS275
A549 Aza+ITF-2357
B
Differentially Expressed Genes
Genes Upregulated
Genes Downregulated
C
GeneName
HDACi
Aza/Aza+HDACi
H460 MS275
H460 ITF
H1299 MS275
H1299 ITF
H23 MS275
H23 ITF
A549 MS275
A549 ITF
H1299 Aza
H1299 Aza MS275
H1299 Aza ITF
H23 Aza
H23 Aza MS275
H23 Aza ITF
H460 Aza
H460 Aza MS275
H460 Aza ITF
A549 Aza
A549 Aza MS275
A549 Aza ITF
row min
row max
D
Antigen processing and presentation
Influenza A
RIG-I-like receptor signaling pathway
Regulating pluripotency of stem cells
TGF-beta signaling pathway
Hippo signaling pathway
Biosynthesis of amino acids
Mineral absorption
-Log10 P Value DAVID Analysis
Metabolism Related
MYC Related
Immune Related

Figure 3

A

AZA + ITF-2357

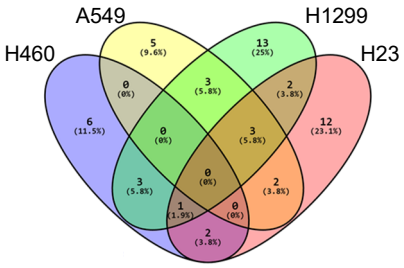

REACTOME INTERFERON ALPHA BETA SIGNALING
REACTOME IMMUNOREGULATORY INTERACTIONS BETWEEN A LYMPHOID AND A NON LYMPHOID CELL
KEGG ECM RECEPTOR INTERACTION

AZA + MS275

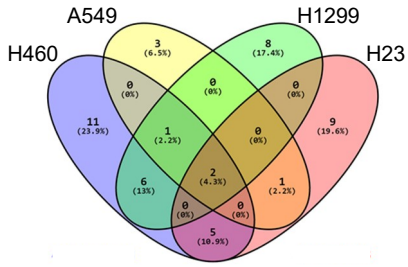

REACTOME INTERFERON ALPHA BETA SIGNALING
REACTOME IMMUNOREGULATORY INTERACTIONS BETWEEN A LYMPHOID AND A NON LYMPHOID CELL
KEGG ECM RECEPTOR INTERACTION

B

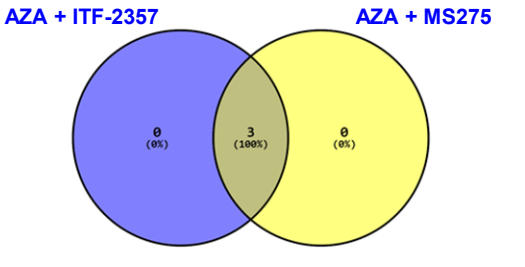

REACTOME INTERFERON ALPHA BETA SIGNALING
REACTOME IMMUNOREGULATORY INTERACTIONS BETWEEN A LYMPHOID AND A NON LYMPHOID CELL
KEGG ECM RECEPTOR INTERACTION

C

Azacitidine + ITF-2357

H23

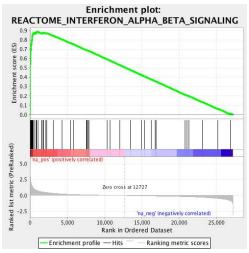

A549

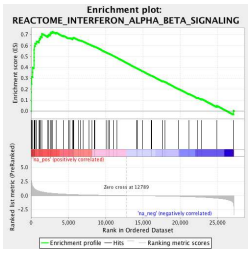

H1299

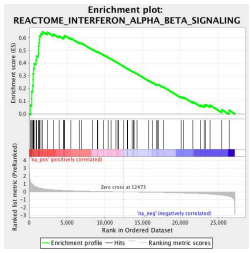

Azacitidine + MS275

H23

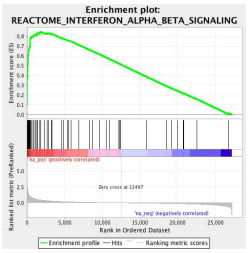

A549

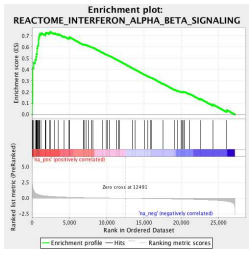

H1299

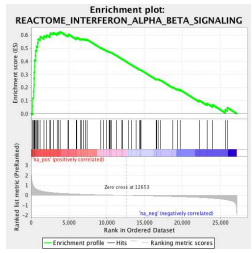

D

AZA + ITF-2357

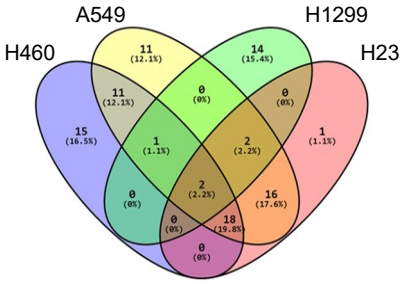

REACTOME MITOTIC M M G1 PHASES
REACTOME MITOTIC PROMETAPHASES
REACTOME G2 M CHECKPOINTS
REACTOME CELL CYCLE
REACTOME CELL CYCLE CHECKPOINTS
REACTOME TRANPORT MATURE TRANSCRIPT TO CYTOPLASM
REACTOME PROCESSING OF CAPPED INTRON CONTAINING MRNA
REACTOME MRNA PROCESSING REACTOME
ACTIVATION OF ATR IN RESPONSE TO REPLICATION STRESS
REACTOME METABOLSIM OF NON CODING RNA
REACTOME INTERACTION OF VPR WITH HOST CELLULAR PROTEINS
REACTOME NEP NS2 INTERACTS WITH THE CELLULAR EXPORT MACHINERY
REACTOME TRANSPORT OF RIBONUCLEOPROTEINS INTO THE HOST NUCLEUS
KEGG SPLICESOME
KEGG CELL CYCLE
KEGG DNA REPLICATION
REACTOME TRNA AMINOACYLATION
REACTOME AMINOACYL TRNA BIOSYNTHESIS
REACTOME CYTOSTOLIC TRNA AMINOACYLATION
KEGG MISMATCH REPAIR
KEGG ONE CARBON POOL BY FOLATE

AZA + MS275

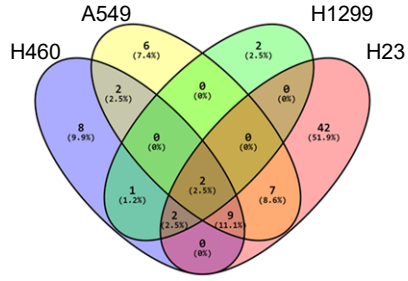

REACTOME MITOTIC M M G1 PHASES
REACTOME MITOTIC PROMETAPHASES
REACTOME CELL CYCLE
REACTOME CELL CYCLE MITOTIC
REACTOME G2 M CHECKPOINTS
REACTOME MRNA PROCESSING REACTOME
ACTIVATION OF ATR IN RESPONSE TO REPLICATION STRESS
KEGG CELL CYCLE
KEGG DNA REPLICATION
REACTOME AMINOACYL TRNA BIOSYNTHESIS
REACTOME TRNA AMINOACYLATION
REACTOME CYTOSTOLIC TRNA AMINOACYLATION
KEGG TERPENOID BACKBONE SYNTHESIS

E

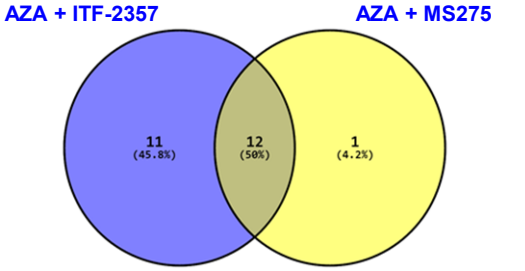

REACTOME MITOTIC M M G1 PHASES
REACTOME MITOTIC PROMETAPHASES
REACTOME CELL CYCLE
REACTOME CELL CYCLE MITOTIC
REACTOME G2 M CHECKPOINTS
REACTOME MRNA PROCESSING REACTOME
ACTIVATION OF ATR IN RESPONSE TO REPLICATION STRESS
KEGG CELL CYCLE
KEGG DNA REPLICATION
REACTOME AMINOACYL TRNA BIOSYNTHESIS
REACTOME TRNA AMINOACYLATION
REACTOME CYTOSTOLIC TRNA AMINOACYLATION

F

Azacitidine + ITF-2357

H23

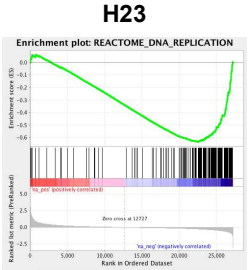

A549

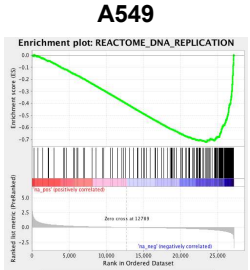

H1299

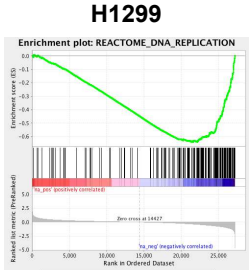

Azacitidine + MS275

H23

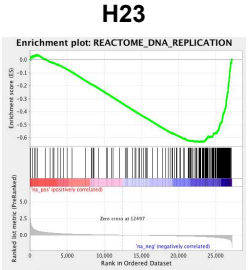

A549

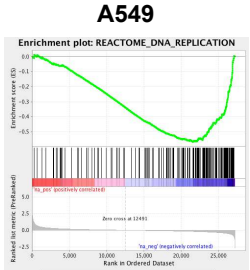

H1299

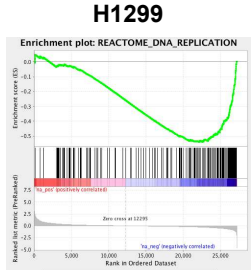

Figure 4

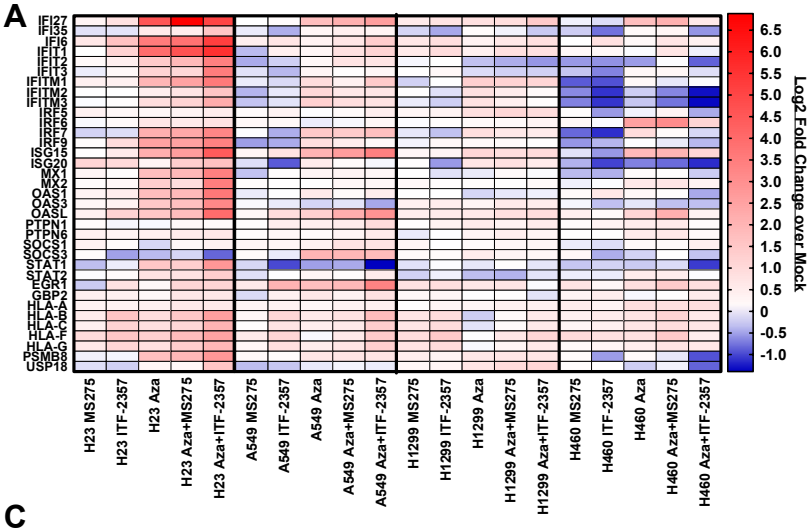
A
IFI27
IFI35
IFI6
IFIT1
IFIT2
IFIT3
IFITM1
IFITM2
IFITM3
IRF5
IRF6
IRF7
IRF9
ISG15
ISG20
MX1
MX2
OAS1
OAS3
OASL
PTPN1
PTPN6
SOCS1
SOCS3
STAT1
STAT2
EGR1
GBP1
HLA-A
HLA-B
HLA-F
HLA-G
PSMB8
USP18
H23 MS275
H23 ITF-2357
H23 Aza
H23 Aza+MS275
H23 Aza+ITF-2357
A549 MS275
A549 ITF-2357
A549 Aza
A549 Aza+MS275
A549 Aza+ITF-2357
H1299 MS275
H1299 ITF-2357
H1299 Aza
H1299 Aza+MS275
H1299 Aza+ITF-2357
H460 MS275
H460 ITF-2357
H460 Aza
H460 Aza+MS275
H460 Aza+ITF-2357
Log2 Fold Change over Mock
6.5
6.0
5.5
5.0
4.5
4.0
3.5
3.0
2.5
2.0
1.5
1.0
0.5
0
-0.5
-1.0

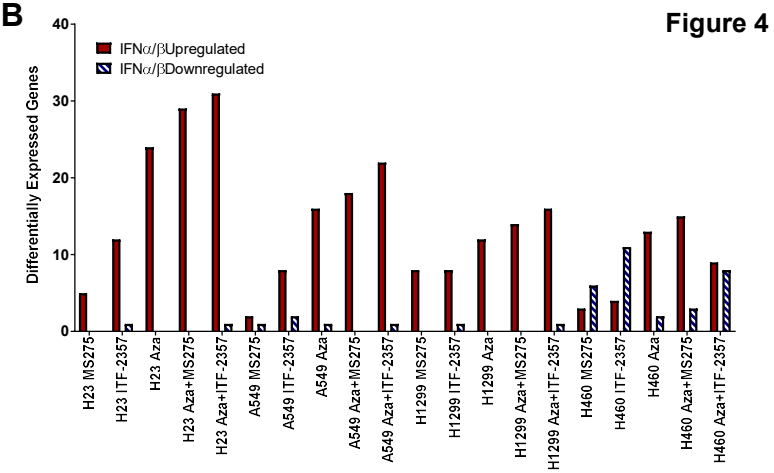
B
IFNα/βUpregulated
IFNα/βDownregulated
Differentially Expressed Genes
40
30
20
10
0
H23 MS275
H23 ITF-2357
H23 Aza
H23 Aza+MS275
H23 Aza+ITF-2357
A549 MS275
A549 ITF-2357
A549 Aza
A549 Aza+MS275
A549 Aza+ITF-2357
H1299 MS275
H1299 ITF-2357
H1299 Aza
H1299 Aza+MS275
H1299 Aza+ITF-2357
H460 MS275
H460 ITF-2357
H460 Aza
H460 Aza+MS275
H460 Aza+ITF-2357

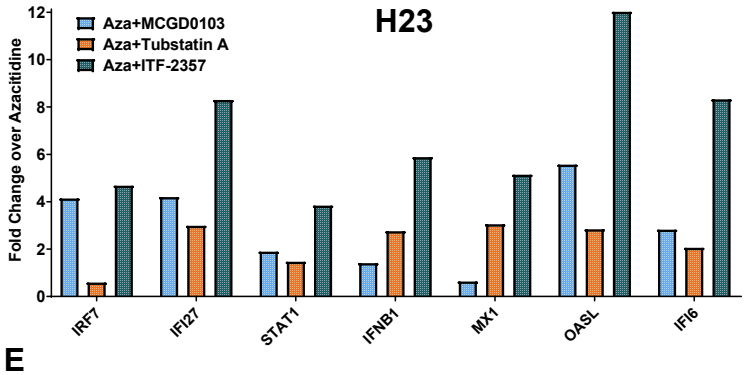
C
H23
Aza+MCGD0103
Aza+Tubstatin A
Aza+ITF-2357
Fold Change over Azacitidine
12
10
8
6
4
2
0
IRF7
IFI27
STAT1
IFNB1
MX1
OASL
IFI6

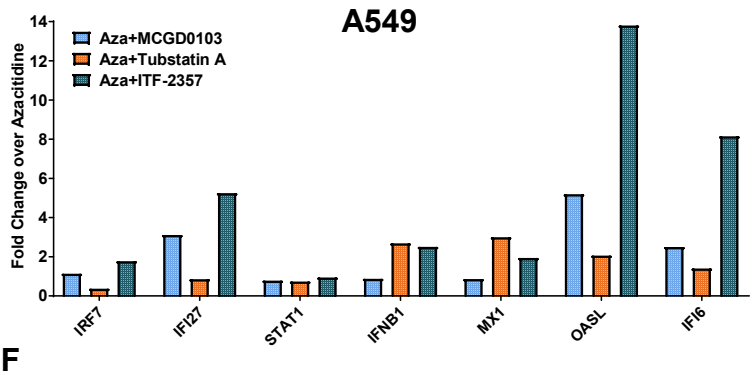
D
A549
Aza+MCGD0103
Aza+Tubstatin A
Aza+ITF-2357
Fold Change over Azacitidine
14
12
10
8
6
4
2
0
IRF7
IFI27
STAT1
IFNB1
MX1
OASL
IFI6

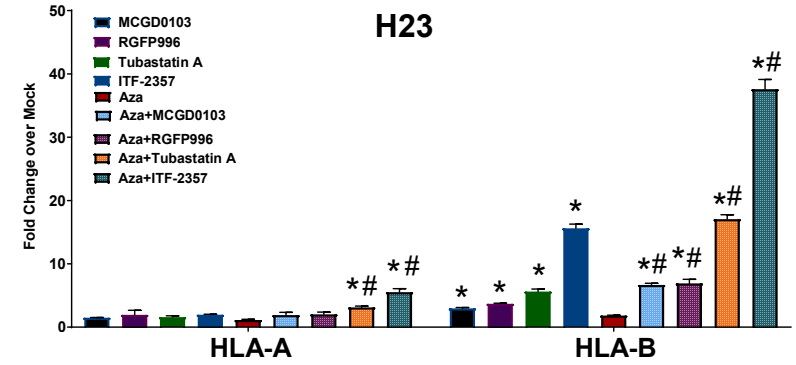
E
H23
MCGD0103
RGFP996
Tubastatin A
ITF-2357
Aza
Aza+MCGD0103
Aza+RGFP996
Aza+Tubastatin A
Aza+ITF-2357
Fold Change over Mock
50
40
30
20
10
0
HLA-A
HLA-B

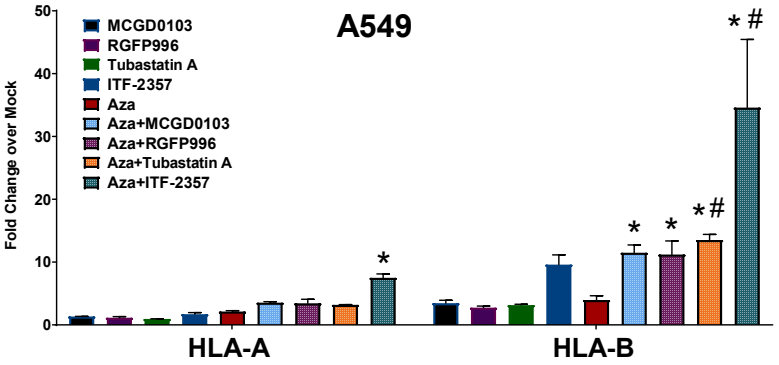
F
A549
MCGD0103
RGFP996
Tubastatin A
ITF-2357
Aza
Aza+MCGD0103
Aza+RGFP996
Aza+Tubastatin A
Aza+ITF-2357
Fold Change over Mock
50
40
30
20
10
0
HLA-A
HLA-B

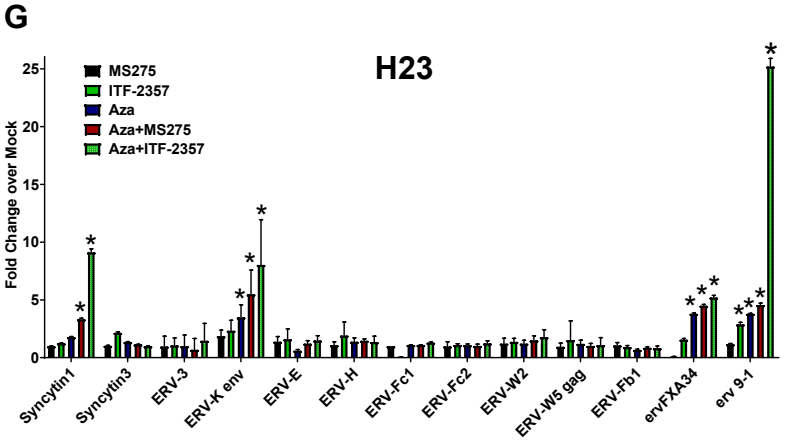
G
H23
MS275
ITF-2357
Aza
Aza+MS275
Aza+ITF-2357
Fold Change over Mock
25
20
15
10
5
0
Syncytin1
Syncytin3
ERV-3
ERV-K env
ERV-E
ERV-H
ERV-Fc1
ERV-Fc2
ERV-W2
ERV-W5 gag
ERV-Fb1
ervFXA34
erv 9-1

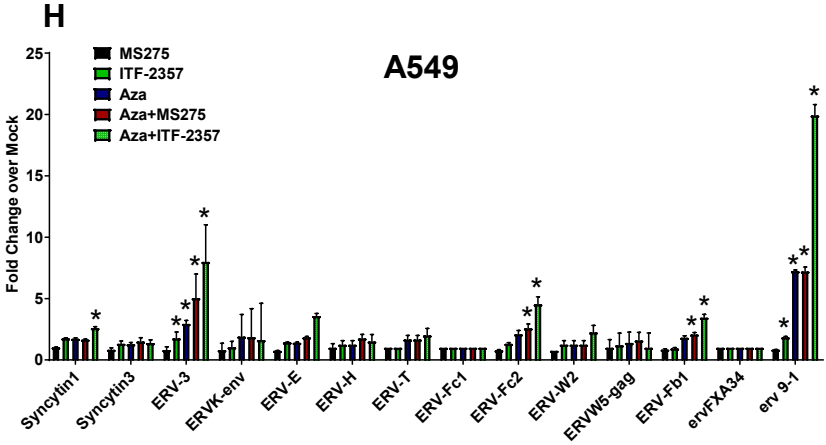
H
A549
MS275
ITF-2357
Aza
Aza+MS275
Aza+ITF-2357
Fold Change over Mock
25
20
15
10
5
0
Syncytin1
Syncytin3
ERV-3
ERVK-env
ERV-E
ERV-H
ERV-T
ERV-Fc1
ERV-Fc2
ERV-W2
ERVW5-gag
ERV-Fb1
ervFXA34
erv 9-1

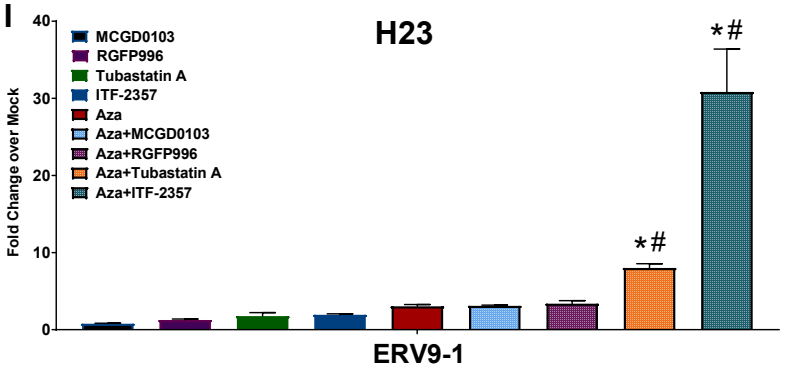
I
H23
MCGD0103
RGFP996
Tubastatin A
ITF-2357
Aza
Aza+MCGD0103
Aza+RGFP996
Aza+Tubastatin A
Aza+ITF-2357
Fold Change over Mock
40
30
20
10
0
ERV9-1

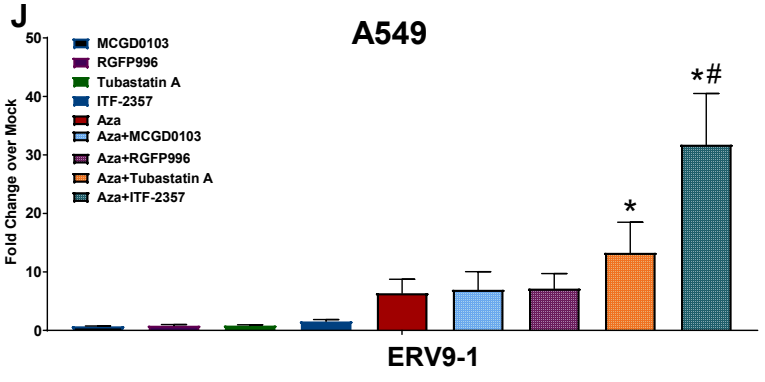
J
A549
MCGD0103
RGFP996
Tubastatin A
ITF-2357
Aza
Aza+MCGD0103
Aza+RGFP996
Aza+Tubastatin A
Aza+ITF-2357
Fold Change over Mock
50
40
30
20
10
0
ERV9-1

Figure 5


A.
Log2 Fold Change over Mock
0.0
-0.5
-1.0
-1.5
-2.0
-2.5
H460 Aza
H1299 Aza
A549 Aza
H23 Aza

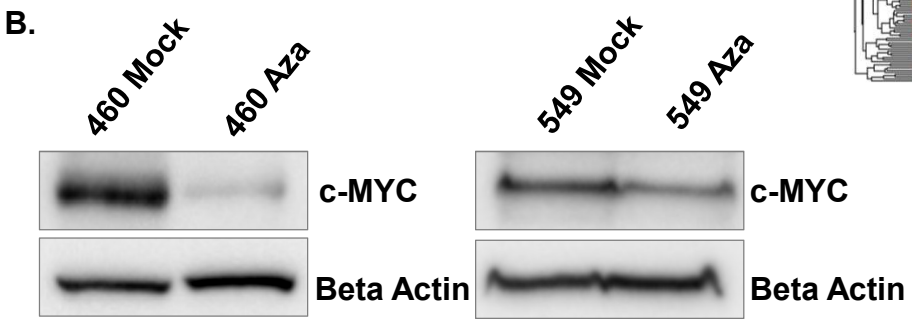
B.
460 Mock
460 Aza
549 Mock
549 Aza
c-MYC
Beta Actin
c-MYC
Beta Actin

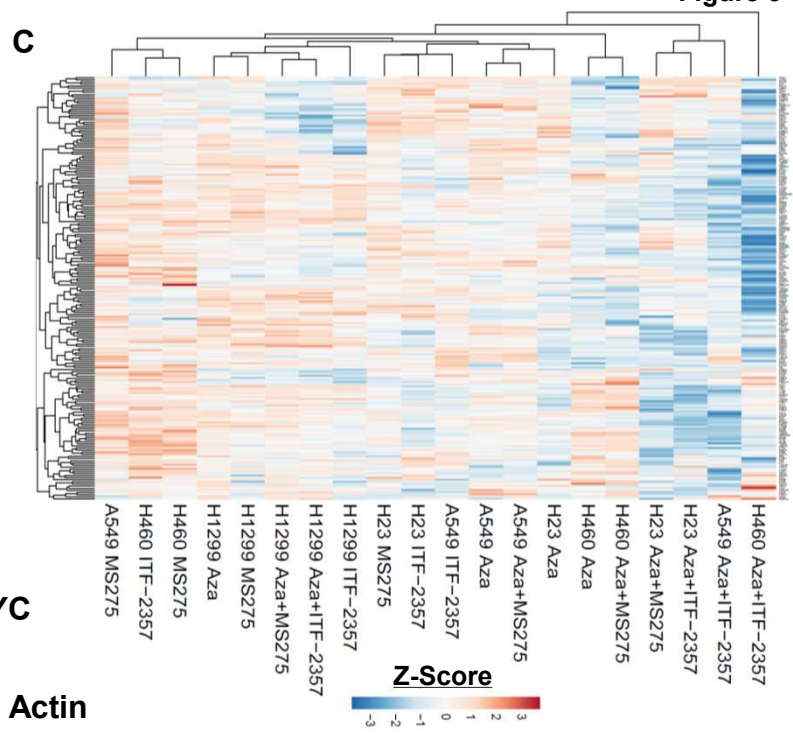
C
A549 MS275
H460 ITF-2357
H460 MS275
H1299 Aza
H1299 MS275
H1299 Aza+MS275
H1299 Aza+ITF-2357
H1299 ITF-2357
H23 MS275
H23 ITF-2357
A549 ITF-2357
A549 Aza
A549 Aza+MS275
H23 Aza
H460 Aza
H460 Aza+MS275
H23 Aza+MS275
H23 Aza+ITF-2357
A549 Aza+ITF-2357
H460 Aza+ITF-2357
Z-Score

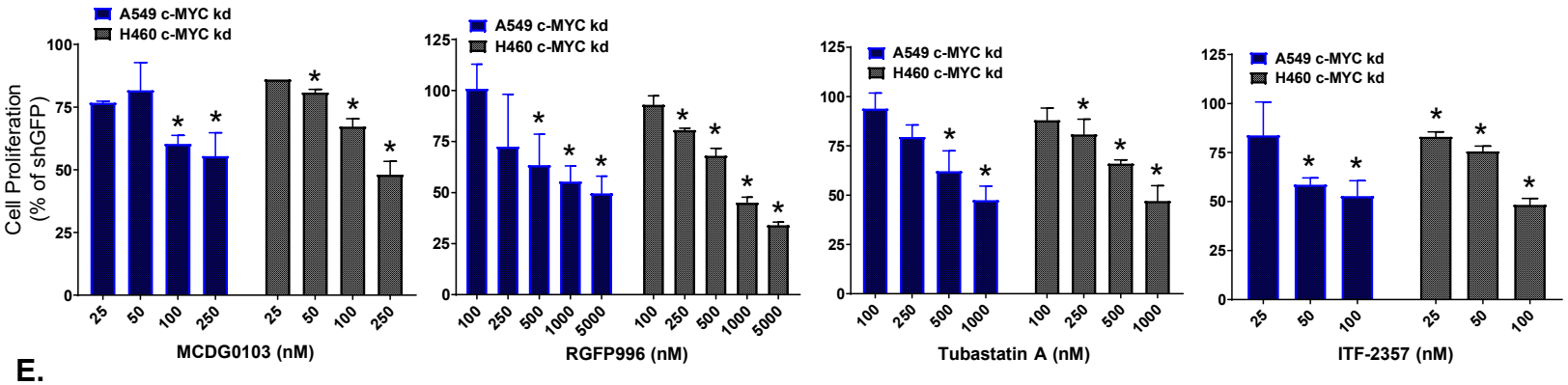
D.
A549 c-MYC kd
H460 c-MYC kd
Cell Proliferation (% of shGFP)
MCDG0103 (nM)
RGFP996 (nM)
Tubastatin A (nM)
ITF-2357 (nM)

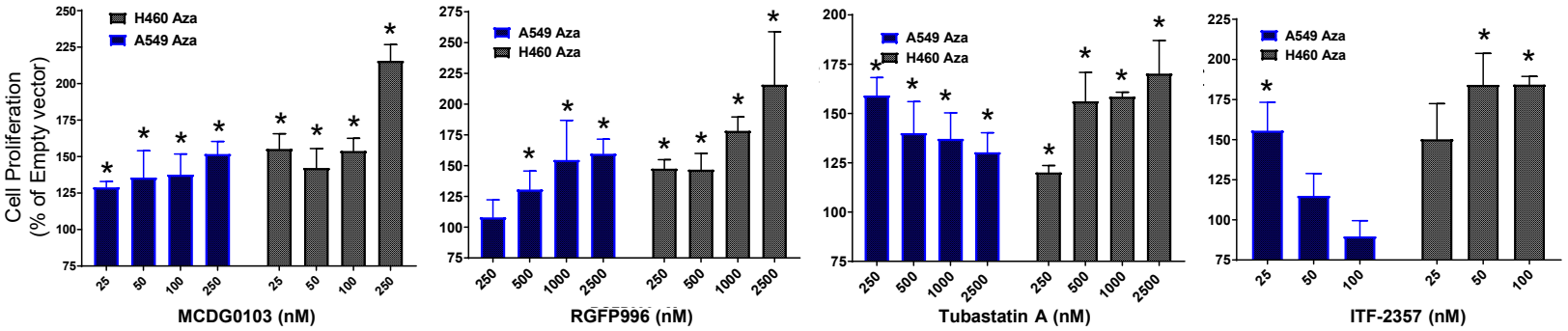
E.
H460 Aza
A549 Aza
Cell Proliferation (% of Empty vector)
MCDG0103 (nM)
RGFP996 (nM)
Tubastatin A (nM)
ITF-2357 (nM)

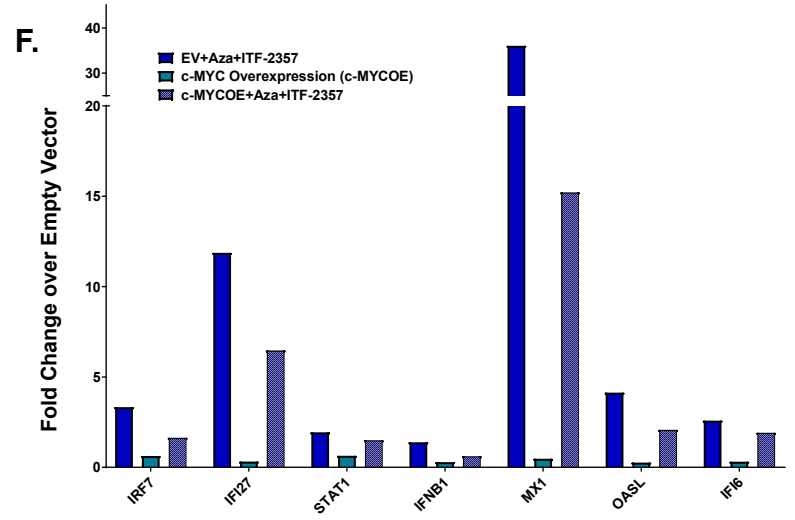
F.
EV+Aza+ITF-2357
c-MYC Overexpression (c-MYCOE)
c-MYCOE+Aza+ITF-2357
Fold Change over Empty Vector
IRF7
IFI27
STAT1
IFNB1
MX1
OASL
IFI6

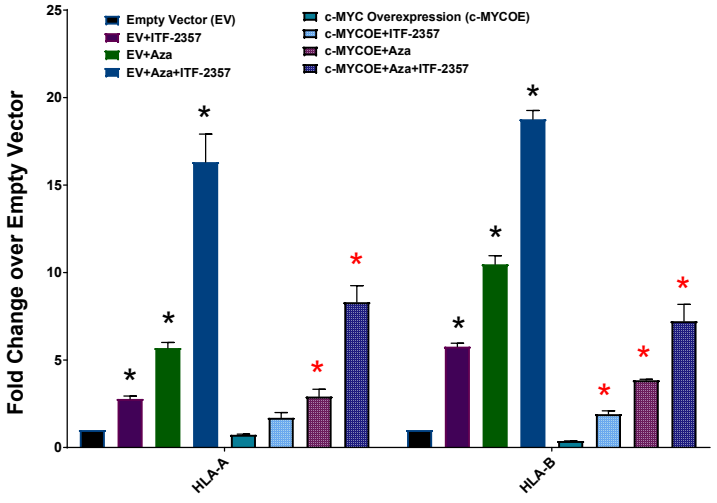
G.
Empty Vector (EV)
EV+ITF-2357
EV+Aza
EV+Aza+ITF-2357
c-MYC Overexpression (c-MYCOE)
c-MYCOE+ITF-2357
c-MYCOE+Aza
c-MYCOE+Aza+ITF-2357
Fold Change over Empty Vector
HLA-A
HLA-B

Figure 6

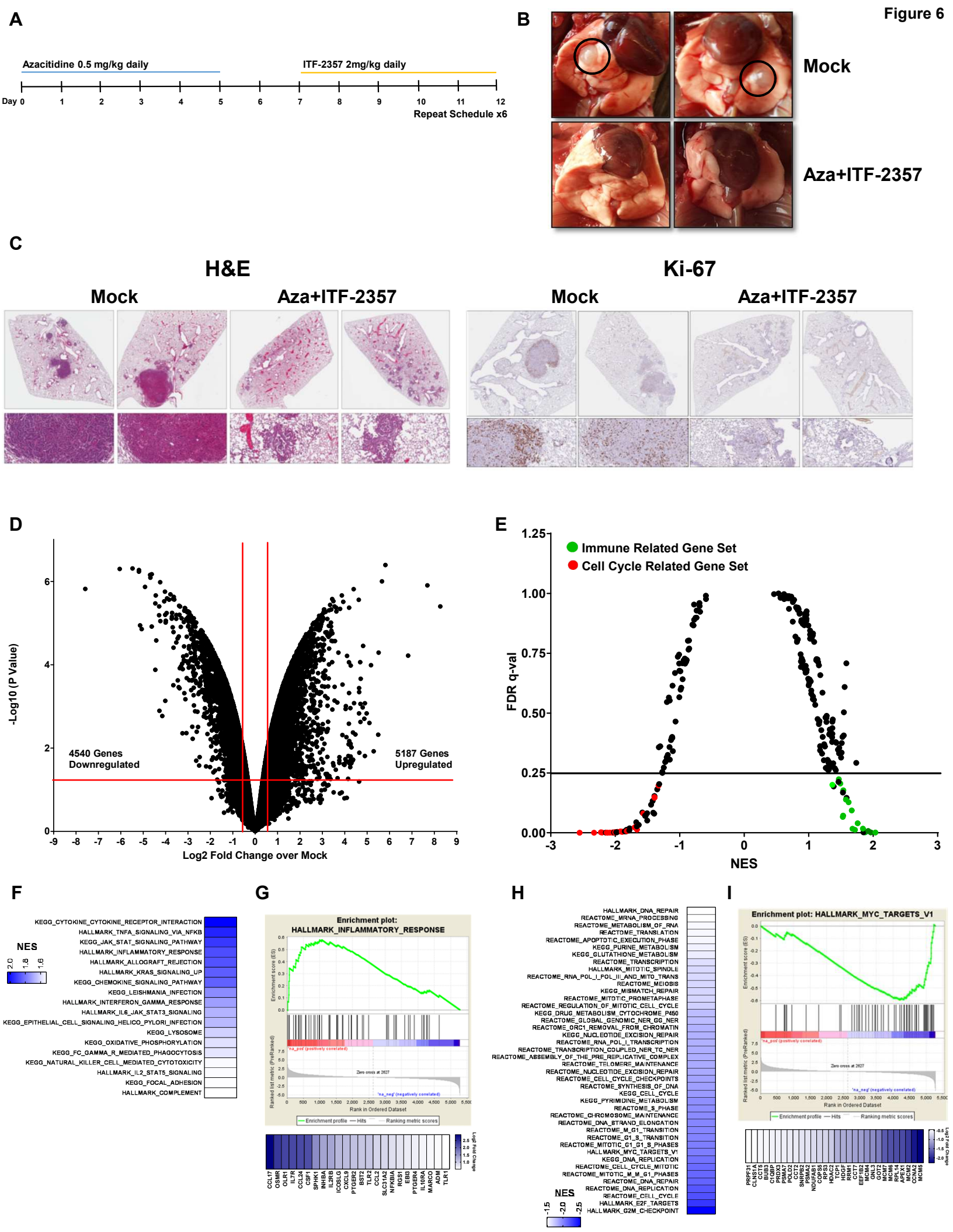
A
Azacitidine 0.5 mg/kg daily
ITF-2357 2mg/kg daily
Day 0 1 2 3 4 5 6 7 8 9 10 11 12
Repeat Schedule x6
B
Mock
Aza+ITF-2357
C
H&E
Mock
Aza+ITF-2357
Ki-67
Mock
Aza+ITF-2357
D
-Log10 (P Value)
Log2 Fold Change over Mock
4540 Genes Downregulated
5187 Genes Upregulated
E
Immune Related Gene Set
Cell Cycle Related Gene Set
FDR q-val
NES
F
NES
KEGG_CYTOKINE_CYTOKINE_RECEPTOR_INTERACTION
HALLMARK_TNFA_SIGNALING_VIA_NFKB
KEGG_JAK_STAT_SIGNALING_PATHWAY
HALLMARK_INFLAMMATORY_RESPONSE
HALLMARK_ALLOGRAFT_REJECTION
HALLMARK_KRAS_SIGNALING_UP
KEGG_CHEMOKINE_SIGNALING_PATHWAY
KEGG_LEISHMANIA_INFECTION
HALLMARK_INTERFERON_GAMMA_RESPONSE
HALLMARK_IL6_JAK_STAT3_SIGNALING
KEGG_EPITHELIAL_CELL_SIGNALING_HELICO_PYLORI_INFECTION
KEGG_LYSOSOME
KEGG_OXIDATIVE_PHOSPHORYLATION
KEGG_FC_GAMMA_R_MEDIATED_PHAGOCYTOSIS
KEGG_NATURAL_KILLER_CELL_MEDIATED_CYTOTOXICITY
HALLMARK_IL2_STAT5_SIGNALING
KEGG_FOCAL_ADHESION
HALLMARK_COMPLEMENT
G
Enrichment plot:
HALLMARK_INFLAMMATORY_RESPONSE
Enrichment score (ES)
Ranked list metric (PreRanked)
Rank in Ordered Dataset
Enrichment profile
Hits
Ranking metric scores
CCL17 OSMR OLR1 IL7R CCL24 CSF1 SPHK1 INHBA IL2RB ICOSLG CXCL9 PTGER2 BST2 TLR2 CCL2 SLC31A2 NFKBIA RGS1 EBI3 PTGER4 IL10RA MARCO ADM TLR1
H
HALLMARK_DNA_REPAIR
REACTOME_MRNA_PROCESSING
REACTOME_METABOLISM_OF_RNA
REACTOME_TRANSLATION
REACTOME_APOPTOTIC_EXECUTION_PHASE
KEGG_PURINE_METABOLISM
KEGG_GLUTATHIONE_METABOLISM
REACTOME_TRANSCRIPTION
HALLMARK_MITOTIC_SPINDLE
REACTOME_RNA_POL_I_POL_III_AND_MITO_TRANS
REACTOME_MEIOSIS
KEGG_MISMATCH_REPAIR
REACTOME_MITOTIC_PROMETAPHASE
REACTOME_REGULATION_OF_MITOTIC_CELL_CYCLE
KEGG_DRUG_METABOLISM_CYTOCHROME_P450
REACTOME_GLOBAL_GENOMIC_NER_GG_NER
REACTOME_ORC1_REMOVAL_FROM_CHROMATIN
KEGG_NUCLEOTIDE_EXCISION_REPAIR
REACTOME_RNA_POL_I_TRANSCRIPTION
REACTOME_TRANSCRIPTION_COUPLED_NER_TC_NER
REACTOME_ASSEMBLY_OF_THE_PRE_REPLICATIVE_COMPLEX
REACTOME_TELOMERE_MAINTENANCE
REACTOME_NUCLEOTIDE_EXCISION_REPAIR
REACTOME_CELL_CYCLE_CHECKPOINTS
REACTOME_SYNTHESIS_OF_DNA
KEGG_CELL_CYCLE
KEGG_PYRIMIDINE_METABOLISM
REACTOME_S_PHASE
REACTOME_CHROMOSOME_MAINTENANCE
REACTOME_DNA_STRAND_ELONGATION
REACTOME_M_G1_TRANSITION
REACTOME_G1_S_TRANSITION
REACTOME_MITOTIC_G1_G1_S_PHASES
HALLMARK_MYC_TARGETS_V1
KEGG_DNA_REPLICATION
REACTOME_CELL_CYCLE_MITOTIC
REACTOME_MITOTIC_M_M_G1_PHASES
REACTOME_DNA_REPAIR
REACTOME_DNA_REPLICATION
REACTOME_CELL_CYCLE
HALLMARK_E2F_TARGETS
HALLMARK_G2M_CHECKPOINT
NES
I
Enrichment plot: HALLMARK_MYC_TARGETS_V1
Enrichment score (ES)
Ranked list metric (PreRanked)
Rank in Ordered Dataset
Enrichment profile
Hits
Ranking metric scores
PRPF31 CLNS1A CCT5 BUB3 C1QBP PRDX3 PSMA7 POLD2 CCT2 SNRPB2 PSMA2 NDUFAB1 COPS5 PSMB3 HDAC2 TCP1 HDAF RANBP1 CCT7 EEF1B2 MRPL4 GOT2 MCM7 MCM6 RPL14 APEX1 MCM2 CCNA2 MCM5

Figure 7

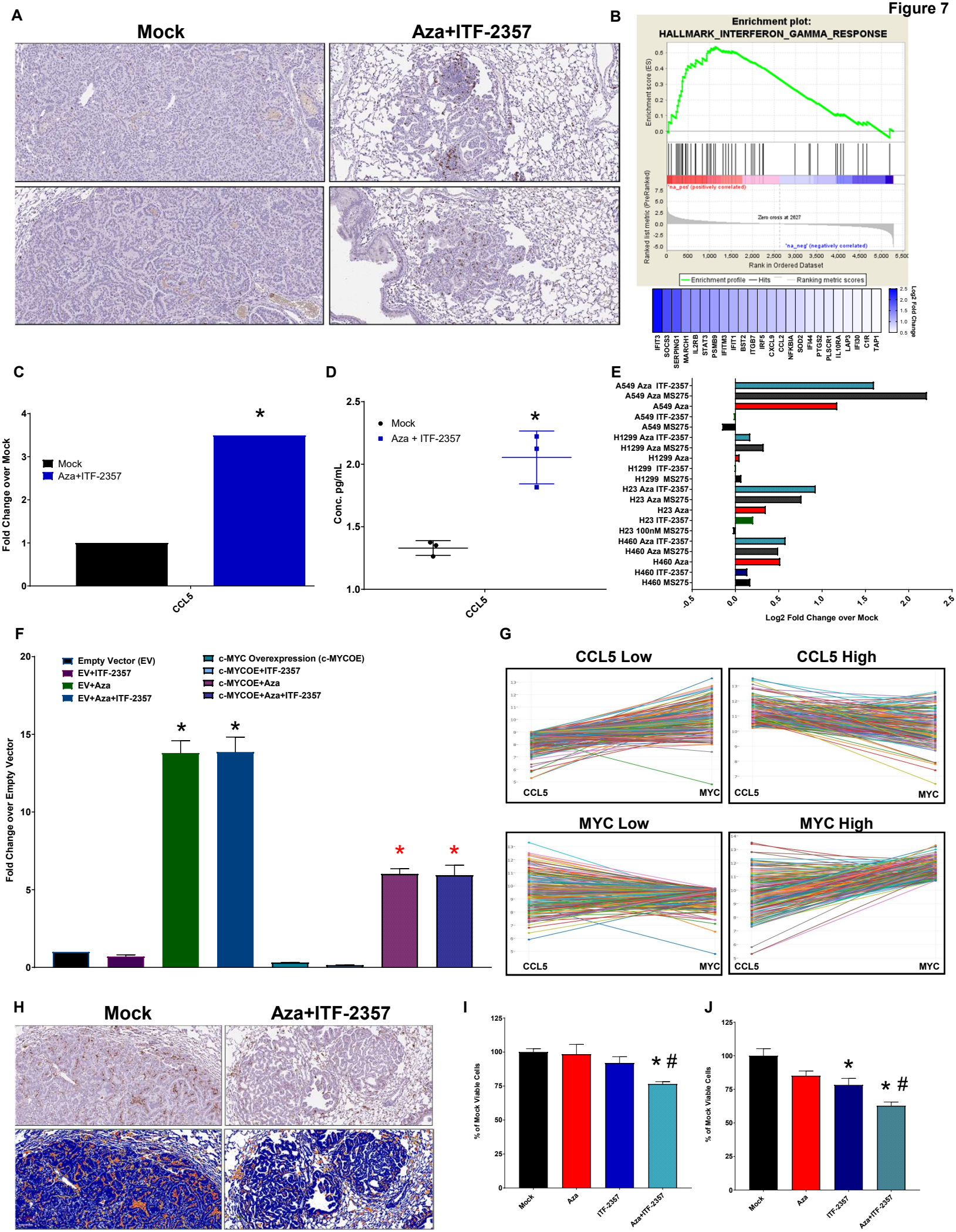
A
Mock
Aza+ITF-2357
B
Enrichment plot:
HALLMARK_INTERFERON_GAMMA_RESPONSE
Enrichment score (ES)
'na_pos' (positively correlated)
Ranked list metric (PreRanked)
Zero cross at 2627
'na_neg' (negatively correlated)
Rank in Ordered Dataset
Enrichment profile
Hits
Ranking metric scores
Log2 Fold Change
IFIT3
SOCS3
SERPING1
MARCH1
IL2RB
STAT3
PSMB9
IFITM3
IFIT1
BST2
ITGB7
IRF5
CXCL9
CCL2
NFKBIA
SOD2
IFI44
PTGS2
PLSCR1
IL10RA
LAP3
IFI30
C1R
TAP1
C
Fold Change over Mock
Mock
Aza+ITF-2357
CCL5
D
Conc. pg/mL
Mock
Aza + ITF-2357
CCL5
E
A549 Aza ITF-2357
A549 Aza MS275
A549 Aza
A549 ITF-2357
A549 MS275
H1299 Aza ITF-2357
H1299 Aza MS275
H1299 Aza
H1299 ITF-2357
H1299 MS275
H23 Aza ITF-2357
H23 Aza MS275
H23 Aza
H23 ITF-2357
H23 100nM MS275
H460 Aza ITF-2357
H460 Aza MS275
H460 Aza
H460 ITF-2357
H460 MS275
Log2 Fold Change over Mock
F
Empty Vector (EV)
EV+ITF-2357
EV+Aza
EV+Aza+ITF-2357
c-MYC Overexpression (c-MYCOE)
c-MYCOE+ITF-2357
c-MYCOE+Aza
c-MYCOE+Aza+ITF-2357
Fold Change over Empty Vector
G
CCL5 Low
CCL5 High
MYC Low
MYC High
CCL5
MYC
H
Mock
Aza+ITF-2357
I
% of Mock Viable Cells
Mock
Aza
ITF-2357
Aza+ITF-2357
J
% of Mock Viable Cells
Mock
Aza
ITF-2357
Aza+ITF-2357

Click here to download Supplemental Figure Topper et al_Supplementary Figures.pdf

A

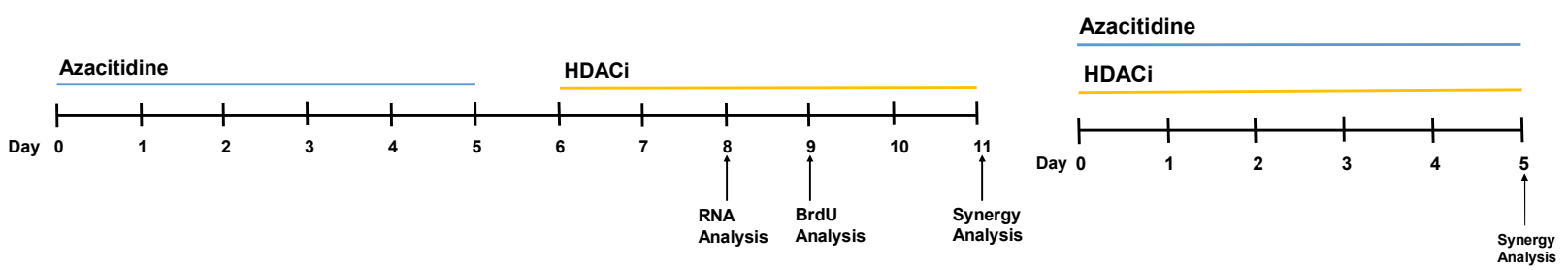

B

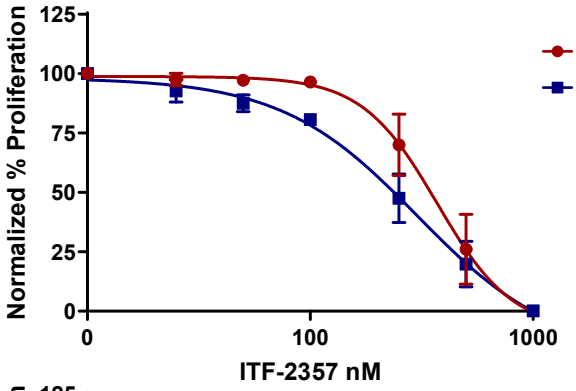

C

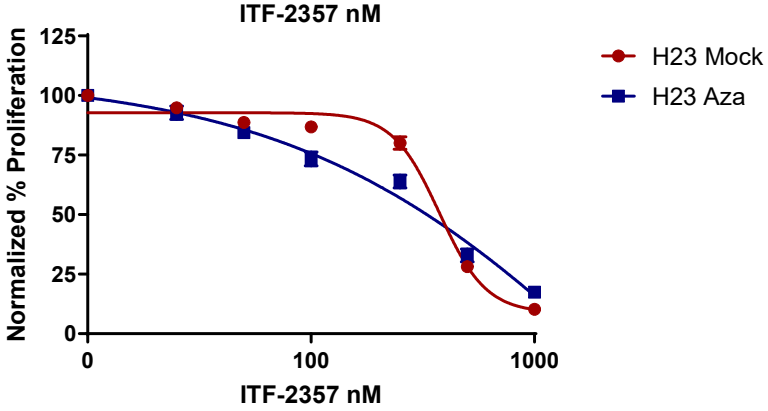

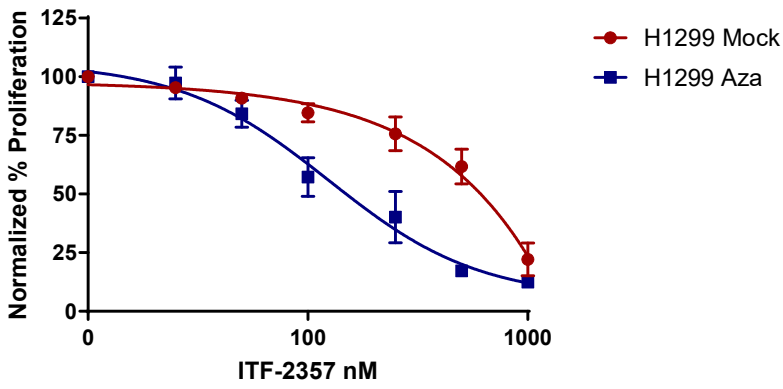

D

Compound	~cMax	~Half-life	HDAC Ki uM			
			1	2	3	6
ITF-2357	300nM	7 hrs.	.002	.003	.003	.0042
SAHA	1.0uM	1.5-2 hrs.	.0013	.0016	.005	.0016
MCGD0103	600nM	9.9 hrs.	.009	.034	.265	
MS275	50nM	105 hrs.	.022		.36	

E

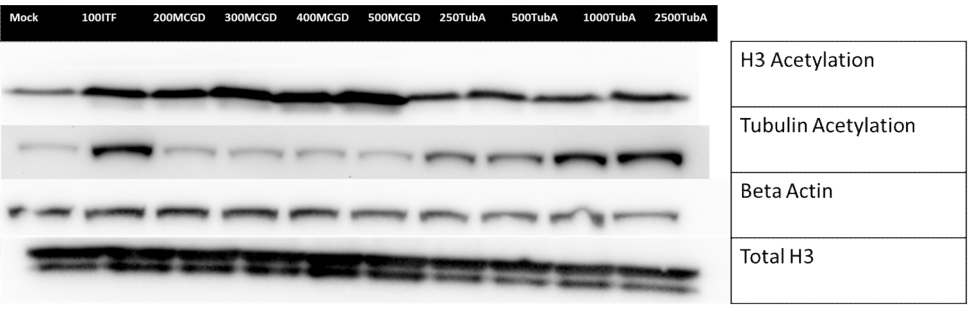

F

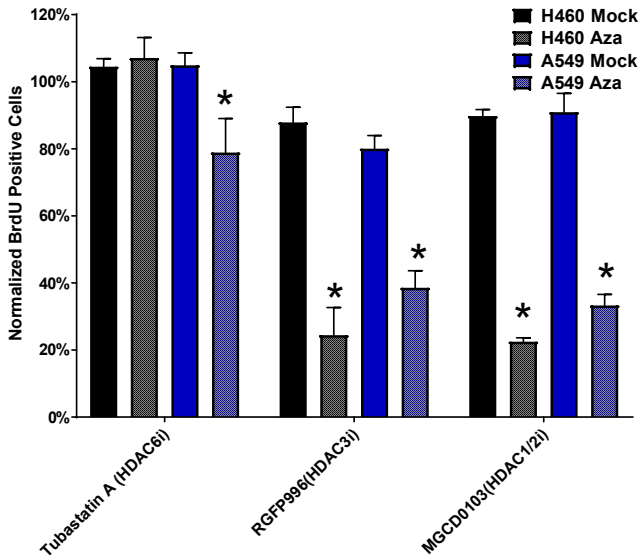

A

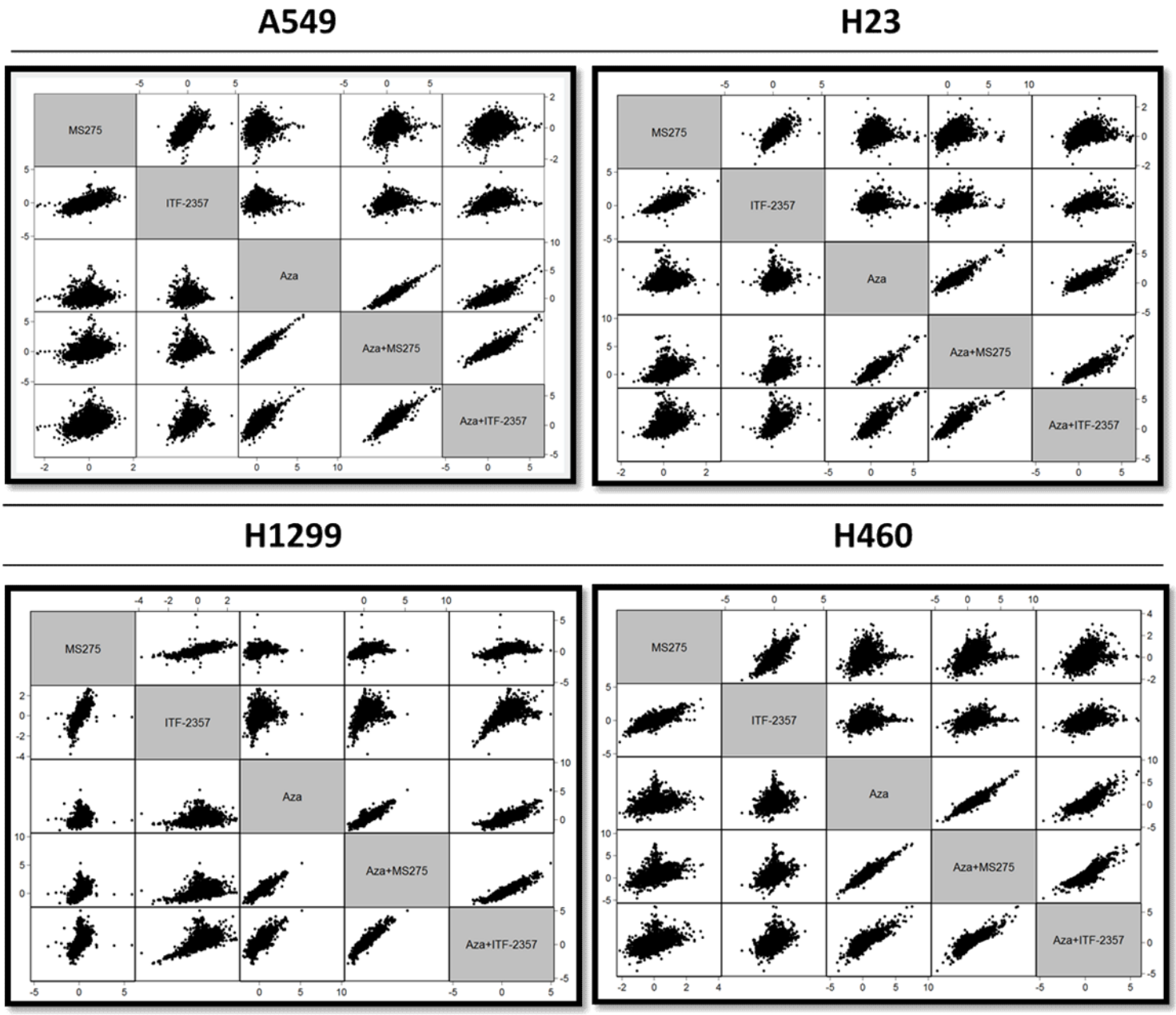
A549
H23
H1299
H460
MS275
ITF-2357
Aza
Aza+MS275
Aza+ITF-2357

B

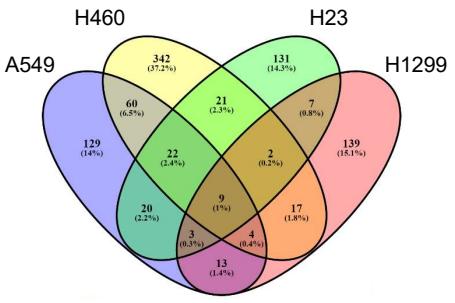
H460
H23
A549
H1299
342 (37.2%)
131 (14.3%)
60 (6.5%)
21 (2.3%)
7 (0.8%)
129 (14%)
139 (15.1%)
22 (2.4%)
2 (0.2%)
20 (2.2%)
9 (1%)
17 (1.8%)
3 (0.3%)
4 (0.4%)
13 (1.4%)

C

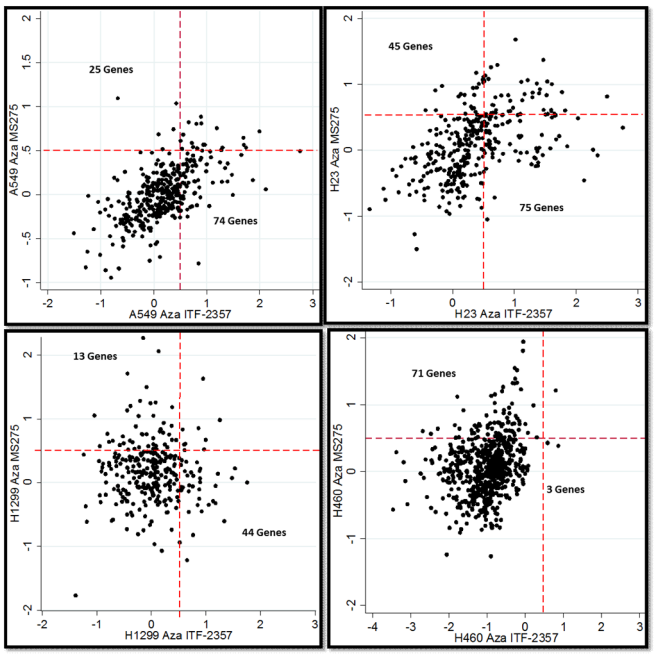
25 Genes
74 Genes
A549 Aza MS275
A549 Aza ITF-2357
45 Genes
75 Genes
H23 Aza MS275
H23 Aza ITF-2357
13 Genes
44 Genes
H1299 Aza MS275
H1299 Aza ITF-2357
71 Genes
3 Genes
H460 Aza MS275
H460 Aza ITF-2357

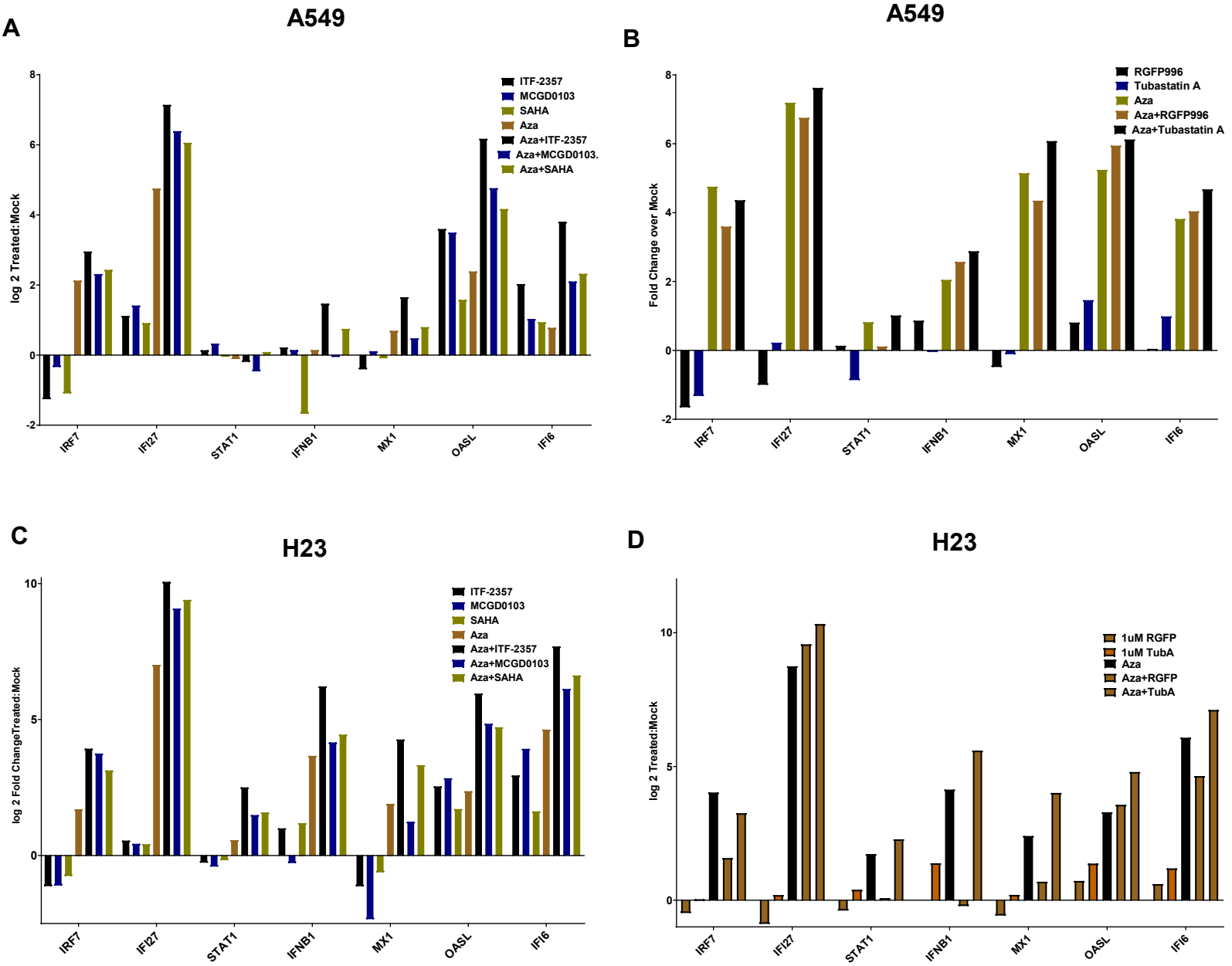
A
A549
log 2 Treated:Mock
ITF-2357
MCGD0103
SAHA
Aza
Aza+ITF-2357
Aza+MCGD0103.
Aza+SAHA
IRF7
IFI27
STAT1
IFNB1
MX1
OASL
IFI6
B
A549
Fold Change over Mock
RGFP996
Tubastatin A
Aza
Aza+RGFP996
Aza+Tubastatin A
C
H23
log 2 Fold ChangeTreated:Mock
ITF-2357
MCGD0103
SAHA
Aza
Aza+ITF-2357
Aza+MCGD0103
Aza+SAHA
D
H23
log 2 Treated:Mock
1uM RGFP
1uM TubA
Aza
Aza+RGFP
Aza+TubA

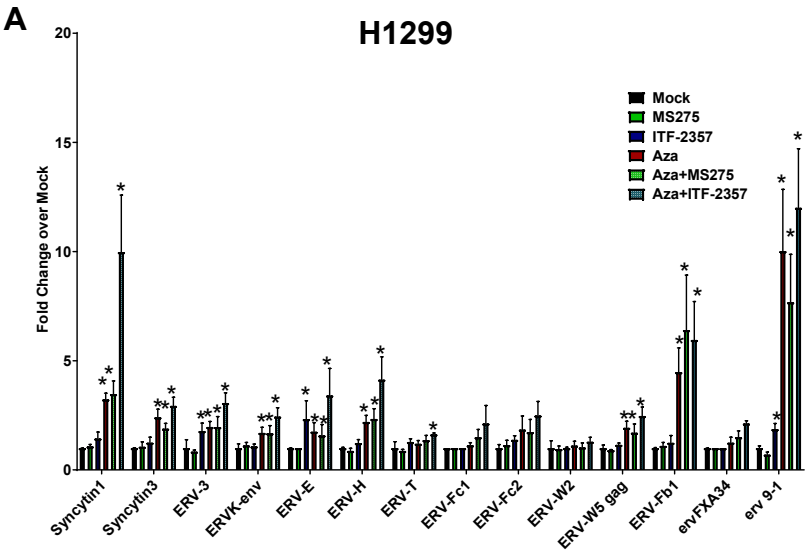
A
H1299
Fold Change over Mock
Mock
MS275
ITF-2357
Aza
Aza+MS275
Aza+ITF-2357
Syncytin1
Syncytin3
ERV-3
ERVK-env
ERV-E
ERV-H
ERV-T
ERV-Fc1
ERV-Fc2
ERV-W2
ERV-W5 gag
ERV-Fb1
ervFXA34
erv 9-1

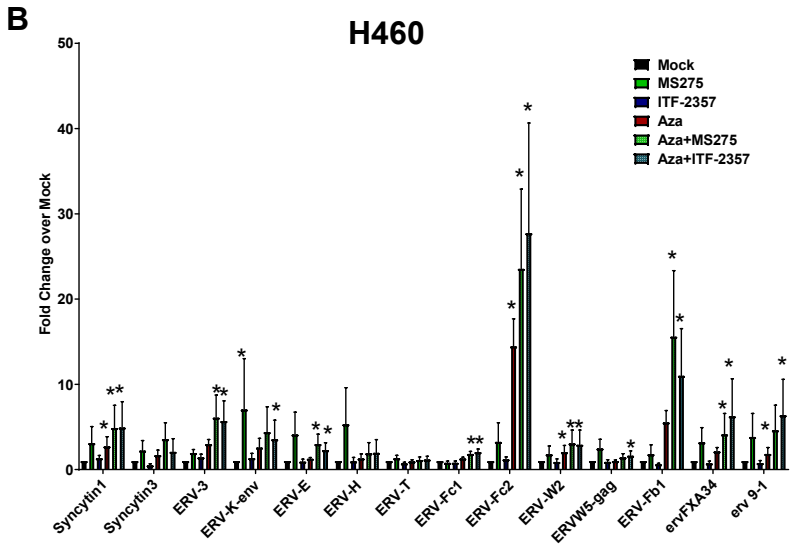
B
H460
Fold Change over Mock
Mock
MS275
ITF-2357
Aza
Aza+MS275
Aza+ITF-2357
Syncytin1
Syncytin3
ERV-3
ERV-K-env
ERV-E
ERV-H
ERV-T
ERV-Fc1
ERV-Fc2
ERV-W2
ERVW5-gag
ERV-Fb1
ervFXA34
erv 9-1

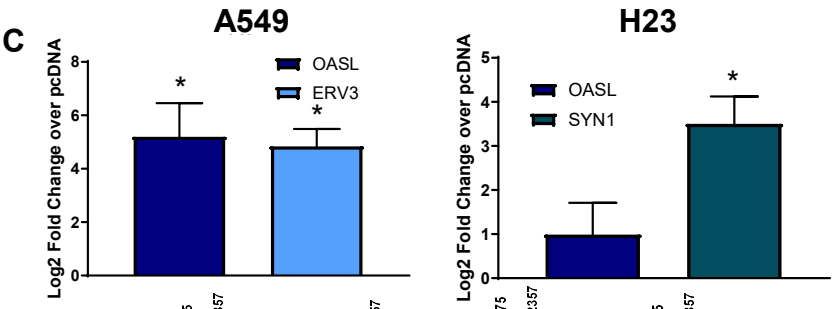
C
A549
Log2 Fold Change over pcDNA
OASL
ERV3
H23
Log2 Fold Change over pcDNA
OASL
SYN1

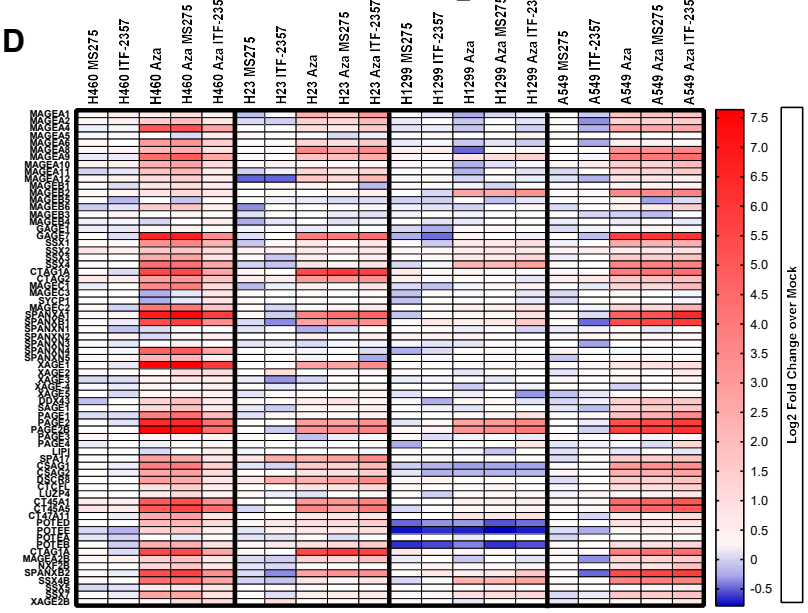
D
H460 MS275
H460 ITF-2357
H460 Aza
H460 Aza MS275
H460 Aza ITF-2357
H23 MS275
H23 ITF-2357
H23 Aza
H23 Aza MS275
H23 Aza ITF-2357
H1299 MS275
H1299 ITF-2357
H1299 Aza
H1299 Aza MS275
H1299 Aza ITF-2357
A549 MS275
A549 ITF-2357
A549 Aza
A549 Aza MS275
A549 Aza ITF-2357
Log2 Fold Change over Mock

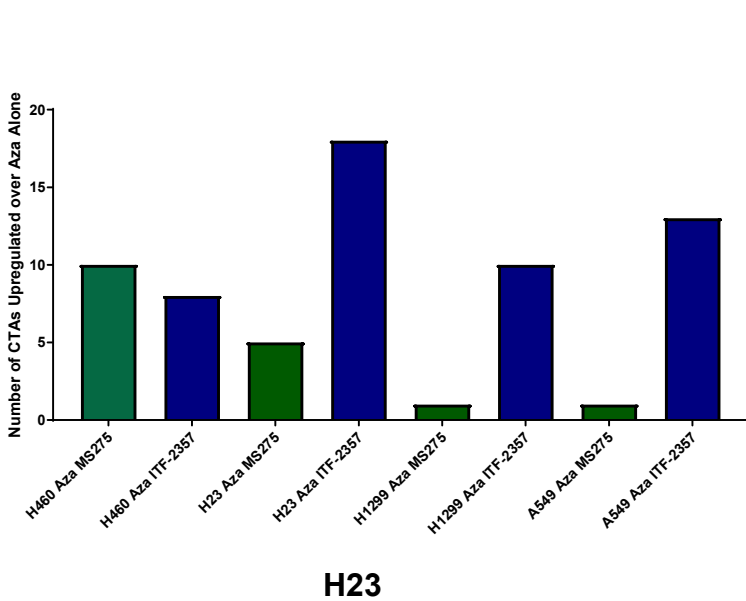
E
Number of CTAs Upregulated over Aza Alone
H460 Aza MS275
H460 Aza ITF-2357
H23 Aza MS275
H23 Aza ITF-2357
H1299 Aza MS275
H1299 Aza ITF-2357
A549 Aza MS275
A549 Aza ITF-2357

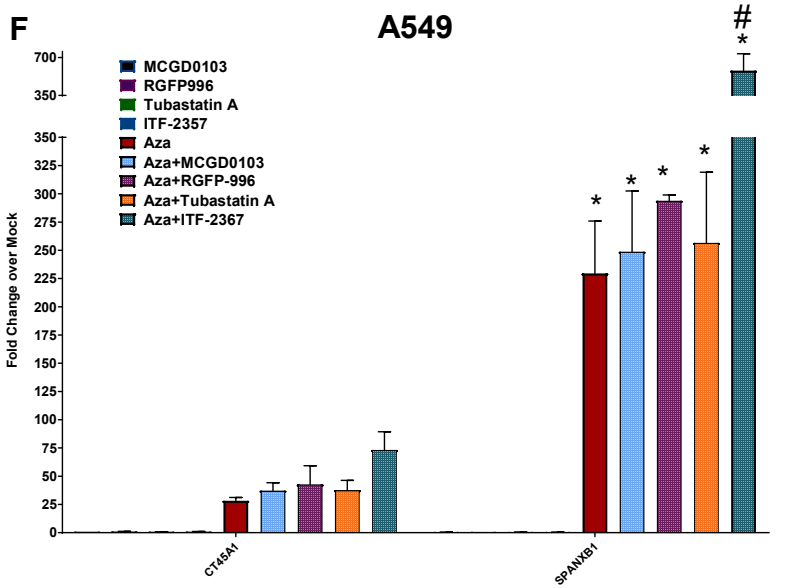
F
A549
Fold Change over Mock
MCGD0103
RGFP996
Tubastatin A
ITF-2357
Aza
Aza+MCGD0103
Aza+RGFP-996
Aza+Tubastatin A
Aza+ITF-2367
CT45A1
SPANXB1

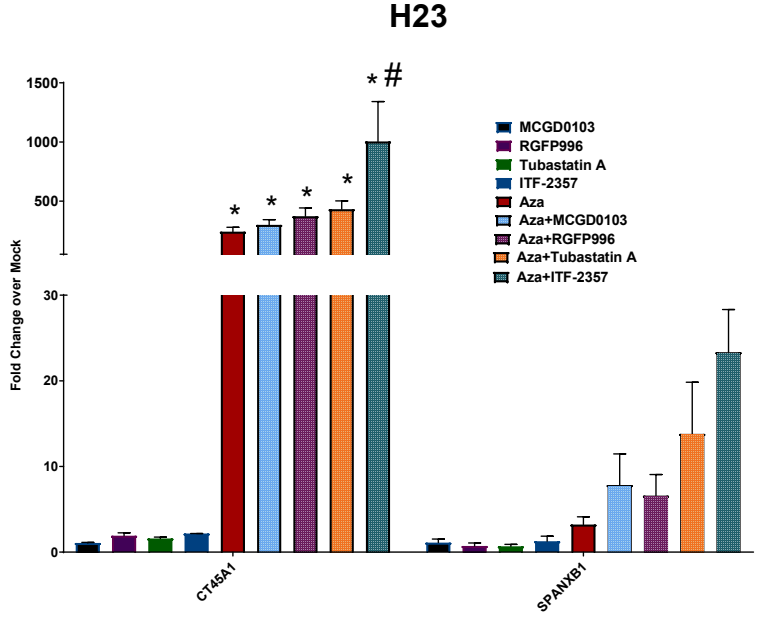
G
H23
Fold Change over Mock
MCGD0103
RGFP996
Tubastatin A
ITF-2357
Aza
Aza+MCGD0103
Aza+RGFP996
Aza+Tubastatin A
Aza+ITF-2357
CT45A1
SPANXB1

A

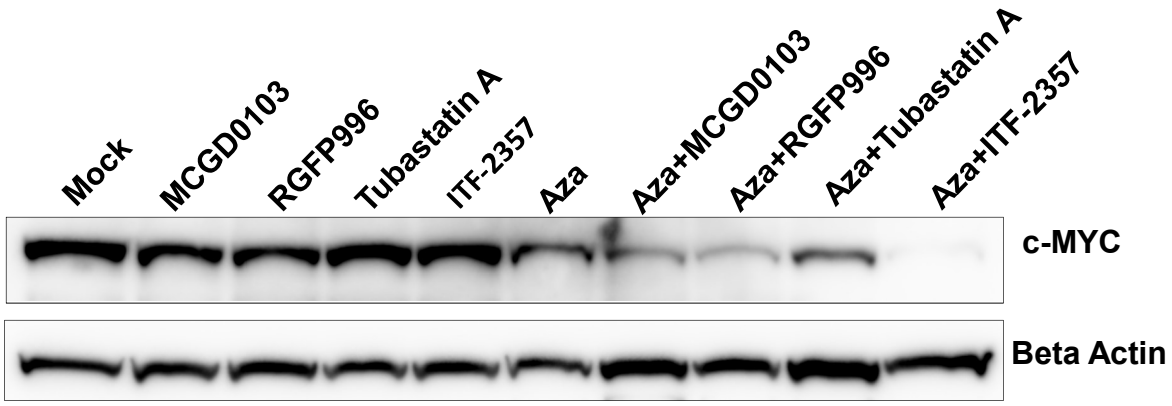
Mock
MCGD0103
RGFP996
Tubastatin A
ITF-2357
Aza
Aza+MCGD0103
Aza+RGFP996
Aza+Tubastatin A
Aza+ITF-2357
c-MYC
Beta Actin

B

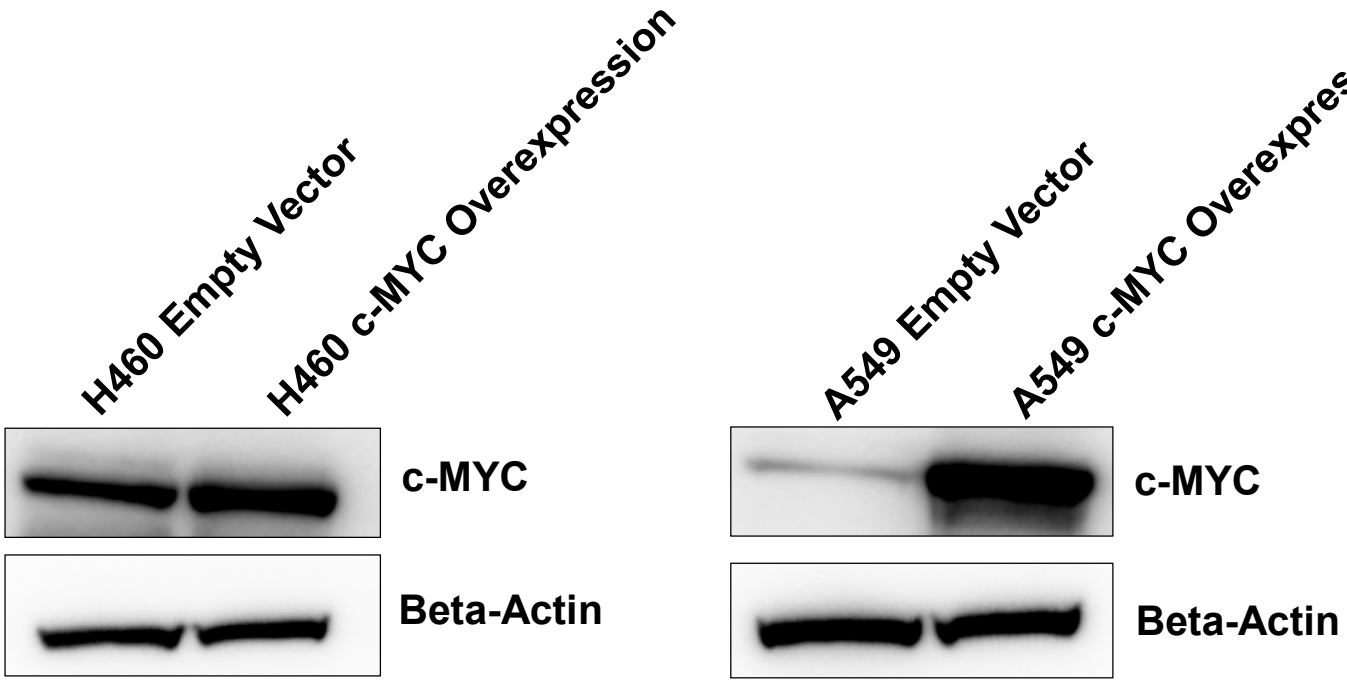
H460 Empty Vector
H460 c-MYC Overexpression
A549 Empty Vector
A549 c-MYC Overexpression
c-MYC
Beta-Actin
c-MYC
Beta-Actin

C

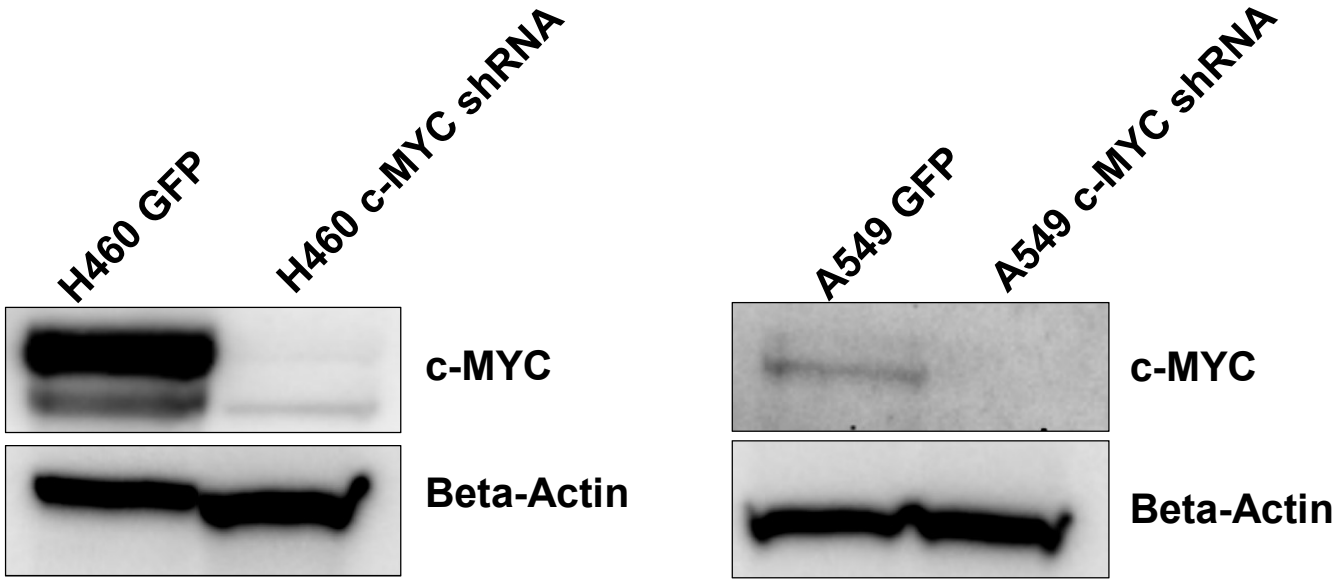
H460 GFP
H460 c-MYC shRNA
A549 GFP
A549 c-MYC shRNA
c-MYC
Beta-Actin
c-MYC
Beta-Actin

A.

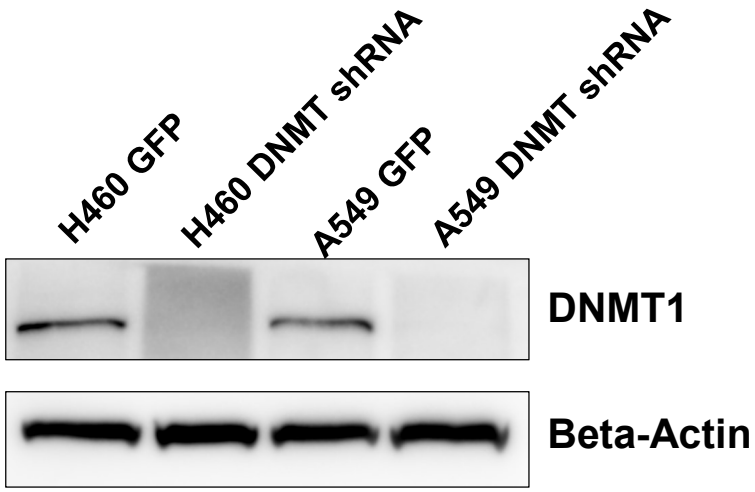
H460 GFP
H460 DNMT shRNA
A549 GFP
A549 DNMT shRNA
DNMT1
Beta-Actin

B

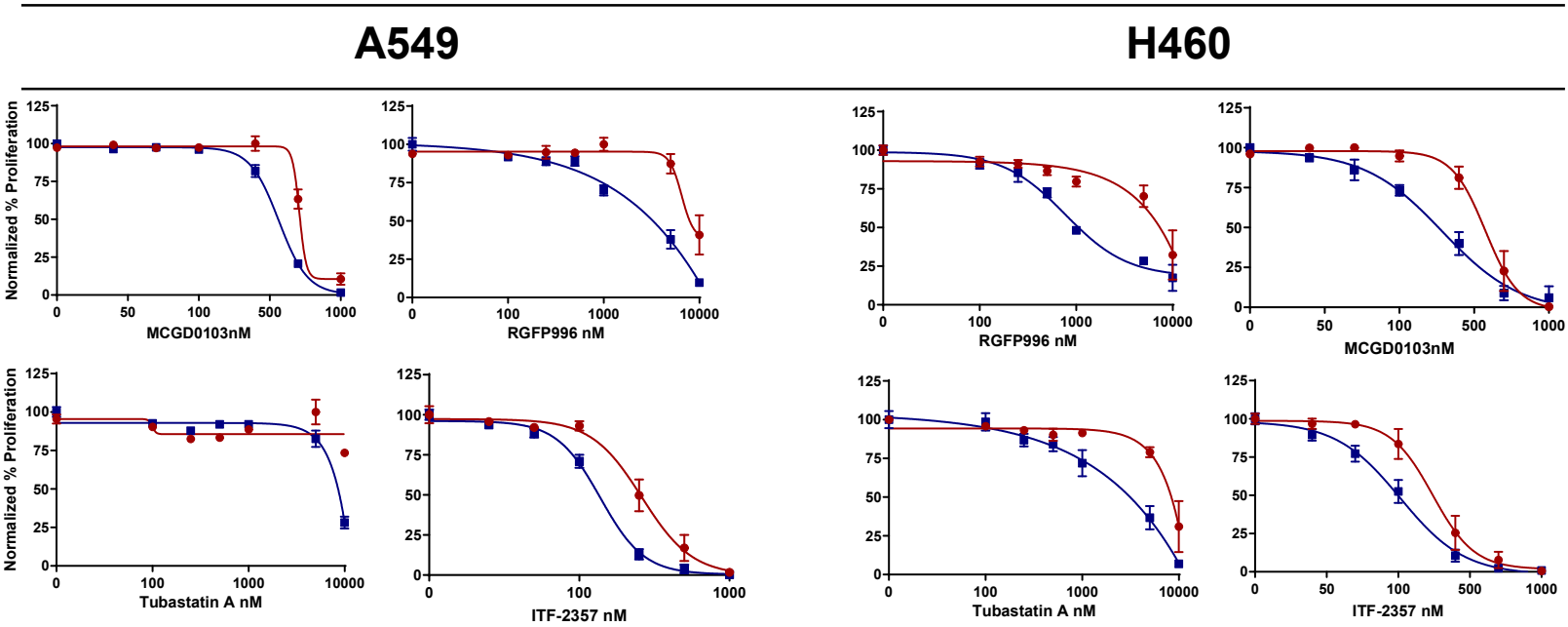
A549
H460
Normalized % Proliferation
MCGD0103nM
RGFP996 nM
Tubastatin A nM
ITF-2357 nM
GFP
DNMTkd

C

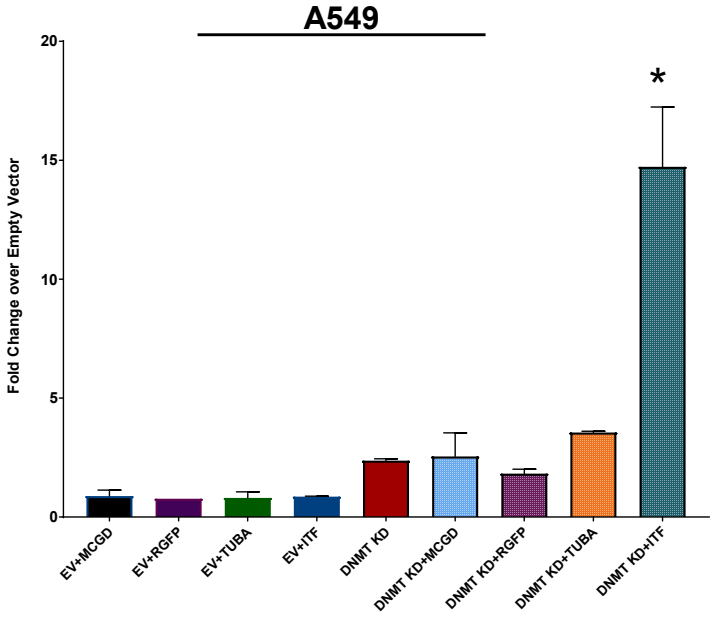
A549
Fold Change over Empty Vector
*
EV+MCGD
EV+RGFP
EV+TUBA
EV+ITF
DNMT KD
DNMT KD+MCGD
DNMT KD+RGFP
DNMT KD+TUBA
DNMT KD+ITF

A

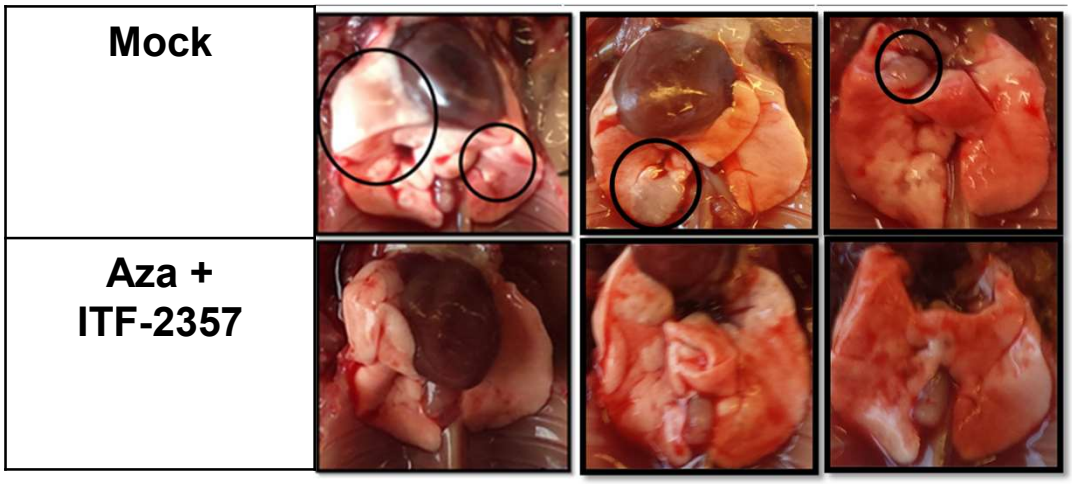
Mock
Aza +
ITF-2357

B

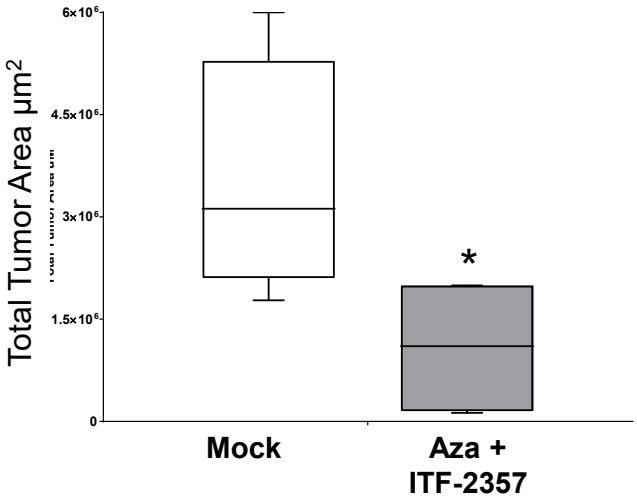
Total Tumor Area µm2
6x10^6
4.5x10^6
3x10^6
1.5x10^6
0
*
Mock
Aza +
ITF-2357

C

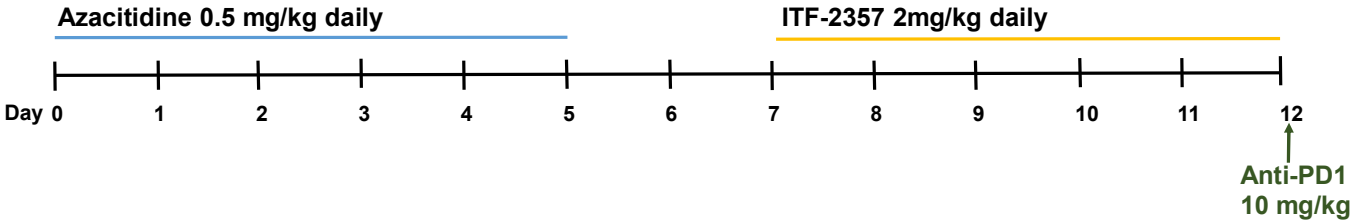
Azacitidine 0.5 mg/kg daily
ITF-2357 2mg/kg daily
Day 0 1 2 3 4 5 6 7 8 9 10 11 12
Anti-PD1
10 mg/kg
Repeat Schedule x6

D

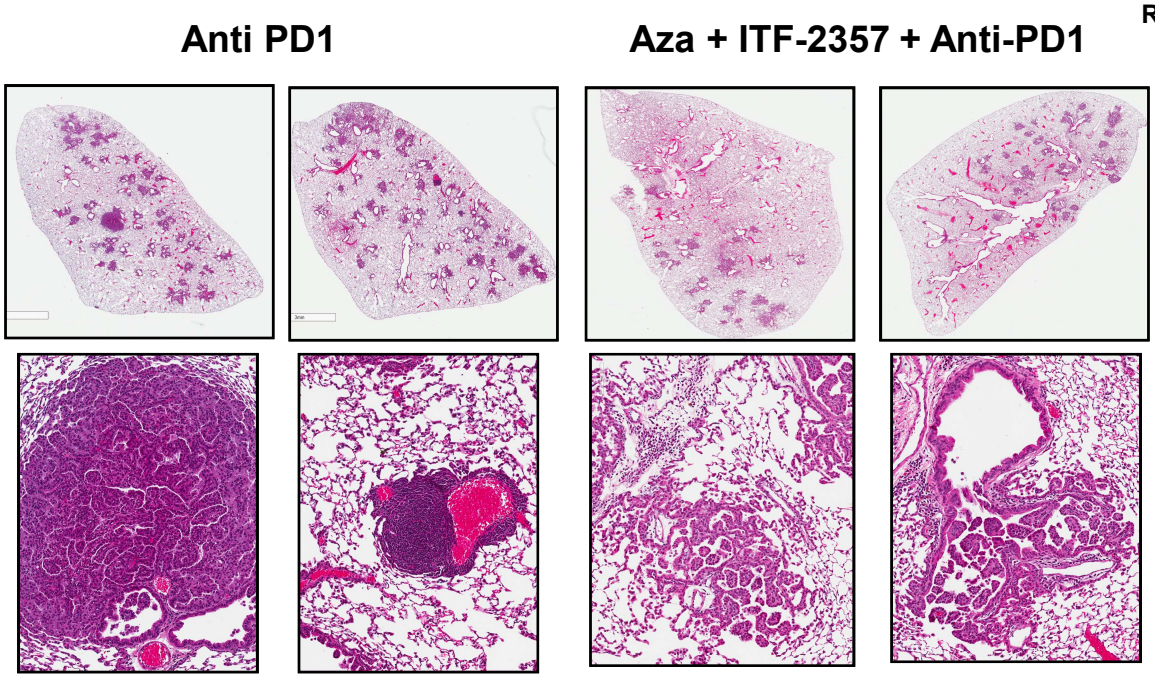
Anti PD1
Aza + ITF-2357 + Anti-PD1